

A systems level characterization of the *Saccharomyces cerevisiae* NuA4 lysine acetyltransferase

Leslie Mitchell

Thesis submitted to the
Faculty of Graduate and Postdoctoral Studies
in partial fulfilment of the requirements
for the PhD degree in Biochemistry

Department of Biochemistry, Microbiology, and Immunology
Faculty of Medicine
University of Ottawa

© Leslie Mitchell, Ottawa, Canada, 2011

ABSTRACT

Lysine acetylation is a post-translational modification (PTM) studied extensively in the context of histone proteins as a regulator of chromatin dynamics. Recent proteomic studies have revealed that as much as 10% of prokaryotic and mammalian proteins undergo lysine acetylation, and as such, the study of its biological consequences is rapidly expanding to include virtually all cellular processes. Unravelling the complex regulatory network governed by lysine acetylation will require an in depth knowledge of the lysine acetyltransferase enzymes that mediate catalysis, and moreover the development of methods that can identify enzyme-substrate relationships *in vivo*. This is complex task and will be aided significantly through the use of model organisms and systems biology approaches. The work presented in this thesis explores the function of the highly conserved NuA4 lysine acetyltransferase enzyme complex in the model organism *Saccharomyces cerevisiae* using systems biology approaches. By exploiting genetic screening tools available to the budding yeast model, I have systematically assessed the cellular roles of NuA4, thereby identifying novel cellular processes impacted by the function of the complex, such as vesicle-mediated transport and the stress response, and moreover identified specific pathways and proteins that are impacted by NuA4 KAT activity, including cytokinesis through the regulation of septin protein dynamics. Moreover, I have developed a mass spectrometry-based technique to identify NuA4-dependent acetylation sites amongst proteins that physically interact with NuA4 *in vivo*. Together this work demonstrates the diversity of processes impacted by NuA4 function *in vivo* and moreover highlights the utility of global screening techniques to characterize KAT function.

ACKNOWLEDGEMENTS

I would like to thank my supervisor Kristin Baetz for providing an inspiring and stimulating lab environment, for continual scientific support and guidance, and for always encouraging independence and initiative.

Long departed Baetz lab members Sharon Berthelet and Maria Gerdes for shaping 'lab life' during the early days in the Baetz lab with your good humour, dedication, and scientific rigour.

Recently departed Baetz lab members Andrea Lau and Ying Fong for months of dedicated effort on the SDL project.

Current Baetz lab members Akil Hamza, Jane Usher, Mike Kennedy, Mojgan Siahbazi, Roya Pourhanifeh, and Sylvain Huard, for unwavering scientific and emotional support.

Drs. Jean-Philippe Lambert and Darren Yip, and Vanja Avdic for helping me understand the characteristics that make a great scientist.

Hilary Phenix and Sujeeve Jeganathan for being enthusiastic colleagues, always willing to discuss interesting topics.

Thienny Mah for thoughtful conversations on work-life balance and demonstrating what is possible through hard work.

And friends and family outside of my scientific network listed above, in particular Laura Chow and Damien Conway, Gad and Joanne Perry, Lorraine Montoya, Ed Bridge, Meagan Fitzpatrick, Pete Meneguzzi, Sarah Bailey, Geordie McConnell, Alexis Tennent, Monica Bisal, Marc Ruus, Dave Lackey, and Kelly Hyndman, all of whom have contributed indirectly but significantly to my completion of this thesis.

TABLE OF CONTENTS

Abstract.....	ii
Acknowledgements	iii
Table of Contents.....	iv
List of Figures.....	vii
List of Tables.....	ix
ABBREVIATIONS	x
Chapter 1: Introduction.....	1
1.1 Lysine acetylation to regulate protein function.....	1
1.1.1 Acetylation of histone proteins	3
1.1.2 Acetylation on chromatin-associated proteins.....	3
1.1.3 Proteome-wide identification of acetylation	6
1.1.4 Acetylation and disease.....	8
1.2 Systems biology approaches in <i>Saccharomyces cerevisiae</i>	9
1.2.1 Global genetic screens	11
1.2.2 Global proteomic screens	16
1.3 NuA4 – a <i>Saccharomyces cerevisiae</i> KAT	18
1.3.1 Subunit composition of NuA4.....	20
1.3.2 KAT activity of NuA4.....	22
1.3.3 Functional insight from analyses of individual NuA4 mutants.....	25
1.3.4 NuA4 cellular processes	26
1.4 Hypothesis and aims.....	29
1.5 References.....	31
Chapter 2:	42
2.1 Abstract.....	43
2.2 Introduction	44
2.3 Materials and Methods	49
2.3.1 Yeast strains and plasmids	49
2.3.2 SL-SGA screens.....	51
2.3.3 NuA4 PrA-tagged protein purification.....	52
2.3.4 Immunoprecipitation and immunoblotting.....	53
2.3.5 Mass spectrometric detection of proteins.....	53
2.3.6 Fluorescence microscopy	54
2.3.7 <i>in vitro</i> binding assay	54
2.3.8 Modified ChIP	55
2.3.9 Northern blot analysis	56
2.4 Results.....	57
2.4.1 An extensive NuA4 genetic interaction map indicates NuA4 impacts a diverse range of cellular processes.....	57

2.4.2	Eaf1 functions primarily as a component of NuA4.....	60
2.4.3	NuA4 function impacts vesicle-mediated transport.....	63
2.4.4	NuA4 and the stress-responsive transcription factor Msn4	67
2.4.5	Eaf1 is required for NuA4 complex integrity	71
2.4.6	Eaf5 and Eaf7 form a sub-complex.....	72
2.5	Discussion.....	76
2.5.1	NuA4 is a genetic hub.....	76
2.5.2	NuA4 as a transcriptional repressor.....	79
2.5.3	NuA4 complex structure and function	81
2.6	Acknowledgements	84
2.7	Supplemental	85
2.8	References.....	86

Chapter 3: 93

3.1	Abstract.....	94
3.2	Introduction	95
3.3	Materials and Methods	97
3.3.1	Yeast strains.....	97
3.3.2	SDL screening	99
3.3.3	Serial spot dilution assays	100
3.3.4	Microscopy	100
3.3.5	Septin TAP immunopurification and NuA4 KAT assay	101
3.3.6	Septin GFP immunopurification and analysis of <i>in vivo</i> acetylation	103
3.3.7	Purification of NuA4, Gcn5, and Eco1 from yeast for <i>in vitro</i> KAT assays	104
3.3.8	Detection of lysine acetylation by mass spectrometry	105
3.4	Results.....	106
3.4.1	A synthetic dosage lethal screen connects NuA4 to cytokinesis	106
3.4.2	NuA4 mutants activate the morphogenesis checkpoint.....	108
3.4.3	Acetyltransferase-deficient NuA4 mutants have defects in septin dynamics	111
3.4.4	NuA4 regulation of septin dynamics is not through histone H4	114
3.4.5	Septin proteins are acetylated <i>in vivo</i>	115
3.4.6	Septin dynamics are regulated by multiple KATs <i>in vivo</i>	120
3.4.7	Unacetylatable <i>shs1</i> mutants have bud morphology and septin localization defects similar to KAT mutants.....	124
3.5	Discussion.....	128
3.5.1	SDL interactions to identify acetylation targets.....	128
3.5.2	A novel role for multiple KATs in regulating septin dynamics	129
3.6	Acknowledgements	132
3.7	Supplemental	133
3.8	References.....	134

Chapter 4: 140

4.1	Abstract.....	141
4.2	Introduction	142
4.3	Materials and methods	145
4.3.1	Yeast strains.....	145

4.3.2	High stringency purification of exogenous NuA4 from yeast for <i>in vitro</i> KAT assays	146
4.3.3	NuA4 modified chromatin immunopurification (mChIP).....	147
4.3.4	<i>in vitro</i> heavy KAT reactions for NuA4 mChIP.....	148
4.3.5	Spindle pole body mChIP-KAT-MS.....	149
4.3.6	Mass spectrometry to detect protein interactions and acetyl lysine residues.....	149
4.3.7	<i>In vitro</i> hot KAT assays.....	150
4.3.8	<i>In vitro</i> unlabelled KAT assays.....	151
4.3.9	Reciprocal co-immunopurifications	151
4.3.10	Microscopy	152
4.4	Results.....	152
4.4.1	mChIP-KAT-MS: A novel method to study NuA4 function.....	152
4.4.2	The NuA4-associated protein interaction network.....	155
4.4.3	Lysine acetylation identified within the NuA4-associated protein network.....	157
4.4.4	NuA4 Auto-acetylation	160
4.4.5	SPB mChIP-KAT-MS uncovers NuA4-dependent acetylation SPB subunits.....	161
4.4.6	NuA4 regulates spindle dynamics.....	167
4.5	Discussion.....	169
4.5.1	mChIP-KAT-MS to characterize NuA4	169
4.5.2	mChIP-MAT-MS to identify putative acetylation targets	172
4.5.3	NuA4 regulation by auto-acetylation	173
4.5.4	NuA4 and SPB function – regulation by acetylation?	174
4.5.5	mChIP-KAT-MS to unravel the lysine acetylation network in yeast	175
4.6	Supplemental	177
4.7	References.....	178
	Chapter 5: General Discussion	185
5.1	Integration of datasets to predict NuA4 function	185
5.1.1	SL and SDL genetic interactions.....	185
5.1.2	Integrating SDL profiles of individual subunits to predict acetylation targets	189
5.1.3	Integrating genetic interaction networks with NuA4 physical interactions and putative acetylation targets	192
5.2	Systems biology approaches to study lysine acetylation	193
5.3	References.....	196

LIST OF FIGURES

Figure 1.1: Reversible lysine acetylation.	2
Figure 1.2: Lysine acetylation on histone proteins.	4
Figure 1.3: Proteome-wide identification of lysine acetylation.	7
Figure 1.4: Synthetic lethal genetic interactions.	13
Figure 1.5: Synthetic genetic array technology applied to SL and SDL genetic interaction profiling.	14
Figure 1.6: Cartoon depicting the identification of an SDL interaction.	15
Figure 1.7: Schematic of the NuA4 lysine acetyltransferase enzyme complex.	21
Figure 1.8: NuA4 mutant phenotypes.	24
Figure 2.1: Synthetic genetic interaction map of five NuA4 subunits.	59
Figure 2.2: Eaf1-TAP purifies the NuA4 complex.	61
Figure 2.3: NuA4 function impacts vesicle-mediated transport.	66
Figure 2.4: NuA4 physically interacts with Msn4 but does not regulate Msn4 binding to the <i>HSP12</i> promoter or heat shock induction of <i>HSP12</i>	68
Figure 2.5: Eaf1 is required for NuA4 complex integrity.	73
Figure 2.6: Eaf5 and Eaf7 form a sub-complex within NuA4.	75
Figure 3.1: NuA4 synthetic dosage lethal genetic interaction network.	107
Figure 3.2: SDL interactions connect NuA4 to cytokinesis through septin proteins.	109
Figure 3.3: <i>eaf1Δ</i> cells have defects in septin dynamics.	112
Figure 3.4: Septin localization defects of <i>eaf1Δ</i> cells are distinct from those of a histone H4 tail mutant.	116
Figure 3.5: Septin proteins are acetylated <i>in vivo</i> and <i>in vitro</i>	117
Figure 3.6: Multiple KATs impact septin dynamics <i>in vivo</i>	122
Figure 3.7: Cell morphology and septin localization is disrupted in 10% of cells expressing an unacetylatable Shs1-HA fusion protein.	125
Figure 4.1: mChIP-KAT-MS methodology.	154
Figure 4.2: The acetyl lysine-enriched NuA4-associated protein network.	156
Figure 4.3: NuA4 subunits are acetylated <i>in vivo</i> and <i>in vitro</i>	162
Figure 4.4: NuA4 acetylates spindle pole body proteins.	164
Figure 4.5: NuA4 acetylation regulates spindle dynamics.	168

Figure 5.1: *ESA1* synthetic lethal genetic interactions link its function to a diverse array of cellular processes. 188

Figure 5.2: Integrating individual NuA4 mutant SDL profiles to predict substrates. 191

LIST OF TABLES

Table 1.1: Conservation of KATs from yeast to human.....	10
Table 1.2: NuA4 conservation across species	19
Table 2.1: Yeast strains.....	50
Table 2.2: Genetic interactions of NuA4 mutants with vesicle-mediated transport genes.....	64
Table 3.1: Yeast strains.....	97
Table 3.2: Quantification of septin localization defects in <i>eaf1Δ</i> cells	113
Table 3.3: Acetylated lysine residues on septin proteins	119
Table 4.1: Yeast strains.....	145
Table 4.2: Acetyl lysine residues in the NuA4-associated protein network.....	159
Table 4.3: Spindle pole body mChIP-KAT-MS acetylation sites.....	166

ABBREVIATIONS

AA	amino acid
<i>ACT1</i>	Actin
AP/MS	affinity purification/mass spectrometry
<i>ARP4</i>	actin related protein
AT	acetyltransferase
ATM	ataxia telangiectasia mutated
ChIP	chromatin immunoprecipitation
DMA	deletion mutant array
DNA	deoxyribonucleic acid
dNTP	deoxyribonucleotide triphosphate
<i>EAF1</i>	Esa1-associated factor 1
<i>EAF3</i>	Esa1-associated factor 3
<i>EAF5</i>	Esa1-associated factor 5
<i>EAF6</i>	Esa1-associated factor 6
<i>EAF7</i>	Esa1-associated factor 7
<i>EPL1</i>	enhancer of polycomb like
E-MAP	epistatic miniarray profile
<i>ESA1</i>	essential SAS family acetyltransferase
GNAT	Gcn5-related N-acetyltransferase
GST	glutathione S-transferase

HAT	histone acetyltransferase
HU	hydroxyurea
IgG	immunoglobulin
KAT	lysine acetyltransferase
KDAC	lysine deacetyltransferase
KDACi	lysine deacetyltransferase inhibitor
Lys	lysine
mChIP	modified chromatin immunoprecipitation
MES	morpholineethanesulfonic
MMS	methyl methanesulfonate
MS	mass spectrometry
MYST	Moz, Ybf2/Sas3, Sas2, Tip60
NuA4	nucleosome acetyltransferase histone H4
OD ₆₀₀	optical density at 600nm
PicNuA4	Piccolo nucleosome acetyltransferase histone H4
PrA	protein A
PTM	post-translational modification
RNAi	ribonucleic acid interference
SDL	synthetic dosage lethal
SDS	synthetic dosage sick
SDS-PAGE	sodium dodecyl sulfate polyacrylamide gel electrophoresis
SILAC	stable isotope labelling with amino acids in cell culture
SL	synthetic lethal
SS	synthetic sick
SUMO	small, ubiquitin-like modifier

<i>SWC4</i>	SWR Complex 4
TAP	tandem affinity purification
Tip60	Tat interactive protein, 60kDa
<i>TRA1</i>	similar to TRRAP
TRRAP	transformation/transcription domain-associated protein
TSA	Trichostatin A
WCE	whole cell extract
<i>YAF9</i>	Yeast homolog of the human leukemogenic protein AF9
<i>YNG2</i>	Yeast homolog of mammalian Ing1
YPD	yeast peptone dextrose

CHAPTER 1: INTRODUCTION

The work described in this thesis examines the function of the *Saccharomyces cerevisiae* NuA4 lysine acetyltransferase enzyme complex using systems biology approaches. In the introduction I will (i) present a brief synopsis of protein lysine acetylation; (ii) describe the global screening approaches I have utilized to probe NuA4 function; and (iii) review NuA4 biology.

1.1 Lysine acetylation to regulate protein function

Conserved lysine acetyltransferase (KAT) enzymes catalyze the acetylation of lysine residues, in which an acetyl moiety from the co-factor acetyl coenzyme A is transferred onto the epsilon amino group of a lysine residue on the substrate, releasing coenzyme A (Figure 1.1). The dynamic equilibrium of acetylation is balanced by the opposing activity of lysine deacetylase enzymes (KDAC), which regenerate the unmodified, positively charged lysine side chain through one of two mechanisms: (i) using a water molecule and releasing acetate or (ii) using NAD^+ and releasing 2'- and 3'-O-acetyl ADP-ribose (Figure 1.1). At the mechanistic level, acetylation not only neutralizes the positive charge of a lysine's side chain, but also modestly increases both the size and hydrophobicity of the modified protein. Any of these features can yield significant conformational changes in a substrate, thereby affecting its function.

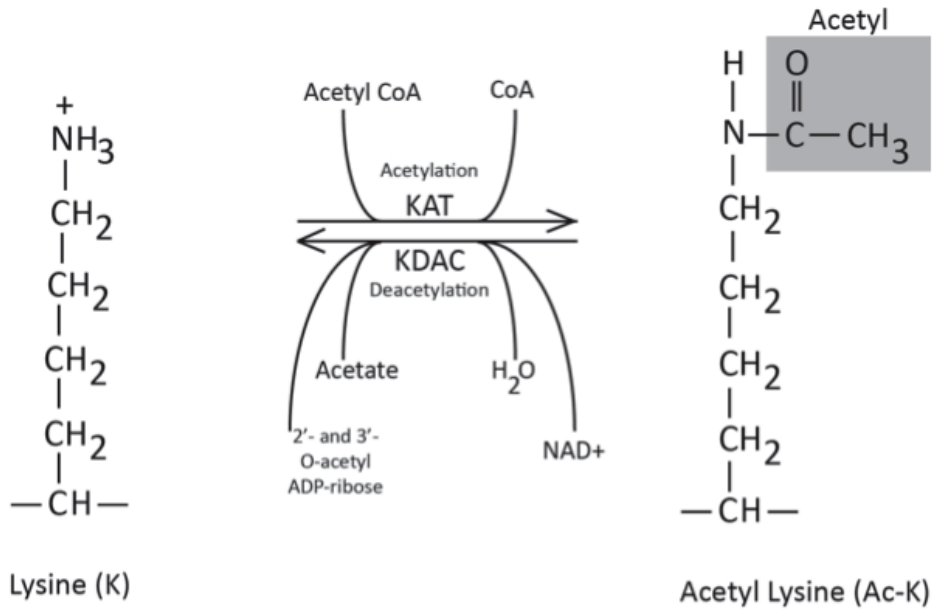


Figure 1.1: Reversible lysine acetylation.

A lysine acetyltransferase (KAT) enzyme catalyzes the transfer of an acetyl group from acetyl coenzyme A (Acetyl CoA) to the epsilon-amino group of the lysine residue. The lysine deacetyltransferase (KDAC) enzyme removes the acetyl group from acetyl-lysine (Ac-K) using water or NAD⁺, thereby regenerating the epsilon-amino group and releasing an acetate molecule or 2'- and 3'-O-acetyl ADP-ribose.

1.1.1 Acetylation of histone proteins

Lysine acetylation was first described on the amino-terminal tails of histone proteins almost 50 years ago (79). Histone proteins package genomic DNA into structural units called nucleosomes, 146 base pairs of DNA wrapped around an octamer of the core histone proteins (two each of H2A, H2B, H3, H4) (64). The complex of DNA and histone proteins, termed the nucleosome that serves as the building block of chromatin, serves to tightly compact the genome within the nucleus and importantly control the access of additional proteins to the DNA. Therefore, lysine acetylation, in cooperation with other histone PTMs, can regulate chromatin structure by changing the accessibility of DNA and/or acting as a docking site for accessory proteins to mediate DNA-templated events (71). As such, *in vivo* acetyl lysine residues within both the N-terminal tails and globular domains of histone proteins (Figure 1.2) (9, 85, 87) have been associated with virtually all DNA-mediated cellular events, including chromosome compaction, transcriptional regulation, DNA damage repair, replication, and silencing (87). For instance, the acetylation of all four N-terminal lysine residues of H4 has been associated with DNA damage repair, combining H4 mutants of Lys5, Lys8, and Lys12 results in transcriptional defects, N-terminal tail acetylation plays a role in nucleosomal deposition of in newly synthesized DNA, and H4 Lys16 acetylation regulates both chromatin compaction and silencing (87).

1.1.2 Acetylation on chromatin-associated proteins

For years evidence has indicated that lysine acetylation also regulates non-histone proteins. Acetyl lysine residues, for instance, were identified on α -



Figure 1.2: Lysine acetylation on histone proteins.

Shown are the amino acid sequences of the four core human histone: H2A, H2B, H3, and H4. All denoted acetylation marks (Ac) have been validated *in vivo* in human cells, and the subset of solid red acetylation marks indicates lysine residues that are conserved in yeast and also known to be modified by acetylation.

tubulin over twenty years ago (80), a modification that stabilizes microtubule structures (81). Further, the cytoplasmic and mitochondrial localization of some KAT and KDAC enzymes suggested the process of reversible lysine acetylation would extend beyond the confines of the nucleus (22, 86). However, given the intimate connection between histone lysine acetylation and the control of DNA-based events, early identification of non-histone acetylation targets focused mainly on proteins involved in chromatin-directed processes. As such, lysine acetylation has been identified and characterized on a variety of transcription factors, and proteins involved in DNA repair, recombination, and replication (108). Importantly, this work demonstrated the diverse functional consequences of the lysine acetylation on protein function. For instance, acetylation may act as a simple on/off switch to regulate a specific aspect of the function of the substrate protein such as enzymatic activity. This has been demonstrated for the ATM kinase, in which acetylation following DNA damage is essential for activation of its kinase activity (94). Acetylation at discrete residues can also serve as a docking site and thereby modulate protein-protein interactions of a substrate. For example, acetylation of p53 at K382 increases the affinity of interaction with the bromodomain of CBP (73). Acetylation can also modify protein function by altering substrate localization, as demonstrated by acetylation-dependent translocation of the WRN DNA helicase from the nucleolus into nucleoplasmic foci following DNA damage (14). Lysine residues can also be modified by ubiquitination and therefore acetylation can regulate protein stability by preventing ubiquitin-mediated proteasomal degradation. An example is the increased stability of SREBP

transcription factors by acetylation at lysine residues to block ubiquitination (38). Finally, another intriguing mechanism of regulation is that of charge neutralization of lysine patches to regulate oligomerization of acetylation targets, for instance the effect of acetylation of multiple C-terminal lysines in p53 regulates its ability to oligomerize (46). In summary, lysine acetylation can regulate substrate function in a number of distinct ways including altering its stability, localization, protein-protein interaction partners, and/or enzymatic activity (91).

1.1.3 Proteome-wide identification of acetylation

More recently, systems level approaches to identify acetyl-lysine residues have unequivocally demonstrated that acetylation is a major player in protein regulation. Multiple groups have employed enrichment strategies to identify acetylation sites, immunopurifying acetylated peptides from tryptically-digested samples using anti-acetyl lysine antibodies, prior to mass spectrometry analysis (Figure 1.3A). The immunopurification step serves to reduce the complexity and dynamic range associated with proteome-wide analysis. These experiments have successfully identified acetylation sites on thousands of proteins with a broad range of functions (Figure 1.3B) (18, 48, 103, 111, 112). Performed in both eukaryotic and prokaryotic systems, these experiments have revealed a number of fundamental properties of protein lysine acetylation. First, acetylation is both an evolutionarily conserved and ubiquitous mechanism of protein regulation; second, most acetylated proteins do not have obvious roles in chromatin-directed cellular processes; third, acetylation is particularly abundant on mitochondrial

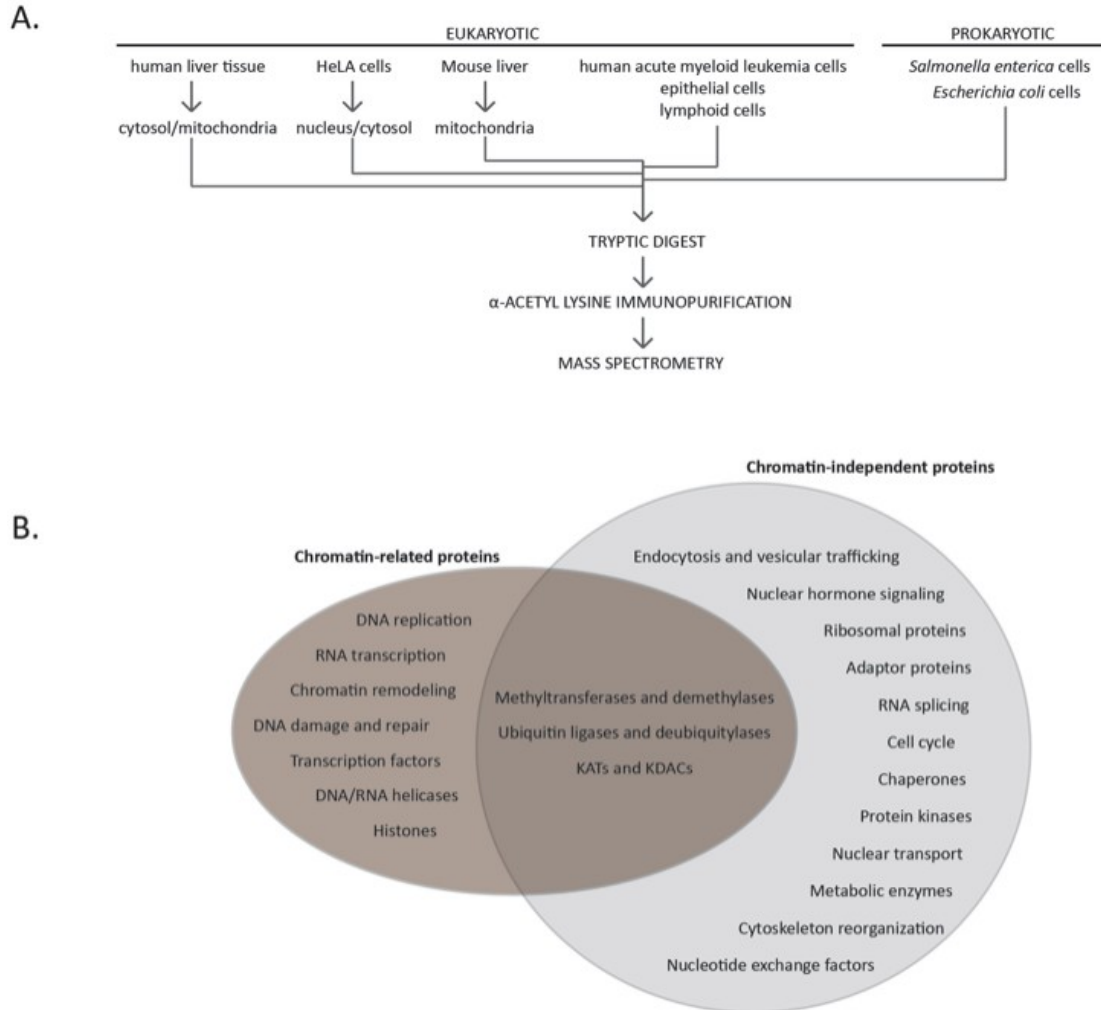


Figure 1.3: Proteome-wide identification of lysine acetylation.

(A) Proteome-wide identification of acetyl-lysine residues in a variety of cells and tissues types has been performed using an enrichment strategy. Briefly, acetylated peptides are isolated from tryptically-digested lysate via immunopurification with anti-acetyl lysine antibodies. Subsequently, mass spectrometric analysis is used to identify acetylated lysine residues. **(B)** Functional classes/biological processes associated with acetylated proteins, organized by chromatin-directed processes (left) and chromatin-independent processes (right). Enzymes that target both histone and non-histone proteins, belong to both classes (middle).

proteins, thereby connecting cellular energy and metabolic processes to this process; fourth, multi-subunit proteins complexes, in particular those involved in modifying chromatin, are often highly acetylated on multiple subunits; and fifth, based on the enrichment of specific amino acids flanking acetyl-lysine residues, acetylation motifs may exist for KATs, similar to those identified for kinases (70). Without question, systems level analyses have fundamentally changed our understanding of the breadth of protein acetylation in all cells, yet the finer details, such as the biological consequences of individual acetylation marks, are only beginning to be explored *in vivo*.

1.1.4 Acetylation and disease

The intimate links to major diseases such as cancer (3), neurodegenerative disorders (28), cardiovascular disease (63), and inflammatory lung disease (43) provide a compelling reason to elucidate pathways governed by protein lysine acetylation. In almost all cases, links between lysine acetylation and the development and/or progression of disease were established based on the effects of treatment with lysine deacetyltransferase inhibitors (KDACi). These small molecule inhibitors induce a hyper-acetylated cellular state by impeding KDAC function, resulting in varied effects on different types of cells. For instance, KDACi treatment exhibits selective toxicity towards cancer cells, by promoting differentiation, cell cycle arrest, senescence, apoptosis, reactive oxygen species production, and mitotic death (91). On the other hand, KDACi drugs exhibit mainly protective properties on neuronal cells (28). While KDACi treatment most certainly alters the expression of specific genes through alterations in chromatin structure

(11), its effects on non-histone targets are only beginning to be explored (18). The broad range of acetylated proteins identified from the global screens (Section 1.1.3) implies important roles will likely be established for the inhibition of non-histone deacetylation in modulating disease.

1.2 Systems biology approaches in *Saccharomyces cerevisiae*

It is clear that elucidating pathways governed by lysine acetylation presents a major challenge due to the sheer cellular abundance of this modification. To this end, model organisms and the application of systems biology approaches represent valuable tools. The budding yeast *Saccharomyces cerevisiae* in particular is an excellent system in which to study lysine acetylation as basic cellular processes are largely conserved with higher eukaryotes, importantly including many of the KAT enzymes that mediate catalysis (Table 1.1). Moreover, post-genomic tools developed in yeast, including genome-wide arrayed yeast libraries, such as the deletion mutant collection (104), the galactose-inducible overexpression array (90), and endogenously epitope-tagged arrays (37, 41), coupled with high throughput screening technology, have revolutionized the ability to systematically study gene and protein function. I have chosen to study the impact of lysine acetylation in budding yeast through the characterization of one particular KAT complex, NuA4. Below I will describe the two genetic and one proteomic screening approaches I have used to probe NuA4 function *in vivo*.

Table 1.1: Conservation of KATs from yeast to human

Yeast KAT	Complex	Histone targets	Non-histone targets	Human Homolog (2)	References
MYST family					
Esa1	NuA4; PicNuA4	H4 (K5,8,12,16); H2A (K4,7); Htz1 (K8,10,14)	Yng2, Pck1	Tip60 (KAT5); HBO1 (KAT7)	(29)
Sas2	SAS	H4 (K16)	---	MOF (KAT8)	(88)
Sas3	NuA3	H3 (K14,23)	---	MOZ (KAT6)	(45)
GNAT family					
Gcn5	SAGA, SLK, ADA, STAGA	H3 (K9,14,18,23,36); Htz1 (14); H2A	Rsc4	GCN5 (KAT2)	(8)
Eco1	---	none	Smc3	ESCO1	(110)
Elp3	Elongator	H3	---	ELP3 (KAT9)	(105)
Hat1	Hat1/2	H4 (K5,12)	---	HAT1 (KAT1)	(77)
Hpa2 (KAT10)	---	H3 (K14)	---	---	(93)
Others					
Rtt109 (KAT11)	trimer with Asf1, Vps75	H3 (K56)	---	p300 (KAT3A)	(97)
Spt10	---	---	---	---	(33)
Taf1	TFIID	<i>in vitro</i> H3	---	TAF1 (KAT4)	(31)

MYST = Moz, Ybf2/Sas3, Sas2, Tip60; GNAT = Gcn5-related N-acetyltransferases

1.2.1 Global genetic screens

Phenotypic analysis of individual mutants provides an important tool to define gene function. However, the effects of gene under- and over-expression, assessed globally, have demonstrated remarkable genetic redundancy within the yeast genome, as over 70% of yeast genes can be deleted and more than 80% over-expressed without dramatic effects on cell fitness in most cases (90, 104). This redundancy, presumably evolved to buffer the negative effects of mutations, has given rise to a powerful alternative approach to study gene function: the identification of synthetic genetic relationships between genes. The premise is that combinations of gene mutations that reduce cell fitness can pinpoint a shared function. The single most important technological development driving the analysis of gene function through synthetic genetic interactions is called Synthetic Genetic Array (SGA), which enables the automated construction of double mutants genome-wide (99). I have applied SGA technology to systematically identify synthetic lethal (SL) (Chapter 2) and synthetic dosage lethal (SDL) (Chapter 3) genetic interaction profiles for NuA4.

1.2.1.1 Synthetic lethal genetic interactions

A synthetic lethal (SL) or synthetic sick (SS) genetic interaction is defined as the combination of two gene mutations, each individually viable, that cause a fitness defect not predicted from the multiplicative effect of combining the single mutations. The classical interpretation of this type of genetic interaction is that the cell cannot tolerate the disruption of a shared function of the two gene mutations, suggesting that the encoded proteins work in parallel to one another (Figure 1.4A).

Conversely, highly similar SL genetic interaction profiles can predict genes that function in the same pathway or protein complex (24, 25) (Figure 1.4B). Using SGA technology, SL screens are performed by introducing a query mutant of interest into the deletion mutant array (DMA) (Figure 1.5A), an ordered array of approximately 4700 non-essential gene deletion mutants (104). Following a series of pinning steps to isolate double mutant haploid cells, SS or SL genetic interactions are identified as slow growing or dead colonies, respectively (Figure 1.5A). SL-SGA analysis has made possible the unbiased screening of a large number of the non-essential genes in yeast as well as alleles encoding mutated essential proteins (25).

1.2.1.2 Synthetic dosage lethal genetic interactions

A second genome-wide screening technique developed to probe gene function is called synthetic dosage lethal (SDL) interaction profiling. An SDL interaction is defined as a reduction in fitness of a mutant cell caused by overexpression of a second gene (Figure 1.6) (90). Genome-wide SDL-SGA screens are performed by introducing a query mutant of interest into the galactose-inducible overexpression library, which contains ~5200 plasmid-borne yeast genes whose over-expression is activated only when grown on galactose-containing media (113). Using SGA technology, double mutants (query deletion mutant and overexpression plasmid) are generated, and synthetic dosage sick (SDS) or SDL interactions are identified by slow growth or death of the mutant specifically when overexpression is induced on galactose media (Figure 1.5B). Importantly, SDL interactions arise from mechanistically distinct genetic origins

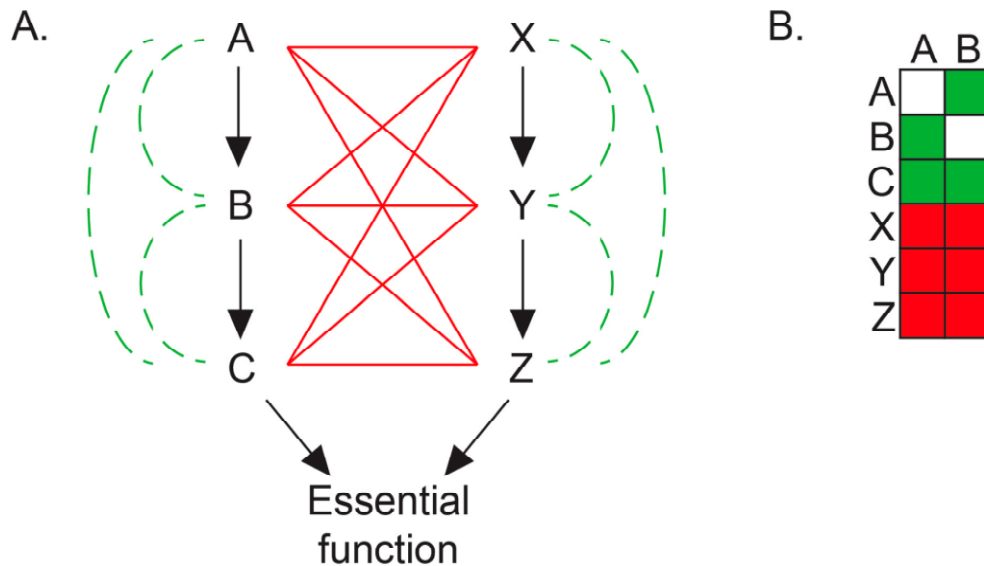


Figure 1.4: Synthetic lethal genetic interactions.

(A) Synthetic lethal or sick genetic interactions (red lines) can be observed when mutations occur between non-essential genes (A, B, C, and X, Y, Z) that function in parallel non-essential pathways (A-C and X-Z) that lead to an important or essential function. Mutation of any of A, B, or C eliminates the pathway A-C, and mutation of any of X, Y, or Z eliminates pathway X-Z. Absence of only one pathway does not affect cellular viability as the intact parallel pathway still achieves the essential cellular function. However, mutation in both pathways leads to synthetic lethality, as the essential cellular function is no longer carried out. Thus, SL or SS genetic interactions tend to occur between pathways. In contrast, non-essential genes functioning within the same pathway do not genetically interact with one another (green dashed lines). **(B)** Genes in the same pathway tend to have similar genetic interactions. Hierarchical clustering exploits this tendency in order to predict pathways. In this example, gene A and gene B have similar genetic interaction profiles and would therefore cluster together.

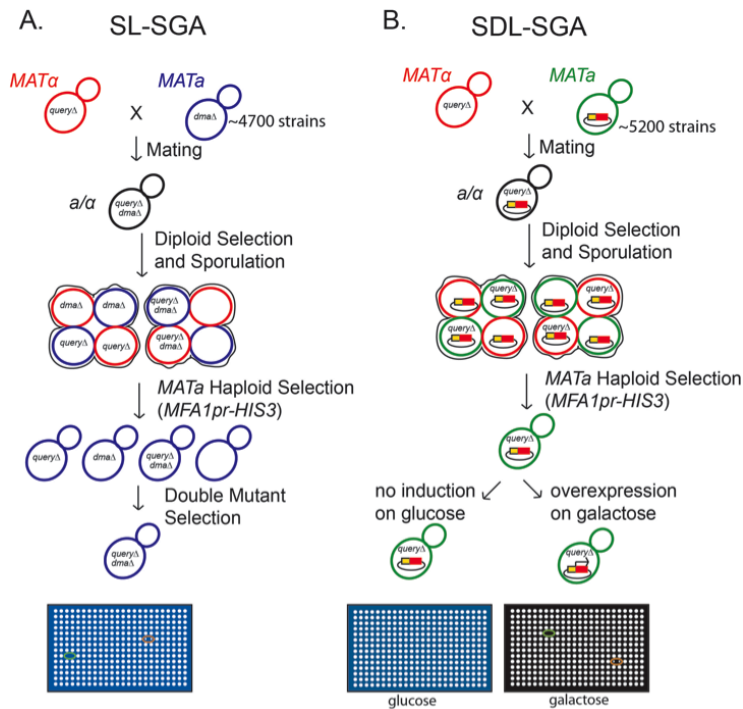


Figure 1.5: Synthetic genetic array technology applied to SL and SDL genetic interaction profiling.

(A) A *MATα* strain carrying a query mutation (*queryΔ*, red cell) linked to a dominant selectable marker, and an *MFA1pr-HIS* reported is crossed to an ordered array of *MATα* viable yeast deletion mutants, each carrying a gene deletion mutation linked to a different selectable marker (*dmaΔ*, blue cell). Growth of resultant heterozygous diploids (black cell) is selected for on medium containing both selectable markers. The heterozygous diploids are then transferred to medium with reduced levels of carbon and nitrogen to induce sporulation and the formation of haploid meiotic spore progeny. Spores are transferred to selective medium lacking histidine, which allows for selective germination of *MATα* meiotic progeny because these cells express the *MFA1pr-HIS* reporter specifically. Finally, the *MATα* meiotic progeny are transferred to medium that contains both selectable markers, which selects for growth of double-mutant meiotic progeny. Dead or slow growing mutants allow for the identification of SL (green circle) or SS (orange circle) genetic interactions. **(B)** SDL-SGA screening is carried out nearly identically, except, the *MATα* query strain is mated to an ordered array of *MATα* yeast overexpression strains (green cell), each carrying a unique *pGAL1/10*-GST-6xHis-ORF high copy plasmid also encoding a selectable marker. Following sporulation and selection of double mutant haploid cells (*queryΔ* plus plasmid) as outlined in (A), cells are pinned onto galactose-containing medium to induce expression from the plasmid-based *GAL1-10* promoter. Colony sizes on galactose are compared to those on glucose to identify those strains with a galactose-specific growth defect reflecting sensitivity to overexpression of the plasmid-borne gene.

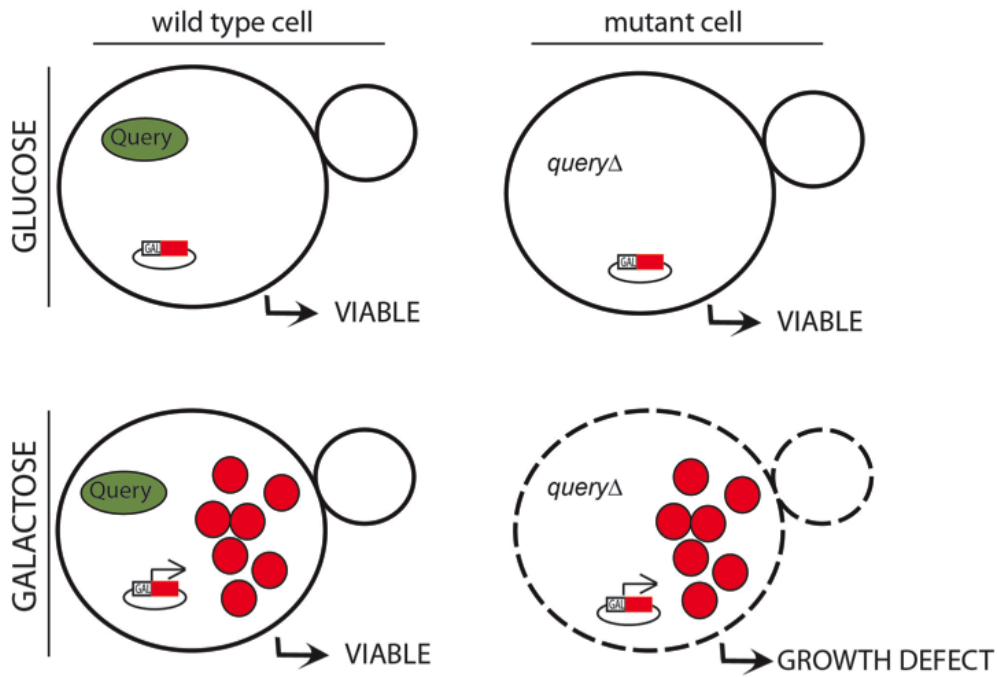


Figure 1.6: Cartoon depicting the identification of an SDL interaction.

Overexpression of the plasmid-borne 'red' gene from the galactose-inducible promoter (*GAL*), encoding the 'red circle protein', is achieved when cells are grown on galactose-containing media (bottom) compared to glucose-containing media (top). SDL interactions are specifically identified when overexpression upon galactose induction, which has no effect on the wild type cell in which the green Query protein is intact (left, bottom), results in a measurable fitness defect (dashed cell wall) in the mutant cell (right, bottom) in which the query gene, encoding the green Query protein, has been deleted (*queryΔ*).

compared to SL genetic interactions, and these two types of screens can therefore provide complementary functional information (7, 90, 114). While SL interactions single out genetic redundancy, generally identifying pathways and proteins that function in parallel pathways, SDL interactions tend to occur between members of the same pathway. Further, based on the premise that an increased amount of inappropriately modified substrate may cause a measurable fitness defect specifically in an enzyme mutant background, genome-wide SDL profiling has proven successful in identifying downstream targets of kinases, as well as targets of specific proteolytic pathways (61, 90, 114). Importantly, the genetic principles suggest the use of genome-wide SDL profiling to identify enzyme-substrate relationships should be universally applicable to all classes of enzymes, including KATs.

1.2.2 Global proteomic screens

While SL and SDL genetic interactions can be used to infer gene function, protein-protein interactions identify direct relationships. (100). In budding yeast, proteome-wide characterizations of protein-protein interactions have been performed using affinity-purification followed by mass spectrometry (AP/MS) (35, 36, 40, 53) as well as yeast-two-hybrid assays (44, 100). These efforts have identified the stably interacting core components of the majority of yeast protein complexes, including NuA4, importantly establishing that proteins that physically interact *in vivo* are likely to be functionally related. However, the success of high throughput screens in discovering physical interactions beyond those of core protein complexes is far more limited. For example, fewer than 10 physical

interactions have been identified for core NuA4 complex members in the high throughput AP/MS and yeast-two-hybrid screens. This represents a major gap in understanding for an enzyme complex such as NuA4, as enzymatic activity necessitates a physical interaction with the substrate; a comprehensive analysis of physical interactions for an enzyme can thus be considered a list of putative substrates. Outlined below is a summary of some approaches that may be used to identify substrates of KAT enzymes.

1.2.2.1 Identification of KAT acetylation targets

A number of approaches have been used to link KATs to their targets. Typically, *in vitro* KAT assays are employed, which involve incubation of a purified KAT and candidate substrate with acetyl coenzyme A. Following gel separation, acetylation can be detected by Western blot using anti-acetyl lysine antibodies, or by fluorography when a radiolabeled version of acetyl coenzyme A (^3H or ^{14}C) is employed. Detection of acetylation using these methods, however, can be hindered due to the poor quality of anti-acetyl lysine antibodies or the low specific activity of the ^3H or ^{14}C radioisotopes. Moreover, *in vitro* assays can lead to spurious enzymatic activity as many regulatory constraints, such as cellular compartmentalization, can only be imposed *in vivo*. The biggest drawback associated with directed *in vitro* KAT assays is the *a priori* requirement for a list of candidate substrates to test. While the application of high-density protein arrays presents one solution to this problem, the availability of such arrays, which require a purified source of all proteins encoded by a genome, presents a significant limiting factor to the widespread use of such technology.

Detection of acetyl-lysine residues *in vivo* has dramatically benefited from the enrichment strategy outlined in (Figure 1.3B) as well as technological advances in mass spectrometry enabling high accuracy assignment of mass-to-charge ratio. However, a global proteomic experiment to connect KAT enzymes to their targeted lysine residues *in vivo* has not yet been attempted. One promising option is the use of stable isotope labelling with amino acids in cell culture (SILAC). Following KDACi treatment, changes in global acetylation can be detected (18), suggesting disruption of KAT or KDAC activity as a possible strategy to identify substrates in a high throughput fashion. However, the detection of low abundance acetylation events such as those regulated by the cell cycle may be difficult to detect due to their transient nature and ultimately while differential acetylation levels may be detected, this may not reflect a direct enzyme-substrate relationship. Therefore, a key challenge in the field of protein lysine acetylation is to connect KAT and KDAC enzymes to their targeted lysine residues on specific proteins to fully elucidate the biological consequences of acetylation.

1.3 NuA4 – a *Saccharomyces cerevisiae* KAT

The work presented in this thesis probes the function of an essential KAT in *Saccharomyces cerevisiae* called NuA4 (nucleosome acetyltransferase H4). NuA4 is a multi-subunit protein complex that is highly conserved across species (Table 1.2), including *Drosophila melanogaster*, *Caenorhabditis elegans*, *Schizosaccharomyces pombe*, and most notably in human cells, in which the orthologous Tip60 complex has been linked to a number of diseases such as

Table 1.2: NuA4 conservation across species

NuA4 <i>S. cerevisiae</i>		Homologs			
Subunit	Other complex? (29)	Human (29)	<i>D. melanogaster</i> (54)	<i>C. elegans</i> (17)	<i>S. pombe</i>
Esa1	PicNuA4	Tip60	dTip60	MYS-1	Mst1
Epl1	PicNua4	Epc	E(Pc)	EPC-1	Epl1
Yng2	PicNuA4	Ing3	dIng3		Png1
Eaf1		p400	Domino	SSL-1	Vid21
Eaf3	Rpd3	MRG15	dMrg15		Alp13
Eaf6	NuA3	hEaf6	dEaf6		Eaf6
Eaf7		MrgBP	dMrgB		Eaf7
Swc4	SWR	DMAP1	dDMA		Swc4
Arp4	SWR/Ino80	BAF53a	BAP55		Alp5
Eaf5					
Tra1	SAGA	TRRAP	dTra1	TRR-1	Tra2
Yaf9	SWR	Gas41	dGas41		Yaf9
Act1	SWR/Ino80	Actin	Act87E		Act1

cancer (5), Alzheimer disease (16, 50) and HIV (23, 26). Importantly, in addition to histone proteins (30, 49), Tip60 acetylates a number of key cellular regulators such p53 (96, 98), the ATM (ataxia telangiectasia mutated) kinase (94), and c-MYC (78). Further, global RNAi screens have linked the *C. elegans* NuA4 complex to a diverse array of cellular processes, including signal transduction (57, 83). Together, studies of orthologous NuA4 complexes have hinted at the mechanisms by which this evolutionary conserved KAT functions. Below I will provide an overview of NuA4 biology in *S. cerevisiae*.

1.3.1 Subunit composition of NuA4

NuA4 was first identified and characterized based on its ability to acetylate histone proteins *in vitro* (39, 92). The *in vitro* histone acetyltransferase (HAT) activity was discovered following chromatographic fractionation of yeast whole cell lysate and indicated NuA4 to be a protein complex of megadalton size (39). Esa1 (essential SAS family acetyltransferase) was quickly established to be the catalytic subunit, (1, 21), but the identities of the remaining subunits were determined over the next several years by AP-MS (1, 32, 34, 51, 52, 55, 62, 75). The full complement of NuA4 subunits is now believed to include thirteen subunits, six of which are essential for cell viability (Act1, Arp4, Epl1, Esa1, Swc4 and Tra1), while the remaining seven are not (Eaf1, Eaf3, Eaf5, Eaf6, Eaf7, Yaf9, and Yng2) (29).

Early analysis of physical interdependencies between subunits defined two sub-complexes within NuA4 (Figure 1.7). The Piccolo sub-complex contains the Esa1 acetyltransferase activity along with Epl1, Yng2, and Eaf6. The

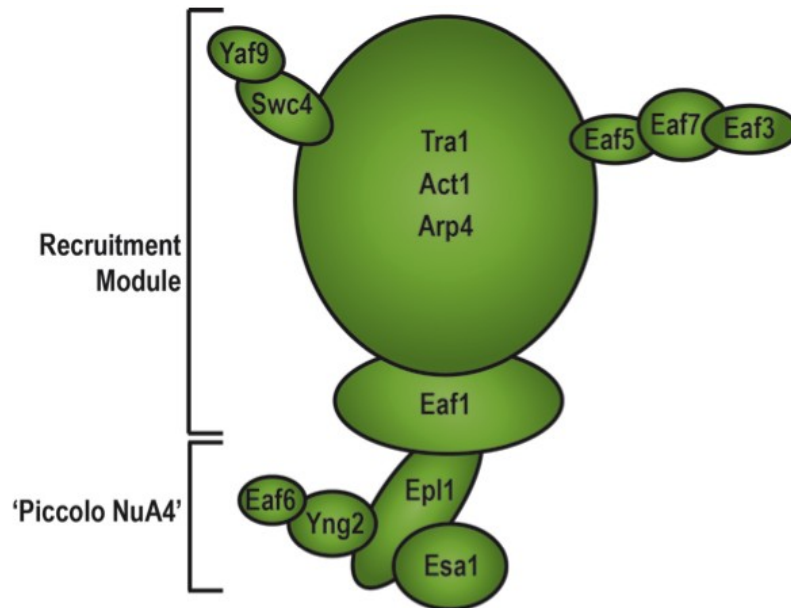


Figure 1.7: Schematic of the NuA4 lysine acetyltransferase enzyme complex.

The catalytic module, also known as Piccolo NuA4, is composed of Yng2, Epl1, Eaf6, and the catalytic subunit Esa1. The recruitment module contains Arp4, Act1, Eaf1, Eaf3, Eaf5, Eaf7, Yaf9, Swc4, and Tra1, and is hypothesized to target the complex to specific genomic loci. Analysis of physical interdependencies between subunits suggests Swc4 bridges the interaction between the Yaf9 and NuA4 (13, 109); Eaf3 and Eaf7 associate through Eaf5 (4, 72); Esa1 and Yng2 interact independently with Epl1 (15); Eaf6 interacts through Yng2 (72); and finally Eaf1 serves as a molecular platform upon which complex assembly depends (4, 72).

recruitment sub-complex is composed of the remaining ten subunits and has been proposed to target NuA4 to specific loci necessary to mediate its varied functions (15). Notably, PicNuA4 exists independently from NuA4 in wild type yeast cells as an acetyltransferase-competent protein complex that has been proposed to globally and non-specifically acetylate histones (15).

Importantly, many of NuA4's subunits participate in additional protein complexes *in vivo* (Table 1.2). This includes Eaf3 as part of the lysine deacetyltransferase (KDAC) complex Rpd3; Eaf6 in the histone H3-specific KAT complex NuA3; Swc4, Yaf9, Act1, and Arp4 in the chromatin re-modelling complex SWR; and finally Act1 and Arp4 in the Ino80 complex. Moreover, Act1 serves as the cytoskeletal structural molecule actin in yeast. Therefore, phenotypes or interactions associated with any of these individual subunits may not derive specifically from their role in the NuA4 complex.

1.3.2 KAT activity of NuA4

The KAT activity of NuA4 is housed within the catalytic subunit Esa1. Esa1 acetylates free histone proteins H4, H2A, and H3 *in vitro* (21, 89), but its activity on nucleosome substrates is dependent on inclusion in either NuA4 (1) or PicNuA4 (15). In the context of either complex, Esa1 predominantly acetylates histone H4, and to a lesser extent H2A both *in vivo* and *in vitro* (15). This work suggested that NuA4 subunits modulate the activity of Esa1 *in vivo* and provide substrate specificity, a property shared with many KAT enzymes (56). In addition to its core nucleosomal histone targets, more recently NuA4 has been shown to acetylate the histone H2A variant Htz1 *in vivo* (6, 47, 67, 68).

Encoded by an essential gene, the study of Esa1's KAT activity *in vivo* has relied almost exclusively on the creation of temperature sensitive mutant alleles. Biochemical characterization of the encoded mutant proteins revealed an inability to acetylate histone H4 *in vivo* or *in vitro*, indicating a loss of catalytic activity and suggesting the essential function of Esa1 to be its acetyltransferase activity (12, 21, 27). Importantly, deleting or mutating other genes encoding NuA4 subunits results in a similar global reduction in H4 acetylation *in vivo* (Figure 1.8), supporting the hypothesis that NuA4 subunits modulate Esa1's target specificity *in vivo*. These mutants include the deletions of the non-essential genes *EAF1* and *YNG2* (6, 47, 52), which can therefore serve as practical tools to study the loss of Esa1-mediated lysine acetylation *in vivo*.

Deciphering the catalytic mechanism of Esa1 has proven controversial. Initial characterization of a partial crystal structure of Esa1 in complex with coenzyme A suggested a 'ping-pong' mechanism involving a Cys304-dependent acetyl-enzyme intermediate (106, 107). However, Cys304 has since been shown to be dispensable for catalytic activity *in vivo* (10), and a mechanism utilizing an Esa1-acetyl-CoA-histone ternary complex was proposed. While the exact mechanism has yet to be deciphered, catalysis is believed to rely on Glu338, which functions as a general base in the reaction. Indeed, mutations at this position result in loss of activity of Esa1 on histone proteins *in vitro* (10, 106). Intriguingly, yeast cells harbouring the mutation *esa1-E338Q* have negligible levels of histone H4 acetylation *in vivo*, yet these cells are viable (albeit barely

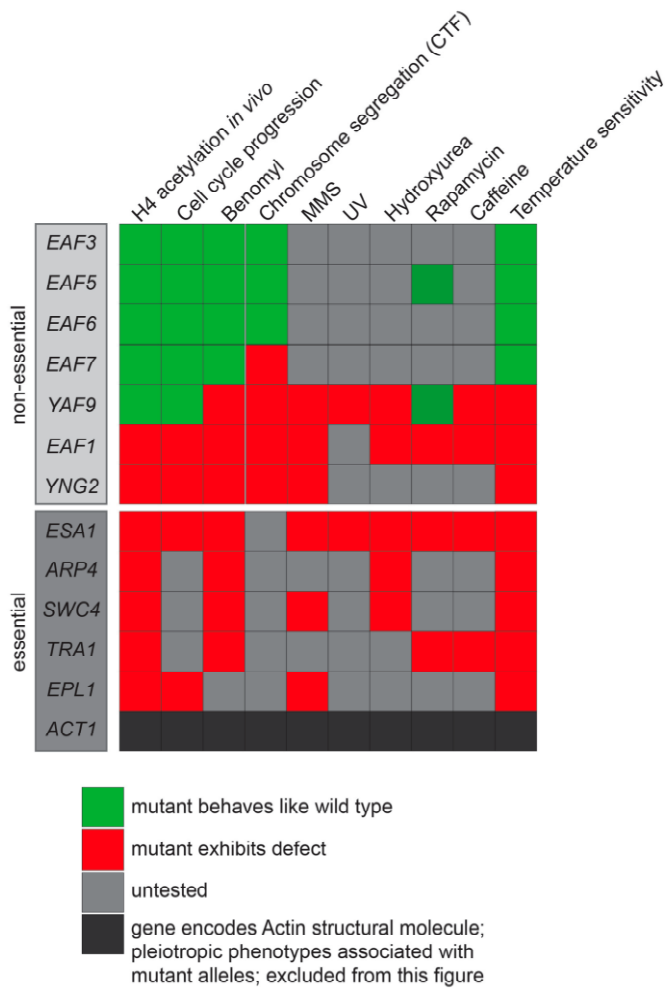


Figure 1.8: NuA4 mutant phenotypes.

Published phenotypes of non-essential and essential NuA4 genes are presented. All references are presented in the text.

so), a result that calls into question whether the essential function of *ESA1* is its KAT activity (27).

1.3.3 Functional insight from analyses of individual NuA4 mutants

The subunit composition is one of the most thoroughly understood aspects of NuA4. Accordingly, characterization of individual NuA4 mutants has offered important insight into the function of the complex (Figure 1.8). For instance, multiple NuA4 mutants exhibit a cell cycle arrest in G2/M, suggesting a role for the complex in cell cycle progression (4, 15, 20, 21). Moreover, that many NuA4 mutants also are hypersensitive to DNA damaging agents such as methyl methanesulfate (MMS) (4, 15, 27, 69, 75, 109) and ultraviolet radiation (UV) (27, 109) suggests the complex regulates DNA damage repair. Another intriguing link has been made between NuA4 function and chromosome stability, as many mutants are sensitive to the microtubule-destabilizing drug Benomyl (27, 51, 52, 55, 69, 76, 102) and exhibit chromosome transmission fidelity defects (52). Moreover, hypersensitivity of NuA4 mutants to a variety of stress-inducing conditions such as high temperature (21, 27, 60, 62, 69, 74, 76, 102, 109), rapamycin (4, 15, 27, 60, 74), hydroxyurea (27, 51, 69, 76, 102, 109), and caffeine (51, 62, 109) indicate pleiotropic roles for NuA4 *in vivo*.

The extensive phenotypic characterization outlined above has highlighted an interesting divide amongst NuA4 subunits, specifically that a subset of mutants share almost none of the chemical sensitivities or phenotypes that have been tested to date; this includes the genes encoding the non-essential subunits Eaf3, Eaf5, Eaf6, and Eaf7. From this, it is clear that NuA4 subunits have differential

roles within the complex and that simple phenotypic analysis is not powerful enough to dissect these roles. Importantly, twelve of the thirteen NuA4 subunits are conserved in orthologous NuA4 complexes in a variety of species, which indicates a functionally important and conserved role for each subunit (Table 1.2).

1.3.4 NuA4 cellular processes

Phenotypic analysis of NuA4 mutants, as outlined above, has shed light on the significant impact of NuA4 on the maintenance of genome stability through cellular processes such as DNA damage repair, cell cycle control, and chromosome stability. Importantly, disruption of NuA4 catalytic activity, assessed by loss of global H4 acetylation *in vivo*, correlates with many of its described phenotypes, suggesting NuA4's cellular functions may largely depend on acetyltransferase activity (Figure 1.8) (15, 21, 27, 51, 52, 95). One hypothesis to explain NuA4's pleiotropic cellular effects is that through the acetylation of histone proteins, NuA4-dependent gene transcription can regulate a myriad of cellular processes. Indeed, NuA4 regulates the transcription of a few specific sets of genes, however, microarray analysis suggests the complex does not significantly contribute to global transcriptional regulation (see below). In fact, NuA4 function has been demonstrated to effectively mediate DNA damage repair and gluconeogenesis through non-transcriptionally mediated pathways (see below). Of utmost importance is to define the mechanism(s) of action and pathways in which NuA4 functions *in vivo*. Below I will describe the established pathways in which NuA4 functions, all of which rely on the KAT activity of the complex.

1.3.4.1 Transcription

The first identified cellular role for NuA4 was that of a transcriptional regulator through histone acetylation. Historically, histone acetylation has been associated with transcriptional upregulation as alterations in chromatin structure associated with this modification can increase the accessibility of DNA and/or serve as a docking site to attract transcriptional accessory proteins (71). Indeed, the ability of NuA4 to remodel nucleosomes (92) and to stimulate transcription from a nucleosomal array in an acetyltransferase-dependent manner *in vitro* has been demonstrated (42, 101). Two specific sets of genes are under the control of NuA4, including ribosomal genes and a subset of stress-responsive genes. Specifically, NuA4 localization and histone H4 acetylation at ribosomal gene promoters positively regulates the expression of rDNA (82, 84), and NuA4 negatively regulates stress-responsive genes under normal conditions when their expression should be low (60, 72). However, microarray analysis, globally assessing gene expression in various NuA4 mutant backgrounds, has indicated the role of NuA4 in the transcription to be fairly minor (20, 52, 55, 109). Together this work suggests NuA4 is not a direct master transcriptional regulator in yeast, but rather functions through additional cellular processes.

1.3.4.2 DNA damage repair

Temperature sensitive mutant alleles of *ESA1* are defective in cell cycle progression and exhibit a Rad9-dependent G2/M arrest (21). As Rad9 is a known component of the DNA damage response, this suggested a role for *Esa1* in maintaining the integrity of genomic DNA in response to DNA damage. Moreover,

given that Rad9-dependent cell cycle arrest is a phenotype shared with unacetylatable histone H4 mutants (65, 66), this indicated the role of Esa1 in DNA damage repair likely relied on histone H4 acetylation. Additional evidence linking the NuA4 complex to DNA repair is that multiple subunits are sensitive to DNA damaging agents such as MMS as outlined above (4, 15, 27, 69, 75, 109) and that multiple NuA4 genes demonstrate synthetic sick (SS) or synthetic lethal (SL) genetic interactions with genes involved in the DNA damage response (19, 72). A direct role for NuA4-mediated histone acetylation has indeed been established in the DNA damage response through the acetylation of histone H4 around double strand breaks (12). NuA4 has been detected at sites of double strand breaks, whereby its recruitment/retention is mediated by the Arp4 subunit, which recognizes phosphorylated H2A around the break site. More recently, a single acetylation site on Yng2 at K170 has been linked to the role of NuA4 KAT activity in DNA damage repair (59). Esa1-dependent acetylation of this residue inhibits proteasomal degradation of Yng2 (59). Upon deacetylation and degradation of Yng2, the other two PicNuA4 subunits, Esa1 and Epl1, are evicted from sites of DNA damage, thereby linking the acetylation of Yng2 K170 specifically to the process of DNA damage repair (59). Moreover this work demonstrates that NuA4 may act in a pathway through both histone and non-histone acetylation.

1.3.4.3 Gluconeogenesis

NuA4 has been linked to metabolism in yeast via acetylation of the key gluconeogenesis regulator Pck1, as well as several additional enzymes or effectors involved in signalling pathways responsive to nutrient availability and energy status

(Atg3, Gph1, Atg11, Sip2, Sip5, Tap42) (58). The intersection between cellular metabolism and protein (de)acetylation is generally reflected in their shared dependency on the key metabolic intermediates acetyl coenzyme A and NAD⁺, the latter serving as a co-factor in sirtuin-mediated deacetylation reactions. Further, the fact that a large proportion of metabolic enzymes are themselves acetylated in both prokaryotic and eukaryotic systems (18, 48, 103, 111, 112), suggests a direct and conserved role for reversible acetylation in regulating a multitude of metabolic processes. In the case of Pck1, which encodes phosphoenolpyruvate carboxykinase and catalyzes the rate-limiting step in gluconeogenesis, NuA4 KAT activity has no effect on *PCK1* mRNA levels, Pck1 protein levels, or localization of Pck1, but rather impacts Pck1 enzymatic activity. It was discovered that NuA4-dependent acetylation of Lys514 on Pck1 is crucial to maintain enzyme function and confer the ability of yeast to grow on non-fermentable carbon sources (58). It was recently reported that the human homolog of Pck1 is also acetylated, however in human cells the modification has been implicated in regulating stability of the protein *in vivo* (112). While the *in vivo* acetylation status of each of Atg3, Gph1, Atg11, Sip2, Sip5, or Tap42 was found to depend on Esa1 catalytic activity, neither the biological consequences nor the acetylated residues on these proteins were identified. However, taken together, this work suggests NuA4 acetyltransferase activity may regulate many different metabolic pathways.

1.4 Hypothesis and aims

We hypothesized that NuA4 function impacts a diverse array of cellular processes through the acetylation of non-histone targets. Using systems biological

approaches, the four main questions addressed in this thesis are: (i) What are the functional roles of the individual subunits within the complex; (ii) Does NuA4 impact additional cellular processes outside of those identified through phenotypic analysis; (iii) In what specific pathways does NuA4 function; and (iv) Does NuA4 have additional, non-histone acetylation substrates?

1.5 References

1. **Allard, S., R. T. Utley, J. Savard, A. Clarke, P. Grant, C. J. Brandl, L. Pillus, J. L. Workman, and J. Cote.** 1999. NuA4, an essential transcription adaptor/histone H4 acetyltransferase complex containing Esa1p and the ATM-related cofactor Tra1p. *Embo J* **18**:5108-5119.
2. **Allis, C. D., S. L. Berger, J. Cote, S. Dent, T. Jenuwien, T. Kouzarides, L. Pillus, D. Reinberg, Y. Shi, R. Shiekhatar, A. Shilatifard, J. Workman, and Y. Zhang.** 2007. New nomenclature for chromatin-modifying enzymes. *Cell* **131**:633-636.
3. **Arif, M., P. Senapati, J. Shandilya, and T. K. Kundu.** 2010. Protein lysine acetylation in cellular function and its role in cancer manifestation. *Biochim Biophys Acta*.
4. **Auger, A., L. Galarneau, M. Altaf, A. Nourani, Y. Doyon, R. T. Utley, D. Cronier, S. Allard, and J. Cote.** 2008. Eaf1 is the platform for NuA4 molecular assembly that evolutionarily links chromatin acetylation to ATP-dependent exchange of histone H2A variants. *Mol Cell Biol* **28**:2257-2270.
5. **Avvakumov, N., and J. Cote.** 2007. The MYST family of histone acetyltransferases and their intimate links to cancer. *Oncogene* **26**:5395-5407.
6. **Babiarz, J. E., J. E. Halley, and J. Rine.** 2006. Telomeric heterochromatin boundaries require NuA4-dependent acetylation of histone variant H2A.Z in *Saccharomyces cerevisiae*. *Genes Dev* **20**:700-710.
7. **Baetz, K., V. Measday, and B. Andrews.** 2006. Revealing hidden relationships among yeast genes involved in chromosome segregation using systematic synthetic lethal and synthetic dosage lethal screens. *Cell Cycle* **5**:592-595.
8. **Baker, S. P., and P. A. Grant.** 2007. The SAGA continues: expanding the cellular role of a transcriptional co-activator complex. *Oncogene* **26**:5329-5340.
9. **Basu, A., K. L. Rose, J. Zhang, R. C. Beavis, B. Ueberheide, B. A. Garcia, B. Chait, Y. Zhao, D. F. Hunt, E. Segal, C. D. Allis, and S. B. Hake.** 2009. Proteome-wide prediction of acetylation substrates. *Proc Natl Acad Sci U S A* **106**:13785-13790.
10. **Berndsen, C. E., B. N. Albaugh, S. Tan, and J. M. Denu.** 2007. Catalytic mechanism of a MYST family histone acetyltransferase. *Biochemistry* **46**:623-629.
11. **Bertrand, P.** 2010. Inside HDAC with HDAC inhibitors. *Eur J Med Chem* **45**:2095-2116.

12. **Bird, A. W., D. Y. Yu, M. G. Pray-Grant, Q. Qiu, K. E. Harmon, P. C. Megee, P. A. Grant, M. M. Smith, and M. F. Christman.** 2002. Acetylation of histone H4 by Esa1 is required for DNA double-strand break repair. *Nature* **419**:411-415.
13. **Bittner, C. B., D. T. Zeisig, B. B. Zeisig, and R. K. Slany.** 2004. Direct physical and functional interaction of the NuA4 complex components Yaf9p and Swc4p. *Eukaryot Cell* **3**:976-983.
14. **Blander, G., N. Zalle, Y. Daniely, J. Taplick, M. D. Gray, and M. Oren.** 2002. DNA damage-induced translocation of the Werner helicase is regulated by acetylation. *J Biol Chem* **277**:50934-50940.
15. **Boudreault, A. A., D. Cronier, W. Selleck, N. Lacoste, R. T. Utley, S. Allard, J. Savard, W. S. Lane, S. Tan, and J. Cote.** 2003. Yeast enhancer of polycomb defines global Esa1-dependent acetylation of chromatin. *Genes Dev* **17**:1415-1428.
16. **Cao, X., and T. C. Sudhof.** 2001. A transcriptionally [correction of transcriptively] active complex of APP with Fe65 and histone acetyltransferase Tip60. *Science* **293**:115-120.
17. **Ceol, C. J., and H. R. Horvitz.** 2004. A new class of *C. elegans* synMuv genes implicates a Tip60/NuA4-like HAT complex as a negative regulator of Ras signaling. *Dev Cell* **6**:563-576.
18. **Choudhary, C., C. Kumar, F. Gnad, M. L. Nielsen, M. Rehman, T. C. Walther, J. V. Olsen, and M. Mann.** 2009. Lysine acetylation targets protein complexes and co-regulates major cellular functions. *Science* **325**:834-840.
19. **Choy, J. S., and S. J. Kron.** 2002. NuA4 subunit Yng2 function in intra-S-phase DNA damage response. *Mol Cell Biol* **22**:8215-8225.
20. **Choy, J. S., B. T. Tobe, J. H. Huh, and S. J. Kron.** 2001. Yng2p-dependent NuA4 histone H4 acetylation activity is required for mitotic and meiotic progression. *J Biol Chem* **276**:43653-43662.
21. **Clarke, A. S., J. E. Lowell, S. J. Jacobson, and L. Pillus.** 1999. Esa1p is an essential histone acetyltransferase required for cell cycle progression. *Mol Cell Biol* **19**:2515-2526.
22. **Close, P., C. Creppe, M. Gillard, A. Ladang, J. P. Chapelle, L. Nguyen, and A. Chariot.** 2010. The emerging role of lysine acetylation of non-nuclear proteins. *Cell Mol Life Sci* **67**:1255-1264.
23. **Col, E., C. Caron, C. Chable-Bessia, G. Legube, S. Gazzeri, Y. Komatsu, M. Yoshida, M. Benkirane, D. Trouche, and S. Khochbin.** 2005. HIV-1 Tat targets Tip60 to impair the apoptotic cell response to genotoxic stresses. *EMBO J* **24**:2634-2645.
24. **Collins, S. R., K. M. Miller, N. L. Maas, A. Roguev, J. Fillingham, C. S. Chu, M. Schuldiner, M. Gebbia, J. Recht, M. Shales, H. Ding, H. Xu, J.**

- Han, K. Ingvarsdottir, B. Cheng, B. Andrews, C. Boone, S. L. Berger, P. Hieter, Z. Zhang, G. W. Brown, C. J. Ingles, A. Emili, C. D. Allis, D. P. Toczyski, J. S. Weissman, J. F. Greenblatt, and N. J. Krogan. 2007. Functional dissection of protein complexes involved in yeast chromosome biology using a genetic interaction map. *Nature* **446**:806-810.
25. Costanzo, M., A. Baryshnikova, J. Bellay, Y. Kim, E. D. Spear, C. S. Sevier, H. Ding, J. L. Koh, K. Toufighi, S. Mostafavi, J. Prinz, R. P. St Onge, B. VanderSluis, T. Makhnevych, F. J. Vizeacoumar, S. Alizadeh, S. Bahr, R. L. Brost, Y. Chen, M. Cokol, R. Deshpande, Z. Li, Z. Y. Lin, W. Liang, M. Marback, J. Paw, B. J. San Luis, E. Shuteriqi, A. H. Tong, N. van Dyk, I. M. Wallace, J. A. Whitney, M. T. Weirauch, G. Zhong, H. Zhu, W. A. Houry, M. Brudno, S. Ragibzadeh, B. Papp, C. Pal, F. P. Roth, G. Giaever, C. Nislow, O. G. Troyanskaya, H. Bussey, G. D. Bader, A. C. Gingras, Q. D. Morris, P. M. Kim, C. A. Kaiser, C. L. Myers, B. J. Andrews, and C. Boone. 2010. The genetic landscape of a cell. *Science* **327**:425-431.
 26. Creaven, M., F. Hans, V. Mutskov, E. Col, C. Caron, S. Dimitrov, and S. Khochbin. 1999. Control of the histone-acetyltransferase activity of Tip60 by the HIV-1 transactivator protein, Tat. *Biochemistry* **38**:8826-8830.
 27. Decker, P. V., D. Y. Yu, M. Iizuka, Q. Qiu, and M. M. Smith. 2008. Catalytic-site mutations in the MYST family histone Acetyltransferase Esa1. *Genetics* **178**:1209-1220.
 28. Dietz, K. C., and P. Casaccia. 2010. HDAC inhibitors and neurodegeneration: at the edge between protection and damage. *Pharmacol Res* **62**:11-17.
 29. Doyon, Y., and J. Cote. 2004. The highly conserved and multifunctional NuA4 HAT complex. *Curr Opin Genet Dev* **14**:147-154.
 30. Doyon, Y., W. Selleck, W. S. Lane, S. Tan, and J. Cote. 2004. Structural and functional conservation of the NuA4 histone acetyltransferase complex from yeast to humans. *Mol Cell Biol* **24**:1884-1896.
 31. Durant, M., and B. F. Pugh. 2006. Genome-wide relationships between TAF1 and histone acetyltransferases in *Saccharomyces cerevisiae*. *Mol Cell Biol* **26**:2791-2802.
 32. Eisen, A., R. T. Utley, A. Nourani, S. Allard, P. Schmidt, W. S. Lane, J. C. Lucchesi, and J. Cote. 2001. The yeast NuA4 and *Drosophila* MSL complexes contain homologous subunits important for transcription regulation. *J Biol Chem* **276**:3484-3491.
 33. Eriksson, P. R., G. Mendiratta, N. B. McLaughlin, T. G. Wolfsberg, L. Marino-Ramirez, T. A. Pompa, M. Jainerin, D. Landsman, C. H. Shen, and D. J. Clark. 2005. Global regulation by the yeast Spt10 protein is mediated through chromatin structure and the histone upstream activating sequence elements. *Mol Cell Biol* **25**:9127-9137.

34. **Galarneau, L., A. Nourani, A. A. Boudreault, Y. Zhang, L. Heliot, S. Allard, J. Savard, W. S. Lane, D. J. Stillman, and J. Cote.** 2000. Multiple links between the NuA4 histone acetyltransferase complex and epigenetic control of transcription. *Mol Cell* **5**:927-937.
35. **Gavin, A. C., P. Aloy, P. Grandi, R. Krause, M. Boesche, M. Marzioch, C. Rau, L. J. Jensen, S. Bastuck, B. Dumpelfeld, A. Edlmann, M. A. Heurtier, V. Hoffman, C. Hoefert, K. Klein, M. Hudak, A. M. Michon, M. Schelder, M. Schirle, M. Remor, T. Rudi, S. Hooper, A. Bauer, T. Bouwmeester, G. Casari, G. Drewes, G. Neubauer, J. M. Rick, B. Kuster, P. Bork, R. B. Russell, and G. Superti-Furga.** 2006. Proteome survey reveals modularity of the yeast cell machinery. *Nature* **440**:631-636.
36. **Gavin, A. C., M. Bosche, R. Krause, P. Grandi, M. Marzioch, A. Bauer, J. Schultz, J. M. Rick, A. M. Michon, C. M. Cruciat, M. Remor, C. Hofert, M. Schelder, M. Brajenovic, H. Ruffner, A. Merino, K. Klein, M. Hudak, D. Dickson, T. Rudi, V. Gnau, A. Bauch, S. Bastuck, B. Huhse, C. Leutwein, M. A. Heurtier, R. R. Copley, A. Edlmann, E. Querfurth, V. Rybin, G. Drewes, M. Raida, T. Bouwmeester, P. Bork, B. Seraphin, B. Kuster, G. Neubauer, and G. Superti-Furga.** 2002. Functional organization of the yeast proteome by systematic analysis of protein complexes. *Nature* **415**:141-147.
37. **Ghaemmaghami, S., W. K. Huh, K. Bower, R. W. Howson, A. Belle, N. Dephoure, E. K. O'Shea, and J. S. Weissman.** 2003. Global analysis of protein expression in yeast. *Nature* **425**:737-741.
38. **Giandomenico, V., M. Simonsson, E. Gronroos, and J. Ericsson.** 2003. Coactivator-dependent acetylation stabilizes members of the SREBP family of transcription factors. *Mol Cell Biol* **23**:2587-2599.
39. **Grant, P. A., L. Duggan, J. Cote, S. M. Roberts, J. E. Brownell, R. Candau, R. Ohba, T. Owen-Hughes, C. D. Allis, F. Winston, S. L. Berger, and J. L. Workman.** 1997. Yeast Gcn5 functions in two multisubunit complexes to acetylate nucleosomal histones: characterization of an Ada complex and the SAGA (Spt/Ada) complex. *Genes Dev* **11**:1640-1650.
40. **Ho, Y., A. Gruhler, A. Heilbut, G. D. Bader, L. Moore, S. L. Adams, A. Millar, P. Taylor, K. Bennett, K. Boutilier, L. Yang, C. Wolting, I. Donaldson, S. Schandorff, J. Shewnarane, M. Vo, J. Taggart, M. Goudreault, B. Muskat, C. Alfarano, D. Dewar, Z. Lin, K. Michalickova, A. R. Willems, H. Sassi, P. A. Nielsen, K. J. Rasmussen, J. R. Andersen, L. E. Johansen, L. H. Hansen, H. Jespersen, A. Podtelejnikov, E. Nielsen, J. Crawford, V. Poulsen, B. D. Sorensen, J. Matthiesen, R. C. Hendrickson, F. Gleeson, T. Pawson, M. F. Moran, D. Durocher, M. Mann, C. W. Hogue, D. Figeys, and M. Tyers.** 2002. Systematic identification of protein complexes in *Saccharomyces cerevisiae* by mass spectrometry. *Nature* **415**:180-183.

41. **Huh, W. K., J. V. Falvo, L. C. Gerke, A. S. Carroll, R. W. Howson, J. S. Weissman, and E. K. O'Shea.** 2003. Global analysis of protein localization in budding yeast. *Nature* **425**:686-691.
42. **Ikeda, K., D. J. Steger, A. Eberharter, and J. L. Workman.** 1999. Activation domain-specific and general transcription stimulation by native histone acetyltransferase complexes. *Mol Cell Biol* **19**:855-863.
43. **Ito, K., C. E. Charron, and I. M. Adcock.** 2007. Impact of protein acetylation in inflammatory lung diseases. *Pharmacol Ther* **116**:249-265.
44. **Ito, T., T. Chiba, R. Ozawa, M. Yoshida, M. Hattori, and Y. Sakaki.** 2001. A comprehensive two-hybrid analysis to explore the yeast protein interactome. *Proc Natl Acad Sci U S A* **98**:4569-4574.
45. **John, S., L. Howe, S. T. Tafrov, P. A. Grant, R. Sternglanz, and J. L. Workman.** 2000. The something about silencing protein, Sas3, is the catalytic subunit of NuA3, a γ TAF(II)30-containing HAT complex that interacts with the Spt16 subunit of the yeast CP (Cdc68/Pob3)-FACT complex. *Genes Dev* **14**:1196-1208.
46. **Kawaguchi, Y., A. Ito, E. Appella, and T. P. Yao.** 2006. Charge modification at multiple C-terminal lysine residues regulates p53 oligomerization and its nucleus-cytoplasm trafficking. *J Biol Chem* **281**:1394-1400.
47. **Keogh, M. C., T. A. Mennella, C. Sawa, S. Berthelet, N. J. Krogan, A. Wolek, V. Podolny, L. R. Carpenter, J. F. Greenblatt, K. Baetz, and S. Buratowski.** 2006. The *Saccharomyces cerevisiae* histone H2A variant Htz1 is acetylated by NuA4. *Genes Dev* **20**:660-665.
48. **Kim, S. C., R. Sprung, Y. Chen, Y. Xu, H. Ball, J. Pei, T. Cheng, Y. Kho, H. Xiao, L. Xiao, N. V. Grishin, M. White, X. J. Yang, and Y. Zhao.** 2006. Substrate and functional diversity of lysine acetylation revealed by a proteomics survey. *Mol Cell* **23**:607-618.
49. **Kimura, A., and M. Horikoshi.** 1998. Tip60 acetylates six lysines of a specific class in core histones in vitro. *Genes Cells* **3**:789-800.
50. **Kinoshita, A., C. M. Whelan, O. Berezovska, and B. T. Hyman.** 2002. The gamma secretase-generated carboxyl-terminal domain of the amyloid precursor protein induces apoptosis via Tip60 in H4 cells. *J Biol Chem* **277**:28530-28536.
51. **Kobor, M. S., S. Venkatasubrahmanyam, M. D. Meneghini, J. W. Gin, J. L. Jennings, A. J. Link, H. D. Madhani, and J. Rine.** 2004. A Protein Complex Containing the Conserved Swi2/Snf2-Related ATPase Swr1p Deposits Histone Variant H2A.Z into Euchromatin. *PLoS Biol* **2**:E131.
52. **Krogan, N. J., K. Baetz, M. C. Keogh, N. Datta, C. Sawa, T. C. Kwok, N. J. Thompson, M. G. Davey, J. Pootoolal, T. R. Hughes, A. Emili, S. Buratowski, P. Hieter, and J. F. Greenblatt.** 2004. Regulation of chromosome stability by the histone H2A variant Htz1, the Swr1 chromatin

- remodeling complex, and the histone acetyltransferase NuA4. *Proc Natl Acad Sci U S A*.
53. **Krogan, N. J., G. Cagney, H. Yu, G. Zhong, X. Guo, A. Ignatchenko, J. Li, S. Pu, N. Datta, A. P. Tikuisis, T. Punna, J. M. Peregrin-Alvarez, M. Shales, X. Zhang, M. Davey, M. D. Robinson, A. Paccanaro, J. E. Bray, A. Sheung, B. Beattie, D. P. Richards, V. Canadien, A. Lalev, F. Mena, P. Wong, A. Starostine, M. M. Canete, J. Vlasblom, S. Wu, C. Orsi, S. R. Collins, S. Chandran, R. Haw, J. J. Rilstone, K. Gandi, N. J. Thompson, G. Musso, P. St Onge, S. Ghanny, M. H. Lam, G. Butland, A. M. Altaf-Ul, S. Kanaya, A. Shilatifard, E. O'Shea, J. S. Weissman, C. J. Ingles, T. R. Hughes, J. Parkinson, M. Gerstein, S. J. Wodak, A. Emili, and J. F. Greenblatt.** 2006. Global landscape of protein complexes in the yeast *Saccharomyces cerevisiae*. *Nature* **440**:637-643.
 54. **Kusch, T., L. Florens, W. H. Macdonald, S. K. Swanson, R. L. Glaser, J. R. Yates, 3rd, S. M. Abmayr, M. P. Washburn, and J. L. Workman.** 2004. Acetylation by Tip60 is required for selective histone variant exchange at DNA lesions. *Science* **306**:2084-2087.
 55. **Le Masson, I., D. Y. Yu, K. Jensen, A. Chevalier, R. Courbeyrette, Y. Boulard, M. M. Smith, and C. Mann.** 2003. Yaf9, a novel NuA4 histone acetyltransferase subunit, is required for the cellular response to spindle stress in yeast. *Mol Cell Biol* **23**:6086-6102.
 56. **Lee, K. K., and J. L. Workman.** 2007. Histone acetyltransferase complexes: one size doesn't fit all. *Nat Rev Mol Cell Biol* **8**:284-295.
 57. **Lehner, B., C. Crombie, J. Tischler, A. Fortunato, and A. G. Fraser.** 2006. Systematic mapping of genetic interactions in *Caenorhabditis elegans* identifies common modifiers of diverse signaling pathways. *Nat Genet* **38**:896-903.
 58. **Lin, Y. Y., J. Y. Lu, J. Zhang, W. Walter, W. Dang, J. Wan, S. C. Tao, J. Qian, Y. Zhao, J. D. Boeke, S. L. Berger, and H. Zhu.** 2009. Protein acetylation microarray reveals that NuA4 controls key metabolic target regulating gluconeogenesis. *Cell* **136**:1073-1084.
 59. **Lin, Y. Y., Y. Qi, J. Y. Lu, X. Pan, D. S. Yuan, Y. Zhao, J. S. Bader, and J. D. Boeke.** 2008. A comprehensive synthetic genetic interaction network governing yeast histone acetylation and deacetylation. *Genes Dev* **22**:2062-2074.
 60. **Lindstrom, K. C., J. C. Vary, Jr., M. R. Parthun, J. Delrow, and T. Tsukiyama.** 2006. Isw1 functions in parallel with the NuA4 and Swr1 complexes in stress-induced gene repression. *Mol Cell Biol* **26**:6117-6129.
 61. **Liu, C., D. van Dyk, Y. Li, B. Andrews, and H. Rao.** 2009. A genome-wide synthetic dosage lethality screen reveals multiple pathways that require the functioning of ubiquitin-binding proteins Rad23 and Dsk2. *BMC Biol* **7**:75.

62. **Loewith, R., M. Meijer, S. P. Lees-Miller, K. Riabowol, and D. Young.** 2000. Three yeast proteins related to the human candidate tumor suppressor p33(ING1) are associated with histone acetyltransferase activities. *Mol Cell Biol* **20**:3807-3816.
63. **Lu, Z., I. Scott, B. R. Webster, and M. N. Sack.** 2009. The emerging characterization of lysine residue deacetylation on the modulation of mitochondrial function and cardiovascular biology. *Circ Res* **105**:830-841.
64. **Luger, K., A. W. Mader, R. K. Richmond, D. F. Sargent, and T. J. Richmond.** 1997. Crystal structure of the nucleosome core particle at 2.8 Å resolution. *Nature* **389**:251-260.
65. **Megee, P. C., B. A. Morgan, B. A. Mittman, and M. M. Smith.** 1990. Genetic analysis of histone H4: essential role of lysines subject to reversible acetylation. *Science* **247**:841-845.
66. **Megee, P. C., B. A. Morgan, and M. M. Smith.** 1995. Histone H4 and the maintenance of genome integrity. *Genes Dev* **9**:1716-1727.
67. **Mehta, M., H. Braberg, S. Wang, A. Lozsa, M. Shales, A. Solache, N. J. Krogan, and M. C. Keogh.** 2010. Individual lysine acetylations on the N-terminus of *S. Cerevisiae* H2A.Z are highly but not differentially regulated. *J Biol Chem*.
68. **Meneghini, M. D., M. Wu, and H. D. Madhani.** 2003. Conserved histone variant H2A.Z protects euchromatin from the ectopic spread of silent heterochromatin. *Cell* **112**:725-736.
69. **Micialkiewicz, A., and A. Chelstowska.** 2008. The essential function of Swc4p - a protein shared by two chromatin-modifying complexes of the yeast *Saccharomyces cerevisiae* - resides within its N-terminal part. *Acta Biochim Pol* **55**:603-612.
70. **Miller, M. L., and N. Blom.** 2009. Kinase-specific prediction of protein phosphorylation sites. *Methods Mol Biol* **527**:299-310, x.
71. **Minard, M. E., A. K. Jain, and M. C. Barton.** 2009. Analysis of epigenetic alterations to chromatin during development. *Genesis* **47**:559-572.
72. **Mitchell, L., J. P. Lambert, M. Gerdes, A. S. Al-Madhoun, I. S. Skerjanc, D. Figeys, and K. Baetz.** 2008. Functional dissection of the NuA4 histone acetyltransferase reveals its role as a genetic hub and that Eaf1 is essential for complex integrity. *Mol Cell Biol* **28**:2244-2256.
73. **Mujtaba, S., Y. He, L. Zeng, S. Yan, O. Plotnikova, Sachchidanand, R. Sanchez, N. J. Zeleznik-Le, Z. Ronai, and M. M. Zhou.** 2004. Structural mechanism of the bromodomain of the coactivator CBP in p53 transcriptional activation. *Mol Cell* **13**:251-263.
74. **Mutiu, A. I., S. M. Hoke, J. Genereaux, C. Hannam, K. MacKenzie, O. Jobin-Robitaille, J. Guzzo, J. Cote, B. Andrews, D. B. Haniford, and C.**

- J. Brandl.** 2007. Structure/function analysis of the phosphatidylinositol-3-kinase domain of yeast tra1. *Genetics* **177**:151-166.
75. **Nourani, A., Y. Doyon, R. T. Utley, S. Allard, W. S. Lane, and J. Cote.** 2001. Role of an ING1 growth regulator in transcriptional activation and targeted histone acetylation by the NuA4 complex. *Mol Cell Biol* **21**:7629-7640.
76. **Ogiwara, H., A. Ui, S. Kawashima, K. Kugou, F. Onoda, H. Iwahashi, M. Harata, K. Ohta, T. Enomoto, and M. Seki.** 2007. Actin-related protein Arp4 functions in kinetochore assembly. *Nucleic Acids Res* **35**:3109-3117.
77. **Parthun, M. R.** 2007. Hat1: the emerging cellular roles of a type B histone acetyltransferase. *Oncogene* **26**:5319-5328.
78. **Patel, J. H., Y. Du, P. G. Ard, C. Phillips, B. Carella, C. J. Chen, C. Rakowski, C. Chatterjee, P. M. Lieberman, W. S. Lane, G. A. Blobel, and S. B. McMahon.** 2004. The c-MYC oncoprotein is a substrate of the acetyltransferases hGCN5/PCAF and TIP60. *Mol Cell Biol* **24**:10826-10834.
79. **Phillips, D. M.** 1963. The presence of acetyl groups of histones. *Biochem J* **87**:258-263.
80. **Piperno, G., and M. T. Fuller.** 1985. Monoclonal antibodies specific for an acetylated form of alpha-tubulin recognize the antigen in cilia and flagella from a variety of organisms. *J Cell Biol* **101**:2085-2094.
81. **Piperno, G., M. LeDizet, and X. J. Chang.** 1987. Microtubules containing acetylated alpha-tubulin in mammalian cells in culture. *J Cell Biol* **104**:289-302.
82. **Reid, J. L., V. R. Iyer, P. O. Brown, and K. Struhl.** 2000. Coordinate regulation of yeast ribosomal protein genes is associated with targeted recruitment of Esa1 histone acetylase. *Mol Cell* **6**:1297-1307.
83. **Rocheleau, C. E., K. Cullison, K. Huang, Y. Bernstein, A. C. Spilker, and M. V. Sundaram.** 2008. The *Caenorhabditis elegans* ekl (enhancer of ksr-1 lethality) genes include putative components of a germline small RNA pathway. *Genetics* **178**:1431-1443.
84. **Rohde, J. R., and M. E. Cardenas.** 2003. The tor pathway regulates gene expression by linking nutrient sensing to histone acetylation. *Mol Cell Biol* **23**:629-635.
85. **Roth, S. Y., J. M. Denu, and C. D. Allis.** 2001. Histone acetyltransferases. *Annu Rev Biochem* **70**:81-120.
86. **Schwer, B., B. J. North, R. A. Frye, M. Ott, and E. Verdin.** 2002. The human silent information regulator (Sir)2 homologue hSIRT3 is a mitochondrial nicotinamide adenine dinucleotide-dependent deacetylase. *J Cell Biol* **158**:647-657.
87. **Shahbazian, M. D., and M. Grunstein.** 2007. Functions of site-specific histone acetylation and deacetylation. *Annu Rev Biochem* **76**:75-100.

88. **Shia, W. J., S. Osada, L. Florens, S. K. Swanson, M. P. Washburn, and J. L. Workman.** 2005. Characterization of the yeast trimeric-SAS acetyltransferase complex. *J Biol Chem* **280**:11987-11994.
89. **Smith, E. R., A. Eisen, W. Gu, M. Sattah, A. Pannuti, J. Zhou, R. G. Cook, J. C. Lucchesi, and C. D. Allis.** 1998. ESA1 is a histone acetyltransferase that is essential for growth in yeast. *Proc Natl Acad Sci U S A* **95**:3561-3565.
90. **Sopko, R., D. Huang, N. Preston, G. Chua, B. Papp, K. Kafadar, M. Snyder, S. G. Oliver, M. Cyert, T. R. Hughes, C. Boone, and B. Andrews.** 2006. Mapping pathways and phenotypes by systematic gene overexpression. *Mol Cell* **21**:319-330.
91. **Spange, S., T. Wagner, T. Heinzl, and O. H. Kramer.** 2009. Acetylation of non-histone proteins modulates cellular signalling at multiple levels. *Int J Biochem Cell Biol* **41**:185-198.
92. **Steger, D. J., A. Eberharter, S. John, P. A. Grant, and J. L. Workman.** 1998. Purified histone acetyltransferase complexes stimulate HIV-1 transcription from preassembled nucleosomal arrays. *Proc Natl Acad Sci U S A* **95**:12924-12929.
93. **Sterner, D. E., and S. L. Berger.** 2000. Acetylation of histones and transcription-related factors. *Microbiol Mol Biol Rev* **64**:435-459.
94. **Sun, Y., X. Jiang, S. Chen, N. Fernandes, and B. D. Price.** 2005. A role for the Tip60 histone acetyltransferase in the acetylation and activation of ATM. *Proc Natl Acad Sci U S A* **102**:13182-13187.
95. **Sunada, R., I. Gorzer, Y. Oma, T. Yoshida, N. Suka, U. Wintersberger, and M. Harata.** 2005. The nuclear actin-related protein Act3p/Arp4p is involved in the dynamics of chromatin-modulating complexes. *Yeast* **22**:753-768.
96. **Sykes, S. M., H. S. Mellert, M. A. Holbert, K. Li, R. Marmorstein, W. S. Lane, and S. B. McMahon.** 2006. Acetylation of the p53 DNA-binding domain regulates apoptosis induction. *Mol Cell* **24**:841-851.
97. **Tang, Y., M. A. Holbert, H. Wurtele, K. Meeth, W. Rocha, M. Gharib, E. Jiang, P. Thibault, A. Verreault, P. A. Cole, and R. Marmorstein.** 2008. Fungal Rtt109 histone acetyltransferase is an unexpected structural homolog of metazoan p300/CBP. *Nat Struct Mol Biol* **15**:998.
98. **Tang, Y., J. Luo, W. Zhang, and W. Gu.** 2006. Tip60-dependent acetylation of p53 modulates the decision between cell-cycle arrest and apoptosis. *Mol Cell* **24**:827-839.
99. **Tong, A. H., M. Evangelista, A. B. Parsons, H. Xu, G. D. Bader, N. Page, M. Robinson, S. Raghizadeh, C. W. Hogue, H. Bussey, B. Andrews, M. Tyers, and C. Boone.** 2001. Systematic genetic analysis with ordered arrays of yeast deletion mutants. *Science* **294**:2364-2368.

100. **Uetz, P., L. Giot, G. Cagney, T. A. Mansfield, R. S. Judson, J. R. Knight, D. Lockshon, V. Narayan, M. Srinivasan, P. Pochart, A. Qureshi-Emili, Y. Li, B. Godwin, D. Conover, T. Kalbfleisch, G. Vijayadamodar, M. Yang, M. Johnston, S. Fields, and J. M. Rothberg.** 2000. A comprehensive analysis of protein-protein interactions in *Saccharomyces cerevisiae*. *Nature* **403**:623-627.
101. **Vignali, M., D. J. Steger, K. E. Neely, and J. L. Workman.** 2000. Distribution of acetylated histones resulting from Gal4-VP16 recruitment of SAGA and NuA4 complexes. *EMBO J* **19**:2629-2640.
102. **Wang, A. Y., J. M. Schulze, E. Skordalakes, J. W. Gin, J. M. Berger, J. Rine, and M. S. Kobor.** 2009. Asf1-like structure of the conserved Yaf9 YEATS domain and role in H2A.Z deposition and acetylation. *Proc Natl Acad Sci U S A* **106**:21573-21578.
103. **Wang, Q., Y. Zhang, C. Yang, H. Xiong, Y. Lin, J. Yao, H. Li, L. Xie, W. Zhao, Y. Yao, Z. B. Ning, R. Zeng, Y. Xiong, K. L. Guan, S. Zhao, and G. P. Zhao.** 2010. Acetylation of metabolic enzymes coordinates carbon source utilization and metabolic flux. *Science* **327**:1004-1007.
104. **Winzeler, E. A., D. D. Shoemaker, A. Astromoff, H. Liang, K. Anderson, B. Andre, R. Bangham, R. Benito, J. D. Boeke, H. Bussey, A. M. Chu, C. Connelly, K. Davis, F. Dietrich, S. W. Dow, M. El Bakkoury, F. Foury, S. H. Friend, E. Gentalen, G. Giaever, J. H. Hegemann, T. Jones, M. Laub, H. Liao, R. W. Davis, and et al.** 1999. Functional characterization of the *S. cerevisiae* genome by gene deletion and parallel analysis. *Science* **285**:901-906.
105. **Wittschieben, B. O., J. Fellows, W. Du, D. J. Stillman, and J. Q. Svejstrup.** 2000. Overlapping roles for the histone acetyltransferase activities of SAGA and elongator in vivo. *EMBO J* **19**:3060-3068.
106. **Yan, Y., N. A. Barlev, R. H. Haley, S. L. Berger, and R. Marmorstein.** 2000. Crystal structure of yeast Esa1 suggests a unified mechanism for catalysis and substrate binding by histone acetyltransferases. *Mol Cell* **6**:1195-1205.
107. **Yan, Y., S. Harper, D. W. Speicher, and R. Marmorstein.** 2002. The catalytic mechanism of the ESA1 histone acetyltransferase involves a self-acetylated intermediate. *Nat Struct Biol* **9**:862-869.
108. **Yang, X. J.** 2004. Lysine acetylation and the bromodomain: a new partnership for signaling. *Bioessays* **26**:1076-1087.
109. **Zhang, H., D. O. Richardson, D. N. Roberts, R. Utlely, H. Erdjument-Bromage, P. Tempst, J. Cote, and B. R. Cairns.** 2004. The Yaf9 component of the SWR1 and NuA4 complexes is required for proper gene expression, histone H4 acetylation, and Htz1 replacement near telomeres. *Mol Cell Biol* **24**:9424-9436.

110. **Zhang, J., X. Shi, Y. Li, B. J. Kim, J. Jia, Z. Huang, T. Yang, X. Fu, S. Y. Jung, Y. Wang, P. Zhang, S. T. Kim, X. Pan, and J. Qin.** 2008. Acetylation of Smc3 by Eco1 is required for S phase sister chromatid cohesion in both human and yeast. *Mol Cell* **31**:143-151.
111. **Zhang, J., R. Sprung, J. Pei, X. Tan, S. Kim, H. Zhu, C. F. Liu, N. V. Grishin, and Y. Zhao.** 2009. Lysine acetylation is a highly abundant and evolutionarily conserved modification in *Escherichia coli*. *Mol Cell Proteomics* **8**:215-225.
112. **Zhao, S., W. Xu, W. Jiang, W. Yu, Y. Lin, T. Zhang, J. Yao, L. Zhou, Y. Zeng, H. Li, Y. Li, J. Shi, W. An, S. M. Hancock, F. He, L. Qin, J. Chin, P. Yang, X. Chen, Q. Lei, Y. Xiong, and K. L. Guan.** 2010. Regulation of cellular metabolism by protein lysine acetylation. *Science* **327**:1000-1004.
113. **Zhu, H., M. Bilgin, R. Bangham, D. Hall, A. Casamayor, P. Bertone, N. Lan, R. Jansen, S. Bidlingmaier, T. Houfek, T. Mitchell, P. Miller, R. A. Dean, M. Gerstein, and M. Snyder.** 2001. Global analysis of protein activities using proteome chips. *Science* **293**:2101-2105.
114. **Zou, J., H. Friesen, J. Larson, D. Huang, M. Cox, K. Tatchell, and B. Andrews.** 2009. Regulation of cell polarity through phosphorylation of Bni4 by Pho85 G1 cyclin-dependent kinases in *Saccharomyces cerevisiae*. *Mol Biol Cell* **20**:3239-3250.

CHAPTER 2:

Functional dissection of the NuA4 histone acetyltransferase reveals its role as a genetic hub and that Eaf1 is essential for complex integrity

Leslie Mitchell^{1,2}, Jean-Phillipe Lambert^{1,2}, Maria Gerdes^{1,2}, Ashraf S. Al-Madhoun², Ilona S. Skerjanc², Daniel Figeys^{1,2}, and Kristin Baetz^{1,2}

¹ Ottawa Institute of Systems Biology, University of Ottawa, Ottawa, Ontario K1H8M5, Canada

² Department of Biochemistry, Microbiology and Immunology, University of Ottawa, Ottawa, Ontario K1H8M5 Canada

Contribution of Authors: LM performed all of the experiments with the exception of the dot assays to assess synthetic lethal genetic interactions of *esa1-L254P*, which were performed by MG. J-PL performed the mass spectrometry in the laboratory of DF. ASA contributed methodological expertise for Northern blot analysis, which was conducted in the laboratory of ISI. LM created all the figures and collaborated with KB to write the manuscript.

Published: Molecular and Cellular Biology. 2008. 28(7): 2244-56.

2.1 Abstract

The *Saccharomyces cerevisiae* NuA4 histone acetyltransferase complex catalyzes the acetylation of histone H4 and the histone variant Htz1 to regulate key cellular events, including transcription, DNA repair, and faithful chromosome segregation. To further investigate the cellular processes impacted by NuA4, we exploited the non-essential subunits of the complex to build an extensive NuA4 genetic interaction network map. The map reveals that NuA4 is a genetic hub whose function buffers a diverse range of cellular processes, many not previously linked to the complex, including Golgi-to-vacuole vesicle-mediated transport. Further, we probe the role that non-essential subunits play in NuA4 complex integrity. We find that most non-essential subunits have little impact on NuA4 complex integrity and display between 12 and 42 genetic interactions. In contrast, deletion of *EAF1* causes the collapse of the NuA4 complex and displays 148 genetic interactions. Our study indicates that Eaf1 plays a crucial function in NuA4 complex integrity. Further, we determine that Eaf5 and Eaf7 form a sub-complex, which reflects their similar genetic interaction profiles and phenotypes. Our integrative study demonstrates that genetic interaction maps are valuable in dissecting complex structure and provides insight into why the human NuA4 complex, Tip60, has been associated with a diverse range of pathologies.

2.2 Introduction

Histone acetyltransferase (HAT) enzyme complexes are key regulators of transcriptional control in all eukaryotic cells and have been linked to a diverse range of biological processes (61). HAT acetylation of specific lysines of N-terminal histone tails is believed to relieve DNA-protein interactions as well as to serve as a molecular beacon to attract additional chromatin remodeling or modifying proteins and/or transcription factors (35). In addition, the cellular processes regulated by HATs may not be governed solely by histone acetylation but, alternatively, may be mediated through the acetylation of nonhistone targets (23). To fully grasp the cellular implications of HATs will require both a comprehensive understanding of their diverse biological roles and a detailed understanding of the proteins within the complexes.

In *Saccharomyces cerevisiae*, the only essential HAT is the NuA4 complex. The known acetylation targets of NuA4 *in vivo* are histone H4 (1, 20, 58) and the histone H2A variant Htz1 (2, 28, 41). Similar to other HATs, NuA4 has been implicated in numerous nuclear events, including regulation of gene expression (17), DNA repair (18, 59), cell cycle progression (58), and chromosome stability (31). Though the various cellular roles of NuA4 are likely mediated through H4 or Htz1 acetylation, the molecular mechanisms by which histone acetylation achieves diverse cellular functions is largely unknown. As the Tip60 complex, the human homolog of the yeast NuA4 complex, has numerous nonhistone targets (51), it is possible that some of the cellular functions of the yeast complex may be fulfilled

through the acetylation of nonhistone substrates. Further, it is unlikely that all of the NuA4-mediated cellular functions have yet been defined. Indeed, NuA4 homologs in both humans and *Caenorhabditis elegans* have been implicated in a much broader range of cellular functions, including cytoplasmic roles in cell signaling (36, 51), suggesting that there may be roles for the yeast complex outside the nucleus.

NuA4 is composed of 13 subunits, including the essential acetyltransferase subunit Esa1 (12, 17). Of the other 12 NuA4 subunits, 5 are essential for cell viability (Act1, Arp4, Epl1, Swc4, and Tra1) and the remaining 7 are not (Eaf1, Eaf3, Eaf5, Eaf6, Eaf7, Yaf9, and Yng2) (17). Despite being the catalytic subunit, Esa1 on its own can target only free histones and is incapable of acetylating nucleosomes or chromatin (1, 7). As with other HAT enzyme complexes, the ability of Esa1 to target nucleosomes is dependent on complex formation. Esa1 has been isolated in two distinct complexes: the complete 13-subunit NuA4 complex and a trimer sub-complex composed of Esa1, Yng2, and Epl1 called Piccolo NuA4 (7). Studies suggest that Piccolo NuA4 cannot be recruited by transcription factors to specific locations, leading to the hypothesis that Piccolo NuA4 is responsible for nontargeted global histone acetylation, whereas the full NuA4 complex is responsible for targeted NuA4-dependent histone acetylation (7, 55).

Esa1 and Yng2 interact independently with the N-terminal portion of Epl1, and it has been demonstrated that the N-terminal Enhancer of Polycomb A (EPcA) region of Epl1 and the N-terminal region of Yng2 are required for Esa1 to recognize and acetylate nucleosomes (7, 55). Though it is known that the C-terminal half of Epl1 is required to bridge Esa1 and Yng2 with the remaining 10

NuA4 subunits (7), very little is known regarding the physical interactions between the remaining NuA4 subunits. Studies have found that Yaf9 interacts with NuA4 through Swc4 *in vivo* (5), and both Eaf3 and Arp4 interact directly with Esa1 *in vitro* (21). As seen in other chromatin modification complexes, such as the SWR1 complex (67) and SWI/SNF (68), it is likely that the non-Piccolo NuA4 subunits may form multiple and distinct sub-complexes that perform a subset of the diverse NuA4 cellular functions.

The functional role of each individual NuA4 subunit remains to be fully understood, particularly with respect to the 10 non-Piccolo NuA4 subunits. One possibility is that some NuA4 subunits may be required for complex integrity, acting as a scaffold upon which other subunits bind. Alternatively, individual subunits or sub-complexes may be required for the targeted recruitment of NuA4 to distinct chromatin loci. Indeed, targeting roles have been characterized for some subunits. For example, upon DNA damage, Arp4 recognizes and interacts with histone H2A phosphorylated at serine 129. This action recruits NuA4 to regions of DNA double-strand breaks where histone H4 acetylation is required for DNA double-strand break repair (4, 16). Similarly, Tra1 directly interacts with the acidic transcriptional activators Gcn4, Hap4, and Gal4 (8). Further, Tra1 is required for both the acetylation of H4 surrounding the promoters and the transcription of Gcn4-dependent genes, suggesting that Tra1 may mediate the recruitment of NuA4 to certain promoters.

While specific targeting roles for the other subunits are undefined, the different phenotypes of the non-essential NuA4 subunits strongly support the

hypothesis that different subunits are required for distinct NuA4 functions. For instance, while *yaf9Δ*, *yng2Δ*, and *eaf1Δ* cells display hypersensitivity to the microtubule-destabilizing drug Benomyl, *eaf5Δ* and *eaf7Δ* cells display no sensitivity to this drug (30, 31, 34). Similarly, while *eaf1Δ* and *yaf9Δ* cells display high rates of chromosome loss (41 and 23 times greater than that of wild-type [WT] cells, respectively), *eaf3Δ*, *eaf5Δ*, *eaf6Δ*, and *eaf7Δ* cells display either no or only modest increases in their rates of chromosome loss compared to WT cells (31) (L. Mitchell and K. Baetz, unpublished data).

Defining the roles of the individual subunits will provide critical insight into the NuA4 enzyme complex as a whole. In *S. cerevisiae*, a genetic method for exploring gene function is through the identification of synthetically lethal (SL) or synthetically sick (SS) genetic interactions by double mutant analysis. Mutants that are defective in the same essential or parallel non-essential pathways often display SL or SS interactions. The development of synthetic genetic array (SGA) analysis has enabled genetic screens to be performed systematically with yeast and has proven to be a powerful tool for predicting the cellular functions of a protein (63). Recently, subunits of NuA4 were analyzed in an epistatic miniarray profile (E-MAP) screen that identified pairwise genetic interaction between 743 genes implicated in various aspects of chromosome biology (13). This study solidified the role of NuA4 in its previously characterized functions, such as chromosome stability, DNA repair, transcription, and chromatin remodeling. However, given that the study was limited to genes involved in chromosome biology, no insights were gained into possible novel cellular functions of NuA4.

To comprehensively explore the global cellular functions of NuA4, we performed genome-wide SL-SGA analysis for five non-essential subunits. Our genetic interaction map reveals over 200 genetic interactions for the NuA4 subunits tested, dramatically expanding our knowledge of the potential cellular functions of the complex. Using the genetic interaction map, we identify a role for NuA4 in Golgi complex-to-vacuole vesicle-mediated transport. In addition, during our complex integrity studies, we discovered that NuA4 physically interacts with the stress response transcription factor Msn4. We also examine the effect of each non-essential subunit on NuA4 complex integrity and discover that the Eaf1 subunit, whose deletion is responsible for a large portion of the genetic interactions in our map, is essential for maintaining the complex integrity of NuA4. Moreover, Eaf5 and Eaf7, which display similar genetic interaction profiles and phenotypes, are found in a sub-complex. This integrative study provides novel insights into the pathways and processes impacted by NuA4 and sheds light on the roles of subunits within the complex.

2.3 Materials and Methods

2.3.1 Yeast strains and plasmids

Yeast strains used in this study are listed in Table 2.1. The MATa deletion mutant array was purchased from Open Biosystems (catalog no. YSC1053). The SGA starting strain Y7092 (62) and the media used in the SL-SGA analysis have been described previously (63, 64). Genomic deletion or epitope tag integrations made for this study were designed with PCR-amplified cassettes as previously described (38, 47) and confirmed by PCR analysis. Plasmid pGST-MSN4 (pKB1) was generated by PCR amplification of MSN4 from genomic DNA using the primers 5'-ATC GGG ATC CAT GCT AGT CTT CGG ACC TAA TAG (forward) and 5'-GCA TGC TCG AGT CAA AAA TCA CCG TGC TTT TTG (reverse). The resulting PCR product was digested with BamHI and XhoI and ligated into pGEX6p-2 (Amersham Bioscience) also digested with BamHI and XhoI.

Table 2.1: Yeast strains

Strain	Auxotrophies	Reference or Source
YPH499	<i>MATa ura3-52 lys2-801 ade2-101 trp1-Δ63 his3-Δ200 leu2-Δ1</i>	(57)
Y7092	<i>MATa□ can1Δ::STE2pr-Sp_his5 lyp1□ his3Δ1 leu2Δ0 ura3Δ0 met15Δ0</i>	(64)
YKB622	<i>MATa□ can1Δ::STE2pr-Sp_his5 lyp1□ his3Δ1 leu2Δ0 ura3Δ0 met15Δ0 eaf1Δ::NAT</i>	(31)
YKB995	<i>MATa□ can1Δ::STE2pr-Sp_his5 lyp1□ his3Δ1 leu2Δ0 ura3Δ0 met15Δ0 eaf3Δ::NAT</i>	This study
YKB852	<i>MATa□ can1Δ::STE2pr-Sp_his5 lyp1□ his3Δ1 leu2Δ0 ura3Δ0 met15Δ0 eaf5Δ::NAT</i>	(31)
YKB623	<i>MATa□ can1Δ::STE2pr-Sp_his5 lyp1□ his3Δ1 leu2Δ0 ura3Δ0 met15Δ0 eaf6Δ::NAT</i>	Gift from J. Greenblatt
YKB853	<i>MATa□ can1Δ::STE2pr-Sp_his5 lyp1□ his3Δ1 leu2Δ0 ura3Δ0 met15Δ0 eaf7Δ::NAT</i>	(31)
LPY3500	<i>MATa his3Δ200 leu2-3,112 trp1Δ1 ura3-52 esa1Δ::his3 esa1(L254P)::URA3</i>	(12)
KLY35	<i>MATa□ can1Δ::STE2pr-Sp_his5 lyp1□ his3Δ1 leu2Δ0 ura3Δ0 met15Δ0 LYS2 htz1-ND-loxP::NAT</i>	Gift from M.C. Keogh
YKB625	<i>MATa□ can1Δ::STE2pr-Sp_his5 lyp1□ his3Δ1 leu2Δ0 ura3Δ0 met15Δ0 htz1Δ::NAT</i>	This study
YKB1007	<i>MATa ura3-52 lys2-801 ade2-101 trp1-Δ63 his3-Δ200 leu2-Δ1 EAF1-TAP::TRP1</i>	This study
YKB44	<i>MATa ura3-52 lys2-801 ade2-101 trp1-Δ63 his3-Δ200 leu2-Δ1 eaf1ΔkanMX</i>	This study
YKB654	<i>MATa ura3-52 lys2-801 ade2-101 trp1-Δ63 his3-Δ200 leu2-Δ1 eaf3ΔTRP1</i>	This study
YKB658	<i>MATa ura3-52 lys2-801 ade2-101 trp1-Δ63 his3-Δ200 leu2-Δ1 eaf5ΔTRP1</i>	This study
YKB662	<i>MATa ura3-52 lys2-801 ade2-101 trp1-Δ63 his3-Δ200 leu2-Δ1 eaf6ΔTRP1</i>	This study
YKB464	<i>MATa ura3-52 lys2-801 ade2-101 trp1-Δ63 his3-Δ200 leu2-Δ1 yaf9ΔkanMX</i>	This study
YKB494	<i>MATa ura3-52 lys2-801 ade2-101 trp1-Δ63 his3-Δ200 leu2-Δ1 yng2ΔkanMX</i>	This study
YKB500	<i>MATa ura3-52 lys2-801 ade2-101 trp1-Δ63 his3-Δ200 leu2-Δ1 htz1ΔkanMX</i>	This study
YKB1035	<i>MATa ura3-52 lys2-801 ade2-101 trp1-Δ63 his3-Δ200 leu2-Δ1 MSN4-TAP::TRP1</i>	This study
YKB518	<i>MATa ura3-52 lys2-801 ade2-101 trp1-Δ63 his3-Δ200 leu2-Δ1 EAF7-MYC::kanMX</i>	This study
YKB1069	<i>MATa ura3-52 lys2-801 ade2-101 trp1-Δ63 his3-Δ200 leu2-Δ1 MSN4-TAP::TRP1 EAF7-MYC::kanMX</i>	This study
YKB440	<i>MATa Δtrp ura3-1 leu2-3,112 his3-11,15 ade2-1 can1-100 ESA1-TAP::TRP1</i>	Gift from N. Krogan
YKB1091	<i>MATa ura3-52 lys2-801 ade2-101 trp1-Δ63 his3-Δ200 leu2-Δ1 MSN4-TAP::TRP1 eaf1Δ::kanMX</i>	This study
YKB855	<i>MATa ESA1-TAP::TRP1 eaf1Δ::kanMX</i>	This study
YKB765	<i>MATa Δtrp ura3-1 leu2-3,112 his3-11,15 ade2-1 can1-100 ESA1-TAP::TRP1 eaf3Δ::kanMX</i>	This study
YKB784	<i>MATa Δtrp ura3-1 leu2-3,112 his3-11,15 ade2-1 can1-100 ESA1-TAP::TRP1 eaf5Δ::kanMX</i>	This study

YKB766	<i>MATa Δtrp ura3-1 leu2-3,112 his3-11,15 ade2-1 can1-100 ESA1-TAP::TRP1 eaf6Δ::kanMX</i>	This study
YKB964	<i>MATa Δtrp ura3-1 leu2-3,112 his3-11,15 ade2-1 can1-100 ESA1-TAP::TRP1 eaf7Δ::kanMX</i>	This study
YKB966	<i>MATa ESA1-TAP::TRP1 yaf9Δ::kanMX</i>	This study
YKB967	<i>MATa ESA1-TAP::TRP1 yng2Δ::kanMX</i>	This study
YKB1054	<i>MATa ESA1-TAP::TRP1 EAF7-MYC::kanMX</i>	This study
YKB1043	<i>MATa ESA1-TAP::TRP1 EAF7-MYC::kanMX eaf5Δ::kanMX</i>	This study
YKB442	<i>MATa his3Δ1 leu2Δ0 met15Δ0 ura3Δ0 EAF7-TAP::HIS</i>	TAP collection
YKB1034	<i>MATa EAF7-TAP::HIS eaf1ΔkanMX</i>	This study
YKB1097	<i>MATa ura3-52 lys2-801 ade2-101 trp1-Δ63 his3-Δ200 leu2-Δ1 msn2Δ::TRP msn4Δ::kanMX eaf1Δ::kanMX</i>	This study

2.3.2 SL-SGA screens

Robotic manipulation of the deletion mutant array was conducted using a Singer RoToR HDA (Singer Instruments), and SL screens were performed as described previously (63). Genome-wide SL screens were conducted three times at 30°C for the following query strains: the *eaf1Δ*, *eaf3Δ*, *eaf5Δ*, *eaf6Δ*, and *eaf7Δ* strains. The resultant double mutants were scored for SL or SS interactions by visual inspection. For the *eaf1Δ* screen, putative genetic interactions, identified in a minimum of two out of three screens, were confirmed by tetrad dissection on yeast-peptone-dextrose (YPD) medium at 25°C. For the *eaf3Δ*, *eaf5Δ*, *eaf6Δ*, and *eaf7Δ* screens, only those putative interactions identified in a minimum of two out of three screens that had not been previously published (as listed at www.thebiogrid.org as of April 2007) were confirmed by tetrad dissection, as described above. Any published interactions in the BioGrid database that were not identified in our screens were incorporated into our data set. The complete list of interactions and references are provided at www.oisb.ca/personal_web_site/Baetz_Lab/publicationsFS.html.

2.3.3 NuA4 PrA-tagged protein purification

One-step affinity purification of protein A (PrA; one epitope of the tandem affinity purification [TAP] tag)-tagged NuA4 components was performed. Cells from 200 ml of mid-log-phase culture (optical density at 600 nm [OD₆₀₀], □0.6 to 0.8) grown in YPD at 25°C were collected by centrifugation, washed in 10 ml lysis buffer (20 mM HEPES, pH 7.4, 0.1% Tween 20, 2 mM MgCl₂, 300 mM NaCl, protease inhibitor cocktail [P-8215; Sigma]) and transferred to a 1.5-ml Eppendorf tube. Cells were resuspended in 300µl lysis buffer plus an equal volume of acid-washed glass beads (catalog no. 35-535; Fisher Scientific), and cells were lysed through vortexing (six 1-minute blasts with incubation on ice in between vortexing). The soluble whole-cell extract (WCE) was isolated by centrifugation at 13,200 rpm for 20 min. Ten milligrams of the WCE was incubated with 25 µl of magnetic Dynabeads (catalog no. 143-01; DYNAL, Invitrogen) cross-linked to rabbit immunoglobulin G (IgG) (catalog no. PP64; Chemicon) as per Invitrogen's instructions. Following 2 hours of end-over-end incubation at 4°C, Dynabeads were collected with a magnet and washed five times with 1 ml cold lysis buffer. The Dynabeads were resuspended in 25 µl of modified 1X loading buffer (50 mM Tris, pH 6.8, 2% sodium dodecyl sulfate [SDS], 0.1% bromophenol blue, 10% glycerol), and PrA-tagged proteins and co-purifying proteins were eluted from the beads with moderate heat (65°C for 10 min). Loading buffer was transferred to a new tube, and 2-β-mercaptoethanol was added to a final concentration of 200 mM. Samples were boiled for 5 min, and 20 µl was resolved on 4 to 12% polyacrylamide gradient gels (catalog no. NP0321BOX; Invitrogen) in 1X MES (morpholineethanesulfonic acid) buffer. Proteins were visualized by silver staining.

2.3.4 Immunoprecipitation and immunoblotting

PrA purification of Msn4-TAP was performed as described above except 15 mg of WCE was incubated with the IgG-coated Dynabeads overnight. Immunoprecipitations were separated by 7.5% SDS-polyacrylamide gel electrophoresis (PAGE). Standard Western blotting procedures were performed using the following antibodies: anti-TAP (CAB1001; Open Biosystems), anti-Myc (catalog no. 11667149; Roche), peroxidase-conjugated goat anti-rabbit IgG (catalog no. AP307P; Chemicon), and peroxidase-conjugated goat anti-mouse IgG (catalog no. 170-6516; Bio-Rad). In cases where the anti-TAP antibody cross-reacted with the IgG eluted from the magnetic beads, the anti-TAP antibody was conjugated to horseradish peroxidase using the SureLINK horseradish peroxidase conjugation kit (catalog no. 84-00-01; KPL) as per the manufacturer's instructions.

2.3.5 Mass spectrometric detection of proteins

Gel bands were excised and subjected to in-gel tryptic digestion by following standard protocols (56). For the knockout analysis, in cases where bands were missing, areas corresponding to the missing bands were also excised to confirm that the proteins were truly missing. Liquid chromatography-tandem mass spectrometry (LC-MS/MS) was performed using the LTQ quadrupole ion trap mass spectrometer (Thermo-Electron, Waltham, MA) as described previously (50). MS/MS data were analyzed and matched to *S. cerevisiae* protein sequences in the NCBI nonredundant database using the Mascot database search engine (Matrix Science Inc., Boston, MA).

2.3.6 Fluorescence microscopy

Cells grown at 25°C in YPD medium were resuspended at 2 to 4 OD₆₀₀ U/ml and stained with FM4-64 (catalog no. T35356; Molecular Probes) at a final concentration of 20 μ M for 25 min at 30°C. Cells were re-suspended in fresh medium and incubated at 30°C for a 2 hour chase period. The *esa1-L254P* cells were incubated at 37°C for the chase period. Cells were then re-suspended at 4 to 8 OD₆₀₀ U/ml in fresh YPD medium. Slides were analyzed with a Leica DM IRE2 microscope using a 625-nm filter. Images were acquired using a Retiga 12-bit camera (Leica) and analyzed using Improvision 3.1 software.

2.3.7 *in vitro* binding assay

Msn4 fused to glutathione S-transferase (GST) (pKB1) as well as GST alone (pGEX-6P2; Amersham) was purified from *Escherichia coli* on glutathione-Sepharose, as recommended by Amersham. GST-Msn4 and GST protein concentrations were normalized by Coomassie blue staining on 10% SDS-PAGE gels. The NuA4 complex from yeast cells expressing Esa1-TAP or background control (WT) yeast cells with no TAP-tagged proteins was purified using IgG-coated magnetic Dynabeads as described above. Twenty-five microlitres of Dynabeads complexed with NuA4 (Esa1-TAP), the background (WT) protein, or beads alone was equilibrated twice with 1-ml washes in cold binding buffer (20mM HEPES, pH 7.4, 0.001% Tween20, 2mM MgCl₂, 100mM NaCl). Equivalent amounts of GST and GST-Msn4 were then incubated with NuA4, the WT protein, or Dynabeads alone for 2 hours at 4°C with end-over-end rotation in a volume of 500 μ l. Dynabeads were washed twice with 1 ml cold binding buffer and then five

times with 1ml cold lysis buffer (see above). Proteins were eluted as described above and resolved by 10% SDS-PAGE. Anti-GST Western blots were carried out with anti-GST (catalog no. A5800; Invitrogen) and peroxidase-conjugated goat anti-rabbit IgG (catalog no. AP307P; Chemicon) using standard procedures.

2.3.8 Modified ChIP

TAP-tagged and untagged strains, grown in YPD medium at 25°C to an OD₆₀₀ of 0.8, were collected by centrifugation, washed with 5 ml chromatin immunoprecipitation (ChIP) lysis buffer (100mM HEPES, pH 8.0, 20mM magnesium acetate, 10% glycerol, 0.1mM EDTA, protease inhibitor cocktail [catalog no. P-8215; Sigma]) and transferred to 1.5-ml Eppendorf tubes. Cells were resuspended in 500µl lysis buffer plus an equal volume of acid-washed glass beads (catalog no. 35–535; Fisher Scientific) and lysed by vortexing (six 1-min blasts, with incubation on ice in between vortexing). The crude WCE was separated from the beads into a fresh Eppendorf tube by centrifugation at 1,000 rpm for 1 min through a hole in the bottom of the Eppendorf tube created using a red-hot 18-gauge needle. Samples were subjected to three rounds of sonication (10 seconds each) (Sonic Dismembrator model 60, at setting 2; Fisher Scientific), with a 30-second incubation on ice between each pulse. NP-40 was added to each sample to a final concentration of 1%. Samples were clarified by centrifugation at 3,000 rpm for 10 min at 4°C. One hundred micrograms of WCE was reserved to serve as an “input” control, while 10 mg of WCE was incubated overnight at 4°C with 25µl of IgG-coated Dynabeads as described above. Beads were washed three times with 1ml cold ChIP wash buffer (ChIP lysis buffer plus 0.5% NP-40). Twenty

percent of the beads were reserved to test for immunopurification of the TAP-tagged proteins by Western blotting as described above. The remainder of the beads and the input WCE were treated with protease K (0.5 mg/ml in Tris-EDTA) for 2 h at 37°C). Protein was extracted using phenol-chloroform, and DNA was ethanol precipitated in the presence of 1 µg of glycogen. DNA pellets were washed with 70% ethanol, air dried, and resuspended in 50µl of Tris-EDTA. Immunoprecipitated DNA was amplified using multiplex PCR with the following primer pairs: HSP12 F (5'-CGC AAG CAT TAA TAC AAC CC) and HSP12 R (5'-CGC AAT TGA GGA AGT AGA AC) and Chr V no-ORF F (5'-GGC TGT CAG AAT ATG GGG CCG TAG TA) and Chr V no-ORF R (5'-CCC CGA AGC TGC TTT CAC AAT AC). PCR products were resolved on a 2% agarose gel and visualized with ethidium bromide.

2.3.9 Northern blot analysis

Yeast strains were grown at 25°C in YPD medium to an OD600 of 0.6 to 0.9. Heat shock conditions were carried out at 39°C for 30 min. RNA was isolated using a hot-phenol extraction method (53), except that TES acid buffer (10mM Tris-HCl, pH 7.5, 10 mM EDTA, pH 8.0, 0.5% SDS) was used, and samples were incubated at 65°C for 1 hour. Northern blotting was carried out as previously described (3). The probes used for the Northern blot analysis were created by PCR amplification of the coding sequences of *HSP12* (5'-GTC TGA CGC AGG TAG AAA AGG [forward]; 5'-CGC AAG CAT TAA TAC AAC CC [reverse]) and *ACT1* (5'-GCA TCA TAC CTT CTA CAA CG [forward]; 5'-GTG ATG ACT TGA CCA TCT GG [reverse]). Probes were labeled using the Megaprime DNA labeling system

(catalog no. RPN1607; Amersham) in the presence of [α - 32 P]dCTP (GE Healthcare).

2.4 Results

2.4.1 An extensive NuA4 genetic interaction map indicates NuA4 impacts a diverse range of cellular processes

In an effort to comprehensively identify the cellular processes potentially impacted by NuA4, we performed genome-wide SL screens using query strains with deletions of all seven non-essential NuA4 genes (*eaf1 Δ* , *eaf3 Δ* , *eaf5 Δ* , *eaf6 Δ* , *eaf7 Δ* , *yaf9 Δ* , and *yng2 Δ*). All seven genome-wide SL screens were performed in triplicate using SGA methodology by mating each query strain to the yeast deletion mutant array and selecting for double mutants (63). Any double mutant combinations that resulted in inviability (SL) or in reduced fitness (SS) that were identified in a minimum of two out of three screens were confirmed by tetrad analysis (genetic interaction data set available at www.oisb.ca/personal_web_site/Baetz_Lab/publicationsFS.html). Despite multiple attempts with *yaf9 Δ* , and *yng2 Δ* query strains, reproducible genetic interaction profiles were not obtained. The resulting confirmed data set contains 172 genetic interactions among 149 genes, of which 18% (31/172) were SL interactions and the remainder were SS interactions. To increase the coverage of our data set, we also incorporated *eaf1 Δ* , *eaf3 Δ* , *eaf5 Δ* , *eaf6 Δ* , and *eaf7 Δ* genetic interactions confirmed in previously published SL-SGA analyses or direct testing (see Materials and Methods for details). The combined data set contains 268 genetic interactions

among 204 genes, of which 38% (101/268) were SL interactions and the remainder were SS interactions.

Given that genetic interactions predict functional relationships (63), the NuA4 genetic interaction map identified many genes that encode proteins implicated in cellular processes previously associated with the NuA4 complex, including chromatin structure, transcription, DNA repair, and chromosome stability, as determined by their gene ontology (GO) annotations (Figure 2.1). Significantly, the NuA4 genetic map enriched for genes encoding proteins within the same protein complexes, suggesting that our screening method provided extensive coverage of the genome and thus the ability to predict interactions between NuA4 and protein complexes. Some examples of this are the SAGA complex (*GCN5*, *SGF9*, *SGF73*, *SGF11*), the SWR complex (*ARP6*, *SWC3*, *SWC5*, *SWR1*, *VPS71*, *VPS72*), and the MRX complex (*MRE11*, *RAD50*, *XRS2*). This is the first time that genetic interactions have been identified for any NuA4 subunit on a genome-wide scale, so in addition to supporting the well-characterized roles for NuA4, the genetic interaction map enriched for numerous other genes implicated in a wide variety of functions, including vesicle-mediated transport, stress response, and arginine biosynthesis.

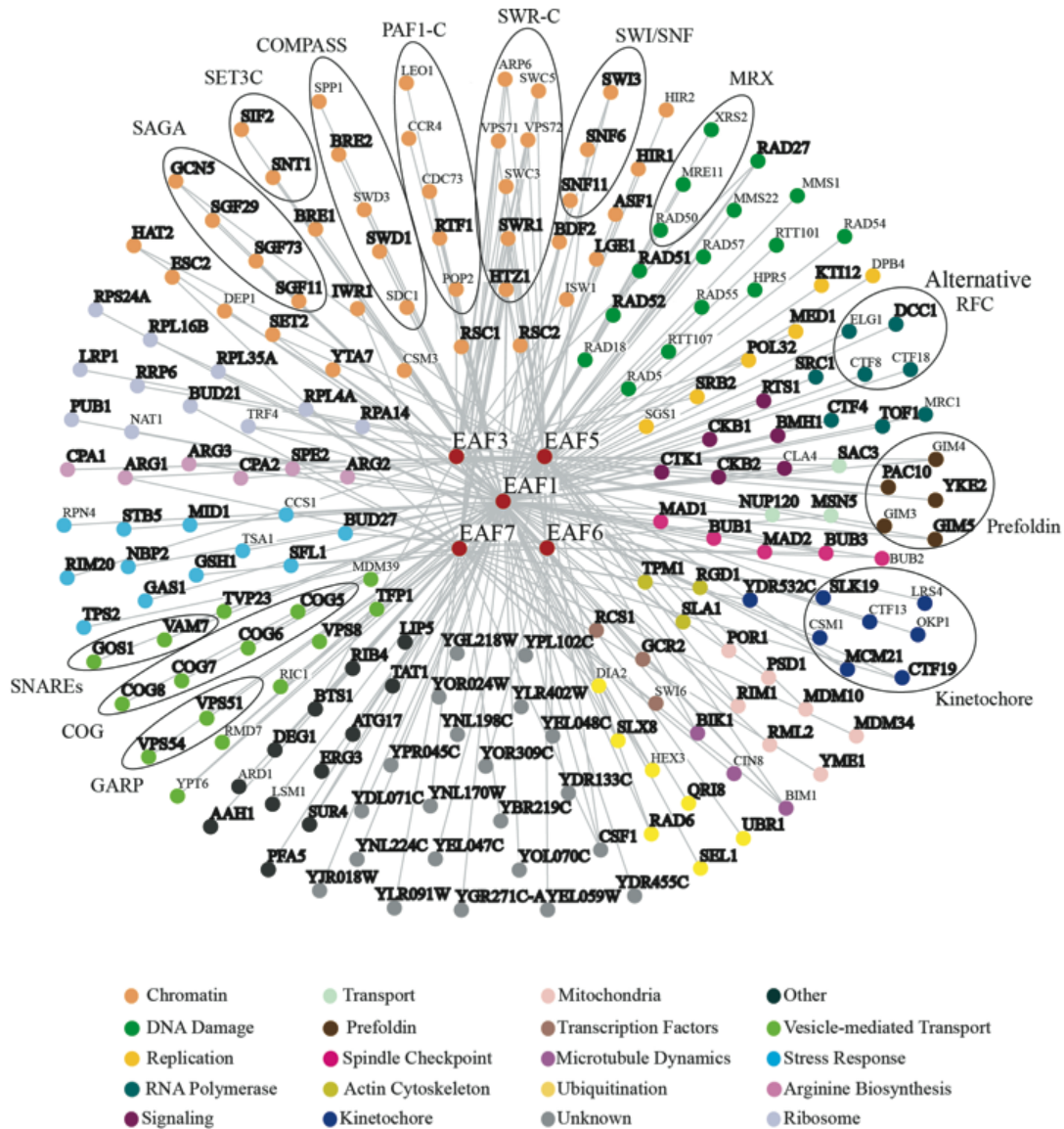


Figure 2.1: Synthetic genetic interaction map of five NuA4 subunits

Genome-wide SL-SGA screens were performed using query strains for five non-essential NuA4 subunits: the *eaf1Δ* (YKB622), *eaf3Δ* (YKB993), *eaf5Δ* (YKB852), *eaf6Δ* (YKB623), and *eaf7Δ* (YKB853) strains. The 199 NuA4 interacting genes are represented by nodes that are colour coded based on the GO process. Gray lines indicate genetic interactions (both SS and SL interactions). The 139 interacting genes highlighted in bold text indicate those genes whose interaction with at least one NuA4 query strain was confirmed by tetrad dissection in our lab. The remaining interacting genes in the map represent previously published genetic interactions that were either identified in our SGA screens but were not confirmed by tetrad dissection or not identified in our screens. Genes encoding subunits of a single protein complex are grouped together with black circles.

2.4.2 Eaf1 functions primarily as a component of NuA4

Although it has been shown that genes that function within the same protein complex have similar genetic interaction profiles (13), we observed that the five NuA4 subunits have remarkably different genetic interaction profiles, particularly with respect to the total number of genetic interaction partners. While *eaf3Δ*, *eaf5Δ*, *eaf6Δ*, and *eaf7Δ* mutants genetically interacted with 31, 42, 12, and 35 genes, respectively, the *eaf1Δ* mutant genetically interacted with 148 genes. Further, 75% of the *eaf1Δ* genetic interactions were specific to the *eaf1Δ* mutant alone (genetic interaction data set available at www.oisb.ca/personal_web_site/Baetz_Lab/publicationsFS.html). This suggests that either Eaf1 plays a crucial role in NuA4 that is not shared by the other non-essential subunits tested or Eaf1 functions on its own or as part of an additional protein complex(es). Previous studies were not able to identify co-purifying proteins when tagged Eaf1 was used as bait (22, 32)(Gavin et al., 2006; Krogan et al., 2006). Therefore, to test the hypothesis that Eaf1 is found only in NuA4, we immunopurified a TAP-tagged version of Eaf1 and identified its interacting proteins using a modified procedure (Figure 2.2). One-step purification was performed using IgG-coated magnetic beads that interact with the PrA component of the TAP tag. Proteins were eluted from the beads in sample buffer at 65°C, separated by SDS-PAGE, and silver stained. This protocol results in low level background binding of non-specific proteins to IgG beads (Figure 2.2, WT lane) and a high yield of TAP purifications. Protein bands were individually cut,

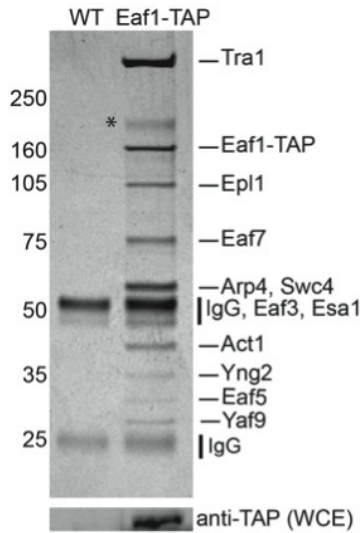


Figure 2.2: Eaf1-TAP purifies the NuA4 complex.

SDS-PAGE (gradient gel) and silver staining comparing NuA4 that was affinity purified via Eaf1-TAP (YKB1007) and NuA4 from an untagged strain (WT; YPH499), using IgG-coated magnetic beads that bind the PrA component of the TAP tag. IgG heavy and light chains co-elute upon heating. Protein bands were identified by MS as indicated. Eaf6 was not efficiently silver stained. The * indicates a non-NuA4, co-purifying protein, Fks1. Anti-TAP Western blotting demonstrates the expression of Eaf1-TAP in the WCE. This gel is representative of those from three purification experiments. Numbers at the left indicate molecular masses (kDa).

and MS was performed to identify the Eaf1-TAP-interacting proteins. We discovered that Eaf1-TAP co-purifies only with subunits of the NuA4 complex and Fks1, which was identified in all NuA4 purifications using this protocol (Figure 2.2 and see Figure 2.5 and 2.6). As Fks1, a subunit of the 1,3-beta-D-glucan synthase enzymatic complex (29), localizes to the plasma membrane and has not previously been reported to interact with NuA4, we suspect that this interaction is an artifact of the purification procedure.

Since Eaf1-TAP co-purified only with NuA4 proteins (and Fks1), this suggests that the 148 *eaf1Δ* genetic interactions are attributable to Eaf1's role in NuA4. Hence, we hypothesized that the *eaf1Δ* genetic interactions would be largely shared with a strain with a mutation in the essential NuA4 catalytic subunit Esa1. To test this, we directly mated the *esa1-L254P* mutant (12), a temperature-sensitive point mutant that displays acetylation defects, with 148 deletion mutants that displayed genetic interactions with the *eaf1Δ* strain. Diploids were sporulated, and tetrads were dissected at 25°C. Of the 148 matings, 140 produced reliable tetrads. Dot assays were performed at 30°C to test for synthetic genetic interactions of these double mutants, except for three double mutants that proved to be SL or extremely SS on the dissection plates (the *YKE2*, *TPM1*, and *RIB4* mutants). Nineteen displayed no growth phenotype defects in combination with the *esa1-L254P* mutation at 30°C, while the remaining 118 deletion mutants were either SL or SS in combination with the *esa1-L254P* mutation (see Supplemental Table 2 at www.oisb.ca/personal_web_site/Baetz_Lab/publicationsFS.html). The facts that 86% of *eaf1Δ* genetic interactions are shared with the acetylation-

deficient *esa1-L254P* mutant and that Eaf1-TAP co-purifies only with NuA4 suggest that Eaf1 functions primarily as a component of NuA4.

2.4.3 NuA4 function impacts vesicle-mediated transport

Surprisingly, the NuA4 genetic map identified 15 genes that encode proteins with well-established roles in vesicle-mediated transport (Figure 2.1 and Table 2.2). Remarkably, most of the vesicle-mediated transport gene deletions displayed only genetic interactions with *eaf1* Δ and the *esa1-L254P* catalytically deficient mutant (Table 2.2). Indeed, no genetic interactions were identified between *eaf3* Δ or *eaf6* Δ mutants and this group of genes. Further, of the 13 *eaf1* Δ mutant genetic interactions with the vesicle-mediated transport genes, eight were SL, including the interactions with all four non-essential subunits of the conserved oligomeric Golgi complex (*COG5*, *COG6*, *COG7*, *COG8*) (65), the soluble N-ethylmaleimide-sensitive factor attachment protein receptors (*GOS1* and *VAM7*) (26), the Golgi complex-associated retrograde protein complex subunit (*VPS54*) (44), and the GTPase (*YPT6*) (46). Many of the vesicle-mediated transport genes identified have specific roles in Golgi complex-to-vacuole transport, and deletion of most of these genes results in altered vacuole morphology (54). The strong genetic interactions of *eaf1* Δ and *esa1-L254P* with these mutants suggest that NuA4 may impact vesicle-mediated transport and that NuA4 mutants may also display aberrant vacuole morphology. To test this hypothesis, we examined vacuolar morphology in all seven non-essential NuA4 mutants and the *esa1-L254P* mutant using the fluorescent vacuolar vital stain

Table 2.2: Genetic interactions of NuA4 mutants with vesicle-mediated transport genes

Interacting Gene	Phenotype with indicated NuA4 gene ^a			
	<i>EAF1</i>	<i>ESA1</i>	<i>EAF5</i>	<i>EAF7</i>
GOS1	SL	SL		
VAM7	SL	SS		
TVP23	SS	ND		
<i>TFP1</i>		ND		SS
<i>VPS8</i>	SS	SS		
<i>COG5</i>	SL	SS		
<i>COG6</i>	SL	SL		
<i>COG7</i>	SL	SL		
<i>COG8</i>	SL	SL		
<i>RIC1</i>		ND		SL
<i>RMD7</i>	SS	ND		
<i>YPT6</i>	SL	SS		SL
<i>VPS51</i>	SS	SS	SS	
<i>VPS54</i>	SL	SL		
<i>MDM39</i>	SS	ND		

^a Empty spaces indicate that no genetic interaction was found by genome-wide SL-SGA screens. ND indicates that no data were obtained from *esa1-L254P* mutant direct tests either because the gene was not identified in the *eaf1Δ* mutant screen (*TFP1* and *RIC1*) or reliable tetrads were not obtained (*TVP23*, *RMD7*, and *MDM23*). *eaf3Δ* and *eaf6Δ* mutants did not display genetic interactions with any of the vesicle-mediated transport genes.

FM4-64 (66). As expected *eaf3Δ*, *eaf5Δ*, *eaf6Δ*, and *eaf7Δ* cells, which do not have any or have only a few genetic interactions with vesicle-mediated transport genes, displayed vacuole morphology similar to that of the WT (Figure 2.3A). In contrast, *eaf1Δ*, *yng2Δ*, *yaf9Δ*, and *esa1-L254P* cells displayed altered vacuole morphology, with the majority of cells displaying one large vacuole (Figure 2.3A). This suggests that Eaf1, Yaf9, Yng2, and the acetyltransferase activity of Esa1 are required for vacuole function. As NuA4 may mediate some of its cellular roles through Htz1 acetylation (2, 27, 41) and *htz1Δ* mutants display some phenotypes similar to those of NuA4 mutants (30, 31), we next tested whether *htz1Δ* and *htz1-ND* cells, in which the N-terminal amino acids 3 to 14 (KAHGGKGKSGAK) are replaced with 24 amino acids (CRSTTLNITSYNVCYTKLLGDIRT), also display defects in vacuole morphology. While the majority of *htz1Δ* cells displayed large vacuoles similar to those of *eaf1Δ*, *yaf9Δ*, *yng2Δ*, and *esa1-L254P* cells, the *htz1-ND* cells displayed WT vacuole morphology (Figure 2.3B). This suggests that the Htz1 globular core, but not the N terminus or N-terminal acetylation sites, is required for vacuole function. We next directly tested whether *htz1Δ* mutants display synthetic genetic interactions with a subset of the identified deletion mutants that interact with both *eaf1Δ* and *esa1-L254P* mutant: the *TVP23*, *VPS51*, *GOS1*, *VPS8*, and *COG6* mutants. *htz1Δ* mutants shared all these genetic interactions (Figure 2.3C). This suggests that both NuA4 and Htz1 have a role in vesicle-mediated transport, likely through the transcriptional regulation of a key gene(s) required for vesicle-mediated transport.

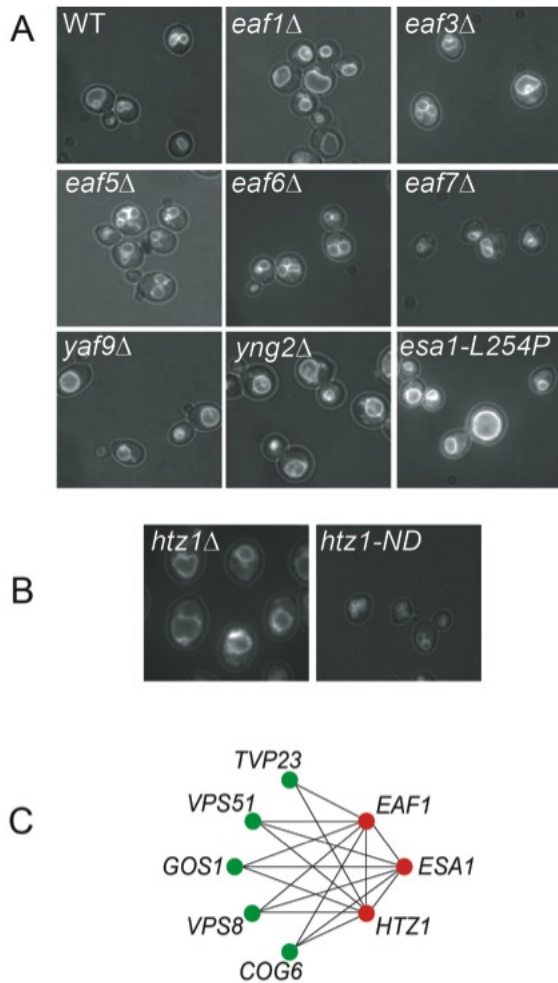


Figure 2.3: NuA4 function impacts vesicle-mediated transport.

(A) *eaf1Δ*, *yaf9Δ*, *yng2Δ*, and *esa1-L254P* cells display vacuolar morphology defects. Vacuole morphology was examined in WT (YPH499) cells, in strains deficient in each of the seven nonessential NuA4 subunits (*eaf1Δ* [YKB44], *eaf3Δ* [YKB654], *eaf5Δ* [YKB658], *eaf6Δ* [YKB662], *eaf7Δ* [YKB853], *yaf9Δ* [YKB464], and *yng2Δ* [YKB494]), and in a temperature sensitive point mutant of the catalytic subunit [*esa1-L254P* (LPY3500)] using the dye FM4-64. The WT and deletion mutants were grown at 30°C, while *esa1-L254P* mutants were grown at 37°C for 2 h after FM4-64 treatment. Images shown were taken after the merger of fluorescent light and transmitted light. **(B)** *htz1-ND* cells (YKL35) do not show vacuolar-morphology defects, while *htz1Δ* (YKB625) cells display defects similar to those of the *eaf1Δ*, *yaf9Δ*, *yng2Δ*, and *esa1-L254P* mutants. Vacuole morphology was examined in mutant cells with FM4-64 as described for panel A. **(C)** *htz1Δ* (YKB500), *esa1-L254P* (LPY3500), and *eaf1Δ* (YKB622) mutants (indicated by the red dots) genetically interact with a subset of vesicle-mediated transport genes (indicated by green dots) identified in the NuA4 SGA screens. Lines connect genes with synthetic genetic interactions.

2.4.4 NuA4 and the stress-responsive transcription factor Msn4

The genetic interaction map also identified 10 genes that have been implicated in the yeast stress response, thereby suggesting a functional connection between NuA4 and the stress response (Figure 2.1). Additionally, during the course of our analysis of NuA4 complex integrity (see below), we identified the general stress-responsive transcription factor Msn4, which co-migrates with Esa1-TAP, in four separate Esa1-TAP purifications. Msn4, along with its functionally related homolog Msn2, are required for the transcriptional induction of numerous stress response genes upon various environmental and metabolic cues (39). We were also interested in the physical interaction between NuA4 and Msn4 because microarray analysis of several NuA4, SWR, and Isw1 mutants previously demonstrated that the complex plays a role in the transcriptional repression of a large number of Msn2/4-dependent stress response genes (25, 37). Further, it was demonstrated that the de-repression of a subset of Msn2/4 target genes in NuA4, SWR, or Isw1 mutants in the absence of environmental stress requires Msn2 and/or Msn4 (37). Having initially identified the physical interaction between NuA4 and Msn4 by MS, we sought to test the validity of the interaction *in vivo* by reciprocal immunopurification of NuA4 using a tagged version of Msn4. To accomplish this, we generated a strain expressing both Msn4-TAP and Eaf7-Myc from their endogenous promoters. IgG-coated magnetic beads were used to immunopurify Msn4-TAP, and Western blot analysis confirmed the presence of Eaf7-Myc (Figure 2.4A). Given that Eaf7

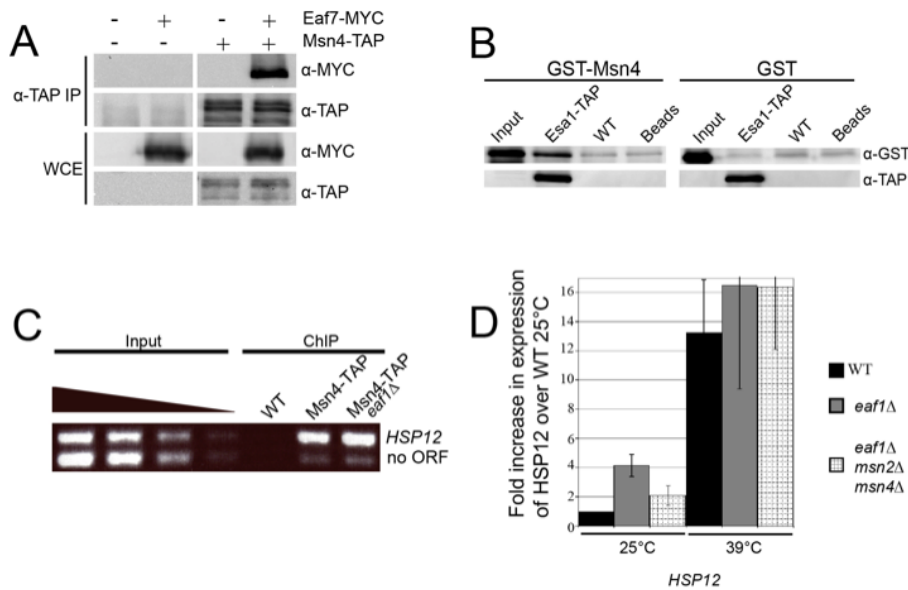


Figure 2.4: NuA4 physically interacts with Msn4 but does not regulate Msn4 binding to the *HSP12* promoter or heat shock induction of *HSP12*.

(A) NuA4 interacts with Msn4 *in vivo*. Protein extracts expressing the indicated tagged proteins (Msn4-TAP [YKB1035], Eaf7-MYC [YKB518], Msn4-TAP/Eaf7-MYC [YKB1069]) or an untagged WT control (YPH499) were immunoprecipitated with magnetic beads coated with IgG antibodies that bind the PrA component of the TAP tag. Total protein extracts (WCE) and immunoprecipitates (α -TAP IP) were resolved by 7.5% SDS-PAGE and subjected to Western blot analysis with anti-Myc and anti-TAP antibodies (α -MYC and α -TAP, respectively), as indicated at the right side of the panels. (B) NuA4 and Msn4 interact *in vitro*. WCE from cells expressing Esa1-TAP (YKB440) were used to purify the NuA4 complex using IgG-coated magnetic beads, and results were compared to those for an untagged strain (WT; YPH499). IgG-coated magnetic beads complexed with NuA4 (lane Esa1-TAP), background yeast proteins (lane WT), or beads alone (lane Beads) were incubated with equivalent amounts of either full-length GST-Msn4 or GST. Resulting immunocomplexes were eluted with heat, resolved by 10% SDS-PAGE, and subjected to Western blotting with anti-TAP and anti-GST antibodies, as indicated. Twenty-five percent of the input GST or GST-Msn4 fusion protein was run alongside the pull-down experiments as an input control (lane Input). (C) Msn4 occupancy at the *HSP12* promoter is independent of NuA4. Modified ChIP (see Materials and Methods) was performed using an untagged strain (WT; YPH499) and the Msn4-TAP (YKB1035) and Msn4-TAP *eaf1* Δ (YKB1091) strains. Immunoprecipitated (ChIP lanes) or WCE (Input lanes) DNA was subjected to multiplex PCR amplification using primers specific to the promoter region of *HSP12* and an intergenic region on chromosome V (no ORF). The results of this ChIP are representative of three experiments. (D) Deletion of *EAF1* causes de-repression of *HSP12* but does not inhibit the heat shock induction of *HSP12*. WT (YPH499), *eaf1* Δ (YKB44), and *eaf1* Δ *msn2* Δ *msn4* Δ (YKB1097) cells were grown in YPD at 25°C to mid-log phase, and samples were collected at 25°C and after 30 min of heat shock treatment at 39°C. Northern blots were probed with labeled DNA fragments of the *HSP12* gene. The signal was quantified using AlphaEase FC (Alpha Innotech) and normalized to the *ACT1* signal. The values are averages from three independent RNA preparations, and error bars indicate standard deviations.

has been identified only within the NuA4 complex, we conclude that Msn4 physically interacts directly or indirectly with the NuA4 enzyme complex. Though Msn4 and Msn2 migrate at the same rate on SDS-PAGE gels, we never identified Msn2 by MS in our Esa1-TAP purification. However, as Msn2 and Msn4 are largely redundant, we also asked whether NuA4 and Msn2 interact. Experiments using Msn2-TAP showed that Msn2-TAP co-immunoprecipitates Eaf7-Myc (data not shown), indicating the NuA4 interacts with both Msn2 and Msn4. While this experiment verified the interaction between NuA4 and both Msn4 and Msn2, it told us little about whether the interaction is mediated by other, non-NuA4 proteins. As Msn2 and Msn4 likely act in the same manner, the remaining experiments were performed with Msn4 alone. To test whether the physical interaction between NuA4 and Msn4 is direct, we performed an *in vitro* binding experiment using recombinant GST-Msn4 purified from *E. coli* and NuA4 isolated from yeast using IgG-coated magnetic beads after extensive washes. We found that while GST alone does not bind to NuA4, GST-Msn4 specifically interacts with the NuA4 enzyme complex (Figure 2.4B), suggesting that the interaction between Msn4 and the NuA4 enzyme complex is likely direct. However, although we believe our NuA4 immunopurification to be extremely clean (Figure 2.5), given that NuA4 was purified from yeast, we cannot rule out the possibility that non-NuA4 co-purifying proteins mediated the interaction with Msn4.

In light of the physical interaction between NuA4 and Msn4/ Msn2 and the de-repression of a subset of Msn2/4 genes in NuA4 mutants, we next decided to further explore the molecular mechanism connecting Msn2/4 and NuA4. Under

non-stress conditions, the majority of Msn2 and Msn4 proteins are localized to the cytoplasm, and upon environmental stress, they enter the nucleus and bind to stress response elements upstream of their target genes (24). However, strains with mutations in NuA4 do not display increased Msn2 or Msn4 nuclear localization, nor is the H4 acetylation of the promoters of de-repressed Msn4/2 target genes significantly changed from that of control promoters in *yaf9Δ* cells (37). This suggests that Msn4 and/or Msn2 may bind stress response element promoters in the absence of stress and that NuA4-dependent modification of the chromatin structure may not regulate Msn2 or Msn4 binding to promoters. To test this, we examined the occupancy of Msn4 on the promoter of the *HSP12* gene by ChIP. The transcriptional induction of *HSP12* is dependent largely on Msn2/4 under stress conditions (39, 52) and is highly de-repressed in NuA4 mutants in a manner dependent on Msn2/4 (37), and Esa1 has been shown to localize to the *HSP12* promoter (49). Using Msn4-TAP, we attempted a traditional ChIP experiment but found that due to the reduced accessibility of the epitope tag upon cross-linking, we were unable to immunoprecipitate Msn4-TAP. We therefore developed a modified ChIP protocol, utilizing a gentle clarification that circumvents the use of formaldehyde cross-linking, and tested for the presence of Msn4-TAP on the promoter of *HSP12*. Our modified ChIP analysis demonstrated that under normal growth conditions, Msn4-TAP associates specifically with the promoter region of *HSP12* but not with an untranscribed control region on chromosome V (Figure 2.4C, row no ORF) (27). Through Northern blot analysis, we determined that *HSP12* is de-repressed at 25°C in log-phase *eaf1Δ* cells and that de-

repression is largely dependent on Msn2 and Msn4 (Figure 2.4D). Therefore, we also performed the modified Msn4-TAP ChIP protocol with *eaf1Δ* cells and determined that the deletion of *EAF1* does not alter Msn4 localization to *HSP12* promoters (Figure 2.4C). As NuA4 has been localized to the *HSP12* promoter in the absence of stress (49) and the deletion of *EAF1* causes the collapse of the NuA4 complex, the ChIP results suggest that Msn4 localization to the *HSP12* promoter does not require NuA4. We were next interested in determining whether NuA4 played a significant role in the activation of *HSP12* under heat shock conditions. To do this, we performed *HSP12* Northern blot analysis and compared WT cells to *eaf1Δ* cells after 30 minutes of heat shock at 39°C (Figure 2.4D). The deletion of *EAF1* did not inhibit the heat shock induction of *HSP12*. This suggests that though NuA4 is important for maintaining the repression of the *HSP12* promoter, NuA4 does not play a significant role in the induction of *HSP12*. Surprisingly, we also determined that in the absence of Eaf1, the heat shock induction of *HSP12* is independent of Msn2 and Msn4 (Figure 2.4D), suggesting that other transcription factors are compensating.

2.4.5 Eaf1 is required for NuA4 complex integrity

The large size of the *eaf1Δ* genetic interaction profile relative to those of the other non-essential NuA4 subunits suggested that Eaf1 might have a unique and critical role in complex integrity. To test this hypothesis, we examined protein association with TAP-tagged Esa1 in cells deficient for one of the seven non-essential subunits (Figure 2.5). Protein bands in the Esa1-TAP lane were identified through MS. Eaf3 co-migrated with the IgG heavy chain, and Eaf7 co-migrated with

Esa1-TAP, so while we detected these subunits by MS in the Esa1-TAP purification, we cannot make reliable predictions as to their interactions with the complex in Esa1-TAP purifications in the various deletion mutant backgrounds. Regardless, we found that the elimination of Eaf3, Eaf5, Eaf6, Eaf7, and Yaf9 had no detectable effect on the association of the remaining visible NuA4 subunits (Figure 2.5), indicating that the overall integrity of the NuA4 complex is not dependent on these subunits. Removal of Yng2 resulted in the loss of Eaf6 (Figure 2.5, compare lane Esa1-TAP to lane Esa1-TAP *yng2Δ*), indicating that Eaf6 interacts with the NuA4 complex through Yng2. Remarkably, the removal of Eaf1 resulted in a dramatic loss of NuA4 complex integrity (Figure 2.5, compare lane Esa1-TAP to lane Esa1-TAP *eaf1Δ*). Though faint bands corresponding to the size of Epl1 and Yng2 were detected on the silver-stained gel as interacting with Esa1-TAP in the absence of Eaf1, no other subunits of NuA4 were detected in multiple purifications. This implies that in the absence of Eaf1, Piccolo NuA4, which is sufficient for cellular viability (7), is still present. These results suggest that Eaf1 is required to maintain the integrity of the NuA4 complex and may link the Piccolo NuA4 sub-complex to the remaining NuA4 components.

2.4.6 Eaf5 and Eaf7 form a sub-complex

We were surprised that the deletion of most non-essential subunits revealed little about the physical interdependencies of the NuA4 subunits within

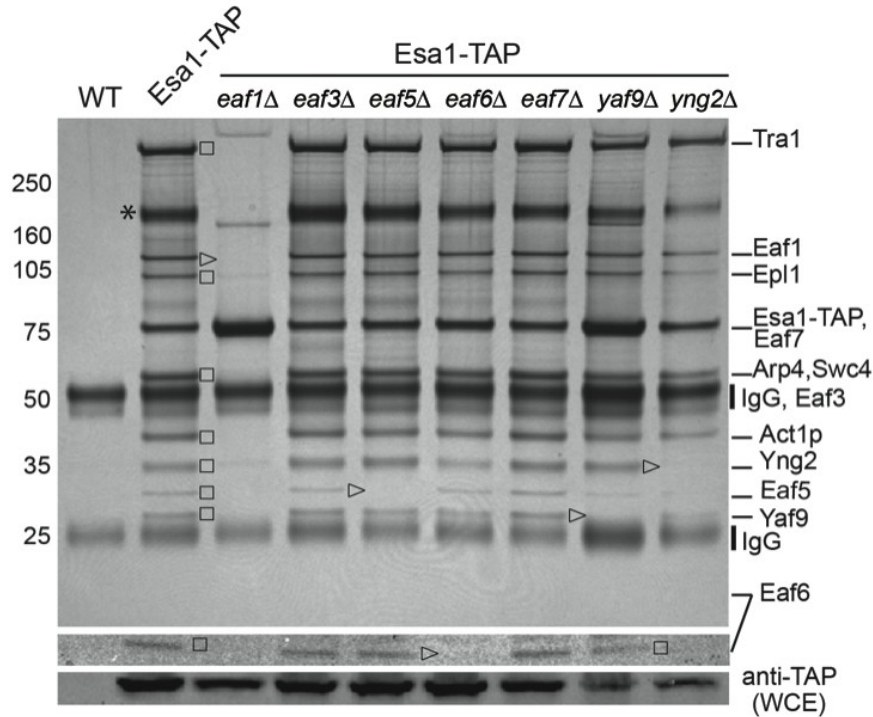


Figure 2.5: Eaf1 is required for NuA4 complex integrity.

SDS-PAGE (gradient gel) and silver staining of NuA4 affinity purified via Esa1-TAP (YKB440) compared to an untagged strain (WT; YPH499) and Esa1-TAP purified from mutant strain backgrounds lacking all seven nonessential subunits (*eaf1Δ* [YKB855], *eaf3Δ* [YKB765], *eaf5Δ* [YKB854], *eaf6Δ* [YKB766], *eaf7Δ* [YKB964], *yaf9Δ* [YKB966], and *yng2Δ* [YKB967] strains). Eaf6, as it does not stain well with silver, was subjected to a longer exposure (middle panel). Proteins bands in the Esa1-TAP lane were identified by MS as indicated. Anti-TAP Western blotting demonstrated the expression of Esa1-TAP in the WCE of all strains tested. Arrowheads point to proteins eliminated by subunit deletion, while squares specify additional subunits lost. The * indicates a non-NuA4, co-purifying protein, Fks1. Numbers at the left are molecular masses (in kDa). The gel is representative of three independent purifications.

the complex. As genes that function within the same complex or sub-complex tend to have similar genetic interaction profiles, to gain further insight into NuA4 complex integrity, we performed two-dimensional hierarchical clustering of our NuA4 genetic interactions (Figure 2.6A). Our analysis revealed that *EAF5*, *EAF7*, and *EAF3* components cluster together. We also performed a two-dimensional hierarchical clustering analysis of our NuA4 genetic interactions in the context of a large combined data set consisting of 12,954 previously published SL or SS interactions that were identified using genome-wide SL-SGA screens (supplementary cluster Treeview files are available at www.oisb.ca/personal_web_site/Baetz_Lab/publicationsFS.html) (40, 45, 48, 64). This analysis further confirmed the idea that *EAF3*, *EAF5*, and *EAF7* cluster together. Similar clustering of *EAF5* and *EAF7* was seen in the recently published chromatin E-MAPs (13), and *eaf5Δ* and *eaf7Δ* strains display similarity in microarray transcriptional profiles (31). The repeated clustering of *EAF5*, *EAF7*, and *EAF3* genetic profiles strongly suggests that Eaf5, Eaf7, and potentially Eaf3 may form a sub-complex that is responsible for mediating only a subset of the cellular functions of NuA4. We have shown that the interaction of Eaf5 with the NuA4 complex is not dependent on Eaf7 (Figure 2.5); however, as Eaf7 was not visible on the silver stained gel, we could not visually determine whether Eaf5 is required for Eaf7's interaction with NuA4. Therefore, to further investigate the possible existence of this sub-complex, we chose to integrate a C-terminal Myc tag at the *EAF7* chromosomal locus in order to determine the effect of *EAF5* gene deletion on the Eaf7-Myc interaction with the NuA4 complex

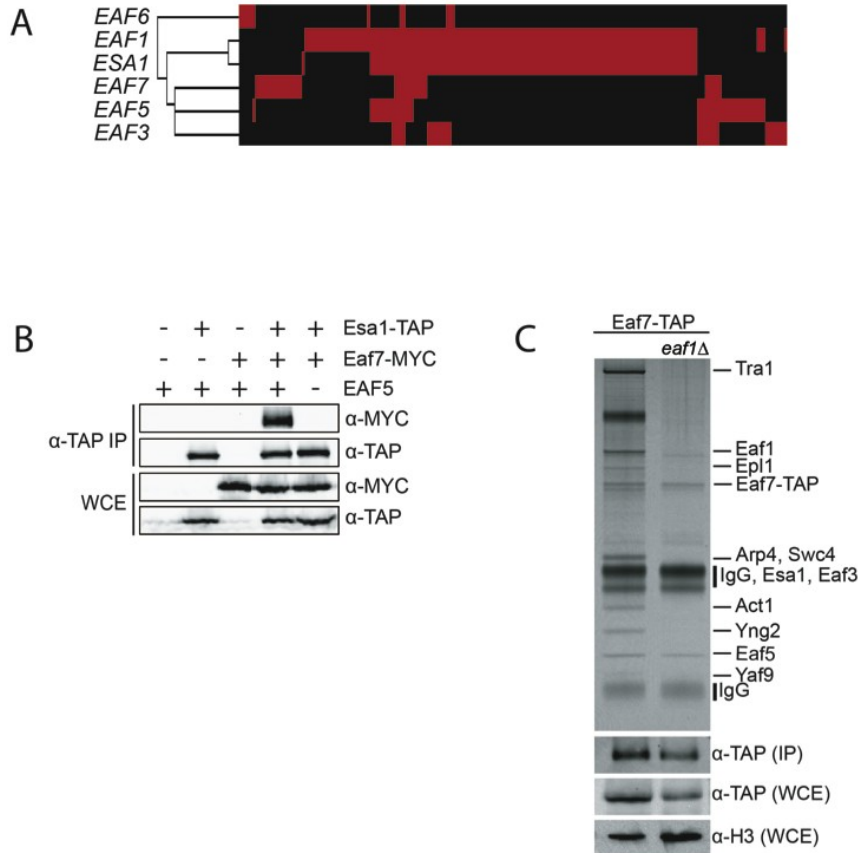


Figure 2.6: Eaf5 and Eaf7 form a sub-complex within NuA4.

(A) Two-dimensional, hierarchical clustering of the NuA4 synthetic genetic interactions. Rows display NuA4 query genes, columns indicate the interacting deletion mutant array genes, and a red box indicates genetic interaction. The cluster includes genetic interactions for the *esa1-L254P* mutant, which were directly tested against all *eaf1Δ* genetic interactions. (B) Eaf7 interacts with NuA4 through Eaf5. Shown are results with protein extracts prepared from strains expressing the indicated tagged proteins (Esa1-TAP [YKB440], Eaf7-Myc [YKB518], Esa1-TAP Eaf7-Myc [YKB1054], and Esa1-TAP Eaf7-Myc *eaf5Δ* [YKB1043]) or an untagged WT (YPH499); immunoprecipitations were performed using magnetic beads coated with IgG antibodies that bind the PrA component of the TAP tag. Total protein extracts (WCE) and anti-TAP immunoprecipitates (IP) were then resolved by 7.5% SDS-PAGE and subjected to Western blot analysis with anti-Myc and anti-TAP antibodies, as indicated on the right side of the panels. α , anti. (C) Eaf7 and Eaf5 form a sub-complex in the absence of Eaf1. SDS-PAGE (gradient gel) and silver staining of NuA4 affinity purified with Eaf7-TAP in the presence (YKB442) and absence (*eaf1Δ*) of Eaf1 (YKB1034). Anti-TAP Western blotting was carried out on WCE as well as on 10% of the IP eluate. An anti-histone H3 (α -H3) Western blot analysis of WCE demonstrates equal protein loadings. The results are representative of three independent purifications.

by Western blotting. We purified the NuA4 complex using Esa1-TAP and found that the *eaf5Δ* mutant disrupted the interaction of Eaf7-Myc with the NuA4 complex (Figure 2.6B). We were next interested in determining whether Eaf7 and Eaf5 form a detectable sub-complex in the absence of NuA4. To explore this, we TAP tagged Eaf7 and studied whether the Eaf5-Eaf7 sub-complex would still form in the absence of Eaf1, which eliminates the full NuA4 complex. We found that while all of the other NuA4 subunits were lost as a result of the Eaf1 deletion, the physical interaction of Eaf7 with Eaf5 remained intact (Figure 2.6C). Taken together, these results indicate the presence of a novel sub-complex forming between Eaf5 and Eaf7 within the NuA4 complex and, moreover, that Eaf7 interacts with NuA4 through Eaf5.

2.5 Discussion

2.5.1 NuA4 is a genetic hub

In an effort to further define the cellular functions of NuA4 and provide insight into the function of individual NuA4 subunits, we performed genome-wide SL-SGA analysis with five non-essential subunits of NuA4. With the inclusion of previously confirmed genetic interactions, the combined data set contains 268 genetic interactions among 204 genes (Figure 2.1). The most remarkable feature of the genetic interaction map is that the *eaf1Δ* query mutant accounted for 148 genetic interactions alone, which is more than four times greater than the average number of interactions per query mutant in other genome-wide screens (64). Further, the genes identified by the *eaf1Δ* mutant were not limited to genes with roles in chromatin biology previously linked to NuA4; rather, the genetic interaction

profile for the *eaf1Δ* mutant indicates new and diverse functional relationships for NuA4, such as protein transport, arginine biosynthesis, stress response, and ubiquitination (Figure 2.1). Though it is possible that Eaf1 has cellular functions outside NuA4, the lack of additional protein interactions (Figure 2.2) and the high degree of overlap in genetic interaction profiles between *eaf1Δ* and *esa1-L254P* cells (Figure 2.6A; see Supplemental Table 2 at www.oisb.ca/personal_web_site/Baetz_Lab/publicationsFS.html) strongly suggest that the sole function of Eaf1 is as a component of NuA4. Of the few *eaf1Δ* mutant genetic interactions that were not shared with *esa1-L254P*, it is possible that the interactions occur at higher temperatures or with other *esa1* alleles. As *Esa1* is essential and part of Piccolo NuA4, *esa1* mutants will likely display numerous genetic interactions distinct from that of the *eaf1Δ* mutant. Regardless, the large number of interactions identified for both *eaf1Δ* and *esa1-L254P* indicates that these are “hub genes” (64). It has been hypothesized that highly connected genetic hub genes are more important for cellular fitness, are more likely to encode essential genes, and are highly conserved across species (14, 36, 64). Genetic hub genes may act as genetic buffers because the loss of hub genes causes an enhancement of mutant phenotypes in otherwise unconnected, diverse cellular functions. This may explain the identification of seemingly disparate genes in the *eaf1Δ* SL-SGA screen. Recently, systematic mapping of genetic interactions in *C. elegans* identified numerous genes encoding chromatin-modifying proteins as genetic hubs, including *mys-1* and *trr-1*, the orthologs of *ESA1* and *TRA1*,

respectively (36). This indicates that NuA4/Tip60 mutants likely act as genetic hubs across species.

How might NuA4 and other chromatin modifiers act as global genetic buffers? The most likely scenario is that a loss of function of NuA4 leads to global changes in acetylation patterns of histones, which subsequently affects transcription. NuA4 mutants alone display relatively minor effects on global transcriptional profiles, as detected in microarray studies (11, 19, 27, 31, 34, 69). However, these transcriptional deficiencies in combination with other mutant genes may result in a dramatic enhancement of phenotypes or fitness defects. For example, we determined that non-essential NuA4 mutants display SS or SL interactions with mutant genes encoding proteins required for arginine biosynthesis (Figure 2.1). Microarray studies have shown that NuA4 mutants display modest two- to three-fold decreases in the transcription of numerous genes in the arginine biosynthesis pathway (11, 19, 31, 34). While the deletion of single genes of this pathway does not result in fitness defects, we suspect that this deletion in combination with decreases in the NuA4-dependent transcription of arginine pathway genes results in fitness defects. Moreover, we hypothesize that NuA4 buffers the effects of the vesicle-mediated transport mutants in a similar manner. Microarray studies of NuA4 or *htz1Δ* mutants (11, 19, 27, 30, 31, 34, 41, 42, 69) provide no insights into the transcriptional mis-regulation of the key gene(s) required for vesicle-mediated transport. However, as *htz1Δ* cells display genetic interactions and vacuolar morphological defects similar to those of *eaf1Δ* and *esa1-L254P* cells (Figure 2.3), we favour a model where NuA4's and Htz1's roles

as genetic buffers are through transcriptional effects. As *htz1-ND* mutants do not display vacuolar morphological defects, it is likely that NuA4's transcriptional effects are not mediated through Htz1 N-terminal tail acetylation but rather through H4 acetylation or alternative targets. Further, numerous strains containing deletions of NuA4, SWR complex, and *HTZ1* genes were identified in a high-throughput screen aimed at identifying diploid, homozygous deletion mutants with carboxypeptidase Y vacuolar sorting defects (6).

Genetic hubs are thought to be major contributors to complex genetic diseases arising from multiple mutations (9). Mutations in genetic hubs may modify the effects of numerous mutations, resulting in the implication of genetic hub genes in a diverse range of apparently unrelated diseases. As mutant components of NuA4/Tip60s in both yeast and *C. elegans* act as genetic hubs, it is likely that this trait is shared with human Tip60. If Tip60 is a genetic hub, it would explain the connection of Tip60 with pleiotropic roles in a diverse range of cancers, neurodegenerative diseases, and viral infections (51). Insights derived from the NuA4 genetic map presented in this paper, along with extension of the map using mutant alleles of essential NuA4 genes, will provide an excellent source of testable hypotheses for determining the exact molecular mechanisms through which Tip60 may contribute to clinical pathology.

2.5.2 NuA4 as a transcriptional repressor

Traditionally, it has been proposed that HAT acetylation of histones is correlated with transcriptional activation and that HDAC deacetylation of histones is correlated with transcriptional repression (33). While NuA4 is required for

transcriptional activation, growing evidence indicates that NuA4 also has a role in the transcriptional repression of a subset of Msn2/4-dependent stress-responsive genes, including *HSP12* (Figure 2.4D) (25, 37). In our study, the identification of 10 genes involved in the stress response in the NuA4 SL-SGA screen (Figure 2.1) and the identification of a physical interaction between Msn4 and NuA4 (Figure 2.4A and B) further support the role of NuA4 in the stress response.

How might NuA4 repress the Msn2/4-dependent transcription of stress response genes? Microarray studies indicate that de-repression of the subset of Msn2/4-dependent genes also occurs in *HTZ1* deletion mutants (41, 43) and histone H4 mutants defective in N-terminal acetylation (15), suggesting that NuA4 could mediate the repression of these genes through the acetylation of these two histones. We do not believe that NuA4 acetylation of histones inhibits the access of Msn2 and/or Msn4 to stress-dependent promoters, as we reproducibly detect Msn4 occupancy at the *HSP12* promoter under non-stress conditions and moreover show that the deletion of *EAF1* does not result in increased Msn4 localization to this promoter (Figure 2.4C). Though it is possible that the localization of Msn4 to *HSP12* promoters is dependent on Piccolo NuA4, which appears to be present in an *eaf1Δ* strain, we believe that this is unlikely, as there is presently no evidence of targeted Piccolo NuA4 activity. Alternatively, the physical interaction between Msn2/4 and NuA4 may target NuA4 histone acetylation to promoters to promote a repressed chromatin state through the recruitment of chromatin remodelers or repressors. Despite multiple ChIP attempts, we were not able to reproducibly determine whether or not Esa1-TAP localization to the *HSP12* promoter is changed

in *msn2Δ/msn4Δ* strains. NuA4 may also directly acetylate Msn4 or Msn2, thereby masking activation domains or regulating additional protein interactions required for the activation or repression of Msn2/4-dependent genes. This may explain the role of the physical interactions seen between NuA4 and Msn2 and/or Msn4. Surprisingly, though *HSP12* heat shock induction has been shown to be largely dependent on Msn2/4, in *eaf1Δ/msn2Δ/msn4Δ* cells, *HSP12* is still induced upon heat shock (Figure 2.4D). This suggests that alternative transcription factors, such as Hsf1 (49), may play a significant role in the absence of NuA4. Unraveling the mysteries of the molecular function of NuA4 in Msn2/4-dependent gene repression will require further in-depth study.

2.5.3 NuA4 complex structure and function

Though it has been proposed that genes encoding proteins in the same pathway or complex should have similar synthetic genetic interactions, a surprising feature of our NuA4 genetic map was the dramatic difference in the numbers of interactions for components and in some cases the lack of overlap between the queries. As genetic interactions that were identified in one screen were not directly tested against all the queries, some of the lack of overlap may be explained by the inherent rate of false negative results of SL-SGA screening. In the case of the *eaf3Δ* and *eaf6Δ* screens, some of the unique genetic interactions may be the result of the Eaf3 and Eaf6 proteins also being part of the Rpd3S and NuA3 complexes, respectively (10, 27, 60). However, in the case of the *eaf1Δ* mutant, the striking number of genetic interactions displayed is likely reflective of the role that Eaf1 plays in NuA4 complex integrity. We determined that in the absence of

Eaf1, the full NuA4 complex collapses (Figures 2.5 and 2.6). Despite the dramatic effect on NuA4 complex integrity, *EAF1* is not an essential gene. This is likely a reflection of the fact that in the absence of Eaf1, Piccolo NuA4 is still detected (Figures 2.5). Piccolo NuA4 contains the only two essential NuA4 proteins, Esa1 and Epl1, that are exclusively found in NuA4, and as previously suggested, Piccolo NuA4 likely mediates the essential non-targeted global acetylation of the histones of NuA4 (7). However, with Eaf1 being a scaffold protein, the diverse genetic interactions identified in the *eaf1Δ* screen may reflect the sum of the proposed recruitment roles of the remaining 10 non-Piccolo NuA4 subunits. Alternatively, Eaf1 may perform unique recruitment or regulatory roles that are not shared with the other nine subunits. The clustering of our genome-wide NuA4 genetic interactions (Figure 2.6A; supplementary cluster Treeview files are available at www.oisb.ca/personal_web_site/Baetz_Lab/publicationsFS.html) and the chromatin E-MAP (13) allowed us to make predictions regarding a possible sub-complex involving Eaf5 and Eaf7. We confirmed that Eaf5 and Eaf7 form a sub-complex and that Eaf7 interacts with the NuA4 complex through Eaf5 (Figure 2.6B and 2.6C). The genetic network also predicts that Eaf3 may be a component of this sub-complex. Work from Jacques Côté's laboratory has confirmed an Eaf3-Eaf5-Eaf7 sub-complex (personal communication). Though we presently do not know if the sub-complex is purely structural in nature, it is likely that it mediates a distinct set of NuA4 cellular functions. As the majority of the genetic interactions shared between the *eaf3Δ*, *eaf5Δ*, and *eaf7Δ* mutants are with SWR complex mutants or the *htz1Δ* mutant, this suggests that the sub-complex performs a function distinct

from NuA4's role in Htz1 acetylation. This idea is further solidified by the fact that *eaf3Δ*, *eaf5Δ*, and *eaf7Δ* mutants do not display mutant phenotypes that are shared with SWR complex, *HTZ1*, and other NuA4 mutants implicated in Htz1 acetylation. For example, *eaf3Δ*, *eaf5Δ*, and *eaf7Δ* mutants display either no or only modest increases in chromosome segregation defects (31) (data not shown), are not sensitive to Benomyl (31), are not defective in Htz1 K14 acetylation (28), and do not display defects in vacuole morphology as detected with FM4-64 (Figure 2.3A). As *eaf5Δ*, and *eaf7Δ* mutants have similar effects on gene expression (31), it is likely that the Eaf3-Eaf5-Eaf7 sub-complex is required for a distinct subset of NuA4 cellular functions, possibly through the recruitment of NuA4 to distinct chromatin loci. Our work indicates that genome-wide genetic interaction maps not only provide valuable insights into query gene function and complex composition but also may be extremely useful in discerning structural integrity and sub-complexes of large, multi-subunit protein complexes. It will be interesting to see whether additional SGA screens using mutants with point or domain mutations in NuA4 genes that specifically abolish protein interactions will provide greater insight into the function of each NuA4 subunit.

2.6 Acknowledgements

We thank M. C. Keogh, J. Dillingham, and J. Greenblatt for providing yeast strains; M. C. Keogh, V. Measday, and members of the Baetz laboratory for helpful discussion and critical reading of the manuscript; A. Rudner and M. C. Keogh for technical support; and J. Côté for communicating results prior to publication. This work was supported by operating grants from the National Cancer Institute of Canada through funds raised by the Terry Fox Research Foundation and an Early Research Award from the Ontario Government (to K.B.). Funding was also received from the Canada Foundation for Innovation, Natural Sciences and Engineering Research Council of Canada; the Canadian Institute of Health Research (CIHR); the Heart and Stroke Foundation of Ontario Centre for Stroke Recovery; La Fondation Jean-Louis Lesveque; and the Ontario Government (to D.F.). K.B. is a Canada Research Chair in Chemical and Functional Genomics. D.F. is a Canada Research Chair in Proteomics and Systems Biology. L.M. was supported by an Ontario Graduate Student Award and a CIHR Doctoral Award. J.-P.L. was supported by an Ontario Graduate Student Award. I.S.S. was supported by a Canadian Institute of Aging Investigator Award. A.S.A.-M. was supported by an Ontario Women's Health Council/CIHR Institute of Gender and Health Fellowship.

2.7 Supplemental

Three supplemental files associated with this manuscript may be found online at www.oisb.ca/personal_web_site/Baetz_Lab/publicationsFS.html

- Supplemental Table 1: NuA4 genetic interactions
- Supplemental Table 2: *ESA1* genetic interactions
- Supplemental File: Clustering information

2.8 References

1. **Allard, S., R. T. Utley, J. Savard, A. Clarke, P. Grant, C. J. Brandl, L. Pillus, J. L. Workman, and J. Cote.** 1999. NuA4, an essential transcription adaptor/histone H4 acetyltransferase complex containing Esa1p and the ATM-related cofactor Tra1p. *Embo J* **18**:5108-5119.
2. **Babiarz, J. E., J. E. Halley, and J. Rine.** 2006. Telomeric heterochromatin boundaries require NuA4-dependent acetylation of histone variant H2A.Z in *Saccharomyces cerevisiae*. *Genes Dev* **20**:700-710.
3. **Baetz, K., J. Moffat, J. Haynes, M. Chang, and B. Andrews.** 2001. Transcriptional coregulation by the cell integrity mitogen-activated protein kinase Slt2 and the cell cycle regulator Swi4. *Mol Cell Biol* **21**:6515-6528.
4. **Bird, A. W., D. Y. Yu, M. G. Pray-Grant, Q. Qiu, K. E. Harmon, P. C. Megee, P. A. Grant, M. M. Smith, and M. F. Christman.** 2002. Acetylation of histone H4 by Esa1 is required for DNA double-strand break repair. *Nature* **419**:411-415.
5. **Bittner, C. B., D. T. Zeisig, B. B. Zeisig, and R. K. Slany.** 2004. Direct physical and functional interaction of the NuA4 complex components Yaf9p and Swc4p. *Eukaryot Cell* **3**:976-983.
6. **Bonangelino, C. J., E. M. Chavez, and J. S. Bonifacino.** 2002. Genomic screen for vacuolar protein sorting genes in *Saccharomyces cerevisiae*. *Mol Biol Cell* **13**:2486-2501.
7. **Boudreault, A. A., D. Cronier, W. Selleck, N. Lacoste, R. T. Utley, S. Allard, J. Savard, W. S. Lane, S. Tan, and J. Cote.** 2003. Yeast enhancer of polycomb defines global Esa1-dependent acetylation of chromatin. *Genes Dev* **17**:1415-1428.
8. **Brown, C. E., L. Howe, K. Sousa, S. C. Alley, M. J. Carrozza, S. Tan, and J. L. Workman.** 2001. Recruitment of HAT complexes by direct activator interactions with the ATM-related Tra1 subunit. *Science* **292**:2333-2337.
9. **Bussey, H., B. Andrews, and C. Boone.** 2006. From worm genetic networks to complex human diseases. *Nat Genet* **38**:862-863.
10. **Carrozza, M. J., B. Li, L. Florens, T. Suganuma, S. K. Swanson, K. K. Lee, W. J. Shia, S. Anderson, J. Yates, M. P. Washburn, and J. L. Workman.** 2005. Histone H3 methylation by Set2 directs deacetylation of coding regions by Rpd3S to suppress spurious intragenic transcription. *Cell* **123**:581-592.
11. **Choy, J. S., and S. J. Kron.** 2002. NuA4 subunit Yng2 function in intra-S-phase DNA damage response. *Mol Cell Biol* **22**:8215-8225.

12. **Clarke, A. S., J. E. Lowell, S. J. Jacobson, and L. Pillus.** 1999. Esa1p is an essential histone acetyltransferase required for cell cycle progression. *Mol Cell Biol* **19**:2515-2526.
13. **Collins, S. R., K. M. Miller, N. L. Maas, A. Roguev, J. Fillingham, C. S. Chu, M. Schuldiner, M. Gebbia, J. Recht, M. Shales, H. Ding, H. Xu, J. Han, K. Ingvarsdottir, B. Cheng, B. Andrews, C. Boone, S. L. Berger, P. Hieter, Z. Zhang, G. W. Brown, C. J. Ingles, A. Emili, C. D. Allis, D. P. Toczyski, J. S. Weissman, J. F. Greenblatt, and N. J. Krogan.** 2007. Functional dissection of protein complexes involved in yeast chromosome biology using a genetic interaction map. *Nature* **446**:806-810.
14. **Davierwala, A. P., J. Haynes, Z. Li, R. L. Brost, M. D. Robinson, L. Yu, S. Mnaimneh, H. Ding, H. Zhu, Y. Chen, X. Cheng, G. W. Brown, C. Boone, B. J. Andrews, and T. R. Hughes.** 2005. The synthetic genetic interaction spectrum of essential genes. *Nat Genet* **37**:1147-1152.
15. **Dion, M. F., S. J. Altschuler, L. F. Wu, and O. J. Rando.** 2005. Genomic characterization reveals a simple histone H4 acetylation code. *Proc Natl Acad Sci U S A* **102**:5501-5506.
16. **Downs, J. A., S. Allard, O. Jobin-Robitaille, A. Javaheri, A. Auger, N. Bouchard, S. J. Kron, S. P. Jackson, and J. Cote.** 2004. Binding of chromatin-modifying activities to phosphorylated histone H2A at DNA damage sites. *Mol Cell* **16**:979-990.
17. **Doyon, Y., and J. Cote.** 2004. The highly conserved and multifunctional NuA4 HAT complex. *Curr Opin Genet Dev* **14**:147-154.
18. **Doyon, Y., W. Selleck, W. S. Lane, S. Tan, and J. Cote.** 2004. Structural and functional conservation of the NuA4 histone acetyltransferase complex from yeast to humans. *Mol Cell Biol* **24**:1884-1896.
19. **Durant, M., and B. F. Pugh.** 2006. Genome-wide relationships between TAF1 and histone acetyltransferases in *Saccharomyces cerevisiae*. *Mol Cell Biol* **26**:2791-2802.
20. **Eberharter, A., S. John, P. A. Grant, R. T. Utley, and J. L. Workman.** 1998. Identification and analysis of yeast nucleosomal histone acetyltransferase complexes. *Methods* **15**:315-321.
21. **Eisen, A., R. T. Utley, A. Nourani, S. Allard, P. Schmidt, W. S. Lane, J. C. Lucchesi, and J. Cote.** 2001. The yeast NuA4 and *Drosophila* MSL complexes contain homologous subunits important for transcription regulation. *J Biol Chem* **276**:3484-3491.
22. **Gavin, A. C., P. Aloy, P. Grandi, R. Krause, M. Boesche, M. Marzioch, C. Rau, L. J. Jensen, S. Bastuck, B. Dumpelfeld, A. Edlmann, M. A. Heurtier, V. Hoffman, C. Hoefert, K. Klein, M. Hudak, A. M. Michon, M. Schelder, M. Schirle, M. Remor, T. Rudi, S. Hooper, A. Bauer, T. Bouwmeester, G. Casari, G. Drewes, G. Neubauer, J. M. Rick, B.**

- Kuster, P. Bork, R. B. Russell, and G. Superti-Furga.** 2006. Proteome survey reveals modularity of the yeast cell machinery. *Nature* **440**:631-636.
23. **Glozak, M. A., N. Sengupta, X. Zhang, and E. Seto.** 2005. Acetylation and deacetylation of non-histone proteins. *Gene* **363**:15-23.
24. **Gorner, W., E. Durchschlag, M. T. Martinez-Pastor, F. Estruch, G. Ammerer, B. Hamilton, H. Ruis, and C. Schuller.** 1998. Nuclear localization of the C2H2 zinc finger protein Msn2p is regulated by stress and protein kinase A activity. *Genes Dev* **12**:586-597.
25. **Gorzer, I., C. Schuller, E. Heidenreich, L. Krupanska, K. Kuchler, and U. Wintersberger.** 2003. The nuclear actin-related protein Act3p/Arp4p of *Saccharomyces cerevisiae* is involved in transcription regulation of stress genes. *Mol Microbiol* **50**:1155-1171.
26. **Jahn, R., and R. H. Scheller.** 2006. SNAREs--engines for membrane fusion. *Nat Rev Mol Cell Biol* **7**:631-643.
27. **Keogh, M. C., S. K. Kurdistani, S. A. Morris, S. H. Ahn, V. Podolny, S. R. Collins, M. Schuldiner, K. Chin, T. Punna, N. J. Thompson, C. Boone, A. Emili, J. S. Weissman, T. R. Hughes, B. D. Strahl, M. Grunstein, J. F. Greenblatt, S. Buratowski, and N. J. Krogan.** 2005. Cotranscriptional set2 methylation of histone H3 lysine 36 recruits a repressive Rpd3 complex. *Cell* **123**:593-605.
28. **Keogh, M. C., T. A. Mennella, C. Sawa, S. Berthelet, N. J. Krogan, A. Wolek, V. Podolny, L. R. Carpenter, J. F. Greenblatt, K. Baetz, and S. Buratowski.** 2006. The *Saccharomyces cerevisiae* histone H2A variant Htz1 is acetylated by NuA4. *Genes Dev* **20**:660-665.
29. **Klis, F. M., P. Mol, K. Hellingwerf, and S. Brul.** 2002. Dynamics of cell wall structure in *Saccharomyces cerevisiae*. *FEMS Microbiol Rev* **26**:239-256.
30. **Kobor, M. S., S. Venkatasubrahmanyam, M. D. Meneghini, J. W. Gin, J. L. Jennings, A. J. Link, H. D. Madhani, and J. Rine.** 2004. A Protein Complex Containing the Conserved Swi2/Snf2-Related ATPase Swr1p Deposits Histone Variant H2A.Z into Euchromatin. *PLoS Biol* **2**:E131.
31. **Krogan, N. J., K. Baetz, M. C. Keogh, N. Datta, C. Sawa, T. C. Kwok, N. J. Thompson, M. G. Davey, J. Pootoolal, T. R. Hughes, A. Emili, S. Buratowski, P. Hieter, and J. F. Greenblatt.** 2004. Regulation of chromosome stability by the histone H2A variant Htz1, the Swr1 chromatin remodeling complex, and the histone acetyltransferase NuA4. *Proc Natl Acad Sci U S A*.
32. **Krogan, N. J., G. Cagney, H. Yu, G. Zhong, X. Guo, A. Ignatchenko, J. Li, S. Pu, N. Datta, A. P. Tikuisis, T. Punna, J. M. Peregrin-Alvarez, M. Shales, X. Zhang, M. Davey, M. D. Robinson, A. Paccanaro, J. E. Bray, A. Sheung, B. Beattie, D. P. Richards, V. Canadien, A. Lalev, F. Mena, P. Wong, A. Starostine, M. M. Canete, J. Vlasblom, S. Wu, C. Orsi, S. R.**

- Collins, S. Chandran, R. Haw, J. J. Rilstone, K. Gandi, N. J. Thompson, G. Musso, P. St Onge, S. Ghanny, M. H. Lam, G. Butland, A. M. Altaf-Ul, S. Kanaya, A. Shilatifard, E. O'Shea, J. S. Weissman, C. J. Ingles, T. R. Hughes, J. Parkinson, M. Gerstein, S. J. Wodak, A. Emili, and J. F. Greenblatt.** 2006. Global landscape of protein complexes in the yeast *Saccharomyces cerevisiae*. *Nature* **440**:637-643.
33. **Kurdistani, S. K., and M. Grunstein.** 2003. Histone acetylation and deacetylation in yeast. *Nat Rev Mol Cell Biol* **4**:276-284.
34. **Le Masson, I., D. Y. Yu, K. Jensen, A. Chevalier, R. Courbeyrette, Y. Boulard, M. M. Smith, and C. Mann.** 2003. Yaf9, a novel NuA4 histone acetyltransferase subunit, is required for the cellular response to spindle stress in yeast. *Mol Cell Biol* **23**:6086-6102.
35. **Lee, K. K., and J. L. Workman.** 2007. Histone acetyltransferase complexes: one size doesn't fit all. *Nat Rev Mol Cell Biol* **8**:284-295.
36. **Lehner, B., C. Crombie, J. Tischler, A. Fortunato, and A. G. Fraser.** 2006. Systematic mapping of genetic interactions in *Caenorhabditis elegans* identifies common modifiers of diverse signaling pathways. *Nat Genet* **38**:896-903.
37. **Lindstrom, K. C., J. C. Vary, Jr., M. R. Parthun, J. Delrow, and T. Tsukiyama.** 2006. Isw1 functions in parallel with the NuA4 and Swr1 complexes in stress-induced gene repression. *Mol Cell Biol* **26**:6117-6129.
38. **Longtine, M. S., A. McKenzie, 3rd, D. J. Demarini, N. G. Shah, A. Wach, A. Brachat, P. Philippsen, and J. R. Pringle.** 1998. Additional modules for versatile and economical PCR-based gene deletion and modification in *Saccharomyces cerevisiae*. *Yeast* **14**:953-961.
39. **Martinez-Pastor, M. T., G. Marchler, C. Schuller, A. Marchler-Bauer, H. Ruis, and F. Estruch.** 1996. The *Saccharomyces cerevisiae* zinc finger proteins Msn2p and Msn4p are required for transcriptional induction through the stress response element (STRE). *EMBO J* **15**:2227-2235.
40. **Measday, V., K. Baetz, J. Guzzo, K. Yuen, T. Kwok, B. Sheikh, H. Ding, R. Ueta, T. Hoac, B. Cheng, I. Pot, A. Tong, Y. Yamaguchi-Iwai, C. Boone, P. Hieter, and B. Andrews.** 2005. Systematic yeast synthetic lethal and synthetic dosage lethal screens identify genes required for chromosome segregation. *Proc Natl Acad Sci U S A* **102**:13956-13961.
41. **Meneghini, M. D., M. Wu, and H. D. Madhani.** 2003. Conserved histone variant H2A.Z protects euchromatin from the ectopic spread of silent heterochromatin. *Cell* **112**:725-736.
42. **Millar, C. B., F. Xu, K. Zhang, and M. Grunstein.** 2006. Acetylation of H2AZ Lys 14 is associated with genome-wide gene activity in yeast. *Genes Dev* **20**:711-722.

43. **Mizuguchi, G., X. Shen, J. Landry, W. H. Wu, S. Sen, and C. Wu.** 2004. ATP-driven exchange of histone H2AZ variant catalyzed by SWR1 chromatin remodeling complex. *Science* **303**:343-348.
44. **Oka, T., and M. Krieger.** 2005. Multi-component protein complexes and Golgi membrane trafficking. *J Biochem (Tokyo)* **137**:109-114.
45. **Pan, X., P. Ye, D. S. Yuan, X. Wang, J. S. Bader, and J. D. Boeke.** 2006. A DNA integrity network in the yeast *Saccharomyces cerevisiae*. *Cell* **124**:1069-1081.
46. **Pfeffer, S., and D. Aivazian.** 2004. Targeting Rab GTPases to distinct membrane compartments. *Nat Rev Mol Cell Biol* **5**:886-896.
47. **Puig, O., F. Caspary, G. Rigaut, B. Rutz, E. Bouveret, E. Bragado-
Nilsson, M. Wilm, and B. Seraphin.** 2001. The tandem affinity purification (TAP) method: a general procedure of protein complex purification. *Methods* **24**:218-229.
48. **Reguly, T., A. Breitkreutz, L. Boucher, B. J. Breitkreutz, G. C. Hon, C. L. Myers, A. Parsons, H. Friesen, R. Oughtred, A. Tong, C. Stark, Y. Ho, D. Botstein, B. Andrews, C. Boone, O. G. Troyanskaya, T. Ideker, K. Dolinski, N. N. Batada, and M. Tyers.** 2006. Comprehensive curation and analysis of global interaction networks in *Saccharomyces cerevisiae*. *J Biol* **5**:11.
49. **Reid, J. L., V. R. Iyer, P. O. Brown, and K. Struhl.** 2000. Coordinate regulation of yeast ribosomal protein genes is associated with targeted recruitment of Esa1 histone acetylase. *Mol Cell* **6**:1297-1307.
50. **Sanchez, C., I. Sanchez, J. A. Demmers, P. Rodriguez, J. Strouboulis, and M. Vidal.** 2007. Proteomics Analysis of Ring1B/Rnf2 Interactors Identifies a Novel Complex with the Fbxl10/Jhdm1B Histone Demethylase and the Bcl6 Interacting Corepressor. *Mol Cell Proteomics* **6**:820-834.
51. **Sapountzi, V., I. R. Logan, and C. N. Robson.** 2006. Cellular functions of TIP60. *Int J Biochem Cell Biol* **38**:1496-1509.
52. **Schmitt, A. P., and K. McEntee.** 1996. Msn2p, a zinc finger DNA-binding protein, is the transcriptional activator of the multistress response in *Saccharomyces cerevisiae*. *Proc Natl Acad Sci U S A* **93**:5777-5782.
53. **Schmitt, M. E., T. A. Brown, and B. L. Trumpower.** 1990. A rapid and simple method for preparation of RNA from *Saccharomyces cerevisiae*. *Nucleic Acids Res* **18**:3091-3092.
54. **Seeley, E. S., M. Kato, N. Margolis, W. Wickner, and G. Eitzen.** 2002. Genomic analysis of homotypic vacuole fusion. *Mol Biol Cell* **13**:782-794.
55. **Selleck, W., I. Fortin, D. Sermwittayawong, J. Cote, and S. Tan.** 2005. The *Saccharomyces cerevisiae* Piccolo NuA4 histone acetyltransferase complex requires the Enhancer of Polycomb A domain and chromodomain to acetylate nucleosomes. *Mol Cell Biol* **25**:5535-5542.

56. **Shevchenko, A., O. N. Jensen, A. V. Podtelejnikov, F. Sagliocco, M. Wilm, O. Vorm, P. Mortensen, A. Shevchenko, H. Boucherie, and M. Mann.** 1996. Linking genome and proteome by mass spectrometry: large-scale identification of yeast proteins from two dimensional gels. *Proc Natl Acad Sci U S A* **93**:14440-14445.
57. **Sikorski, R. S., and P. Hieter.** 1989. A system of shuttle vectors and yeast host strains designed for efficient manipulation of DNA in *Saccharomyces cerevisiae*. *Genetics* **122**:19-27.
58. **Smith, E. R., A. Eisen, W. Gu, M. Sattah, A. Pannuti, J. Zhou, R. G. Cook, J. C. Lucchesi, and C. D. Allis.** 1998. ESA1 is a histone acetyltransferase that is essential for growth in yeast. *Proc Natl Acad Sci U S A* **95**:3561-3565.
59. **Squatrito, M., C. Gorrini, and B. Amati.** 2006. Tip60 in DNA damage response and growth control: many tricks in one HAT. *Trends Cell Biol* **16**:433-442.
60. **Taverna, S. D., S. Ilin, R. S. Rogers, J. C. Tanny, H. Lavender, H. Li, L. Baker, J. Boyle, L. P. Blair, B. T. Chait, D. J. Patel, J. D. Aitchison, A. J. Tackett, and C. D. Allis.** 2006. Yng1 PHD finger binding to H3 trimethylated at K4 promotes NuA3 HAT activity at K14 of H3 and transcription at a subset of targeted ORFs. *Mol Cell* **24**:785-796.
61. **Thomas, T., and A. K. Voss.** 2007. The diverse biological roles of MYST histone acetyltransferase family proteins. *Cell Cycle* **6**:696-704.
62. **Tong, A. H., and C. Boone.** 2006. Synthetic genetic array analysis in *Saccharomyces cerevisiae*. *Methods Mol Biol* **313**:171-192.
63. **Tong, A. H., M. Evangelista, A. B. Parsons, H. Xu, G. D. Bader, N. Page, M. Robinson, S. Raghizadeh, C. W. Hogue, H. Bussey, B. Andrews, M. Tyers, and C. Boone.** 2001. Systematic genetic analysis with ordered arrays of yeast deletion mutants. *Science* **294**:2364-2368.
64. **Tong, A. H., G. Lesage, G. D. Bader, H. Ding, H. Xu, X. Xin, J. Young, G. F. Berriz, R. L. Brost, M. Chang, Y. Chen, X. Cheng, G. Chua, H. Friesen, D. S. Goldberg, J. Haynes, C. Humphries, G. He, S. Hussein, L. Ke, N. Krogan, Z. Li, J. N. Levinson, H. Lu, P. Menard, C. Munyana, A. B. Parsons, O. Ryan, R. Tonikian, T. Roberts, A. M. Sdicu, J. Shapiro, B. Sheikh, B. Suter, S. L. Wong, L. V. Zhang, H. Zhu, C. G. Burd, S. Munro, C. Sander, J. Rine, J. Greenblatt, M. Peter, A. Bretscher, G. Bell, F. P. Roth, G. W. Brown, B. Andrews, H. Bussey, and C. Boone.** 2004. Global mapping of the yeast genetic interaction network. *Science* **303**:808-813.
65. **Ungar, D., T. Oka, M. Krieger, and F. M. Hughson.** 2006. Retrograde transport on the COG railway. *Trends Cell Biol* **16**:113-120.
66. **Vida, T. A., and S. D. Emr.** 1995. A new vital stain for visualizing vacuolar membrane dynamics and endocytosis in yeast. *J Cell Biol* **128**:779-792.

67. **Wu, W. H., S. Alami, E. Luk, C. H. Wu, S. Sen, G. Mizuguchi, D. Wei, and C. Wu.** 2005. Swc2 is a widely conserved H2AZ-binding module essential for ATP-dependent histone exchange. *Nat Struct Mol Biol* **12**:1064-1071.
68. **Yang, X., R. Zaurin, M. Beato, and C. L. Peterson.** 2007. Swi3p controls SWI/SNF assembly and ATP-dependent H2A-H2B displacement. *Nat Struct Mol Biol* **14**:540-547.
69. **Zhang, H., D. O. Richardson, D. N. Roberts, R. Utlej, H. Erdjument-Bromage, P. Tempst, J. Cote, and B. R. Cairns.** 2004. The Yaf9 component of the SWR1 and NuA4 complexes is required for proper gene expression, histone H4 acetylation, and Htz1 replacement near telomeres. *Mol Cell Biol* **24**:9424-9436.

CHAPTER 3:

A NuA4 SDL screen reveals that septin proteins are acetylated and that multiple KATs regulate septin dynamics

Leslie Mitchell^{1,2}, Andrea Lau^{1,2}, Jean-Philippe Lambert^{1,2}, Hu Zhou^{1,2}, Ying Fong^{1,2}, Jean-François Couture^{1,2}, Daniel Figeys^{1,2}, and Kristin Baetz^{1,2}

¹ Ottawa Institute of Systems Biology, University of Ottawa, Ottawa, Ontario K1H8M5, Canada

² Department of Biochemistry, Microbiology and Immunology, University of Ottawa, Ottawa, Ontario K1H8M5 Canada

Contribution of Authors: AL and YF performed the SDL screens and confirmation of all hits. LM performed the rest of the experiments. J-PL and HZ performed the mass spectrometry in the laboratory of DF. J-FC contributed critical structure-function analysis of septin proteins to predict sites of acetylation undetectable by mass spectrometry. LM created all the figures and wrote the manuscript with review by KB.

3.1 Abstract

In the budding yeast *Saccharomyces cerevisiae*, the lysine acetyltransferase NuA4 has been linked to a host of cellular processes through the acetylation of both histone and non-histone targets. To discover proteins that may be regulated by NuA4-dependent acetylation, we performed genome-wide synthetic dosage lethal screens to identify genes whose overexpression is toxic to non-essential NuA4 deletion mutants. The resulting genetic network identified a novel link between NuA4 and septin proteins, a group of highly conserved GTP-binding proteins that function in cytokinesis. We show that acetyltransferase-deficient NuA4 mutants have defects in septin collar formation resulting in activation of the Swe1-dependent morphogenesis checkpoint and elongated buds. We have discovered multiple sites of acetylation on four of the five yeast mitotic septins, Cdc3, Cdc10, Cdc12 and Shs1, and determined that NuA4 can acetylate all but Cdc10 *in vitro*. *In vivo* we find that septin dynamics rely on the activity of two additional lysine acetyltransferase enzymes, Gcn5 and Eco1, however only Eco1 and NuA4 impact septin acetylation levels *in vivo*. Finally, we explore the cause-effect relationship between septin acetylation and KAT function by determining that cells encoding an unacetylatable Shs1 protein have defects in septin dynamics that are highly similar to those observed in KAT mutants. These findings provide the first evidence that yeast septin proteins are acetylated and that acetylation impacts septin dynamics.

3.2 Introduction

Lysine acetylation is traditionally associated with histone proteins and the regulation of a variety of chromatin-based cellular processes (8). More recently, systematic efforts have revealed that thousands of additional proteins are acetylated *in vivo*, dramatically altering our view of the abundance of this modification and the multitude of cellular pathways it impacts (9, 31, 71, 73). The next major challenge will be to connect lysine acetyltransferase (KAT) enzymes to their substrates and target lysine residues in order to understand the biological consequences of acetylation.

NuA4 is a KAT complex in the budding yeast *S. cerevisiae* (57) whose function has been linked to a variety of processes including transcription (14), DNA repair (5), chromosome segregation (33), cell cycle control (10, 11), the stress response (36, 45), vesicle-mediated transport (45) and gluconeogenesis (34). Accordingly, the orthologous human complex, Tip60, which is highly conserved both structurally and functionally (15), is known to be misregulated in a number of human pathologies, including Alzheimer's disease (60) and cancer (68). NuA4 is a multi-subunit complex, composed of the essential catalytic subunit Esa1 (57), five other essential subunits Act1, Arp4, Epl1, Swc4, Tra1, and seven non-essential subunits Eaf1, Eaf3, Eaf5, Eaf6, Eaf7, Yaf9, and Yng2. Importantly, the non-essential proteins Eaf1 and Yng2 are each required for Esa1's acetyltransferase activity on histone targets *in vivo* (2, 30, 33) and can therefore serve as genetic tools for studying NuA4-related functions. *In vivo*, the best-characterized acetylation targets of NuA4 are histones H4 (1, 17, 57), and the H2A variant Htz1

(2, 30, 44). Surprisingly, microarray analysis indicates the role of NuA4 in regulating global gene expression is relatively minor (33, 36, 70), suggesting the diverse cellular functions of NuA4 cannot be explained by histone acetylation alone. To date, two non-histone NuA4 acetylation targets have been characterized *in vivo*, including the NuA4 subunit Yng2 (35), and the gluconeogenesis regulator Pck1 (34). Several non-histone targets have been documented *in vivo* for the human NuA4 complex, Tip60, including p53, c-myc, and ATM kinase (61, 64). Finally using a protein acetylation microarray, a broad range of both nuclear and non-nuclear proteins shown to be *in vitro* targets of NuA4 (34). The full extent and the biological consequence of NuA4 dependent *in vivo* acetylation have yet to be established.

To date, NuA4 function has been assessed extensively using genome-wide synthetic lethal (SL) genetic interaction screens (13, 26, 35, 45, 48), which highlight genetic redundancy between pairs of hypomorphic gene mutations. Though highly informative in regards to biological function, SL screens generally identify proteins that function in parallel rather than direct pathways (6). Here we have taken advantage of a new genome-wide genetic screen called synthetic dosage lethal (SDL) profiling, which systematically assesses the effect of gene overexpression in a mutant background and has been successful at identifying kinase targets (59). Our NuA4 SDL network identifies a novel link between NuA4 and septins, a group of highly conserved proteins that function in cytokinesis in many organisms (42). We discovered that acetylation-deficient NuA4 mutants have defects in septin dynamics that result in activation of the Swe1-dependent morphogenesis

checkpoint. Further, we determine that septin proteins are acetylated *in vivo*, likely by multiple KATs. Specifically we find that Shs1 acetylation *in vivo* depends on the concerted action of NuA4 and Eco1. In cells encoding an unacetylatable Shs1-HA fusion protein, bud morphology and septin localization defects are remarkably similar to those observed in KAT mutants, suggesting a direct relationship between septin acetylation and septin dynamics. Together, this work highlights acetylation as a novel form of regulation of septin dynamics and cytokinesis.

3.3 Materials and Methods

3.3.1 Yeast strains

Yeast strains used in this study are described in Table 3.1. The galactose-inducible overexpression array (59) was a gift from Brenda Andrews. Genomic deletion or epitope tag integrations made for this study were designed with PCR-amplified cassettes as previously described and confirmed by PCR analysis (39).

Table 3.1: Yeast strains

Strain	Genotype	Reference or Source
YKB779	<i>MATα ura3-52 lys2-801 ade2-101 trp1-Δ200 leu2-Δ1</i>	(53)
YKB780	<i>MATα ura3-52 lys2-801 ade2-101 trp1-Δ200 leu2-Δ1</i>	(53)
YKB622	<i>MATα can1Δ::STE2pr-Sp_his5 lyp1Δ his3Δ1 leu2Δ0 ura3Δ0 met15Δ0 eaf1Δ::NAT</i>	(33)
YKB995	<i>MATα can1Δ::STE2pr-Sp_his5 lyp1Δ his3Δ1 leu2Δ0 ura3Δ0 met15Δ0 eaf3Δ::NAT</i>	(45)
YKB852	<i>MATα can1Δ::STE2pr-Sp_his5 lyp1Δ his3Δ1 leu2Δ0 ura3Δ0 met15Δ0 eaf5Δ::NAT</i>	(33)
YKB623	<i>MATα can1Δ::STE2pr-Sp_his5 lyp1Δ his3Δ1 leu2Δ0 ura3Δ0 met15Δ0 eaf6Δ::NAT</i>	Gift from N. Krogan
YKB853	<i>MATα can1Δ::STE2pr-Sp_his5 lyp1Δ his3Δ1 leu2Δ0 ura3Δ0 met15Δ0 eaf7Δ::NAT</i>	(33)
YKB44	<i>MATα ura3-52 lys2-801 ade2-101 trp1-Δ200 leu2-Δ1 eaf1Δ::kanMX</i>	(45)
YKB1224	<i>MATα ura3-52 lys2-801 ade2-101 trp1-Δ200 leu2-Δ1 eaf1Δ::NAT</i>	This study

YKB1162	<i>MATa ura3-52 lys2-801 ade2-101 trp1-Δ200 leu2-Δ1 eaf3Δ::kanMX</i>	(45)
YKB658	<i>MATa ura3-52 lys2-801 ade2-101 trp1-Δ200 leu2-Δ1 eaf5Δ::TRP1</i>	(45)
YKB504	<i>MATa ura3-52 lys2-801 ade2-101 trp1-Δ200 leu2-Δ1 eaf6Δ::kanMX</i>	(45)
YKB530	<i>MATa ura3-52 lys2-801 ade2-101 trp1-Δ200 leu2-Δ1 eaf7Δ::kanMX</i>	(45)
YKB464	<i>MATa ura3-52 lys2-801 ade2-101 trp1-Δ200 leu2-Δ1 yaf9Δ::kanMX</i>	(45)
YKB494	<i>MATa ura3-52 lys2-801 ade2-101 trp1-Δ200 leu2-Δ1 yng2Δ::kanMX</i>	(45)
YKB1443	<i>MATa his3Δ1 leu2Δ0 met15Δ0 ura3Δ0 CDC10-TAP::HIS3</i>	TAP Collection
YKB1455	<i>MATa his3Δ1 leu2Δ0 met15Δ0 ura3Δ0 CDC11-TAP::HIS3</i>	TAP Collection
YKB1466	<i>MATa his3Δ1 leu2Δ0 met15Δ0 ura3Δ0 SHS1-TAP::HIS3</i>	TAP Collection
YKB440	<i>MATa his3Δ1 leu2Δ0 met15Δ0 ura3Δ0 ESA1-TAP::URA3</i>	(45)
YKB2272	<i>MATa his3Δ1 leu2Δ0 met15Δ0 ura3Δ0 GCN5-TAP::HIS3</i>	TAP Collection
YKB2303	<i>MATa his3Δ1 leu2Δ0 met15Δ0 ura3Δ0 ECO1-TAP::HIS3</i>	TAP Collection
YKB1807	<i>MATa his3Δ1 leu2Δ0 met15Δ0 ura3Δ0 swe1Δ::kanMX</i>	DMA collection
YKB1266	<i>MATa swe1Δ::kanMX eaf1Δ::kanMX</i>	This study
YKB1648	<i>MATa swe1::pGAL-SWE1-HA::LEU2</i>	Gift from A. Rudner
YKB1806	<i>MATa swe1::pGAL-SWE1-HA::LEU2 eaf1Δ::kanMX</i>	This study
YKB1311	<i>MATa CDC11-GFP::HIS3</i>	This study
YKB1312	<i>MATα CDC11-GFP::HIS3</i>	This study
YKB2250	<i>MATa CDC11-GFP::HIS3 eaf1Δ::kanMX</i>	This study
YKB1385	<i>MATα CDC11-GFP::HIS3 yng2Δ::kanMX</i>	This study
YKB1664	<i>MATα CDC11-GFP::HIS3 gcn5Δ::kanMX</i>	This study
YKB1668	<i>MATα CDC11-GFP::HIS3 sas2Δ::kanMX</i>	This study
YKB1672	<i>MATα CDC11-GFP::HIS3 rtt109Δ::kanMX</i>	This study
YKB1676	<i>MATα CDC11-GFP::HIS3 elp3Δ::kanMX</i>	This study
YKB1679	<i>MATα CDC11-GFP::HIS3 hpa2Δ::kanMX</i>	This study
YKB1682	<i>MATα CDC11-GFP::HIS3 hat1Δ::kanMX</i>	This study
YKB1796	<i>MATα CDC11-GFP::HIS3 spt10Δ::kanMX</i>	This study
YKB1800	<i>MATα CDC11-GFP::HIS3 sas3Δ::kanMX</i>	This study
YKB1878	<i>MATα SHS1-GFP::HIS3</i>	This study
YKB2145	<i>MATα CDC11-GFP::HIS3 eco1-203</i>	This study
YKB2138	<i>MATa eco1-203 pep4Δ ::G418 ura3-52 leu2-3,112 his3-11,15 bar1 GAL+</i>	(56)
YKB1665	<i>MATa his3Δ1 leu2Δ0 met15Δ0 ura3Δ0 gcn5Δ::kanMX</i>	This study
YKB2160	<i>MATα CDC11-GFP::HIS3 hht1-hhf1::pWZ405-F2F9-LEU2 hht2-hhf2::pWZ403-F4F10-HIS3 [HHT2-HHF2::TRP1]</i>	This study; (72)
YKB2161	<i>MATα CDC11-GFP::HIS3 hht1-hhf1::pWZ405-F2F9-LEU2 hht2-hhf2::pWZ403-F4F10-HIS3 [HHT2-hhf2Δ4-19::TRP1]</i>	This study; (72)
YKB1804	<i>MATα CDC11-GFP::HIS3 esa1Δ::HIS3 esa1(L254P)::URA3</i>	This study
YKB2145	<i>MATα CDC11-GFP::HIS3 eco1-203</i>	This study
YKB2517	<i>MATα CDC11-GFP::HIS3 esa1Δ::HIS3 esa1(L254P)::URA3 eco1-203</i>	This study

YKB2254	<i>MAT_a CDC11-GFP::HIS3 shs1ΔTRP [pRS415::LEU2]</i>	This study
YKB2255	<i>MAT_a CDC11-GFP::HIS3 shs1ΔTRP [SHS1-3HA::LEU2]</i>	This study
YKB2518	<i>MAT_α CDC11-GFP::HIS3 SHS1-3HA::kanMX</i>	This study
YKB2519	<i>MAT_α CDC11-GFP::HIS3 shs1ΔTRP [pRS415::LEU2]</i>	This study
YKB2520	<i>MAT_α CDC11-GFP::HIS3 shs1ΔTRP [SHS1::LEU2]</i>	This study
YKB2521	<i>MAT_α CDC11-GFP::HIS3 shs1ΔTRP [shs1-66Δ::LEU2]</i>	This study
YKB2522	<i>MAT_α CDC11-GFP::HIS3 shs1ΔTRP [shs1-K536R::LEU2]</i>	This study
YKB2523	<i>MAT_α CDC11-GFP::HIS3 shs1ΔTRP [shs1-K16R-K19R-K57R-K82R-K204R-K443R-K478R-K488R-K536R::LEU2]</i>	This study

3.3.2 SDL screening

Media used for the genome-wide SDL screens was prepared as described (59), except that as the five non-essential NuA4 deletion mutants used for genome-wide SDL analysis were linked to the dominant selectable marker NAT diploid and final haploid selections were achieved using clonNAT (Werner Bioagents, 5.0000) at a final concentration of 100ug/mL. The SDL library (~5300 yeast strains) was initially condensed in duplicate at a density of 1536 colonies per plate, yielding 9 high-density library plates maintained on medium lacking uracil to select for the presence of the overexpression plasmids. All replica pinning steps were carried out as described (59). Screens were performed in triplicate at 25°C using the following query strains: *eaf1Δ* (YKB622), *eaf3Δ* (YKB995), *eaf5Δ* (YKB852), *eaf6Δ* (YKB623), *eaf7Δ* (YKB853). For the final scoring analysis, plate images were acquired using the ChemiDoc XRS Molecular Imaging System (BioRad) two days after pinning onto synthetic medium lacking uracil and containing either glucose or galactose as the sugar source. Images were analyzed using an in-house automated scoring method. SDL interactions that appeared in a list of “toxic genes”, whose overexpression alone is known to kill wild type cells (59), were

discarded from further analysis. For each query strain, interactions identified in at least two screens were confirmed by direct transformation followed by serial spot dilution assays. All SDL and synthetic dosage sick (SDS) interactions were then directly tested in all seven non-essential NuA4 deletion mutant backgrounds, *eaf1Δ* (YKB44), *eaf3Δ* (YKB1162), *eaf5Δ* (YKB658), *eaf6Δ* (YKB504), *eaf7Δ* (YKB530), *yaf9Δ* (KYB464) and *yng2Δ* (YKB494), by direct transformation followed by streak test.

3.3.3 Serial spot dilution assays

Wild type and NuA4 mutant strains, transformed with galactose-inducible overexpression plasmids or an empty vector control (pRS416) using traditional methods (20), were grown to mid-log phase at 25°C in synthetic defined liquid medium lacking uracil. Ten-fold serial dilutions (OD_{600} = 0.1, 0.01, 0.001, 0.0001) were spotted onto medium lacking uracil and containing either galactose or glucose. Plates were incubated for 5 days at 25°C and images were collected using the ChemiDoc XRS Molecular Imaging system (Biorad).

3.3.4 Microscopy

All cells were grown to mid-log phase at 25°C in YPD supplemented with adenine unless otherwise noted. For *in vivo* time-lapse studies, slides and samples were prepared as described (25), but coverslips were sealed with VALAP (1 vasoline: 1 lanolin: 1 paraffin). Z-stacks (0.5μm steps) were collected across 20μm every 5 minutes for wild type cells and every 15 minutes for *eaf1Δ* cells. Briefly, the cells from 1mL of culture grown to mid-logarithmic phase were collected by

centrifugation and re-suspended in 50 μ L of synthetic defined medium. 2 μ L were then spotted onto a freshly prepared agarose pad, sealed, and imaged immediately. For quantification, only mother cells were tracked post-cytokinesis. For examining septin localization and bud morphology in all KAT mutants (Figures 3.6A and 3.6B) cells from mid-log phase cultures were fixed with paraformaldehyde as previously described (4) and Z-stack images were collected (0.3 μ m steps) across 5-6 μ m. Microscopy was performed using a Leica DMI 6000 florescent microscope (Leica Microsystems GmbH, Wetzlar Germany), equipped with a Sutter DG4 light source (Sutter Instruments, California, USA), Ludl emission filter wheel with Chroma band pass emission filters (Ludl Electronic Products Ltd., NY, USA) and Hamamatsu Orca AG camera (Hamamatsu Photonics, Herrsching am Ammersee, Germany). Images were collected and analyzed using Velocity 4.3.2 Build 23 (Perkin Elmer). Analysis was performed on images collapsed into two dimensions using the “extended focus” option in Velocity.

3.3.5 Septin TAP immunopurification and NuA4 KAT assay

Septin protein complexes were isolated from exponentially growing yeast cultures via single step affinity purification of protein A, one epitope of the tandem affinity purification (TAP) tag. Cells from 300ml of mid-log phase culture grown in YPD at 30°C were collected by centrifugation, washed in 25mL of ice-cold water and transferred to 1.5mL Eppendorf tubes where they were flash frozen on dry ice. Cell pellets were re-suspended in 300mL of lysis buffer (100mM HEPES pH 8.0, 20mM magnesium acetate, 10% glycerol (V/V), 10mM EGTA, 0.1mM EDTA, 300mM sodium acetate, and fresh protease inhibitor cocktail (Sigma, P8215)) plus

an equal volume of glass beads, and cells were lysed through vortexing (six 1-minute blasts with incubation on ice between vortexing). Lysates were subjected to sonication (3x20sec; 1 minute incubation on ice between each pulse) using a Misonix Sonicator 3000 at setting four. Prior to centrifugation (10min, 3000rpm, 4°C), Nonidet P-40 was added to a final concentration of 1%. Forty milligrams of whole cell extract was incubated with 100µL of magnetic beads (Invitrogen, 143.02D) cross-linked to rabbit immunoglobulin (IgG) (Chemicon, PP64) as per the manufacturer's instructions. Following 2 hours of end-over-end rotation at 4°C, the beads were collected on a magnet and washed 3 times with 1mL of ice cold wash buffer (100mM HEPES pH 8.0, 20mM magnesium acetate, 10% glycerol (V/V), 10mM EGTA, 0.1mM EDTA, 300mM sodium acetate, 0.5% Nonidet P-40). The KAT assay was performed with the septins proteins bound to the magnetic beads. To the septin-magnetic bead matrix was added 3µL of 5X KAT buffer (250mM Tris pH 8.0, 250mM NaCl, 25mM MgCl₂, 5mM DTT), 0.5µCi of [³H]-acetyl coenzyme A (Perkin-Elmer, NET290L050UC), and 5µL of NuA4, purified from yeast cells (described below) in a final volume of 15µL. The reaction was incubated for 1 hour at 30°C with end-over-end rotation. As the NuA4 preparation included the TEV enzyme, TAP-tagged septin proteins were cleaved from the magnetic beads during the KAT assay. An equal volume of 2x loading dye (100mM Tris, pH 6.8, 4% SDS, 0.2% bromophenol blue, 200mM β-2-mercaptoethanol, 20% glycerol) was added and the samples heated at 65°C for 10 minutes. Proteins were separated by SDS-PAGE (7.5%). Following Coomassie staining and destaining, a image was taken of the gel. Next, the gel was treated for

fluorography, dried, and exposed to film for 1 month at -80°C. To ensure NuA4's activity, a control reaction was performed on 2ug of chicken core histones (Upstate, 13-107) using 3μL of purified NuA4 and 5μCi of [³H]-acetyl coenzyme A in a final volume of 10μL. This sample was processed as described above except proteins were separated on by 15% SDS-PAGE.

3.3.6 Septin GFP immunopurification and analysis of *in vivo* acetylation

Cells expressing endogenously GFP-tagged *CDC11* genes were grown to mid-log phase at 25°C in YPD supplemented with adenine. For temperature shift experiments, cells were harvested and re-suspended in pre-heated YPD medium supplemented with adenine (25°C or 37°C) and incubated for 4 hours at 250rpm. Harvesting of cells, lysate preparation, and immunopurifications were carried out as described above for Septin TAP Immunopurifications, except lysates were sonicated 1x10sec and 40μL of GFP-trap magnetic beads (Chromotek, GTM-20) was used with 10-15mg of whole cell lysate. Proteins were eluted in 25μl of 2x loading dye (50mM Tris, pH 6.8, 2% SDS, 0.1% bromophenol blue, 200mM beta-2-mercaptoethanol, 10% glycerol) with heating at 65°C for 10 minutes. Western blotting was performed using a semi-dry transfer apparatus from Biorad (Trans-Blot SD Semi Dry Electrophoretic Transfer Cell; 170-3940) and buffers recommended by the manufacturer. Protein transfer was performed for 1 hour using constant milliamps (mA) based on the following calculation: 0.8mA x area of gel x # of gels. Acetylation was detected using two anti-acetyl lysine antibodies at the indicated dilutions: Cell Signalling, 1/500 (9681); Upstate 1/1000 (06-933). Other primary antibodies used were: α-Act1 1/1000 (Novus Biologicals, NB600-505); α-MYC

1/1000 (Roche, 11667149001); α -G6PDH 1/10000 (Sigma, A9521), α -HA 1/1000 (Covance, MMS101P); α -GFP 1/1000 (Roche, 11814460001); 1/1000 α -hyperacetylated histone H4 (06-946). All blocking, primary, and secondary antibody incubations were performed with 5% milk dissolved in PBS plus 0.1% Tween20 (PBS-T), except the Cell Signalling anti-acetyl lysine antibody, in which the manufacturer's recommendation of 5% BSA in PBS-T was followed. Primary incubations were carried out overnight at 4°C and secondary incubations at room temperature for 2 hours. Secondary antibodies, all used at a dilution of 1/5000, were peroxidase-conjugated goat anti-rabbit IgG (Chemicon; AP307P), and peroxidase-conjugated goat anti-mouse IgG (Bio-Rad; 170-6516) where appropriate. Chemiluminescence was detected using Immobilon Western Chemiluminescent HRP substrate (Millipore; WBKLS0500) and developed on a ChemiDoc XRS system (Biorad; 170-8070). All experiments were repeated a minimum of three times and a representative image is shown.

3.3.7 Purification of NuA4, Gcn5, and Eco1 from yeast for *in vitro* KAT assays

Endogenously TAP-tagged Esa1, Gcn5, and Eco1 were used to purify the three KATs from yeast cells as described (45), except the proteins were eluted from magnetic beads by enzymatic cleavage in TC Buffer (50mM Tris, pH 8.0, 1mM DTT, 0.1% Nonidet P-40, 150mM NaCl, 10% glycerol) using tobacco etch virus (TEV). Briefly, cells from 1L of exponentially growing culture (in YPD, at 30°C) were lysed and KATs were purified in a single step using magnetic beads coupled to IgG. After washing, the KAT-bead matrix was resuspended in TC buffer

(100mL) to which was added 20mL of TEV. The cleavage reaction was incubated overnight at 4°C with end-over-end rotation. Finally, the supernatant was isolated from the beads, aliquoted, and stored at -80°C. The purity of each KAT preparation was assessed by silver stain using 2mL of TEV-cleaved sample separated by SDS-PAGE (7.5%). Activity of the purified KAT complexes with histone acetyltransferase activity (NuA4 and Gcn5-containing complexes) was tested by KAT assay (described above) using 2mg of chicken core histones (Upstate, 13-107) and 2mg of acetyl coenzyme A (Sigma, A2056) in a final volume of 15mL. The acetylation signal was assessed by Western blot using an anti-acetyl lysine antibody (Upstate, 06-933).

3.3.8 Detection of lysine acetylation by mass spectrometry

Purified TAP tagged septin proteins were resolved on SDS-PAGE gel, silver stained and bands excised. Following in-gel digestion with trypsin, samples were analyzed by LC-MS/MS using an Agilent 1100 HPLC system (Agilent Technologies) coupled to either an LTQ or an LTQ-Orbitrap XL spectrometer (Thermo-Electron) as indicated. Acetylated lysine residues on septin proteins were identified using mass spectrometry as previously described (9). MS/MS corresponding to putative lysine acetylation sites were all manually validated.

3.4 Results

3.4.1 A synthetic dosage lethal screen connects NuA4 to cytokinesis

To elucidate pathways regulated by the NuA4 lysine acetyltransferase complex and to discover putative substrates, we identified SDL interactions for the seven non-essential NuA4 subunits. Genome-wide SDL analysis was performed with five NuA4 query genes (*eaf1Δ*, *eaf3Δ*, *eaf5Δ*, *eaf6Δ*, *eaf7Δ*) using synthetic genetic array (SGA) technology (59, 65). Any gene whose overexpression caused an SDL phenotype in at least one NuA4 query strain was directly tested in all non-essential NuA4 deletion mutant backgrounds, including the remaining two, *yaf9Δ* and *yng2Δ*. The resulting NuA4 SDL genetic network encompasses 173 interactions among 89 genes, of which 16% (27/173) are SDL interactions and the remainder are SDS (synthetic dosage sick) interactions. (Figure 3.1A, Supplemental Table 3.1). Similar to previous NuA4 SL screens (26, 35, 45, 48), our SDL analysis successfully identified biologically relevant genes in cellular processes known to be impacted by NuA4, such as transcription (14), DNA damage (5), cell cycle progression (10, 11), and the stress response (36, 45). As SDL and SL interactions identify different types of genetic relationships (59, 74), as expected there was only minimal overlap between the NuA4 SDL interactions with previously published genome-wide SL (Figure 3.1B and Supplemental Table 3.2). The most remarkable feature of the SDL map was the large proportion of genes (~20%) in the map implicated in cytokinesis, suggesting a hitherto unknown role for NuA4 in this process (Figure 3.1A and

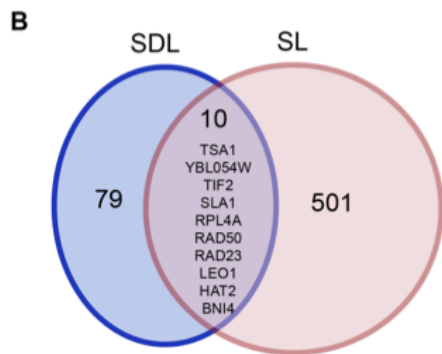
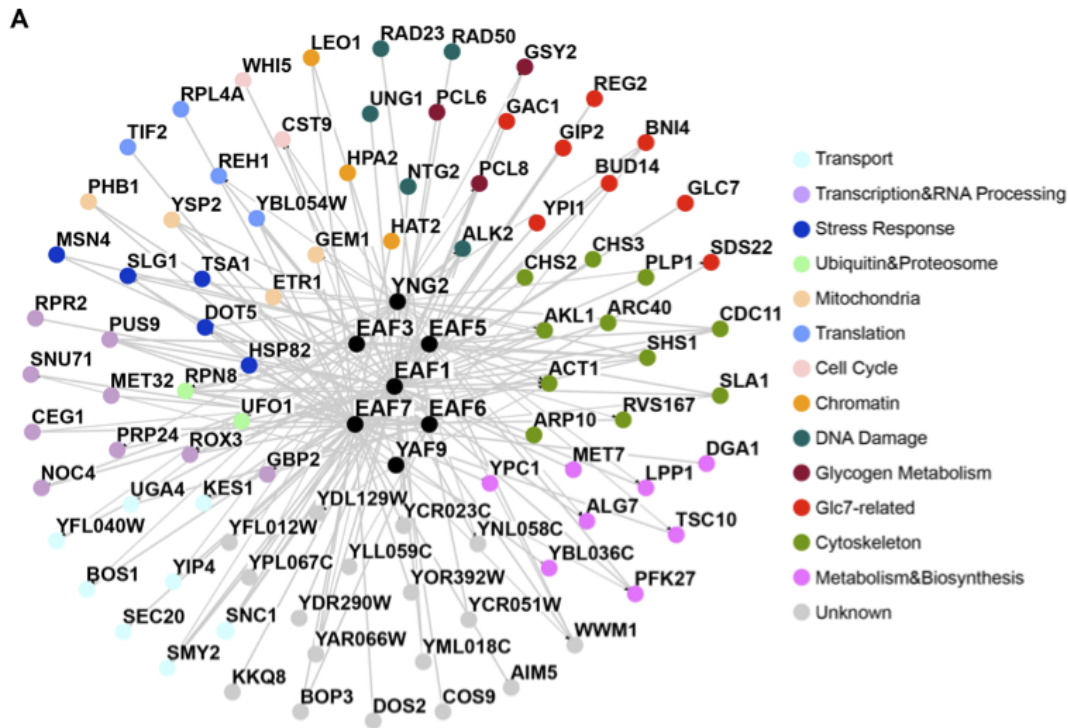


Figure 3.1: NuA4 synthetic dosage lethal genetic interaction network.

(A) NuA4 SDL Genetic Network. Black nodes represent NuA4 genes. Interacting genes are represented by colour-coded nodes grouped according to gene ontology. Edges indicate interactions. See also Supplemental Table 1. (B) Comparison of the NuA4 SDL and SL genetic interactions identified by genome-wide screens for the five non-essential NuA4 subunits *EAF1*, *EAF3*, *EAF5*, *EAF6*, *EAF7*. See Supplemental Table 3.2 for the list of SL interactions.

Supplemental Table 3.1). In the budding yeast, the successful completion of cytokinesis depends on many processes, including formation of a septin ring at the incipient bud site early in G1, remodelling of the actin cytoskeleton to support vesicle-mediated transport of cellular material to the growing bud, as well as formation of both the septum and actomyosin ring at the bud neck to facilitate invagination and cell separation (47). Our SDL network includes many genes that impact these processes, including two chitin synthase enzymes, Chs2 and Chs3, that function at the primary septum and throughout the cell wall respectively (51, 54); the multifunctional protein phosphatase 1, Glc7, and its regulator Bni4, that together localize Chs2 to the bud neck (32); several additional regulators of Glc7 (Bud14, Gip2, Ypi1, Reg2, Gac1, Sds22) (38); a number of proteins involved in both formation and regulation of the actin cortical patch and cytoskeleton, Arc40, Rvs167, Akl1, Sla1, as well as the actin structural molecule itself, Act1 (47); and finally two mitotic septin proteins, Cdc11 and Shs1 (reviewed in 7, 42, 69). Taken together the SDL network predicts a novel role for NuA4 in cytokinesis, and further supports the dual use of SL and SDL screening to identify the complete spectrum of cellular processes impacted by query genes.

3.4.2 NuA4 mutants activate the morphogenesis checkpoint

The identification of cytokinesis-related genes in the NuA4 SDL network prompted us to investigate the relationship between NuA4 and cytokinesis. We focused on the two most highly connected cytokinesis-related genes within the network: *CDC11* and *SHS1*, whose overexpression was toxic to almost all non-essential NuA4 deletion mutants (Figure 3.2A). Along with *CDC3*, *CDC10* and

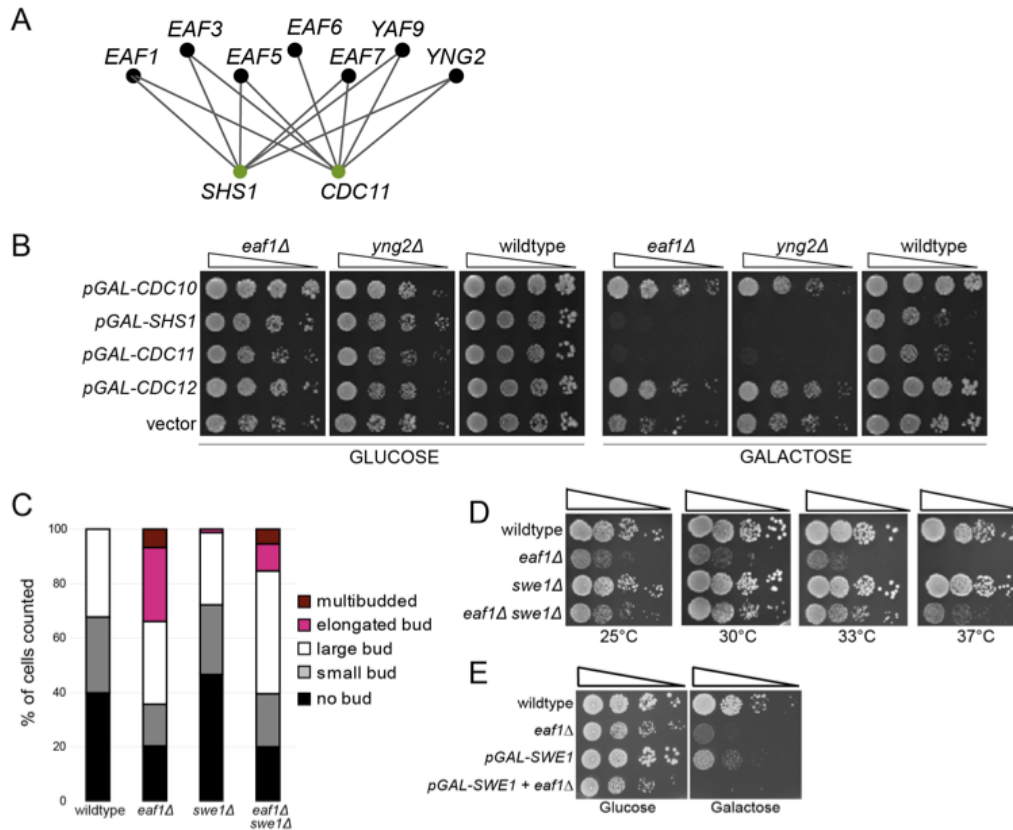


Figure 3.2: SDL interactions connect NuA4 to cytokinesis through septin proteins.

(A) Overexpression of the septin genes *CDC11* and *SHS1* (green nodes) is toxic to non-essential NuA4 deletion mutants (black nodes). Edges represent interactions. **(B)** Overexpression of the septin genes *SHS1* and *CDC11* cause death in the absence of *EAF1* or *YNG2*. Isogenic wild type (YKB779), *eaf1Δ* (YKB44) and *yng2Δ* (YKB494) cells containing galactose-inducible, plasmid-borne copy of galactose inducible *CDC10*, *SHS1*, *CDC11*, *CDC12*, or an empty vector control (pRS416) were spotted in serial ten-fold dilutions on either glucose (left) or galactose (right) at 25°C for 3 or 5 days, respectively. **(C)** *eaf1Δ* mutants exhibit elongated buds due to activation of the morphogenesis checkpoint. Bud morphology was scored for at least 100 cells each of wild type (YKB779), *eaf1Δ* (YKB42), *swe1Δ* (YKB1807), and *eaf1Δ swe1Δ* (YKB1266). The average of three replicates is presented. **(D)** Deletion of *SWE1* rescues the temperature sensitivity of *eaf1Δ* cells. The strains used in (C) were spotted in ten-fold serial dilutions at the temperatures indicated on YPD plates. **(E)** Overexpression of *SWE1* is toxic to *eaf1Δ* cells. Wild type (YKB779), *eaf1Δ* (YKB42), *pGAL-SWE1* (YKB1648), and *eaf1Δ pGAL-SWE1* (YKB1806) cells were spotted in 10-fold serial dilutions on either glucose (left) or galactose (right) at 25°C for 2 days.

CDC12, these genes encode the five mitotic septin proteins in yeast, which are GTP-binding proteins that form oligomeric protein complexes localized to the bud neck (reviewed in 7, 42, 69). Septins serve as a molecular platform for the actomyosin ring and septum, as well as a diffusion barrier. Overexpression of *CDC11* and *SHS1* was lethal to the NuA4 acetyltransferase-deficient mutant cells *eaf1Δ* and *yng2Δ* (Figure 3.2B), suggesting the acetyltransferase activity associated with the full NuA4 complex is required to buffer the effects of *SHS1* and *CDC11* overexpression. As septin localization and organization at the bud neck is a precursor to a host of downstream events that contribute to successful cytokinesis, NuA4 regulation of septin proteins could explain the broad range of cytokinesis-related genes identified in the NuA4 SDL network. A hallmark phenotype associated with mutations in septin genes and their regulators is the development of elongated buds (23, 40), which results from activation of the Swe1-dependent morphogenesis checkpoint that can detect defects in septin organization (29). Briefly, this checkpoint coordinates mitotic progression and bud growth through the Swe1 kinase, which inhibits mitosis via phosphorylation and inactivation of the mitotic Cdk1 (Cdc28). As a consequence, cells accumulate in G2/M with hyper-elongated buds due to an inability to switch from apical to isotropic growth. We reasoned that if NuA4 regulated septins, then NuA4 mutants might display Swe1-dependent bud morphology defects. To test this, we assessed bud morphology of *eaf1Δ* cells. We discovered that ~25% of *EAF1* deletion mutants displayed elongated buds as compared to wild type cells and that inactivation of the morphogenesis checkpoint via deletion of *SWE1* partially

suppressed both the elongated bud morphology (Figure 3.2C) and temperature sensitivity of *eaf1* Δ cells (Figure 3.2D). Conversely, constitutive activation of the checkpoint induced by overexpression of *SWE1* was lethal to *eaf1* Δ cells (Figure 3.2E). This data strongly suggests that one of the defects associated with *eaf1* Δ cells is activation of the morphogenesis checkpoint. As these phenotypes are shared with septin mutants and their regulators, this supports a role for NuA4 in septin regulation.

3.4.3 Acetyltransferase-deficient NuA4 mutants have defects in septin dynamics

To explore the role of NuA4 in septin regulation, using time-lapse fluorescence microscopy, we examined the localization of Cdc11-GFP in both wild type and *eaf1* Δ cells. During the cell cycle, septins adopt two main structures: a ring that assembles at the incipient bud site in early G1, and an hourglass-shaped collar that develops upon bud emergence. Just prior to cytokinesis, the collar splits into two rings that are inherited by the mother and daughter and then disassembled following cytokinesis, thereby resetting the cycle (reviewed in 7, 42, 69). The transition between the ring and collar relies on structural changes in the organization of oligomeric septin complexes, but the molecular basis is poorly understood (43). In wild type cells, Cdc11-GFP localized as expected in all cells examined (Figure 3.3A; Table 3.2; Supplemental Movie 3.1). However, we observed a defect in septin localization in 24% of *eaf1* Δ cells (Figure 3.3B and 3.3C; Table 3.2). While formation of the septin ring appeared normal in all cells examined, rather than re-structuring into the collar

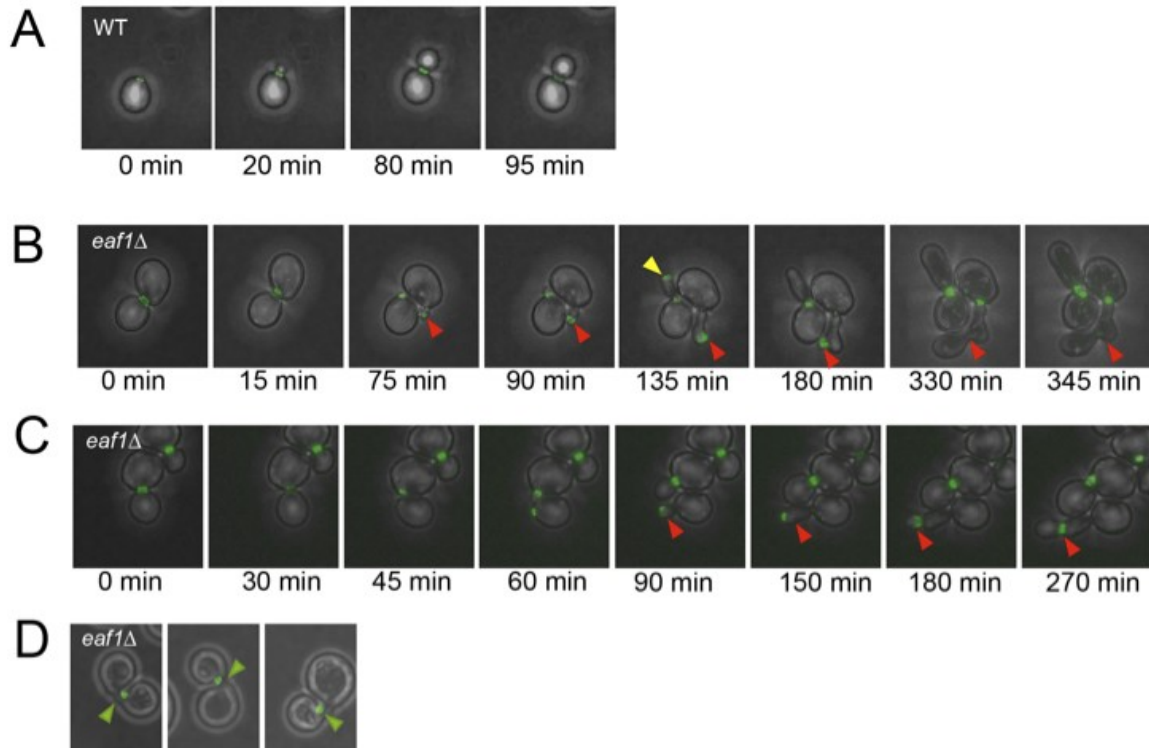


Figure 3.3: *eaf1Δ* cells have defects in septin dynamics.

Time lapse imaging of cells expressing Cdc11-GFP in the presence (WT (YKB1312)) or absence of *EAF1* (*eaf1Δ* (YKB1310)). Images were collected at five or fifteen minute intervals for wild type and *eaf1Δ* cells, respectively, at room temperature. Representative images of cells over time are shown panel (A) for wild type cells and panels (B) and (C) for *eaf1Δ* mutants. Red arrows point to septins mislocalized into the bud. The yellow arrow points out initially mislocalized septins that return to the bud neck and the cell successfully divided. (D) Different cells exhibiting septins misorganized to one side of the neck. Quantification of is presented in Table 3.2.

Table 3.2: Quantification of septin localization defects in *eaf1Δ* cells

Bud	Morphology Septin	WT (n=15)	<i>eaf1Δ</i> (n=43)
Normal	Normal	100%	65%
Elongated	Mis-localized in bud	0%	19%
No bud	Ring did not re-assemble (>1 hour)	0%	11%
Normal	Localized to one side of neck	0%	5%

Using time lapse imaging of cells expressing Cdc11-GFP in the presence (WT (YKB1312)) or absence of *EAF1* (*eaf1Δ* (YKB1310)), mother cells (immediately after cytokinesis) were followed through a cell cycle and bud and septin morphology was scored. Images were collected at five or fifteen minute intervals for wild type and *eaf1Δ* cells, respectively, at room temperature.

upon bud emergence, Cdc11-GFP diffused into the bud in 19% of the cells examined (Supplemental Movie 3.2). In these cells, Cdc11-GFP either assembled into a new ring at the bud tip and a new bud emerged, or it remained diffusely localized near or in the bud tip. In both cases the cells developed elongated buds. Interestingly, in some of the *eaf1* Δ cells with ectopically localized septins, the defect was corrected as Cdc11-GFP re-localized to the bud neck followed by collar splitting and cell division (Figure 3.3B and 3.3C). Another interesting phenotype associated with 5% of *eaf1* Δ cells was the misorganization of Cdc11-GFP to one side of the bud neck (Figure 3.3D); while bud morphology appeared largely normal, over time the Cdc11-GFP re-structured into a collar that spanned the bud neck, albeit lacking the crisp structure of wild type cells, and the cells eventually divided. We also examined Cdc11-GFP localization in the other six non-essential deletion mutants and found that only *yng2* Δ mutants exhibited defects similar to *eaf1* Δ cells (data not shown). As Yng2 is the only other non-essential subunit required for Esa1 catalytic activity *in vivo* (33), our work indicates that NuA4 acetyltransferase activity is required for faithful septin dynamics, in particular during the re-organization of septin filaments into the collar upon bud emergence.

3.4.4 NuA4 regulation of septin dynamics is not through histone H4

It was previously reported that both Esa1 and the N-terminal tail of histone H4 become essential when the morphogenesis checkpoint is constitutively activated (41, 50). This suggests the basis of these genetic interactions might lie in altered chromatin structure or transcriptional misregulation derived from defects in histone modifications. To test the hypothesis that histone H4 acetylation by NuA4

controls septin dynamics *in vivo*, we examined Cdc11-GFP localization and bud morphology in cells expressing a plasmid-borne copy of wild type or N-terminal deletion mutant (amino acids 4 to 19) (H4-ΔN) as the sole source of histone H4 (72). We discovered that H4-ΔN cells were strikingly more oblong in both mothers and buds than their wild type counterparts (Figure 3.4A and 3.4B), however, in the vast majority of mutants cells (98.3%), septins were localized to the bud neck as in wild type (100%). We did observe a few cells with ectopically localized Cdc11-GFP in addition to the correctly formed ring or collar, but in only 1.7% of H4-ΔN cells were septins mislocalized to the bud tip (Figure 3.4C). As the phenotypes we observed in H4-ΔN mutants were largely distinct from those observed in *eaf1Δ* mutants, this suggests NuA4 is not regulating septin dynamics and bud morphology solely through the acetylation of the N-terminal tail of histone H4 or altered chromatin structure.

3.4.5 Septin proteins are acetylated *in vivo*

As other studies have shown that SDL screens can identify targets of enzymes (59, 74), the SDL interactions between NuA4 mutants and *CDC11* and *SHS1* encouraged us to directly test whether one or more septin proteins are acetylated *in vivo*. Septin protein complexes were immunopurified through endogenously tagged Cdc11-GFP and Shs1-GFP. Western blot analysis of the purified septins using two different anti-acetyl lysine antibodies suggested that Cdc10 and Shs1 are acetylated *in vivo* (Figure 3.5A). While both antibodies recognized Shs1, only one recognized Cdc10, suggesting variability in epitope

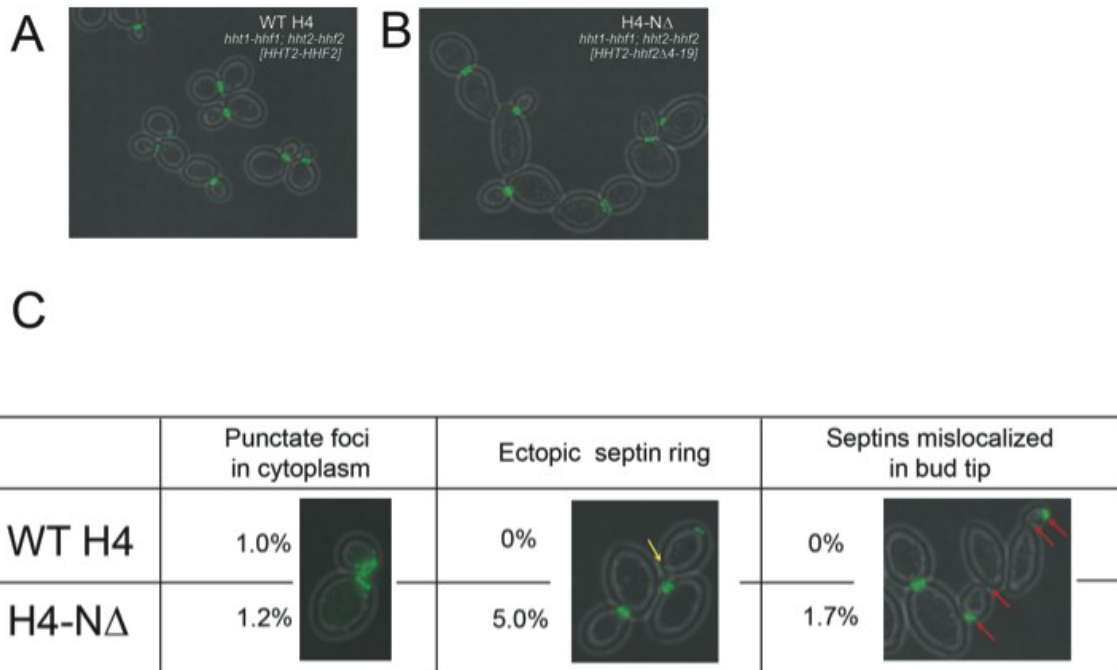


Figure 3.4: Septin localization defects of *eaf1Δ* cells are distinct from those of a histone H4 tail mutant.

Cells expressing Cdc11-GFP whose only source of histone H4 was expressed from a wild type (WT H4 (YKB1260)) or N-terminal tail mutant plasmid (H4-ΔN (YKB1261)) were used. Representative images of WT H4 and H4-ΔN cells are shown in (A) and (B), respectively. (C) Quantification of the defects observed in bud morphology and Cdc11-GFP localization in cells whose sole source of histone H4 came from a plasmid encoding a WT H4 gene or a mutant version of H4 from which amino acids 4 to 19 were deleted (H4-NΔ). The experiment was repeated in triplicate scoring more than 100 cells in each replicate. The yellow arrow points to an ectopic septin ring and the red arrows point to cells with septin in both the bud tip and neck.

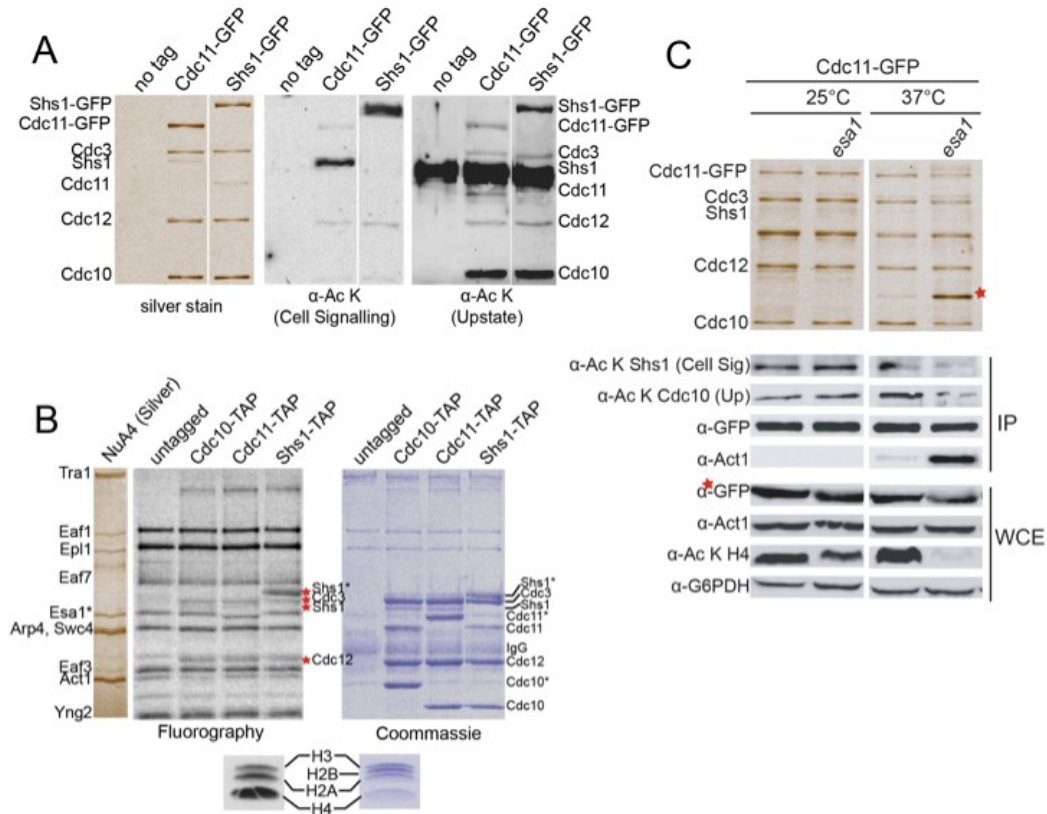


Figure 3.5: Septin proteins are acetylated *in vivo* and *in vitro*.

(A) Cdc10 and Shs1 are acetylated *in vivo*. Cells expressing Cdc11-GFP (YKB1312) or Shs1-GFP (YKB1878) and an untagged strain (YKB780) were used to immunopurify septins. Proteins were separated by SDS-PAGE (7.5%) and acetylation was determined using two anti-acetyl lysine (α -Ac K) antibodies, as indicated (right panels). Ten percent of the purification was separated on SDS-PAGE and silver stained (left panel). (B) NuA4 acetylates septins *in vitro*. *In vitro* KAT assays were carried out on septins immunopurified through Cdc10-TAP (YKB1443), Cdc11-TAP (YKB1455), or Shs1-TAP (YKB1466), relative to an untagged control purification (YKB779) using highly purified NuA4 from yeast in the presence of [3 H]-acetyl coenzyme A. Reactions were separated by SDS-PAGE (7.5%) and visualized by Coomassie staining (right panel). Gels were treated for fluorography and labeled proteins were visualized on film (middle panel). A silver stain of purified NuA4 is shown (left panel) to denote the migration of NuA4 subunits, as labeled. Chicken core histones were used as a control substrate to monitor NuA4's activity (bottom panel). A star (*) indicates a shift in mobility due to the presence of the calmodulin binding peptide fused to the protein. (C) Acetylation of Shs1 and Cdc10 is dependent on Esa1 KAT activity *in vivo*. Septin proteins were immunopurified through Cdc11-GFP in cells expressing a wild type (YKB1312) or mutant *esa1-L254P* allele (YKB1804), grown at 25°C (left side) or 37°C (right side) for four hours. Immunopurified products were separated by SDS-PAGE and either silver stained (10%) or subjected to Western blot analysis using the indicated antibodies. Shs1 acetylation was detected using an antibody from Cell Signalling (α -Ac K Cell Sig) and Cdc10 acetylation was detected using an antibody from Upstate (α -Ac K Up). Whole cell extract (WCE) samples were used to demonstrate equal loading (G6PDH = glyceraldehyde-6-phosphate dehydrogenase) and protein expression. The red star (*) denotes the co-purification of actin, both on the silver stain and determined by Western blot with an Act1 antibody (α -Act1).

recognition. To confirm the *in vivo* acetylation and to identify the modified lysine residues, septins were purified through endogenously TAP-tagged Cdc11-TAP or Shs1-TAP, and mass spectrometry was performed. To enrich acetylation levels within the immunopurified septins, half of each sample was subjected to an *in vitro* KAT reaction using highly purified NuA4 (45) and acetyl coenzyme A. Remarkably, this analysis identified eighteen acetylation sites on four septin proteins, as well as N-terminal acetylation sites on all five septins (Table 3.3 and Supplemental Table 3.3). While a few of these sites were unique to the NuA4 *in vitro* KAT assay samples (Cdc12 K193 and K338; Shs1 K443 and K488), the rest were also identified in the untreated samples, indicating that all four septins are acetylated *in vivo*. To test if NuA4 could directly acetylate septin proteins, we next performed *in vitro* NuA4 KAT assays using radiolabeled acetyl coenzyme A on septins immunopurified from yeast. This analysis confirmed that in addition to acetylating itself, NuA4 was capable of acetylating Cdc3, Cdc12 and Shs1 *in vitro*, however acetylation on Cdc10 was not detected (Figure 3.5B). Finally, to test whether septin acetylation *in vivo* required NuA4 function, we assessed the acetylation status of Shs1 and Cdc10, immunopurified through Cdc11-GFP, by Western blot in a strain harbouring a thermosensitive copy of the *ESA1* gene, *esa1-L254P* (11). The protein encoded by the *esa1-L254P* is catalytically inactive when grown at the restrictive temperature of 37°C (11). We discovered that while acetylation of Cdc10 and Shs1 was identical in *esa1-L254P* cells relative to WT cells at 25°C, a reduction in septin acetylation was observed in cells grown at 37°C for 4 hours (Figure 3.5C *esa1-L254P* lanes compared to WT), indicating

Table 3.3: Acetylated lysine residues on septin proteins

Septin	Protein Coverage	Acetylation site
Cdc3	77.3%	K4, K137, K316
Cdc10	60.2%	K73, K78, K128, K166
Cdc11	73.7%	----
Cdc12	81.3%	K193*, K251, K338*
Shs1	62.3%	K57, K82, K204, K352, K443*, K478, K488*, K536

* = Acetylation site was only identified in sample subjected to NuA4 *in vitro* KAT assay

that acetylation of both Cdc10 and Shs1 is at least partially dependent on Esa1 *in vivo*. Taken together, these data implicate NuA4 in the acetylation of Shs1 both *in vivo* and *in vitro*, and indicate Cdc10 acetylation relies on Esa1 activity *in vivo*, although NuA4 cannot directly acetylate this protein *in vitro*. Moreover, as acetylation was not abolished in the *esa1-L254P* mutant, this work suggested the involvement of additional KATs in the acetylation of septin proteins *in vivo*.

A surprising discovery we made during this analysis was a marked change in the proteins co-purifying with septins immunopurified at 37°C in the *esa1-L254P* background (Figure 3.5C and 3.6C). Mass spectrometry identified these proteins to be components of the actin cytoskeleton: Actin (Act1), which interacted with septin protein complexes in greater than stoichiometric proportion (Figure 3.5C (red star), and 3.6C), as well as components of actin cortical patches, such as Crn1 and Abp1 (reviewed in 47). Further, by Western blot analysis with anti-Act1 antibodies, we determined that the septin-actin interaction also occurs in wild type cells grown at 37°C, although possibly transiently, based on the reduced amount of co-purifying actin, and also irreproducibly (Figure 3.6C). This is the first report of a physical association between septins and components of the actin cytoskeleton in yeast, but we have not explored this interaction in detail.

3.4.6 Septin dynamics are regulated by multiple KATs *in vivo*

Our analysis of NuA4-dependent septin acetylation *in vitro* and *in vivo* suggested one or more additional KATs to be involved in septin acetylation. As our data also suggest that acetylation may regulate septin dynamics *in vivo*, we examined Cdc11-GFP localization in eight additional KAT mutants by fluorescence

microscopy using fixed cells grown to mid-log phase. With the exception of Taf1, an essential TFIID subunit involved in RNA polymerase II transcription initiation whose KAT activity *in vivo* has not been substantiated (16), this analysis included all known KATs in yeast. We detected cell morphology defects in three of eight KAT mutants examined (Figure 3.6A and 3.6B), however only two of these mutants also displayed septin mis-organization and/or localization defects. Specifically, cells lacking *SPT10*, which encodes a putative KAT with no known targets (19), displayed long, narrow cell morphology in both mothers and buds, however Cdc11-GFP localization was normal in all cells examined (Figure 3.6B). Moreover, the level of acetylation on Cdc10 and Shs1, as assessed by Western blot, was unchanged relative to wild type cells in *spt10Δ* mutants (data not shown). On the other hand, the phenotypes we observed in both *gcn5Δ* and *eco1-203* cells were highly reminiscent of the defects described in *eaf1Δ* mutants. As part of multiple KAT complexes, the predominant acetylation target of Gcn5 *in vivo* is histone H3 (24). We found that deletion of *GCN5* resulted in mis-organization of septins and elongated buds in 3% of cells. Eco1 is an essential KAT that promotes sister chromatid cohesion through the acetylation of the cohesin subunit Smc3 (reviewed in 55). Cells harbouring the *eco1-203* allele (56) displayed elongated buds and mislocalized septins in 10% of cells with a further 1% exhibiting punctate foci of Cdc11-GFP throughout the cytoplasm of normally shaped cells, even at the permissive temperature of 25°C. Intriguingly, Eco1 was previously reported to physically interact with proteins that

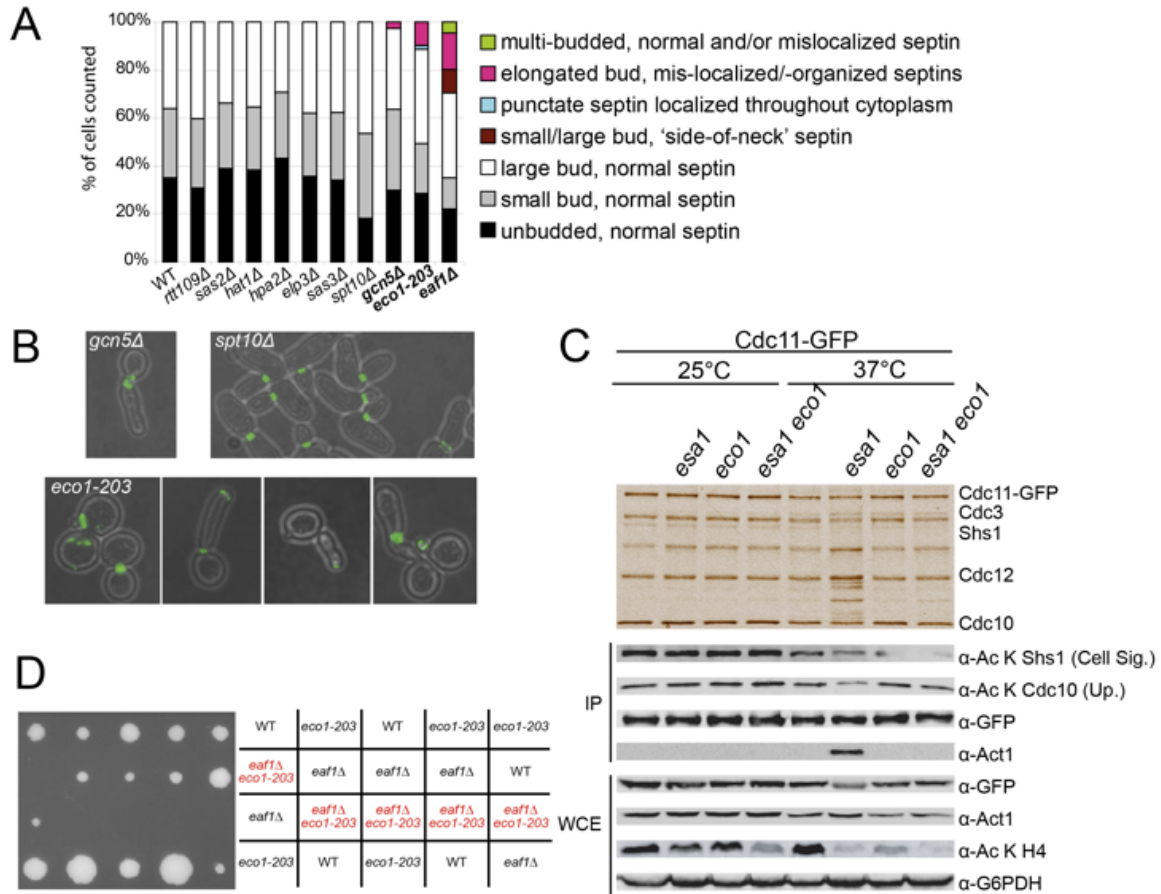


Figure 3.6: Multiple KATs impact septin dynamics *in vivo*.

(A) Cdc11-GFP localization in KAT mutants. Bud morphology and septin localization in KAT mutant strains grown at 25°C. One hundred cells were analyzed for each strain. **(B)** *SPT10*, *GCN5*, and *ECO1* mutants have defects in cell morphology and/or septin localization. Representative images of Cdc11-GFP localization and bud morphology in the KAT mutants strains *spt10Δ* (YKB1796), *gcn5Δ* (YKB1664), *eco1-203* (YKB2145), are shown. **(C)** Septin acetylation depends on *Esa1* and *Eco1* KAT activity *in vivo*. Septin complexes were immunopurified through Cdc11-GFP in wild type cells (YKB1312), or cells expressing the following mutant KAT alleles *esa1-L254P* (YKB1804), *eco1-203* (YKB2145), and *esa1-L254P eco1-203* (2517). Cells were grown at 25°C (left side) or 37°C (right side) for four hours. Ten percent of the immunopurified products (IP) were separated by SDS-PAGE (7.5%) and silver stained (top panel). IP samples and whole cell extract (WCE) samples were probed with the antibodies as indicated (bottom). Shs1 acetylation was detected using an antibody from Cell Signalling (α -Ac K Cell Sig.) and Cdc10 acetylation was detected using an antibody from Upstate (α -Ac K Up). Whole cell extract (WCE) samples were used to demonstrate equal loading (G6PDH = glyceraldehyde-6-phosphate dehydrogenase) and protein expression. **(D)** Mutation of *EAF1* and *ECO1* causes synthetic lethality. *eaf1Δ* (YKB1224) cells were mated to *eco1-203* (YKB2138) mutants and the resulting diploid cells were sporulated. No double mutants grew on the dissection plate, as assessed by replica plating.

localize to the bud neck (46). Given these defects, we hypothesized that one or both of these KATs were functioning in concert with NuA4 to acetylate septin proteins. To address this, we first tested the ability of Gcn5, purified from yeast in the context of all of its associated KAT complexes, and Eco1 also purified from yeast, to acetylate septin proteins *in vitro* using the same radioactive KAT assay as outlined for NuA4 above. We discovered that while Gcn5 could robustly acetylate septin proteins, Eco1 was catalytically inactive (Supplemental Figure 3.1). However, in the absence of the expected Eco1 auto-acetylation reaction (27), the Eco1 sample used in this assay may not have been functional. We next assessed Cdc10 and Shs1 acetylation levels by Western blot in *gcn5Δ* and *eco1-203* mutants, either singly or in combination with *esa1-L254P*, by immunopurifying septin protein complexes through Cdc11-GFP. While we observed no changes in septin acetylation in either *gcn5Δ* or *esa1-L254P gcn5Δ* cells relative to wild type or *esa1-L254P* cells, respectively, at either 25°C or 37°C (data not shown), we discovered Shs1 acetylation to be moderately reduced in *eco1-203* cells and moreover virtually eliminated in *esa1-L254P eco1-203* double mutants at the non-permissive temperature of 37°C (Figure 3.6C). While the reduction in acetylation on Shs1 was reproducible over three independent biological replicates with unique isolates, the level of Cdc10 acetylation in these same experiments was variable, as either no or only a small decrease in acetylation was observed in single or double mutants (Figure 3.6C). Together, these data support the model that multiple KATs impact septin function, as both *ECO1* and *GCN5* mutants display defects in septin dynamics similar to those observed in *EAF1* mutants, and furthermore NuA4 and

Eco1 together account for the maximal acetylation of Shs1 *in vivo*. Indeed, we discovered a SL genetic interaction between *eaf1* Δ and *eco1-203*, even at 25°C (Figure 3.6D), suggesting functional redundancy between NuA4 and Eco1.

3.4.7 Unacetylatable *shs1* mutants have bud morphology and septin localization defects similar to KAT mutants

To establish the possibility of a direct cause-and-effect relationship between septin acetylation and the defects in septin organization and localization observed in KAT mutants, we next tested whether loss of acetylation on septins could recapitulate the phenotypes observed in the KAT mutants. To this end, we set out to generate unacetylatable septin point mutants by mutating acetyl lysine residues identified by mass spectrometry to arginine. We focused our efforts on Shs1, the most abundantly acetylated septin protein (Table 3.3) and the acetylation target of NuA4 and Eco1 *in vivo* (Figure 3.6C). We initially cloned a C-terminally epitope-tagged (3HA, three copies of the hemagglutinin epitope) version of *SHS1* into a low copy plasmid under the control of the endogenous *SHS1* promoter, (~500 base pairs upstream of the start site). However, we quickly established that the Shs1-HA fusion protein, whether expressed from a plasmid or the genomically integrated copy, could not be acetylated *in vivo* (Figure 3.7A). This result suggested that the presence of the relatively small HA tag (~3kDa, 25AA) effectively blocked KAT activity on Shs1, and moreover indicated that despite detection of acetylation sites in multiple domains of Shs1 (Table 3.3, Figure 3.7D) the predominant site(s) of acetylation might lie in the C-terminal region of Shs1.

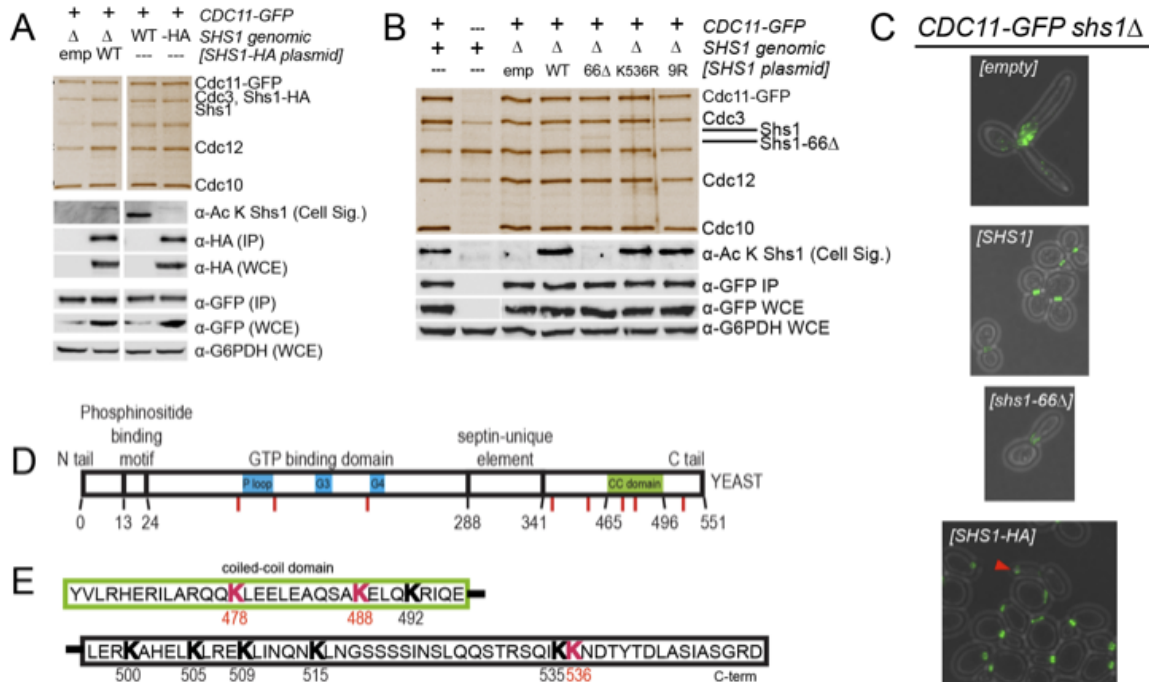


Figure 3.7: Cell morphology and septin localization is disrupted in 10% of cells expressing an unacetylatable Shs1-HA fusion protein.

(A) The Shs1-HA fusion protein is unacetylatable *in vivo*. Cells expressing Cdc11-GFP in which the genomic copy of SHS1 was deleted (Δ) but covered by either an empty vector (emp; YKB2254) or wild type (WT; YKB2255) plasmid-borne copy of SHS1, or expressed normally from the genomic locus (WT; YKB1312) or expressed from the genomic locus as an HA fusion protein (-HA; YKB2518) were immunopurified using GFP-trap magnetic beads. Immunopurified products were separated by SDS-PAGE and either silver stained (10%) or subjected to Western blot analysis using the indicated antibodies. Shs1 acetylation was detected using an anti-acetyl lysine antibody from Cell Signaling (α -Ac K Cell Sig). Whole cell extract (WCE) samples were used to demonstrate equal loading (G6PDH = glyceraldehyde-6-phosphate dehydrogenase) and protein expression. (B) Shs1 acetylation is abolished in a C-terminal tail truncation mutant. Cells expressing (+; YKB1312) or not expressing (-; YKB780) *CDC11-GFP* (top row of legend; *CDC11-GFP*) in which the genomic copy of SHS1 was either intact (+) or deleted (Δ) (second row; *SHS1* genomic); and harboring a plasmid expressing SHS1 (labels) or not (---) (third row of legend; [*SHS1* plasmid]) were used. Plasmids encode either an empty vector (emp; YKB2519); a wild type SHS1 gene (WT; YKB2520); a C-terminal truncation mutant (66 Δ ; YKB2521); a single point mutant (K536R; YKB2522); or 9 lysine-to-arginine mutations (K16, K19, K57, K82, K204, K443, K478, K488, K536; YKB2523). Septin complexes were immunopurified through Cdc11-GFP using GFP-trap magnetic beads. Immunopurified products were separated by SDS-PAGE and either silver stained (10%) or subjected to Western blot analysis using the indicated antibodies, as outlined in (A). (C) Bud morphology and septin localization in *shs1* mutants. Cdc11-GFP was examined by fluorescent microscopy in *shs1 Δ* mutants in the presence of an empty vector (*[empty]*), or a plasmid encoding a wild type (*[SHS1]*), C-terminal truncation mutant (*[shs1-66 Δ]*), Shs1-HA fusion protein (*[SHS1-HA]*). Cells were grown to mid-log phase at 25°C and fixed prior to imaging. The red arrow points a cell with an elongated bud and mislocalized septins (D) Schematic depicting domain structure of Shs1, including acetylation sites identified by mass spectrometry (red lines). Regions critical for GTP binding within the GTP binding domain are noted in blue (P-loop; G3; G4), and the coiled-coil (CC) domain within the C-terminal tail is in green. Numbers indicate amino acid residues. (E) Amino acid sequence of the coiled-coil domain and the C-terminal tail of Shs1. All lysines and their corresponding residue number are indicated. Red K's represent lysines on which acetylation has been identified by mass spectrometry. The coiled-coil domain is boxed in green and the remainder of the C-terminal tail in black.

To test these hypotheses, we first eliminated the 3HA epitope tag from the *SHS1* plasmid and subsequently introduced a series of additional mutations, including a lysine to arginine substitution at amino acid 536 (K536R), a known acetyl lysine residue identified by mass spectrometry (Table 3.3) and notably the C-terminal most lysine residue in the protein (Figure 3.7E); a '9R mega-mutant', in which seven of the eight identified acetylated lysine residues on Shs1, plus two additional sites in the N-terminal tail, were mutated to arginine, which we hypothesized would create an 'unacetylatable mutant' assuming that all acetylation sites had been identified by mass spectrometry (Table 3.3). Finally, we also generated a C-terminal truncation mutant (Shs1-66 Δ) in which the final 66 amino acids of Shs1 were eliminated. We then immunopurified septin protein complexes from exponentially growing yeast cells via Cdc11-GFP and assessed the acetylation status of Shs1 by Western blot. We discovered the level of Shs1 acetylation was indistinguishable whether Shs1 was expressed from its endogenous genomic locus, or a plasmid encoding a wild type, K536R, or 9R mega mutant Shs1 protein (Figure 3.7B), indicating that these lysine residues do not contribute significantly to the acetylation on Shs1 *in vivo*. However, in the truncation mutant shs1-66 Δ , the acetylation signal on Shs1 was completely abolished, despite incorporation of the truncated protein into the septin protein complex to the same degree as the wild type and other mutant proteins (Figure 3.7B silver stain). This result suggested that acetylation of Shs1 occurs exclusively within the C-terminal tail region.

Given the loss of acetylation, we wondered whether these cells would display the same phenotypes observed in KAT mutants. Thus, using fluorescence

microscopy, we examined bud morphology and septin localization through Cdc11-GFP in these cells. We found that cells lacking *SHS1* entirely (Figure 3.7C [*empty*]) displayed highly elongated bud morphology and were oftentimes multi-budded, with severely fragmented Cdc11-GFP signal throughout the cell but concentrated near the bud neck(s). Bud morphology and septin localization could be nearly completely restored to normal by expression of a wild type copy of Shs1 from a plasmid (Figure 3.7C [*SHS1*]). However, in the truncation mutant, we observed elongated buds and a septin morphology phenotype previously described as parallel bars (23) at the bud neck in about 40% of cells (Figure 3.7C [*shs1-66Δ*]). Though acetylation was eliminated from the truncated *shs1-66Δ* mutant, this phenotype did not correspond to the defects observed in *eaf1Δ*, *eco1-203*, or *gcn5Δ* mutant cells (Figures 3.3B, 3.3C, and 3.6B). Shs1 is heavily post-translationally modified by both phosphorylation (18) and sumoylation (28) in its C-terminus and a role for the C-terminal domain of Shs1 has been suggested for septin structural transitions (3). We therefore considered that the phenotype observed in the *shs1-66D* mutant might be attributable to a combination of these factors. To more specifically examine the consequence of abolishing Shs1 acetylation without truncating the protein, we next examined the bud morphology and septin localization in the Shs1-HA fusion protein. As shown in Figure 3.7A and described above, acetylation in this mutant is virtually eliminated. Remarkably, we discovered that cells expressing the unacetylatable Shs1-HA protein had a phenotype extremely similar to the KAT mutants, in that a relatively small portion of cells in the population (~10%) demonstrated elongated buds with septins mis-

localized into the tip (Figure 3.7A, [*SHS1-HA*], red arrows). Importantly, all small, unbudded cells contained a correctly formed septin ring, suggesting that loss of Shs1 acetylation does not impact this stage of septin organization. This result provides strong support for the hypothesis that acetylation directly impacts septin dynamics. We are currently generating individual and combinatorial arginine substitutions of all lysine residues within the Shs1 C-terminal tail to determine which are acetylated (Figure 3.7E). Notably, we have already determined that K488 (as part of the 9R mega mutant) and K536 are dispensable for Shs1 acetylation (Figure 3.7B).

3.5 Discussion

3.5.1 SDL interactions to identify acetylation targets

In this work, we performed genome-wide SDL screens to assess the function of the NuA4 lysine acetyltransferase complex and uncovered a novel role for NuA4 in cytokinesis. To date, only a few other genome-wide SDL screens have been performed in yeast, two of which assessed the function of kinases, while the other explored the function of a specific proteolytic degradation pathway (37, 59, 74). These efforts have established that SDL interactions can occur between components of the same pathway, and have successfully identified enzyme-substrate relationships. Indeed, our work indicates that SDL screens will also be useful for predicting substrates of KATs, as we have shown that a highly connected gene in the NuA4 SDL network, *SHS1*, encodes a protein whose acetylation depends, in part, on Esa1 activity *in vivo* (Figure 3.5C, 3.6C). Importantly, we have demonstrated that the elongated bud and septin mislocalization phenotypes

observed in acetyltransferase-deficient NuA4 mutant *eaf1Δ* cells can be recapitulated when Shs1 is expressed as an unacetylatable, C-terminally HA-tagged fusion protein (Figure 3.7C), thereby suggesting a cause-and-effect relationship between Shs1 acetylation and septin dynamics. To rule out the possibility that the HA tag alone causes the phenotype and that the loss of acetylation is just a coincidence, we are presently identifying the acetyl lysine residue(s) on the C-terminal tail of Shs1 by mutational analysis.

3.5.2 A novel role for multiple KATs in regulating septin dynamics

While the primary goal of the SDL screen was to discover NuA4 substrates, through this analysis we have made the more general discovery that multiple KATs regulate septin dynamics *in vivo* (Figures 3.3 3.6A and 3.6B). In addition to acetyltransferase NuA4 mutants, mutation of either *GCN5* or *ECO1* results in defects in septin localization and organization. Notably, in addition to NuA4, these are the only other KATs in yeast for which non-histone acetylation targets have been described to date (55, 66). Our discovery that KATs regulate septin proteins adds an additional layer of complexity into an already complicated regulatory network implicated in septin dynamics, as the function of numerous kinases (18, 46, 58, 63, 67) and a SUMO (small ubiquitin-like modifier)-conjugating enzyme (28, 62) have been linked to this process. As such, a plethora of phosphorylation and sumoylation sites have been identified on multiple septin proteins. The biological consequences of these modifications, which have generally proven difficult to dissect, have by-and-large been linked to some aspect of septin assembly or disassembly (42). Indeed, our time-lapse imaging specifically implicates NuA4

function in the transition of septin proteins from the ring structure, which assembles at the incipient bud site, into the hourglass shaped collar that develops upon bud emergence. That *eco1* and *gcn5* mutants display similar phenotypes, suggests common or redundant roles for KATs in regulating this transition. A host of proteins have been implicated in the ring-to-collar transition, including Cdc42, Cla4, Elm1, Gin4, Bni5, Bud3, Bud4, Bud5, Bni1, Cln1, and Cln2 (7, 21, 22, 67, 74) yet the mechanistic understanding of the process is quite poor as it is likely regulated by multiple parallel pathways. This hypothesis is supported by the incomplete phenotypic penetrance observed in virtually all mutants linked to the ring-to-collar transition, and the exacerbation of phenotypes observed by combining mutations (23). Indeed, that NuA4 mutants (*esa1-L254P*, *eaf1Δ*) display synthetic sickness with *cla4Δ* mutants (12, 45) suggests that NuA4 and Cla4 may work in parallel to promote septin organization.

While we have preliminarily linked the function of Shs1 acetylation to a defect in septin dynamics that is similar to phenotypes of KAT mutants, the biological consequences of acetylation on Cdc3, Cdc12, and Cdc10 remain to be determined. For instance, do acetylation of any of these proteins mediate the novel, 'side-of-neck' phenotype observed uniquely in the NuA4 *eaf1Δ* mutant cells (Figure 3.3D)? Moreover, while we did not identify acetyl lysine residues on Cdc11 through Western blot analysis or mass spectrometry, the high degree of SDL interconnectivity of *CDC11* with non-essential NuA4 mutants (Figure 2.3A and 2.3B) and the interchangeable role described for Cdc11 with Shs1 in septin oligomeric protein complex structure (3) suggest that acetylation sites may still be

mapped onto Cdc11. Dissecting the functional consequences of acetylation presents many challenges, including identifying the biologically relevant sites of acetylation, dissecting temporal changes, and assigning KATs to each site. Importantly, septin acetylation has also been identified in high throughput proteomic studies in human cells (9, 73) pointing toward acetylation being a conserved mechanism for the regulation of cytokinesis. Intriguingly, at least one component of the human homolog of NuA4, the Tip60 complex, is known to localize to the cytokinetic furrow during mitosis (52). The impetus to unravel the complexities of septin regulation is driven in large part by the links that have been established between mutations in human septin proteins and diseases such as cancer and neurodegeneration (49).

3.6 Acknowledgements

We thank Jeremy Thorner and members of the Baetz Lab for their thoughtful comments. This research is funded by the Canadian Cancer Society (grant # 20309) and an Early Researcher Award from the Ontario Government to K.B. K.B. is a Canada Research Chair (CRC) in Chemical and Functional Genomics. D.F. is a CRC in Proteomics and Systems Biology and J.F.C is a CRC in Structural Biology and Epigenetics. L.M. was supported by a Canada Institute for Health Research Ph.D. scholarship. A.L. was supported by a Natural Sciences and Engineering Research Council of Canada M.Sc Scholarship. J-P.L. was supported by an Ontario Graduate Scholarship.

3.7 Supplemental

Supplemental files associated with this chapter may be found online at www.oisb.ca/personal_web_site/Baetz_Lab/publicationsFS.html:

- Supplemental Table 3.1: SDL interactions for non-essential NuA4 mutants.
- Supplemental Table 3.2: SL interactions of five non-essential NuA4 mutants.
- Supplemental Table 3.3: Acetyl lysine residues identified by mass spectrometry.
- Supplemental Movie 3.1: Time lapse imaging of wild type yeast expressing Cdc11-GFP.
- Supplemental Movie 3.2: Time lapse imaging of *eaf1Δ* mutants expressing Cdc11-GFP.
- Supplemental Figure 3.1: Gcn5 but not Eco1 can acetylate septin proteins *in vitro*.

3.8 References

1. **Allard, S., R. T. Utley, J. Savard, A. Clarke, P. Grant, C. J. Brandl, L. Pillus, J. L. Workman, and J. Cote.** 1999. NuA4, an essential transcription adaptor/histone H4 acetyltransferase complex containing Esa1p and the ATM-related cofactor Tra1p. *Embo J* **18**:5108-5119.
2. **Babiarz, J. E., J. E. Halley, and J. Rine.** 2006. Telomeric heterochromatin boundaries require NuA4-dependent acetylation of histone variant H2A.Z in *Saccharomyces cerevisiae*. *Genes Dev* **20**:700-710.
3. **Bertin, A., M. A. McMurray, P. Grob, S. S. Park, G. Garcia, 3rd, I. Patanwala, H. L. Ng, T. Alber, J. Thorner, and E. Nogales.** 2008. *Saccharomyces cerevisiae* septins: supramolecular organization of heterooligomers and the mechanism of filament assembly. *Proc Natl Acad Sci U S A* **105**:8274-8279.
4. **Biggins, S., F. F. Severin, N. Bhalla, I. Sassoon, A. A. Hyman, and A. W. Murray.** 1999. The conserved protein kinase Ipl1 regulates microtubule binding to kinetochores in budding yeast. *Genes Dev* **13**:532-544.
5. **Bird, A. W., D. Y. Yu, M. G. Pray-Grant, Q. Qiu, K. E. Harmon, P. C. Megee, P. A. Grant, M. M. Smith, and M. F. Christman.** 2002. Acetylation of histone H4 by Esa1 is required for DNA double-strand break repair. *Nature* **419**:411-415.
6. **Boone, C., H. Bussey, and B. J. Andrews.** 2007. Exploring genetic interactions and networks with yeast. *Nat Rev Genet* **8**:437-449.
7. **Cao, L., W. Yu, Y. Wu, and L. Yu.** 2009. The evolution, complex structures and function of septin proteins. *Cell Mol Life Sci* **66**:3309-3323.
8. **Choi, J. K., and L. J. Howe.** 2009. Histone acetylation: truth of consequences? *Biochem Cell Biol* **87**:139-150.
9. **Choudhary, C., C. Kumar, F. Gnad, M. L. Nielsen, M. Rehman, T. C. Walther, J. V. Olsen, and M. Mann.** 2009. Lysine acetylation targets protein complexes and co-regulates major cellular functions. *Science* **325**:834-840.
10. **Choy, J. S., B. T. Tobe, J. H. Huh, and S. J. Kron.** 2001. Yng2p-dependent NuA4 histone H4 acetylation activity is required for mitotic and meiotic progression. *J Biol Chem* **276**:43653-43662.
11. **Clarke, A. S., J. E. Lowell, S. J. Jacobson, and L. Pillus.** 1999. Esa1p is an essential histone acetyltransferase required for cell cycle progression. *Mol Cell Biol* **19**:2515-2526.
12. **Collins, S. R., K. M. Miller, N. L. Maas, A. Roguev, J. Fillingham, C. S. Chu, M. Schuldiner, M. Gebbia, J. Recht, M. Shales, H. Ding, H. Xu, J. Han, K. Ingvarsdottir, B. Cheng, B. Andrews, C. Boone, S. L. Berger, P. Hieter, Z. Zhang, G. W. Brown, C. J. Ingles, A. Emili, C. D. Allis, D. P. Toczyski, J. S. Weissman, J. F. Greenblatt, and N. J. Krogan.** 2007. Functional dissection of protein complexes involved in yeast chromosome biology using a genetic interaction map. *Nature* **446**:806-810.

13. **Costanzo, M., A. Baryshnikova, J. Bellay, Y. Kim, E. D. Spear, C. S. Sevier, H. Ding, J. L. Koh, K. Toufighi, S. Mostafavi, J. Prinz, R. P. St Onge, B. VanderSluis, T. Makhnevych, F. J. Vizeacoumar, S. Alizadeh, S. Bahr, R. L. Brost, Y. Chen, M. Cokol, R. Deshpande, Z. Li, Z. Y. Lin, W. Liang, M. Marback, J. Paw, B. J. San Luis, E. Shuteriqi, A. H. Tong, N. van Dyk, I. M. Wallace, J. A. Whitney, M. T. Weirauch, G. Zhong, H. Zhu, W. A. Houry, M. Brudno, S. Ragibzadeh, B. Papp, C. Pal, F. P. Roth, G. Giaever, C. Nislow, O. G. Troyanskaya, H. Bussey, G. D. Bader, A. C. Gingras, Q. D. Morris, P. M. Kim, C. A. Kaiser, C. L. Myers, B. J. Andrews, and C. Boone.** 2010. The genetic landscape of a cell. *Science* **327**:425-431.
14. **Doyon, Y., and J. Cote.** 2004. The highly conserved and multifunctional NuA4 HAT complex. *Curr Opin Genet Dev* **14**:147-154.
15. **Doyon, Y., W. Selleck, W. S. Lane, S. Tan, and J. Cote.** 2004. Structural and functional conservation of the NuA4 histone acetyltransferase complex from yeast to humans. *Mol Cell Biol* **24**:1884-1896.
16. **Durant, M., and B. F. Pugh.** 2006. Genome-wide relationships between TAF1 and histone acetyltransferases in *Saccharomyces cerevisiae*. *Mol Cell Biol* **26**:2791-2802.
17. **Eberharter, A., S. John, P. A. Grant, R. T. Utley, and J. L. Workman.** 1998. Identification and analysis of yeast nucleosomal histone acetyltransferase complexes. *Methods* **15**:315-321.
18. **Egelhofer, T. A., J. Villen, D. McCusker, S. P. Gygi, and D. R. Kellogg.** 2008. The septins function in G1 pathways that influence the pattern of cell growth in budding yeast. *PLoS One* **3**:e2022.
19. **Eriksson, P. R., G. Mendiratta, N. B. McLaughlin, T. G. Wolfsberg, L. Marino-Ramirez, T. A. Pompa, M. Jainerin, D. Landsman, C. H. Shen, and D. J. Clark.** 2005. Global regulation by the yeast Spt10 protein is mediated through chromatin structure and the histone upstream activating sequence elements. *Mol Cell Biol* **25**:9127-9137.
20. **Gietz, R. D., and R. H. Schiestl.** 2007. High-efficiency yeast transformation using the LiAc/SS carrier DNA/PEG method. *Nat Protoc* **2**:31-34.
21. **Gladfelter, A. S., I. Bose, T. R. Zyla, E. S. Bardes, and D. J. Lew.** 2002. Septin ring assembly involves cycles of GTP loading and hydrolysis by Cdc42p. *J Cell Biol* **156**:315-326.
22. **Gladfelter, A. S., L. Kozubowski, T. R. Zyla, and D. J. Lew.** 2005. Interplay between septin organization, cell cycle and cell shape in yeast. *J Cell Sci* **118**:1617-1628.
23. **Gladfelter, A. S., T. R. Zyla, and D. J. Lew.** 2004. Genetic interactions among regulators of septin organization. *Eukaryot Cell* **3**:847-854.
24. **Grant, P. A., L. Duggan, J. Cote, S. M. Roberts, J. E. Brownell, R. Candau, R. Ohba, T. Owen-Hughes, C. D. Allis, F. Winston, S. L. Berger, and J. L. Workman.** 1997. Yeast Gcn5 functions in two multisubunit complexes to acetylate nucleosomal histones: characterization of an Ada complex and the SAGA (Spt/Ada) complex. *Genes Dev* **11**:1640-1650.

25. **Hoepfner, D., A. Brachat, and P. Philippsen.** 2000. Time-lapse video microscopy analysis reveals astral microtubule detachment in the yeast spindle pole mutant *cnm67*. *Mol Biol Cell* **11**:1197-1211.
26. **Hoke, S. M., J. Guzzo, B. Andrews, and C. J. Brandl.** 2008. Systematic genetic array analysis links the *Saccharomyces cerevisiae* SAGA/SLIK and NuA4 component Tra1 to multiple cellular processes. *BMC Genet* **9**:46.
27. **Ivanov, D., A. Schleiffer, F. Eisenhaber, K. Mechtler, C. H. Haering, and K. Nasmyth.** 2002. Eco1 is a novel acetyltransferase that can acetylate proteins involved in cohesion. *Curr Biol* **12**:323-328.
28. **Johnson, E. S., and G. Blobel.** 1999. Cell cycle-regulated attachment of the ubiquitin-related protein SUMO to the yeast septins. *J Cell Biol* **147**:981-994.
29. **Keaton, M. A., and D. J. Lew.** 2006. Eavesdropping on the cytoskeleton: progress and controversy in the yeast morphogenesis checkpoint. *Curr Opin Microbiol* **9**:540-546.
30. **Keogh, M. C., T. A. Mennella, C. Sawa, S. Berthelet, N. J. Krogan, A. Wolek, V. Podolny, L. R. Carpenter, J. F. Greenblatt, K. Baetz, and S. Buratowski.** 2006. The *Saccharomyces cerevisiae* histone H2A variant Htz1 is acetylated by NuA4. *Genes Dev* **20**:660-665.
31. **Kim, S. C., R. Sprung, Y. Chen, Y. Xu, H. Ball, J. Pei, T. Cheng, Y. Kho, H. Xiao, L. Xiao, N. V. Grishin, M. White, X. J. Yang, and Y. Zhao.** 2006. Substrate and functional diversity of lysine acetylation revealed by a proteomics survey. *Mol Cell* **23**:607-618.
32. **Kozubowski, L., H. Panek, A. Rosenthal, A. Bloecher, D. J. DeMarini, and K. Tatchell.** 2003. A Bni4-Glc7 phosphatase complex that recruits chitin synthase to the site of bud emergence. *Mol Biol Cell* **14**:26-39.
33. **Krogan, N. J., K. Baetz, M. C. Keogh, N. Datta, C. Sawa, T. C. Kwok, N. J. Thompson, M. G. Davey, J. Pootoolal, T. R. Hughes, A. Emili, S. Buratowski, P. Hieter, and J. F. Greenblatt.** 2004. Regulation of chromosome stability by the histone H2A variant Htz1, the Swr1 chromatin remodeling complex, and the histone acetyltransferase NuA4. *Proc Natl Acad Sci U S A*.
34. **Lin, Y. Y., J. Y. Lu, J. Zhang, W. Walter, W. Dang, J. Wan, S. C. Tao, J. Qian, Y. Zhao, J. D. Boeke, S. L. Berger, and H. Zhu.** 2009. Protein acetylation microarray reveals that NuA4 controls key metabolic target regulating gluconeogenesis. *Cell* **136**:1073-1084.
35. **Lin, Y. Y., Y. Qi, J. Y. Lu, X. Pan, D. S. Yuan, Y. Zhao, J. S. Bader, and J. D. Boeke.** 2008. A comprehensive synthetic genetic interaction network governing yeast histone acetylation and deacetylation. *Genes Dev* **22**:2062-2074.
36. **Lindstrom, K. C., J. C. Vary, Jr., M. R. Parthun, J. Delrow, and T. Tsukiyama.** 2006. Isw1 functions in parallel with the NuA4 and Swr1 complexes in stress-induced gene repression. *Mol Cell Biol* **26**:6117-6129.
37. **Liu, C., D. van Dyk, Y. Li, B. Andrews, and H. Rao.** 2009. A genome-wide synthetic dosage lethality screen reveals multiple pathways that require the functioning of ubiquitin-binding proteins Rad23 and Dsk2. *BMC Biol* **7**:75.

38. **Logan, M. R., T. Nguyen, N. Szapiel, J. Knockleby, H. Por, M. Zadworny, M. Neszt, P. Harrison, H. Bussey, C. A. Mandato, J. Vogel, and G. Lesage.** 2008. Genetic interaction network of the *Saccharomyces cerevisiae* type 1 phosphatase Glc7. *BMC Genomics* **9**:336.
39. **Longtine, M. S., A. McKenzie, 3rd, D. J. Demarini, N. G. Shah, A. Wach, A. Brachat, P. Philippsen, and J. R. Pringle.** 1998. Additional modules for versatile and economical PCR-based gene deletion and modification in *Saccharomyces cerevisiae*. *Yeast* **14**:953-961.
40. **Longtine, M. S., C. L. Theesfeld, J. N. McMillan, E. Weaver, J. R. Pringle, and D. J. Lew.** 2000. Septin-dependent assembly of a cell cycle-regulatory module in *Saccharomyces cerevisiae*. *Mol Cell Biol* **20**:4049-4061.
41. **Ma, X. J., Q. Lu, and M. Grunstein.** 1996. A search for proteins that interact genetically with histone H3 and H4 amino termini uncovers novel regulators of the Swe1 kinase in *Saccharomyces cerevisiae*. *Genes Dev* **10**:1327-1340.
42. **McMurray, M. A., and J. Thorner.** 2009. Reuse, replace, recycle. Specificity in subunit inheritance and assembly of higher-order septin structures during mitotic and meiotic division in budding yeast. *Cell Cycle* **8**:195-203.
43. **McMurray, M. A., and J. Thorner.** 2009. Septins: molecular partitioning and the generation of cellular asymmetry. *Cell Div* **4**:18.
44. **Millar, C. B., F. Xu, K. Zhang, and M. Grunstein.** 2006. Acetylation of H2AZ Lys 14 is associated with genome-wide gene activity in yeast. *Genes Dev* **20**:711-722.
45. **Mitchell, L., J. P. Lambert, M. Gerdes, A. S. Al-Madhoun, I. S. Skerjanc, D. Figeys, and K. Baetz.** 2008. Functional dissection of the NuA4 histone acetyltransferase reveals its role as a genetic hub and that Eaf1 is essential for complex integrity. *Mol Cell Biol* **28**:2244-2256.
46. **Mortensen, E. M., H. McDonald, J. Yates, 3rd, and D. R. Kellogg.** 2002. Cell cycle-dependent assembly of a Gin4-septin complex. *Mol Biol Cell* **13**:2091-2105.
47. **Moseley, J. B., and B. L. Goode.** 2006. The yeast actin cytoskeleton: from cellular function to biochemical mechanism. *Microbiol Mol Biol Rev* **70**:605-645.
48. **Pan, X., P. Ye, D. S. Yuan, X. Wang, J. S. Bader, and J. D. Boeke.** 2006. A DNA integrity network in the yeast *Saccharomyces cerevisiae*. *Cell* **124**:1069-1081.
49. **Peterson, E. A., and E. M. Petty.** 2010. Conquering the complex world of human septins: implications for health and disease. *Clin Genet* **77**:511-524.
50. **Ruault, M., and L. Pillus.** 2006. Chromatin-modifying enzymes are essential when the *Saccharomyces cerevisiae* morphogenesis checkpoint is constitutively activated. *Genetics* **174**:1135-1149.
51. **Shaw, J. A., P. C. Mol, B. Bowers, S. J. Silverman, M. H. Valdivieso, A. Duran, and E. Cabib.** 1991. The function of chitin synthases 2 and 3 in the *Saccharomyces cerevisiae* cell cycle. *J Cell Biol* **114**:111-123.

52. **Sigala, B., M. Edwards, T. Puri, and I. R. Tsaneva.** 2005. Relocalization of human chromatin remodeling cofactor TIP48 in mitosis. *Exp Cell Res* **310**:357-369.
53. **Sikorski, R. S., and P. Hieter.** 1989. A system of shuttle vectors and yeast host strains designed for efficient manipulation of DNA in *Saccharomyces cerevisiae*. *Genetics* **122**:19-27.
54. **Silverman, S. J., A. Sburlati, M. L. Slater, and E. Cabib.** 1988. Chitin synthase 2 is essential for septum formation and cell division in *Saccharomyces cerevisiae*. *Proc Natl Acad Sci U S A* **85**:4735-4739.
55. **Skibbens, R. V.** 2009. Establishment of sister chromatid cohesion. *Curr Biol* **19**:R1126-1132.
56. **Skibbens, R. V., L. B. Corson, D. Koshland, and P. Hieter.** 1999. Ctf7p is essential for sister chromatid cohesion and links mitotic chromosome structure to the DNA replication machinery. *Genes Dev* **13**:307-319.
57. **Smith, E. R., A. Eisen, W. Gu, M. Sattah, A. Pannuti, J. Zhou, R. G. Cook, J. C. Lucchesi, and C. D. Allis.** 1998. ESA1 is a histone acetyltransferase that is essential for growth in yeast. *Proc Natl Acad Sci U S A* **95**:3561-3565.
58. **Smolka, M. B., S. H. Chen, P. S. Maddox, J. M. Enserink, C. P. Albuquerque, X. X. Wei, A. Desai, R. D. Kolodner, and H. Zhou.** 2006. An FHA domain-mediated protein interaction network of Rad53 reveals its role in polarized cell growth. *J Cell Biol* **175**:743-753.
59. **Sopko, R., D. Huang, N. Preston, G. Chua, B. Papp, K. Kafadar, M. Snyder, S. G. Oliver, M. Cyert, T. R. Hughes, C. Boone, and B. Andrews.** 2006. Mapping pathways and phenotypes by systematic gene overexpression. *Mol Cell* **21**:319-330.
60. **Stante, M., G. Minopoli, F. Passaro, M. Raia, L. D. Vecchio, and T. Russo.** 2009. Fe65 is required for Tip60-directed histone H4 acetylation at DNA strand breaks. *Proc Natl Acad Sci U S A* **106**:5093-5098.
61. **Sykes, S. M., H. S. Mellert, M. A. Holbert, K. Li, R. Marmorstein, W. S. Lane, and S. B. McMahon.** 2006. Acetylation of the p53 DNA-binding domain regulates apoptosis induction. *Mol Cell* **24**:841-851.
62. **Takahashi, Y., M. Iwase, M. Konishi, M. Tanaka, A. Toh-e, and Y. Kikuchi.** 1999. Smt3, a SUMO-1 homolog, is conjugated to Cdc3, a component of septin rings at the mother-bud neck in budding yeast. *Biochem Biophys Res Commun* **259**:582-587.
63. **Tang, C. S., and S. I. Reed.** 2002. Phosphorylation of the septin cdc3 in g1 by the cdc28 kinase is essential for efficient septin ring disassembly. *Cell Cycle* **1**:42-49.
64. **Tang, Y., J. Luo, W. Zhang, and W. Gu.** 2006. Tip60-dependent acetylation of p53 modulates the decision between cell-cycle arrest and apoptosis. *Mol Cell* **24**:827-839.
65. **Tong, A. H., M. Evangelista, A. B. Parsons, H. Xu, G. D. Bader, N. Page, M. Robinson, S. Raghizadeh, C. W. Hogue, H. Bussey, B. Andrews, M. Tyers, and C. Boone.** 2001. Systematic genetic analysis with ordered arrays of yeast deletion mutants. *Science* **294**:2364-2368.

66. **VanDemark, A. P., M. M. Kasten, E. Ferris, A. Heroux, C. P. Hill, and B. R. Cairns.** 2007. Autoregulation of the rsc4 tandem bromodomain by gcn5 acetylation. *Mol Cell* **27**:817-828.
67. **Versele, M., and J. Thorner.** 2004. Septin collar formation in budding yeast requires GTP binding and direct phosphorylation by the PAK, Cla4. *J Cell Biol* **164**:701-715.
68. **Voss, A. K., and T. Thomas.** 2009. MYST family histone acetyltransferases take center stage in stem cells and development. *Bioessays* **31**:1050-1061.
69. **Weirich, C. S., J. P. Erzberger, and Y. Barral.** 2008. The septin family of GTPases: architecture and dynamics. *Nat Rev Mol Cell Biol* **9**:478-489.
70. **Zhang, H., D. O. Richardson, D. N. Roberts, R. Utley, H. Erdjument-Bromage, P. Tempst, J. Cote, and B. R. Cairns.** 2004. The Yaf9 component of the SWR1 and NuA4 complexes is required for proper gene expression, histone H4 acetylation, and Htz1 replacement near telomeres. *Mol Cell Biol* **24**:9424-9436.
71. **Zhang, J., R. Sprung, J. Pei, X. Tan, S. Kim, H. Zhu, C. F. Liu, N. V. Grishin, and Y. Zhao.** 2009. Lysine acetylation is a highly abundant and evolutionarily conserved modification in *Escherichia coli*. *Mol Cell Proteomics* **8**:215-225.
72. **Zhang, W., J. R. Bone, D. G. Edmondson, B. M. Turner, and S. Y. Roth.** 1998. Essential and redundant functions of histone acetylation revealed by mutation of target lysines and loss of the Gcn5p acetyltransferase. *EMBO J* **17**:3155-3167.
73. **Zhao, S., W. Xu, W. Jiang, W. Yu, Y. Lin, T. Zhang, J. Yao, L. Zhou, Y. Zeng, H. Li, Y. Li, J. Shi, W. An, S. M. Hancock, F. He, L. Qin, J. Chin, P. Yang, X. Chen, Q. Lei, Y. Xiong, and K. L. Guan.** 2010. Regulation of cellular metabolism by protein lysine acetylation. *Science* **327**:1000-1004.
74. **Zou, J., H. Friesen, J. Larson, D. Huang, M. Cox, K. Tatchell, and B. Andrews.** 2009. Regulation of cell polarity through phosphorylation of Bni4 by Pho85 G1 cyclin-dependent kinases in *Saccharomyces cerevisiae*. *Mol Biol Cell* **20**:3239-3250.

CHAPTER 4:

A novel proteomic method, mChIP-KAT-MS, to simultaneously map protein interactions and acetylation targets for the lysine acetyltransferase NuA4

Leslie Mitchell^{1,2}, Jean-Phillipe Lambert^{1,2}, Hu Zhou^{1,2}, Sylvain Huard^{1,2},
Daniel Figeys^{1,2}, and Kristin Baetz^{1,2}

¹ Ottawa Institute of Systems Biology, University of Ottawa, Ottawa, Ontario K1H8M5, Canada

² Department of Biochemistry, Microbiology and Immunology, University of Ottawa, Ottawa, Ontario K1H8M5 Canada

Contribution of Authors: LM performed all experiments with the exception of microscopy, which was performed by SH. JPL and HZ performed the mass spectrometry in the laboratory of DF. LM created all the figures and wrote the manuscript with review by KB.

4.1 Abstract

The biological consequences of protein lysine acetylation are only beginning to be characterized outside the context of histone proteins. NuA4 is an essential lysine acetyltransferase (KAT) in the budding yeast *S. cerevisiae* that genetic studies have linked to a myriad of cellular processes beyond its traditional chromatin roles mediated by histone acetylation, including chromosome stability. We hypothesize that proteins that physically interact with NuA4 are predictive of the cellular pathways in which this KAT functions and may be acetylation targets. To explore this, we have developed a novel mass spectrometry method that generates a protein interaction network from which we can simultaneously identify both *in vivo* acetylation sites and NuA4-dependent *in vitro* acetylation sites. Our NuA4 protein interaction network consists of 124 reproducible protein interactions, of which more than 10% have detectable acetyl lysine residues. Moreover, we discovered acetylation sites on 10 NuA4 subunits, suggesting auto-acetylation as a means of NuA4 regulation. Notably, numerous spindle pole body proteins were identified in the NuA4 protein interaction network. We determine that acetyltransferase-deficient NuA4 mutants have defects in microtubule dynamics including broken or “hooked” spindles. Through a series of mass spectrometry studies we identify *in vivo* lysine acetylation on 8 spindle pole body components, 4 of which are *in vitro* targets of NuA4, including Cnm67, Nud1, Bfa1 and Spc42. Our study has dramatically increased our knowledge of NuA4’s protein interaction

network, identified novel non-histone targets, and uncovered a role for NuA4 in spindle dynamics.

4.2 Introduction

Lysine acetyltransferase (KAT) enzymes catalyze the transfer of an acetyl group from acetyl coenzyme A onto the epsilon-amino group of lysine residues. Acetylation can then regulate protein function in a number of ways, including altering the localization, activity, stability, and/or physical interactions of the target protein (70). Through the acetylation of histone proteins, KATs have traditionally been associated with a variety of chromatin-based cellular processes such as transcription, silencing, and DNA repair (11). More recently, systematic screens aimed at identifying acetylated lysine peptides in both prokaryotic and mammalian systems have established acetylation as a ubiquitous and conserved mechanism of protein regulation that affects thousands of proteins (12, 39, 77, 79, 80). Further, these screens have revealed fundamental properties associated with lysine acetylation, such as the abundance of acetylation sites found on metabolic enzymes and mitochondrial proteins, the tendency of multi-subunit protein complexes to be heavily acetylated, and that most acetylated proteins do not have an obvious role in chromatin-directed processes. However, in the vast majority of cases the biological consequence(s) of lysine acetylation and the KAT responsible for catalysis have yet to be studied.

NuA4 is a KAT complex in the budding yeast *Saccharomyces cerevisiae* composed of thirteen subunits (2, 18). Along with the catalytic subunit, Esa1 (2), five additional NuA4 members are essential proteins (Arp4, Act1, Epl1, Swc4, and

Tra1) while the remaining seven are not (Eaf1, Eaf3, Eaf5, Eaf6, Eaf7, Yaf9 and Yng2). Genetic and phenotypic analyses have linked NuA4 function to a diverse array of cellular processes, including transcription (22, 25), DNA repair (7), chromosome stability (41), cell cycle control (13, 14), the stress response (51, 59), vesicle-mediated transport (59), and gluconeogenesis (49). Currently, only a limited number of pathways have been established for NuA4 function *in vivo*, all of which rely on the KAT activity of the complex. For instance, through the acetylation of histone proteins, NuA4 regulates the transcription of both ribosomal and stress responsive genes (51, 64), and also promotes the repair of DNA damage (7). NuA4's histone acetylation targets *in vivo* include H4 (2, 18, 69), and the H2A variant Htz1 (3, 38, 56, 58). A specific role for NuA4 in gluconeogenesis has also been demonstrated as Esa1-dependent acetylation regulates the enzymatic activity of Pck1, a key regulator of gluconeogenesis (49). Finally, a single Esa1-dependent acetylation site that regulates protein stability has been identified on the NuA4 subunit Yng2, and this modification may modulate NuA4's response to DNA damage (50). To fully elucidate the cellular functions of NuA4 *in vivo* will require a detailed understanding of the direct pathways in which the complex functions, and a focused analysis of the role of NuA4-dependent acetylation within those pathways.

Surprisingly, lysine acetylation on non-histone proteins is remarkably understudied in yeast despite the propensity to develop and demonstrate proof-of-concept systematic screening techniques in this model organism. To date, one systematic analysis of lysine acetylation has been undertaken, whereby a protein

acetylation microarray encompassing more than 90% of the proteins encoded in the *S. cerevisiae* genome was used to identify putative NuA4 substrates *in vitro* (49). This work demonstrated the promise of identifying novel NuA4 targets by first defining a list of putative candidates *in vitro* and ultimately succeeded in discovering thirteen novel Esa1 substrates *in vivo* (49); importantly, the list of candidate substrates implicates NuA4 activity in a broad range of nuclear and non-nuclear processes. Despite its success, the technological challenges associated with a protein acetylation microarray as well as the inability to identify targeted lysine residues represent major drawbacks to this approach. Novel techniques need to be developed to connect KAT enzymes to their substrates and acetyl-lysine residues *in vivo* to fully elucidate the pathways governed by acetylation.

To this end, we have developed a method to generate a NuA4-associated protein interaction network in which the level of acetylated lysine residues is enriched *in vitro*. As proteins that physically interact are likely functionally related, identification of the NuA4-associated protein network serves to indicate pathways in which NuA4 functions. While all interacting partners represent putative acetylation targets, given that acetylation resulting from NuA4 catalysis *in vivo* may be low or rare, we have introduced a NuA4 *in vitro* KAT reaction to boost the level of acetylation within the interacting protein network. The resulting network of 124 NuA4 physically associated proteins, of which 23 are acetylated, significantly broadens our perspective on the pathways in which NuA4 may function *in vivo*. We next apply the methodology in an inverse fashion to explore the relationship between NuA4 and the spindle pole body, one of the many protein complexes we

find that physically associate with NuA4 *in vivo*. Finally, we discover that NuA4 plays a critical role in spindle morphology *in vivo*. This work provides proof-of-concept of a novel methodology to identify KAT targets.

4.3 Materials and methods

4.3.1 Yeast strains

Yeast strains used in this study are listed in Table 4.1. Genomic deletions or epitope tag integrations made for this study were designed with PCR-amplified cassettes as previously described (53).

Table 4.1: Yeast strains

Strain	Genotype	Source
YPH499	<i>MATa ade2-101 his3-Δ200 leu2-Δ1 lys2-801 trp1-Δ63 ura3-52</i>	(68)
YKB440	<i>MATa Δtrp1 ura3-1 leu2-3,112 his3-11,15 ade2-1 can1-100 ESA1-TAP::TRP</i>	(59)
YKB1994	<i>MATa his3Δ1 leu2Δ0 met15Δ0 ura3Δ0 CNM67-TAP::HIS</i>	TAP collection
YKB1996	<i>MATa his3Δ1 leu2Δ0 met15Δ0 ura3Δ0 BBP1-TAP::HIS</i>	TAP collection
YKB1999	<i>MATa his3Δ1 leu2Δ0 met15Δ0 ura3Δ0 SPC72-TAP::HIS</i>	TAP collection
YKB518	<i>MATa ade2-101 his3-Δ200 leu2-Δ1 lys2-801 trp1-Δ63 ura3-52 EAF7-MYC::kanMX</i>	(59)
YKB1306	<i>MATa SPC72-TAP::HIS EAF7-MYC::kanMX</i>	This study
YKB1296	<i>MATa BBP1-TAP::HIS EAF7-MYC::kanMX</i>	This study
YKB44	<i>MATa ade2-101 his3-Δ200 leu2-Δ1 lys2-801 trp1-Δ63 ura3-52 eaf1ΔKAN</i>	(59)
YKB1130	<i>MATa ade2-101 his3-Δ200 leu2-Δ1 lys2-801 trp1-Δ63 ura3-52 rpd3ΔTRP</i>	This study
YKB1154	<i>MATa ade2-101 his3-Δ200 leu2-Δ1 lys2-801 trp1-Δ63 ura3-52 rpd3ΔTRP eaf1ΔKAN</i>	This study
YKB1233	<i>MATa ade2-101 his3-Δ200 leu2-Δ1 lys2-801 trp1-Δ63 ura3-52 URA3::TUB1-GFP</i>	This study
YKB1235	<i>MATa ade2-101 his3-Δ200 leu2-Δ1 lys2-801 trp1-Δ63 ura3-52 URA3::TUB1-GFP eaf1ΔKAN</i>	This study
LPY3500	<i>MATa his3-Δ200 leu2-3,112 trp1Δ1 ura3-52 esa1Δ::HIS3 esa1(L254P)::URA3</i>	(14)
YKB1250	<i>MATa 52 URA3::TUB1-GFP esa1Δ::HIS3 esa1(L254P)::URA3</i>	This study

4.3.2 High stringency purification of exogenous NuA4 from yeast for *in vitro* KAT assays

High stringency purification of NuA4 from yeast was carried out using Esa1-TAP as described (59), except the complex was eluted from magnetic beads by enzymatic cleavage in TC Buffer (50mM Tris, pH 8.0, 1mM DTT, 0.1% Nonidet P-40, 150mM NaCl, 10% glycerol) using tobacco etch virus (TEV) protease, which was prepared and generously donated by the laboratory of Dr. Jean-François Couture. Briefly, 1L of exponentially growing yeast cells (in YPD, at 30°C) expressing endogenously TAP-tagged *ESA1* were lysed and NuA4 was purified in a single step using 600µL of magnetic beads coupled to IgG. After washing, the NuA4-bead matrix was re-suspended in TC buffer (100µL) to which was added 20µL of TEV. The cleavage reaction was incubated overnight at 4°C with end-over-end rotation. Finally, the supernatant was isolated from the beads, aliquoted, and stored at -80°C. The purity of each NuA4 preparation was assessed by silver stain using 2µL of TEV-cleaved NuA4 separated by SDS-PAGE (7.5%). Activity of all high stringency NuA4 complex preparations was confirmed by performing a KAT reaction using 2µg of chicken core histones (Upstate, 13-107) and 2µg of standard, unlabeled acetyl coenzyme A (Sigma, A2056) in a final volume of 15µL. The acetylation signal was assessed by Western blot using an anti-acetyl lysine antibody (Upstate, 06-933). An untagged control strain was also taken through immunopurification procedure to ensure the purity of the purification (by silver stain) and to confirm that KAT activity did not non-specifically associate with the IgG-coated magnetic beads

4.3.3 NuA4 modified chromatin immunopurification (mChIP)

NuA4 and its associated protein network were isolated from exponentially growing yeast cultures via mChIP (44) of protein A (one epitope of the tandem affinity purification [TAP] tag) through endogenously tagged *ESA1*. Six replicates of the experiment were performed, and a flow chart is presented in Supplemental Figure 1 with specific details of each replicate. Briefly, cells from 400-700mL mid-log phase cultures grown in YPD at 30°C were collected by centrifugation, washed in 25mL of ice-cold water, transferred to 1.5mL Eppendorf tubes and frozen on dry ice. Cell pellets were re-suspended in 300uL of lysis buffer (100mM HEPES pH 8.0, 20mM magnesium acetate, 10% glycerol (V/V), 10mM EGTA, 0.1mM EDTA, 300mM sodium acetate, and fresh protease inhibitor cocktail (Sigma, P8215)) plus an equal volume of glass beads, and cells were lysed through vortexing (six 1-minute blasts with incubation on ice between vortexing). Lysates were subjected to sonication (3x20sec; 1 minute incubation on ice between each pulse) using a Misonix Sonicator 3000 at setting four. Prior to centrifugation (10min, 3000rpm, 4°C), Nonidet P-40 was added to a final concentration of 1%. 40-150mg of whole cell extract was incubated with 100-600µL magnetic beads (Invitrogen, 143.02D) cross-linked to rabbit immunoglobulin (IgG) (Chemicon, PP64) as per the manufacturer's instructions. Following 2 hours of end-over-end rotation at 4°C, the beads were collected on a magnet and washed three times with 1mL of ice cold wash buffer (100mM HEPES pH 8.0, 20mM magnesium acetate, 10% glycerol (V/V), 10mM EGTA, 0.1mM EDTA, 300mM sodium acetate, 0.5% Nonidet P-40). At this point, immunopurified proteins were either eluted from the magnetic beads

in 1X loading dye (50mM Tris, pH 6.8, 2% SDS, 0.1% bromophenol blue, 10% glycerol) with gentle heating (65°C for 10 minutes) (3 replicates); eluted from the magnetic beads by incubating in 1mL of elution buffer (0.5M NH₄OH, 0.5M EDTA) at room temperature for 20 minutes (1 replicate); or washed once in 1mL 1X KAT buffer (50mM Tris pH 8.0, 50mM NaCl, 5mM MgCl₂, 1mM DTT) and subjected to a KAT reaction using isotopically labeled acetyl coenzyme A (see below) (2 replicates). The loading dye eluate samples were transferred to new tubes and boiled for 10 minutes at 95°C following the addition of β-2-mercaptoethanol to 100mM. Proteins were separated by SDS-PAGE (NuPAGE Novex 4-12% Bis-Tris Gel, Invitrogen, NP0321), visualized by silver stain, and bands were excised and processed for mass spectrometry (see below). The sample in elution buffer was transferred to a new tube and evaporated to dryness using a speed vac and processed on the proteomic reactor (see below).

4.3.4 *in vitro* heavy KAT reactions for NuA4 mChIP

NuA4 *in vitro* heavy KAT assays using isotopically labeled acetyl coenzyme A (herein referred to as 'heavy') were carried out with immunopurified proteins still bound to the magnetic beads by adding to the protein-magnetic bead matrix 5X KAT buffer (250mM Tris pH 8.0, 250mM NaCl, 25mM MgCl₂, 5mM DTT), ¹³C₂-acetyl coenzyme A (Isotec, 658650), and stringently purified, exogenous NuA4 (see above). As the exogenous NuA4 preparation included the TEV enzyme, immunopurified proteins still bound to magnetic beads were enzymatically cleaved during the KAT reactions. Heavy KAT reactions were performed on two NuA4 mChIP replicates (Supplemental Figure 1) and were carried out in a total volume of

100uL using 6ug of $^{13}\text{C}_2$ -acetyl coenzyme A and 10uL of exogenous NuA4 at 30°C for 1 hour with end-over-end rotation. Samples were separated from the beads and processed directly on the proteomic reactor, as described below (81).

4.3.5 Spindle pole body mChIP-KAT-MS

SPB protein complexes were isolated from 700mL of exponentially growing yeast cultures in YPD at 30°C using endogenously TAP-tagged *CNM67* or *SPC72*. The mChIP procedure was carried out identically as described above for NuA4 except 100uL of magnetic beads coupled to IgG and 100mg of whole cell lysate were used. Following immunopurification and washing, beads were equilibrated in 1X KAT buffer, and then subjected to a heavy KAT reaction in a final volume of 20uL including 5uL highly purified exogenous NuA4, 2ug of $^{13}\text{C}_2$ -acetyl coenzyme A, and 4uL 5X KAT buffer. Following incubation at 30°C for one hour with end-over-end rotation, an equal volume of 2X loading dye was added directly to the beads and the samples were heated at 65°C for 10 minutes. The loading dye eluate samples were transferred to new tubes and boiled for 10 minutes at 95°C following the addition of β -2-mercaptoethanol to 100mM. Each of the two SPB mChIP-KAT-MS assays was performed once and proteins were separated by SDS-PAGE (NuPAGE Novex 4-12% Bis-Tris Gel, Invitrogen, NP0321), and visualized by silver stain.

4.3.6 Mass spectrometry to detect protein interactions and acetyl lysine residues

For three replicates of NuA4 and SPB mChIP samples separated on SDS-PAGE, the entire lane was excised, reduced, alkylated, and digested as previously

described (78). The other three replicates of NuA4 mChIP, including the two subjected to the heavy KAT assay, were prepared using a novel proteomic sample processing device termed the proteomic reactor (81). Briefly, the proteomic reactor enables the enrichment, clean up, and chemical and enzymatic processing within capillary tubing packed with either strong anion or strong cation exchange (SAX or SCX, respectively) beads. Processed peptides were eluted using 10 step pH buffers as described (81). One of three replicates was subjected to both SAX and SCX proteomic reactor conditions, and the remaining two subjected to only SAX conditions (Supplemental Figure 1). Liquid chromatography coupled to tandem mass spectrometry (LC-MS/MS) was performed as previously described (44) using an Agilent 1100 HPLC system (Agilent Technologies) coupled to either an LTQ or an LTQ-Orbitrap XL mass spectrometer (Thermo-Electron) as indicated (Supplemental Table 1). Acetylated lysine residues were identified as previously described (12). MS/MS corresponding to putative lysine acetylation sites were all manually validated. Acetyl lysine residues were identified on NuA4 components in both the NuA4 and SPB mChIP-KAT-MS experiments (Supplemental Tables 4.1 and 4.2). The combined results all identified NuA4 acetyl lysine residues are presented in Figure 4.2 and Tables 4.2.

4.3.7 *In vitro* hot KAT assays

Radiolabelled KAT reactions were performed using 0.5 μ Ci of [³H]-acetyl coenzyme A (Perkin-Elmer, NET290L050UC), the equivalent of 10% of a high stringency NuA4 preparation (as described above) still on beads, and 3 μ L of 5X KAT buffer in a final volume of 15 μ L. Each reaction also contained 2 μ g of chicken

core histones (Upstate, 13-107) to serve as an internal positive control for KAT activity. The KAT reaction was incubated at 30°C for 1 hour with end-over-end rotation. An equal volume of 2x loading dye with BME (100mM Tris, pH 6.8, 4% SDS, 0.2% bromophenol blue, 200mM β -2-mercaptoethanol, 20% glycerol) was then added and the samples heated at 65°C for 10 minutes. Proteins were separated by SDS-PAGE (NuPAGE Novex 4-12% Bis-Tris Gel, Invitrogen, NP0321) and visualized by Coomassie staining. Next, the gel was treated for fluorography, dried, and exposed to film for 2 weeks at -80°C.

4.3.8 *In vitro* unlabelled KAT assays

KAT assays using unlabeled acetyl coenzyme A (Sigma, A2056) were performed as described for the radiolabelled experiments except 5 μ L of stringently purified NuA4 that had been TEV cleaved from magnetic beads was used in the reaction along with 1 μ g of unlabelled acetyl coenzyme A. Histone controls, using 2 μ g of core histone, were incubated separately. Following SDS-PAGE (7.5% for NuA4 or 15% for histones; gels made in-house), acetylation was assessed by Western blot using anti-acetyl lysine antibodies from Cell Signaling (9681) and Upstate (06-933).

4.3.9 Reciprocal co-immunopurifications

Reciprocal co-immunopurifications were carried out as previously described (44) except cells extracts were prepared using the mChIP technique and 100mg of total protein was incubated with 100 μ L of coupled magnetic beads (as per manufacturer's instructions) for 2 hours.

4.3.10 Microscopy

Microscopy was performed using a Leica DMI 6000 fluorescent microscope (Leica Microsystems GmbH, Wetzlar Germany), equipped with a Sutter DG4 light source (Sutter Instruments, California, USA), Ludl emission filter wheel with Chroma band pass emission filters (Ludl Electronic Products Ltd., NY, USA) and Hamamatsu Orca AG camera (Hamamatsu Photonics, Herrsching am Ammersee, Germany). Images were collected and analyzed using Velocity 4.3.2 Build 23 (Perkin Elmer). All cells were grown to mid-log phase at 25°C in YPD supplemented with adenine unless otherwise noted. Cells were fixed with paraformaldehyde (6) and stored at 4°C for no longer than one month. Z-stack images were collected (0.2µm steps) across 5-6µm. Analysis was performed on images collapsed into 2D using the “extended focus” option in Velocity.

4.4 Results

4.4.1 mChIP-KAT-MS: A novel method to study NuA4 function

The multi-functional NuA4 KAT complex in the budding yeast has been linked to a variety of cellular processes. To gain insight into the mechanisms of action and specific pathways in which NuA4 functions, we have developed a method to identify the network of proteins that physically interact with NuA4 *in vivo*, as well as to simultaneously identify acetyl lysine residues arising from either pre-existing *in vivo* or NuA4-dependent *in vitro* catalysis within that network. The methodology, which we have termed the NuA4 mChIP-KAT-MS, consists of three steps: (i) isolating NuA4 and its associated protein network from yeast cells; (ii) enriching the level of acetylated lysine residues within the network using a NuA4 *in*

in vitro KAT reaction; and (iii) identifying interacting proteins and acetylation sites by LC-MS/MS (Figure 4.1). To isolate NuA4 and interacting proteins, we purified NuA4 through Esa1-TAP using a variant of the traditional immunopurification strategy, termed modified chromatin immunopurification (mChIP) (44). The mChIP method, originally developed to study chromatin-associated proteins, has now been used successfully to increase the depth of coverage of protein interactions of wide range of bait proteins *in vivo* (43). Briefly, yeast whole cell lysates are subjected to mild sonication followed by gentle centrifugation, thereby promoting the retention of poorly soluble cellular components in solution. Immunopurification is performed in a single step using magnetic beads coated with IgG antibodies that specifically recognize the protein A component of the TAP tag. Next, to boost the level of acetyl lysine residues on proteins within the network an *in vitro* KAT assay is performed where exogenous, stringently purified NuA4 and isotopically labelled acetyl coenzyme A ($^{13}\text{C}_2$ -acetyl CoA; herein referred to as heavy acetyl CoA) are incubated with the immunopurified bead matrix. Finally, the acetyl lysine enriched network is

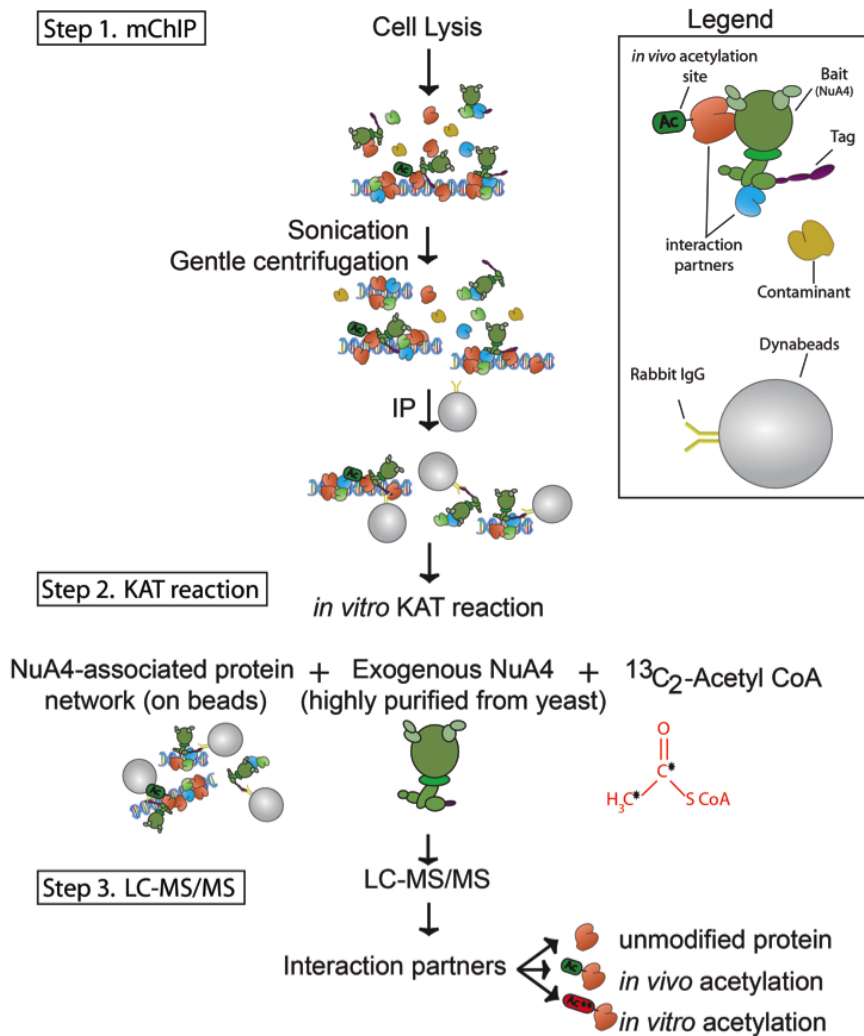


Figure 4.1: mChIP-KAT-MS methodology.

Step 1: NuA4 and the associated protein interaction network are purified from yeast using mChIP technology. Briefly, yeast whole cell lysate is mildly sonicated and gently clarified prior to NuA4 immunopurification through endogenously TAP-tagged Esa1 with magnetic beads coupled to IgG antibodies. **Step 2:** NuA4 and co-purifying proteins are subjected to an *in vitro* KAT assay. Highly purified exogenous NuA4 and isotopically acetyl coenzyme A ($^{13}\text{C}_2$ -Acetyl CoA) are added to the NuA4-bead-matrix under conditions promoting NuA4 KAT activity. **Step 3:** Proteins and acetylation sites are identified by liquid chromatography coupled to tandem mass spectrometry (LC-MS/MS). Acetyl-lysine on identified on sequenced peptides be unlabelled or light, resulting from pre-existing *in vivo* catalysis (green 'Ac' tag). Alternatively NuA4-dependent *in vitro* catalysis will yield labelled, or heavy acetyl-lysine residues (red 'Ac' tag).

analyzed by LC-MS/MS. Due to the shift in mass-to-charge ratio, heavy acetyl groups resulting from NuA4 *in vitro* KAT activity can be distinguished from unlabelled, pre-existing acetyl moieties (herein referred to as 'light' acetyl coA). Therefore, this methodology allows us to (i) identify the network of proteins associated with Esa1-TAP and NuA4 under normal growth conditions; (ii) generate a list of light or 'in vivo' acetylation sites, thereby increasing our general knowledge of yeast acetylation; and (iii) define a set of NuA4-specific *in vitro* acetylation sites on proteins that physically associate with NuA4 *in vivo*.

4.4.2 The NuA4-associated protein interaction network

To generate the NuA4-associated protein network (Figure 4.2), the Esa1-TAP mChIP assay was repeated six times. To identify and exclude non-specific interacting proteins from our final dataset, an untagged control strain was processed in parallel for each replicate. Additionally, proteins previously identified as contaminants due to their co-purification with a large number of unrelated bait proteins by mChIP (43) were excluded from the final dataset, (Supplemental Table 4.1). The resulting protein network includes the thirteen core members of the NuA4 KAT complex, as well as an additional 124 proteins (Figure 4.2 and Supplemental Table 4.1). As expected this network contains proteins that had previously been shown to interact with one or more NuA4 subunits, including histone proteins H4 (Hhf1), H2A (Hta1 and Hta2), H2B (Htb2), and H3 (Hht1) (14); the stress responsive transcription factors (Msn2, Msn4, and Yap1) (59); subunits of the Chaperonin Containing Tcp1 (CCT) complex (Tcp1, Cct8, Cct4) (17), the 14-3-3 protein Bmh1 (54); and the RNA polymerase II(Rpo21) (25).

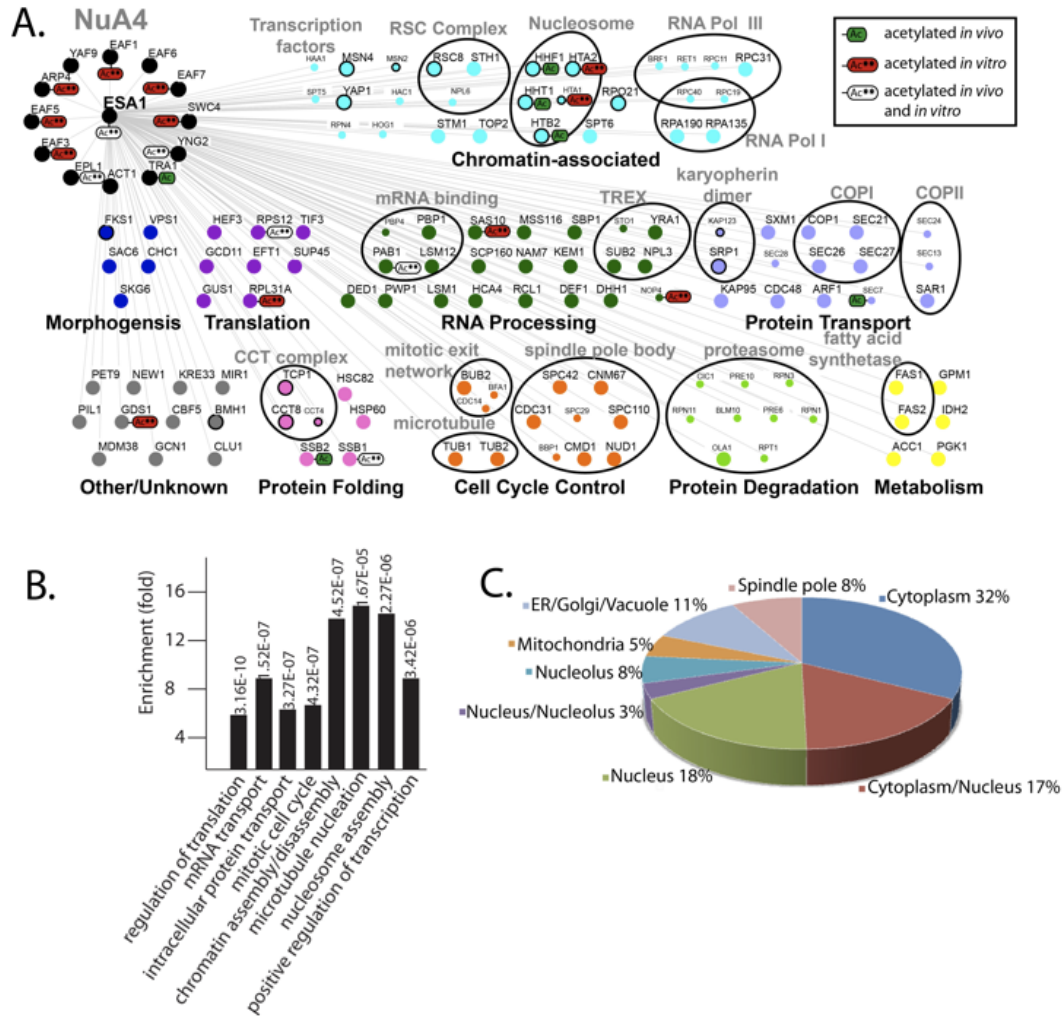


Figure 4.2: The acetyl lysine-enriched NuA4-associated protein network.

(A) NuA4 subunits, including the bait protein Esa1-TAP, are represented by black nodes (top left). Other interacting proteins are grouped by cellular process (node colour/label) and further organized into complexes where appropriate (circled). Eighty-nine interactions were identified in a minimum of two out of six replicates and are represented in the network with large nodes. An additional thirty-five proteins, denoted by small nodes/text, were identified once, however co-purified with reproducibly identified complexes (e.g. spindle pole body) or harboured one or more acetyl lysine residues. Previously identified NuA4 protein interactions are indicated by a black circle around the node (as published at www.theBiogrid.org version 3.1.70). Only physical interactions for Esa1, Yng2, Epl1, and Eaf1 were considered, as these proteins function exclusively with NuA4 *in vivo*. (B) The NuA4-associated protein network was analyzed for enrichment of gene ontology (GO) groups with Funspec (65) using a p-value threshold of 0.01 and the Bonferroni correction. (C) Cellular localization of proteins in the network. Localization annotation is based on a global study (32) (see Supplemental Table 1 for individual annotations). The thirteen NuA4 subunits were excluded from bioinformatic analyses presented in this figure.

Remarkably, the network includes an additional 108 proteins, dramatically expanding our knowledge of NuA4 interacting proteins and potential cellular functions of NuA4. As expected the gene ontology (GO) molecular functions assigned to the NuA4 interacting proteins were significantly enriched for processes previously associated with NuA4 such as (i) chromatin assembly/disassembly, (ii) the positive regulation of transcription, and (iii) mitotic cell cycle, and further suggests NuA4 may directly contribute to processes such as (i) the regulation of translation, (ii) mRNA transport, and (iii) intracellular protein transport (Figure 4.2B). We were intrigued to discover that the more than half of the proteins in the network localize outside the nucleus (Figure 4.2C). This suggests a broad localization pattern for NuA4 within the yeast cell. This work represents the first in depth analysis of proteins that physically associated with NuA4 *in vivo* and indicates the extent to which NuA4 may function directly in a diverse array of cellular processes in addition to chromatin-mediated roles.

4.4.3 Lysine acetylation identified within the NuA4-associated protein network

The mChIP-KAT-MS methodology presented here enables the discovery of acetylation sites on proteins within the network resulting from either *in vivo* acetylation (light acetyl groups) or *in vitro* catalysis (heavy acetyl groups), where the latter is specifically NuA4-dependent. While the mChIP-MS was performed six times, enabling identification of light acetyl-lysine residues in each replicate, only the final two replicates included the isotopically labelled NuA4 KAT assay to enrich NuA4-dependent acetyl lysine residues *in vitro* (Supplemental Figure 4.1). Within

the interaction network 78 acetyl lysine residues were identified on 23 proteins (Figure 4.2A, Table 4.2 Supplemental Table 1 and 2). Twenty-eight lysines were modified only by a light acetyl group, including most previously identified histone acetylation sites. The 13 novel sites on non-histone proteins increase our knowledge of *in vivo* acetylation in yeast. Moreover, as these proteins co-purify with NuA4 it suggests, but does not confirm, that their acetylation could be dependent on NuA4. Forty-three lysines were modified by only a heavy acetyl group. As we detected no other KAT enzymes in the NuA4 protein interaction network, (Figure 4.2 and Supplemental Table 4.1), heavy acetylation implicates NuA4-dependent catalysis in the acetylation of these sites *in vitro*. The set of heavy acetylation sites includes 12 lysines on eight novel NuA4 interacting proteins, none of whose acetylation has been previously reported; two heavy sites on histone H2A (Hta1 K124, K127), a protein acetylated by NuA4 *in vivo* at K5 (40), and an *in vivo* modification recently reported on the conserved K127 residue of human histone H2A (4); and 28 heavy sites on NuA4 subunits themselves, of which only Eaf7 K343 acetylation has previously been reported *in vivo* (4). The final 7 acetyl lysine residues, identified on 5 proteins, were represented by peptides modified by both light and heavy acetyl groups. Importantly, these sites represent excellent candidates as novel NuA4 acetylation targets in yeast cells, as their *in vivo* occurrence suggests biological relevance, and their acetylation *in vitro* indicates NuA4 is capable of catalyzing the reaction. All but one of these proteins (Pab1) belongs to the NuA4 complex.

Table 4.2: Acetyl lysine residues in the NuA4-associated protein network

Protein	Acetylation site(s)	Description
light (<i>in vivo</i>) acetylation		
H2A (Hta2)	K5 ^{#*} , K8 ^{#*}	histone
H2B (Htb1)	K8 [*] , K12 ^{#*} , K17 ^{#*}	histone
H2B (Htb2)	K7 ^{#*} , K22 ^{#*} , K23 ^{#*}	histone
H3 (Hht1)	K19 ^{#*} , K24 ^{#*} , K28 [*]	histone
H4 (Hhf1)	K5 ^{#*} , K8 ^{#*} , K12 ^{#*} , K16 ^{#*}	histone
Rps12	K114, K125	ribosome
Sec7	K1237, K1238	transport
Ssb1	K466, K538, K539	protein folding
Ssb2	K428 [*]	protein folding
Esa1	K232 [*]	NuA4
Epl1	K345 [*] , K353 [*] , K376, K379	NuA4
Tra1	K552 [*]	NuA4
heavy (<i>in vitro</i>) acetylation		
Gds1	K343 or K345, K348, K351, K354	unknown
Hca4	K570	RNA processing
Nop4	K144	RNA processing
Rpl31A	K86, K102	ribosome
Rps12	K95	ribosome
Sas10	K10	RNA processing
Ssb1	K90 or K95, K571 or K573	protein folding
H2A (Hta1)	K124, K127 [#]	histone
Esa1	K92, K96 or K97, K97	NuA4
Epl1	K16, K96, K100, K116, K118, K395, K429, K446, K470, K496, K512, K569, K721, K821	NuA4
Eaf1	K280, K848	NuA4
Arp4	K350	NuA4
Eaf7	K343 [#] , K381, K399, K409	NuA4
Eaf3	K45, K54, K156	NuA4
Swc4	K345, K350	NuA4
light and heavy (<i>in vivo</i> and <i>in vitro</i>) acetylation		
Esa1	K135	NuA4
Eaf5	K3	NuA4
Epl1	K39, K427	NuA4
Yng2	K170 [#] , K208	NuA4
Pab1	K7	RNA processing

= Acetyl lysine residues previously identified *in vivo* (4, 50, 66). 'or' indicates that unambiguous assignment of the acetyl group to one of two lysine residues within a single peptide was not possible. *Cannot be distinguished from tri-methylation.

Moreover, this set includes the Yng2 K170 site, a known acetylation target of Esa1 that regulates Yng2 protein stability *in vivo* (50). Together this work dramatically expands our knowledge of lysine acetylation in yeast by identifying *in vivo* acetylated proteins and putative targets of NuA4.

4.4.4 NuA4 Auto-acetylation

One of the most striking features of the acetylation dataset is the number of acetyl lysine residues identified on NuA4 subunits: 41 of the 79 acetylation sites we uncovered occurred on 10 NuA4 subunits (Table 4.2, Supplemental Tables 4.1 and 4.2). While the relative abundance of NuA4 subunits within the immunopurified samples increased the likelihood of acetyl lysine residue identification, this is an extremely interesting observation for a number of reasons. First, acetylation of multi-subunit protein complexes, in particular those that associated with chromatin, is a recognized phenomenon, and acetylation sites on 7 homologous human NuA4 subunits have been identified (12). Second, as mentioned, NuA4 auto-acetylates Yng2 *in vivo* and the modification stabilizes the protein (50). Third, *in vitro* acetylation of Epl1, Esa1, and Yng2, the NuA4 subunits that form a related complex called Piccolo NuA4 KAT complex which is proposed to globally and non-specifically acetylate histone H4 *in vivo* (9), has been shown by a radioactive *in vitro* KAT assay (5). Fourth, *in vivo* auto-acetylation in response to DNA damage has been described for the human ortholog of Esa1, Tip60, and this modification regulates Tip60's activity (76). Using the mChIP-KAT-MS methodology has enabled for the first time the identification of the specific sites of acetylation and the extent to which this modification exists on subunits such as Epl1, which was

modified by 20 acetyl lysine residues. Importantly, six sites were identified with both heavy and light acetyl groups, implicating NuA4 in their catalysis (Table 4.2). To confirm the *in vivo* and *in vitro* acetylation status of the complex, highly purified NuA4 was subjected to an *in vitro* KAT assay in the presence and absence of unlabelled acetyl coenzyme A. Following separation on SDS-PAGE, acetylation was detected by Western blot using two different anti-acetyl lysine antibodies. In the absence of acetyl coenzyme A, acetylation was detected on Epl1, Esa1, and Yng2, indicating each of these three proteins are acetylated *in vivo* (Figure 4.3A), corresponding to the results of our mChIP-KAT-MS analysis. Furthermore, in the presence of acetyl coenzyme A, hyper-acetylation of Yng2, Esa1, Eaf7, Eaf1, and Epl1 was observed (Figure 4.3B). To circumvent antibody specificity and epitope variability issues associated with lysine acetylation detection by Western blot, an *in vitro* KAT reaction was also performed using radiolabeled acetyl coenzyme A. Using this technique, we discovered acetylation on Yng2, Eaf5, Eaf1, and Epl1, and one or both of the co-migrating proteins Esa1-TAP/Eaf7 and Arp4/Swc4 (Figure 4.3B). Together, this data confirms that NuA4 subunits are acetylated *in vivo* and suggests the intriguing possibility that NuA4 auto-acetylation regulates one or more aspects of its function.

4.4.5 SPB mChIP-KAT-MS uncovers NuA4-dependent acetylation SPB subunits

Within the NuA4-associated protein network we discovered that NuA4 co-purifies eight proteins of the spindle pole body (SPB) complex (Figure 4.2A). The SPB,

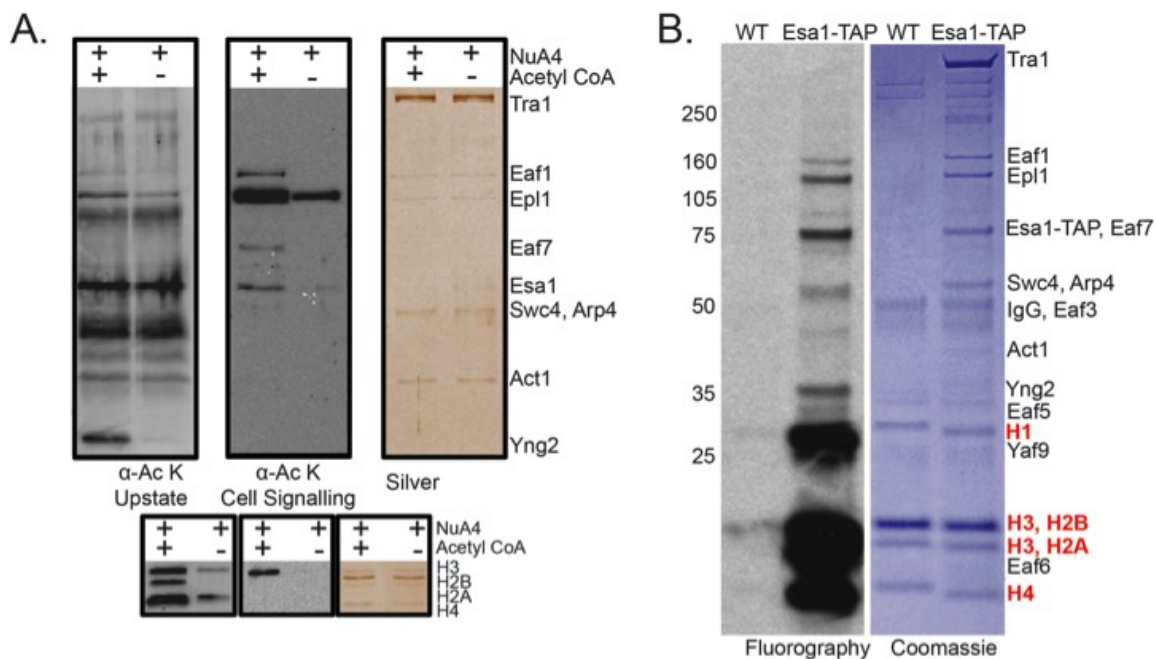


Figure 4.3: NuA4 subunits are acetylated *in vivo* and *in vitro*.

(A) Western blot analysis of NuA4 acetylation. *In vitro* KAT assays were performed with highly purified NuA4 incubated with or without acetyl coenzyme A (Acetyl CoA) (top panel). Reactions were separated by 7.5% SDS-PAGE and either silver stained, or subjected to Western blot analysis with two anti-acetyl lysine (α -Ac K) antibodies as indicated. The position of each NuA4 subunit is noted. To ensure NuA4 catalytic activity under experimental conditions, control reactions were also carried out on core histone proteins (bottom panel), separated by 15% SDS-PAGE. (B) Radioactive KAT assay to assess NuA4 auto-acetylation *in vitro*. [3 H]-acetyl coenzyme A was added directly to bead matrix of a stringently immunopurified NuA4 preparation (Esa1-TAP; YKB440) versus an untagged control immunopurification (WT; YKB779). Histone proteins were added to the reaction to serve as a positive control for acetylation. The reactions were separated on a gradient gel, Coomassie stained to visualize proteins (right panel), treated for fluorography, and finally exposed to film for 2 weeks (left panel). Proteins are identified on the right side and protein size is indicated on the left (kDa).

equivalent to the mammalian centrosome, is the sole microtubule-organizing centre in budding yeast and serves as a platform for nucleation of both nuclear and cytoplasmic microtubules (48). Within our network we also identified Tub1 and Tub2, the yeast tubulin proteins, as well as Bub1 and Bfa2, spindle checkpoint proteins that localize to the cytoplasmic face of the SPB (35) (Figure 4.2A). The core SPB complex is composed of roughly 20 unique proteins that assemble within the nuclear envelope, and play a critical role in chromosome segregation (35) (Figure 4.4C). A connection between NuA4 and chromosome segregation has been established through both phenotypic and genetic means, as some NuA4 mutant genes are sensitive to the microtubule destabilizing drug Benomyl (16, 40, 41, 46, 57, 60, 75), have elevated rates of chromosome loss (41), and display synthetic lethal genetic interactions with genes that impact microtubule dynamics (*BIK1*, *CIN8*, *BIM1*) and the spindle assembly checkpoint (*BUB1*, *BUB2*, *BUB3*, *MAD1*, *MAD2*) (15, 50, 59, 61). The physical interaction with the SPB that we have identified using the mChIP-KAT-MS technique suggests a potential mechanism through which NuA4 regulates chromosome stability. To explore this possibility, we first sought to test the validity of the SPB-NuA4 physical interaction by performing a reciprocal co-immunopurification of NuA4 using cells expressing endogenously tagged versions of two SPB components, Cnm67-TAP and Spc72-TAP, as well as a MYC-tagged version of the NuA4 subunit Eaf7. IgG-coated magnetic beads were used to immunopurify the TAP-tagged proteins, and Western blot analysis confirmed the co-purification of Eaf7-MYC with both SPB bait proteins (Figure 4.4A).

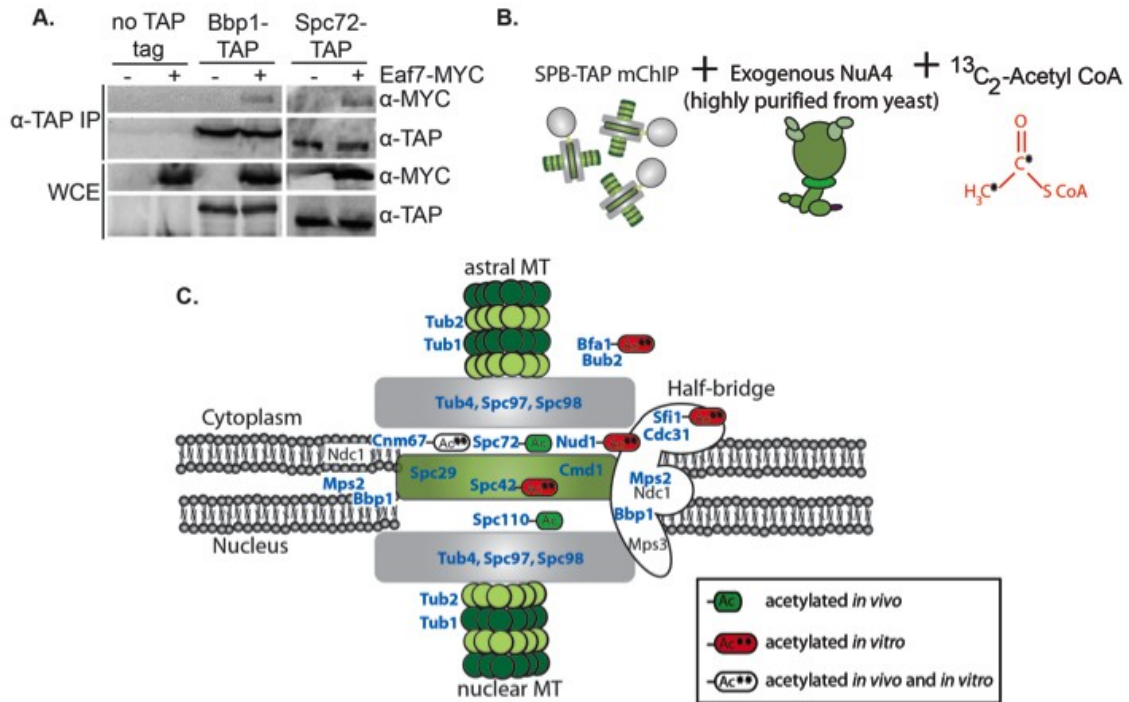


Figure 4.4: NuA4 acetylates spindle pole body proteins.

(A) NuA4 interacts with the SPB *in vivo*. Protein extracts expressing the indicated tagged proteins (Bbp1-TAP [YKB1996], Spc72-TAP [YKB1999], Eaf7-MYC [YKB518], Bbp1-TAP Eaf7-MYC [YKB1296], Spc72-TAP Eaf7-MYC [YKB1306]) or an untagged control (no TAP tag) (YKB779) were immunoprecipitated with magnetic beads coated with IgG antibodies that recognize the protein A component of the TAP tag. Total protein extracts (WCE) and immunoprecipitates (α-TAP IP) were resolved by 7.5% SDS-PAGE and subjected to Western blot analysis with anti-MYC and anti-TAP (α-MYC, α-TAP respectively), as indicated at the right side of the panels. (B) Schematic outlining the application of the mChIP-KAT-MS technique to identify acetylation on SPB proteins. ‘SPB-TAP mChIP’ represents the result of immunopurifying the SPB from yeast cells via mChIP through a TAP-tagged SPB component. (C) Cartoon of the yeast SPB. The relative positions of all core SPB components are shown with respect to the nuclear and cytoplasmic faces of the nuclear lipid bilayer. Astral and nuclear microtubules (MT) emanate into the cytoplasm and nucleus, respectively. SPB proteins identified in the Cnm67 and/or Spc72 SPB mChIP-KAT-MS experiments are indicated by blue text, otherwise protein names are in black. Acetylated proteins are noted (as described in the legend; Table 4.3). For a detailed review of the physical interactions of proteins within the SPB see (35).

Together with the unbiased identification of multiple SPB components through Esa1-TAP in the NuA4 interaction network (Figure 4.2A), and a previously reported yeast-two-hybrid interaction between Yaf9 and the SPB protein Mps2 (46), we conclude that NuA4 and the SPB physically interact *in vivo*.

While no acetylation sites were identified on the SPB in our initial NuA4 mChIP-KAT-MS experiment, a number of lines of evidence suggest NuA4 may directly acetylate one more subunits of the SPB. First, the SPB-NuA4 protein interaction we identified provides the required physical connection mandated (although not necessarily detectable) for an enzyme-substrate relationship. Second, the SPB component Cnm67 was discovered as an *in vitro* substrate of NuA4 in the protein acetylation microarray (49). Finally, hyper-acetylation has been suggested as a conserved mechanism of multi-subunit protein complex regulation (12). We suspected that the low SPB protein coverage, which ranged from 2-25%, might be a limiting factor in detecting acetylation. To circumvent this problem, we therefore performed the mChIP-KAT-MS technique using Spc72-TAP or Cnm67-TAP as the bait and NuA4 as the KAT (Figure 4.4B). Using the inverse approach enabled significantly improved coverage of SPB proteins, and thus the identification of ten novel acetylation sites on seven SPB or SPB-associated proteins (Table 4.3, Figure 4.4C, Supplemental Table 4.2). Importantly, seven of these sites are heavy, implicating NuA4-dependent KAT activity in their acetylation. This experiment validates the inverse application of the mChIP-KAT-MS technique to identify putative acetylation targets.

Table 4.3: Spindle pole body mChIP-KAT-MS acetylation sites

Protein	Acetylation site(s)	light or heavy
Cnm67	K220, K221, K222	light
Cnm67	K128, K433	heavy
Nud1	K35	heavy
Sfi1	K868, K869	heavy
Spc110	K331	light
Spc42	K13	heavy
Spc72	K222, K590	light
Bfa1	K328	heavy

4.4.6 NuA4 regulates spindle dynamics

Identification of NuA4-dependent acetylation on SPB proteins suggests a mechanism of direct regulation. As the sole microtubule-organizing centre in yeast, disruption of SPB function by mutation of any subunit can lead to specific defects in nuclear and/or astral microtubule dynamics that can be monitored by fluorescent microscopy in cells expressing an appropriately tagged (e.g. GFP) tubulin protein. For instance, cells lacking the non-essential SPB protein Cnm67 display frequent detachment of astral microtubules from the SPB despite maintaining normal nuclear microtubule morphology, evidenced by the formation and extension of a mitotic spindle during anaphase (30). To assess specific defects associated with loss of NuA4 acetylation, we examined cells expressing Tub1-GFP using fluorescence microscopy in either a wild type strain or a strain harboring a mutant allele of the NuA4 catalytic subunit, *esa1-L254P* (14). The protein encoded by the mutant allele exhibits reduced KAT activity both *in vivo* and *in vitro* at permissive temperatures, and is catalytically inactive at 37°C (14). In unbudded and small budded cells, we observed no difference in microtubule morphology between cells expressing the wild type or mutant alleles of *ESA1* (Figure 4.5). However, in large budded cells in which the mitotic spindle had begun to extend, we observed multiple defects in *esa1-L254P* mutant cells (Figure 4.5). Specifically, while 90% of large budded wild type cells had straight anaphase mitotic spindles, extending continuously to opposing edges of the mother and daughter bud, only 40% of large budded mutant cells displayed this

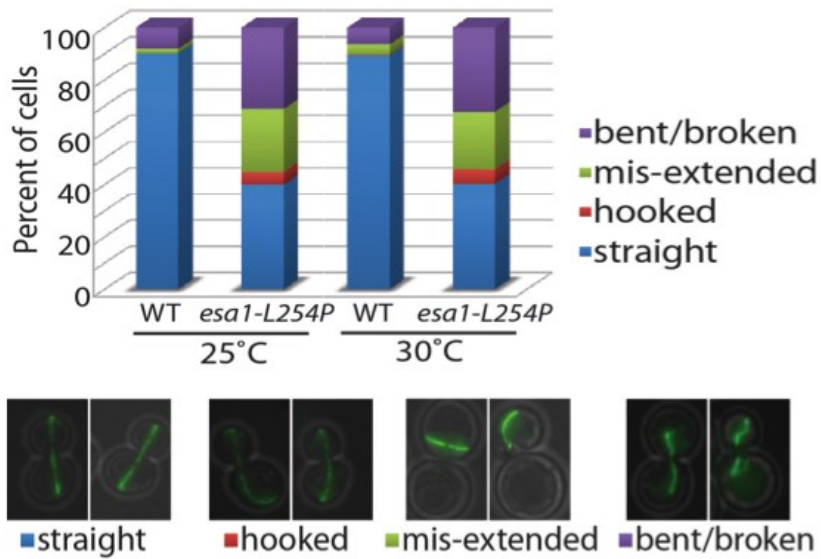


Figure 4.5: NuA4 acetylation regulates spindle dynamics.

esa1 mutants have microtubule morphology defects. Fixed cells expressing Tub1-GFP encoding either a wild type (YKB1233) or mutant allele of *ESA1* (YKB1268) (wild type or *esa1-L254P*) were examined by fluorescence microscopy. Cells were grown to mid-log phase in standard YPD medium supplemented with adenine at 25°C or 30°C as indicated. The average of three experimental replicates is shown and at least 50 large budded cells with extended microtubules were scored for each replicate.

expected morphology. Rather, in about 5% of cells, the mitotic spindle had a 'hooked' phenotype, 30% of cells exhibited bent and/or broken spindles, and in about 20% of cells the spindle was characterized as 'mis-extended', as it had elongated within the mother cell (Figure 4.5). We observed similar defects in *eaf1Δ* cells (data not shown) and a recently published high throughput screen to identify mutants with microtubule defects uncovered the 'hooked' microtubule phenotype in multiple non-essential NuA4 mutants (74). Importantly, our work connects the catalytic subunit of NuA4 to this phenotype, and moreover indicates the critical importance of lysine acetylation as only a moderate reduction in NuA4 acetyltransferase activity results in dramatic, pleiotropic defects. We are presently dissecting the biological consequences of acetylation on unacetylatable SPB mutant proteins and given the multiple defects associated with *esa1-L254P* cells we predict the role of lysine acetylation to be complex.

4.5 Discussion

4.5.1 mChIP-KAT-MS to characterize NuA4

Here we characterize the molecular functions of the NuA4 KAT complex using novel methodology we have developed called mChIP-KAT-MS (Figure 4.1). We hypothesized that proteins that physically interact with NuA4 can provide insight into the biological roles of the complex and further that a subset of interacting proteins are acetylation targets. Despite multiple global affinity purification surveys in yeast (24, 29, 42), only a limited number of NuA4 interaction partners had been identified prior to the work we present here and almost all of these derived from directed studies (17, 25, 54, 59). Application of the mChIP-KAT-

MS technique to the NuA4 protein complex has increased our knowledge of physical interaction partners for the complex by ten-fold (Figure 4.2A). We cannot, however, exclude the possibility that at least a portion of proteins in the physical interaction network co-purify through Esa1 as part of PicNuA4 (9). It is also possible that some interactions may be mediated through DNA, although the non-nuclear localization pattern of more than half of the proteins in the network (Figure 4.2C) suggests that in most cases this is likely not the case.

Importantly, this work places NuA4 in the context of various new biological pathways. For instance, we identified a large number of proteins involved in RNA processing, including all four components of the Transcription-Export complex (TREX complex; Yra1, Sub2, Sto1, Npl3) implicated in both transcriptional elongation and nuclear export (37); four proteins that together bind to and regulate polyadenylation of mRNA (Pab1, Pbp1, Pbp4, Lsm12) (72); as well as proteins involved in both mRNA decay (Kem1, Nam7, Lsm1) and rRNA maturation (Sik1, Hca4, Pwp1, Rcl1) (Figure 2A). These physical interactions are the first indication that NuA4 may participate directly in one or more aspects of mRNA processing. It is also of interest to note that both Esa1 and Eaf3 contain chromodomains, best known for their methylated histone binding capability, but are also able to bind RNA (1). Another pair of protein complexes identified in the NuA4-associated network are the COPI and COPII transport complexes, which promote vesicle formation and cargo transport at the Golgi and ER membranes, respectively (47). These interactions may provide functional insight into previously reported synthetic lethal genetic interactions that suggest a role for NuA4 in vesicle-mediated transport, and

phenotypic analysis indicating that acetyltransferase-deficient NuA4 mutants have defects in vacuole morphology (59).

Even with respect to known interaction partners the network serves to broaden our perspective on these connections. An interesting example is the interaction discovered between NuA4 and components of the Chaperonin Containing Tcp1 (CCT) complex (Tcp1, Cct8, Cct4), which is responsible for folding a large number of proteins in the cell, including actin and tubulin (20). Where the NuA4 subunit Eaf5 previously co-purified with various CCT bait proteins (17), here we demonstrate the opposite, uncovering the reciprocal co-purification of CCT complex subunits with NuA4; while it is possible that multiple NuA4 subunits depend on CCT for folding, it is intriguing to consider that NuA4 may regulate some aspect of CCT function, as has been shown for other co-chaperones (17). Notably, CCT subunits are acetylated in yeast and the acetylation state of the complex modulates its ability to fold actin *in vitro* (52) and Cct2 subunit was discovered as an *in vitro* acetylation target of NuA4 (49). Additionally, acetylated lysine residues have been identified on the homologous human TCP1 ring complex (39). Together these results suggest the possibility that one or more CCT subunits may be NuA4 acetylation targets. Clearly, by integrating the NuA4-associated protein interaction network presented here with NuA4 synthetic lethal (50, 59, 61, 73) and synthetic dosage lethal genetic interaction networks, functional connections and testable hypotheses can be developed with respect to identifying specific pathways in which NuA4 functions.

4.5.2 mChIP-MAT-MS to identify putative acetylation targets

Using mChIP-KAT-MS, we have identified an extensive network of acetylation sites within the NuA4-associated protein network (Table 4.2). Though acetylation may be identified on co-purifying proteins by LC-MS/MS, one potential limitation is the inability to detect low abundance acetyl-lysine residues. Moreover, despite co-purifying with NuA4, the catalytically responsible enzyme, in principle, remains unknown. The heavy *in vitro* KAT reaction, making use of $^{13}\text{C}_2$ -acetyl coenzyme A, circumvents these issues by (i) enriching the pool of acetyl-lysine residues within the co-purified proteins; and (ii) introducing an isotopically labelled acetyl moiety which is easily distinguished from pre-existing 'light' acetyl groups of *in vivo* origin. In this way, the mChIP-KAT-MS technique builds on the success of the NuA4 *in vitro* protein acetylation microarray (49) in predicting novel substrates for NuA4, but introduces significant advantages. For instance, the mChIP-KAT-MS technique enables the identification of not only the putative acetylation target, but also the specific lysine residue(s) modified by acetylation, as mass spectrometry is used to detect the modification rather than incorporation of radioactive acetyl moieties. Moreover, as enzymatic activity demands a physical interaction between the substrate and enzyme *in vivo*, acetylated proteins identified using mChIP-KAT-MS inherently meet this important constraint, thereby providing a highly relevant functional connection *in vivo* between NuA4 and the acetylated proteins. A direct comparison of the twenty-three acetylated proteins identified within the NuA4-associated protein network (Table 4.2) with the set of *in vitro* candidate substrates discovered on the protein acetylation microarray revealed no overlap. However, broadening the comparison to include any protein identified a minimum of one time

co-purifying with NuA4 reveals an overlap of three proteins, including, the SPB protein Cnm67; Rnr4, a protein involved in dNTP synthesis; and Hsp104, a heat shock protein. We postulate the low abundance, and hence minimal MS protein sequence coverage, of many NuA4 co-purifying proteins might result in undetected acetyl lysine residues. This is specifically demonstrated by application of the mChIP-KAT-MS technique in reverse to identify multiple acetylation sites, including two NuA4-dependent heavy acetyl-lysine residues on Cnm67, on SPB components (Figure 4.4B, Table 4.2). Together, testable hypotheses may be derived from the overlap of the NuA4 interactome and the *in vitro* protein microarray candidate list.

4.5.3 NuA4 regulation by auto-acetylation

We have discovered that multiple NuA4 subunits are acetylated *in vivo*, and further that at least ten subunits can be acetylated by Esa1 *in vitro* (Table 4.2; Figure 4.4), suggesting that auto-acetylation may regulate one or more aspects of NuA4 function. Many examples of enzyme regulation by self-modification have been discovered, such as ATM kinase auto-phosphorylation promoting its activation following DNA damage (17) and auto-acetylation of the KAT p300 to induce a conformational change in its catalytic domain that alters its affinity for DNA (8). Hyper-acetylation of human protein complexes has been described, both with respect to KAT complexes and numerous other classes of protein complexes, but the biological consequences are unknown (12). One possibility is that acetylation regulates protein-protein interactions between subunits, as charge neutralization is a one consequence of lysine acetylation. Another possibility is that acetylation modulates enzymatic activity. For instance, acetylation of the

human KAT enzyme p300 correlates positively with histone acetyltransferase activity (36). To date, the biological function of only a single acetylation site on the NuA4 subunit Yng2 has been explored. Lin *et al.* found that K170 acetylation of Yng2 regulates the stability of the protein (50). As the presence of Yng2 in the NuA4 complex is required to maintain Esa1-catalytic activity *in vivo* (41), this implies a potential feedback loop to control function. Notably, the Yng2 K170 was identified as both a heavy and light acetyl lysine residue in the NuA4 mChIP-KAT-MS, highlighting the utility of our method in identifying biologically significant acetylation. Dissecting the biological consequences of the acetyl lysine residues on NuA4 subunits will likely unravel additional regulatory roles for auto-acetylation.

4.5.4 NuA4 and SPB function – regulation by acetylation?

Numerous links between NuA4 function and the structural integrity of the spindle apparatus have been discovered yet the specific functions of NuA4 have yet to be established. It is likely NuA4 has pleiotropic roles, potentiated through a combination of histone acetylation (41, 46), kinetochore protein regulation (55, 60), and our data now suggest the possibility of direct acetylation of the SPB. Phosphorylation of at least four SPB proteins (Spc42, Spc110, Spc29 and Mps1) results in varied functional consequences including SPB duplication and spindle checkpoint activation (10, 19, 31, 33, 34), but this is the first evidence of lysine acetylation on the SPB. It will be interesting to determine if the accumulation of hyper-acetylation, rather than specific individual acetylation events, may be the predominant mechanism by which acetylation regulates SPB components. The heavy, NuA4-dependent acetylation sites we identified clustered exclusively on

SPB components that reside on the cytoplasmic face of the complex, both in core SPB proteins Cnm67, Nud1, and Spc42, as well as the half-bridge protein Sfi1, and the spindle checkpoint protein Bfa1 (35) (Figure 4.5D). Another important question to address is whether NuA4 has a role in regulating tubulin proteins and hence the function of microtubules directly. Tubulin proteins are acetylated in mammalian systems, which serves to stabilize microtubule structures (62, 63), and alter the interactions of motor proteins (21, 27), yet this modification has not yet been described in yeast. While the exact role of NuA4 at the SPB remains to be dissected, that multiple subunits of the human homolog of NuA4, Tip60, either co-localize to centromeres (23, 67) or have been co-immunoprecipitated with core centrosome proteins or centrosome-localized proteins (26, 28, 45, 71) suggests the possibility of conserved function.

4.5.5 mChIP-KAT-MS to unravel the lysine acetylation network in yeast

Though a proteome-wide analysis of yeast acetyl lysine residues *in vivo* has yet to be published, it is likely just a matter of time. The drawback of such a dataset is the lack of context for the identified acetyl lysine residues, for example, which KAT is responsible for catalyzing the modification and what are the biological consequences? We postulate that the mChIP-KAT-MS methodology presented here can serve as a valuable complementary analysis tool in the elucidation of pathways governed by lysine acetylation due to its ability to connect KATs to their substrates. Moreover, phenotypes previously associated with KATs through genetic analyses can provide additional context as to the potential biological

relevance of identified acetyl lysine residues. The mChIP-KAT-MS technique should be universally applicable to the study of KATs in all model systems.

4.6 Supplemental

Supplemental files associated with this manuscript may be found online at www.oisb.ca/personal_web_site/Baetz_Lab/publicationsFS.html

- Supplemental Figure 4.1: NuA4 mChIP-KAT-MS.
- Supplemental Table 4.1: NuA4-associated protein network and acetylation sites discovered therein
- Supplemental Table 4.2: SPB mChIP-KAT-MS.

4.7 References

1. **Akhtar, A., D. Zink, and P. B. Becker.** 2000. Chromodomains are protein-RNA interaction modules. *Nature* **407**:405-409.
2. **Allard, S., R. T. Utley, J. Savard, A. Clarke, P. Grant, C. J. Brandl, L. Pillus, J. L. Workman, and J. Cote.** 1999. NuA4, an essential transcription adaptor/histone H4 acetyltransferase complex containing Esa1p and the ATM-related cofactor Tra1p. *Embo J* **18**:5108-5119.
3. **Babiarz, J. E., J. E. Halley, and J. Rine.** 2006. Telomeric heterochromatin boundaries require NuA4-dependent acetylation of histone variant H2A.Z in *Saccharomyces cerevisiae*. *Genes Dev* **20**:700-710.
4. **Basu, A., K. L. Rose, J. Zhang, R. C. Beavis, B. Ueberheide, B. A. Garcia, B. Chait, Y. Zhao, D. F. Hunt, E. Segal, C. D. Allis, and S. B. Hake.** 2009. Proteome-wide prediction of acetylation substrates. *Proc Natl Acad Sci U S A* **106**:13785-13790.
5. **Berndsen, C. E., B. N. Albaugh, S. Tan, and J. M. Denu.** 2007. Catalytic mechanism of a MYST family histone acetyltransferase. *Biochemistry* **46**:623-629.
6. **Biggins, S., F. F. Severin, N. Bhalla, I. Sassoon, A. A. Hyman, and A. W. Murray.** 1999. The conserved protein kinase Ipl1 regulates microtubule binding to kinetochores in budding yeast. *Genes Dev* **13**:532-544.
7. **Bird, A. W., D. Y. Yu, M. G. Pray-Grant, Q. Qiu, K. E. Harmon, P. C. Megee, P. A. Grant, M. M. Smith, and M. F. Christman.** 2002. Acetylation of histone H4 by Esa1 is required for DNA double-strand break repair. *Nature* **419**:411-415.
8. **Black, J. C., J. E. Choi, S. R. Lombardo, and M. Carey.** 2006. A mechanism for coordinating chromatin modification and preinitiation complex assembly. *Mol Cell* **23**:809-818.
9. **Boudreault, A. A., D. Cronier, W. Selleck, N. Lacoste, R. T. Utley, S. Allard, J. Savard, W. S. Lane, S. Tan, and J. Cote.** 2003. Yeast enhancer of polycomb defines global Esa1-dependent acetylation of chromatin. *Genes Dev* **17**:1415-1428.
10. **Castillo, A. R., J. B. Meehl, G. Morgan, A. Schutz-Geschwender, and M. Winey.** 2002. The yeast protein kinase Mps1p is required for assembly of the integral spindle pole body component Spc42p. *J Cell Biol* **156**:453-465.
11. **Choi, J. K., and L. J. Howe.** 2009. Histone acetylation: truth of consequences? *Biochem Cell Biol* **87**:139-150.
12. **Choudhary, C., C. Kumar, F. Gnad, M. L. Nielsen, M. Rehman, T. C. Walther, J. V. Olsen, and M. Mann.** 2009. Lysine acetylation targets protein complexes and co-regulates major cellular functions. *Science* **325**:834-840.
13. **Choy, J. S., B. T. Tobe, J. H. Huh, and S. J. Kron.** 2001. Yng2p-dependent NuA4 histone H4 acetylation activity is required for mitotic and meiotic progression. *J Biol Chem* **276**:43653-43662.

14. **Clarke, A. S., J. E. Lowell, S. J. Jacobson, and L. Pillus.** 1999. Esa1p is an essential histone acetyltransferase required for cell cycle progression. *Mol Cell Biol* **19**:2515-2526.
15. **Costanzo, M., A. Baryshnikova, J. Bellay, Y. Kim, E. D. Spear, C. S. Sevier, H. Ding, J. L. Koh, K. Toufighi, S. Mostafavi, J. Prinz, R. P. St Onge, B. VanderSluis, T. Makhnevych, F. J. Vizeacoumar, S. Alizadeh, S. Bahr, R. L. Brost, Y. Chen, M. Cokol, R. Deshpande, Z. Li, Z. Y. Lin, W. Liang, M. Marback, J. Paw, B. J. San Luis, E. Shuteriqi, A. H. Tong, N. van Dyk, I. M. Wallace, J. A. Whitney, M. T. Weirauch, G. Zhong, H. Zhu, W. A. Houry, M. Brudno, S. Ragibizadeh, B. Papp, C. Pal, F. P. Roth, G. Giaever, C. Nislow, O. G. Troyanskaya, H. Bussey, G. D. Bader, A. C. Gingras, Q. D. Morris, P. M. Kim, C. A. Kaiser, C. L. Myers, B. J. Andrews, and C. Boone.** 2010. The genetic landscape of a cell. *Science* **327**:425-431.
16. **Decker, P. V., D. Y. Yu, M. Iizuka, Q. Qiu, and M. M. Smith.** 2008. Catalytic-site mutations in the MYST family histone Acetyltransferase Esa1. *Genetics* **178**:1209-1220.
17. **Dekker, C., P. C. Stirling, E. A. McCormack, H. Filmore, A. Paul, R. L. Brost, M. Costanzo, C. Boone, M. R. Leroux, and K. R. Willison.** 2008. The interaction network of the chaperonin CCT. *EMBO J* **27**:1827-1839.
18. **Eberharter, A., S. John, P. A. Grant, R. T. Utleay, and J. L. Workman.** 1998. Identification and analysis of yeast nucleosomal histone acetyltransferase complexes. *Methods* **15**:315-321.
19. **Friedman, D. B., J. W. Kern, B. J. Huneycutt, D. B. Vinh, D. K. Crawford, E. Steiner, D. Scheiltz, J. Yates, 3rd, K. A. Resing, N. G. Ahn, M. Winey, and T. N. Davis.** 2001. Yeast Mps1p phosphorylates the spindle pole component Spc110p in the N-terminal domain. *J Biol Chem* **276**:17958-17967.
20. **Frydman, J.** 2001. Folding of newly translated proteins in vivo: the role of molecular chaperones. *Annu Rev Biochem* **70**:603-647.
21. **Fukushima, N., D. Furuta, Y. Hidaka, R. Moriyama, and T. Tsujiuchi.** 2009. Post-translational modifications of tubulin in the nervous system. *J Neurochem* **109**:683-693.
22. **Galarneau, L., A. Nourani, A. A. Boudreault, Y. Zhang, L. Heliot, S. Allard, J. Savard, W. S. Lane, D. J. Stillman, and J. Cote.** 2000. Multiple links between the NuA4 histone acetyltransferase complex and epigenetic control of transcription. *Mol Cell* **5**:927-937.
23. **Gartner, W., J. Rossbacher, B. Zierhut, T. Daneva, W. Base, M. Weissel, W. Waldhausl, M. S. Pasternack, and L. Wagner.** 2003. The ATP-dependent helicase RUVBL1/TIP49a associates with tubulin during mitosis. *Cell Motil Cytoskeleton* **56**:79-93.
24. **Gavin, A. C., M. Bosche, R. Krause, P. Grandi, M. Marzioch, A. Bauer, J. Schultz, J. M. Rick, A. M. Michon, C. M. Cruciat, M. Remor, C. Hofert, M. Schelder, M. Brajenovic, H. Ruffner, A. Merino, K. Klein, M. Hudak, D. Dickson, T. Rudi, V. Gnau, A. Bauch, S. Bastuck, B. Huhse, C. Leutwein, M. A. Heurtier, R. R. Copley, A. Edelmann, E. Querfurth, V.**

- Rybin, G. Drewes, M. Raida, T. Bouwmeester, P. Bork, B. Seraphin, B. Kuster, G. Neubauer, and G. Superti-Furga.** 2002. Functional organization of the yeast proteome by systematic analysis of protein complexes. *Nature* **415**:141-147.
25. **Ginsburg, D. S., C. K. Govind, and A. G. Hinnebusch.** 2009. NuA4 lysine acetyltransferase Esa1 is targeted to coding regions and stimulates transcription elongation with Gcn5. *Mol Cell Biol* **29**:6473-6487.
26. **Giorgio, G., M. Alfieri, C. Prattichizzo, A. Zullo, S. Cairo, and B. Franco.** 2007. Functional characterization of the OFD1 protein reveals a nuclear localization and physical interaction with subunits of a chromatin remodeling complex. *Mol Biol Cell* **18**:4397-4404.
27. **Hammond, J. W., C. F. Huang, S. Kaech, C. Jacobson, G. Banker, and K. J. Verhey.** 2010. Posttranslational modifications of tubulin and the polarized transport of kinesin-1 in neurons. *Mol Biol Cell* **21**:572-583.
28. **Harborth, J., K. Weber, and M. Osborn.** 2000. GAS41, a highly conserved protein in eukaryotic nuclei, binds to NuMA. *J Biol Chem* **275**:31979-31985.
29. **Ho, Y., A. Gruhler, A. Heilbut, G. D. Bader, L. Moore, S. L. Adams, A. Millar, P. Taylor, K. Bennett, K. Boutilier, L. Yang, C. Wolting, I. Donaldson, S. Schandorff, J. Shewnarane, M. Vo, J. Taggart, M. Goudreault, B. Muskat, C. Alfarano, D. Dewar, Z. Lin, K. Michalickova, A. R. Willems, H. Sassi, P. A. Nielsen, K. J. Rasmussen, J. R. Andersen, L. E. Johansen, L. H. Hansen, H. Jespersen, A. Podtelejnikov, E. Nielsen, J. Crawford, V. Poulsen, B. D. Sorensen, J. Matthiesen, R. C. Hendrickson, F. Gleeson, T. Pawson, M. F. Moran, D. Durocher, M. Mann, C. W. Hogue, D. Figeys, and M. Tyers.** 2002. Systematic identification of protein complexes in *Saccharomyces cerevisiae* by mass spectrometry. *Nature* **415**:180-183.
30. **Hoepfner, D., A. Brachat, and P. Philippsen.** 2000. Time-lapse video microscopy analysis reveals astral microtubule detachment in the yeast spindle pole mutant *cnm67*. *Mol Biol Cell* **11**:1197-1211.
31. **Holinger, E. P., W. M. Old, T. H. Giddings, Jr., C. Wong, J. R. Yates, 3rd, and M. Winey.** 2009. Budding yeast centrosome duplication requires stabilization of Spc29 via Mps1-mediated phosphorylation. *J Biol Chem* **284**:12949-12955.
32. **Huh, W. K., J. V. Falvo, L. C. Gerke, A. S. Carroll, R. W. Howson, J. S. Weissman, and E. K. O'Shea.** 2003. Global analysis of protein localization in budding yeast. *Nature* **425**:686-691.
33. **Huisman, S. M., M. F. Smeets, and M. Segal.** 2007. Phosphorylation of Spc110p by Cdc28p-Clb5p kinase contributes to correct spindle morphogenesis in *S. cerevisiae*. *J Cell Sci* **120**:435-446.
34. **Jaspersen, S. L., B. J. Huneycutt, T. H. Giddings, Jr., K. A. Resing, N. G. Ahn, and M. Winey.** 2004. Cdc28/Cdk1 regulates spindle pole body duplication through phosphorylation of Spc42 and Mps1. *Dev Cell* **7**:263-274.
35. **Jaspersen, S. L., and M. Winey.** 2004. The budding yeast spindle pole body: structure, duplication, and function. *Annu Rev Cell Dev Biol* **20**:1-28.

36. **Karukurichi, K. R., L. Wang, L. Uzasci, C. M. Manlandro, Q. Wang, and P. A. Cole.** 2010. Analysis of p300/CBP histone acetyltransferase regulation using circular permutation and semisynthesis. *J Am Chem Soc* **132**:1222-1223.
37. **Katahira, J., and Y. Yoneda.** 2009. Roles of the TREX complex in nuclear export of mRNA. *RNA Biol* **6**:149-152.
38. **Keogh, M. C., T. A. Mennella, C. Sawa, S. Berthelet, N. J. Krogan, A. Wolek, V. Podolny, L. R. Carpenter, J. F. Greenblatt, K. Baetz, and S. Buratowski.** 2006. The *Saccharomyces cerevisiae* histone H2A variant Htz1 is acetylated by NuA4. *Genes Dev* **20**:660-665.
39. **Kim, S. C., R. Sprung, Y. Chen, Y. Xu, H. Ball, J. Pei, T. Cheng, Y. Kho, H. Xiao, L. Xiao, N. V. Grishin, M. White, X. J. Yang, and Y. Zhao.** 2006. Substrate and functional diversity of lysine acetylation revealed by a proteomics survey. *Mol Cell* **23**:607-618.
40. **Kobor, M. S., S. Venkatasubrahmanyam, M. D. Meneghini, J. W. Gin, J. L. Jennings, A. J. Link, H. D. Madhani, and J. Rine.** 2004. A Protein Complex Containing the Conserved Swi2/Snf2-Related ATPase Swr1p Deposits Histone Variant H2A.Z into Euchromatin. *PLoS Biol* **2**:E131.
41. **Krogan, N. J., K. Baetz, M. C. Keogh, N. Datta, C. Sawa, T. C. Kwok, N. J. Thompson, M. G. Davey, J. Pootoolal, T. R. Hughes, A. Emili, S. Buratowski, P. Hieter, and J. F. Greenblatt.** 2004. Regulation of chromosome stability by the histone H2A variant Htz1, the Swr1 chromatin remodeling complex, and the histone acetyltransferase NuA4. *Proc Natl Acad Sci U S A*.
42. **Krogan, N. J., G. Cagney, H. Yu, G. Zhong, X. Guo, A. Ignatchenko, J. Li, S. Pu, N. Datta, A. P. Tikuisis, T. Punna, J. M. Peregrin-Alvarez, M. Shales, X. Zhang, M. Davey, M. D. Robinson, A. Paccanaro, J. E. Bray, A. Sheung, B. Beattie, D. P. Richards, V. Canadian, A. Lalev, F. Mena, P. Wong, A. Starostine, M. M. Canete, J. Vlasblom, S. Wu, C. Orsi, S. R. Collins, S. Chandran, R. Haw, J. J. Rilstone, K. Gandi, N. J. Thompson, G. Musso, P. St Onge, S. Ghanny, M. H. Lam, G. Butland, A. M. Altaf-Ul, S. Kanaya, A. Shilatifard, E. O'Shea, J. S. Weissman, C. J. Ingles, T. R. Hughes, J. Parkinson, M. Gerstein, S. J. Wodak, A. Emili, and J. F. Greenblatt.** 2006. Global landscape of protein complexes in the yeast *Saccharomyces cerevisiae*. *Nature* **440**:637-643.
43. **Lambert, J. P., J. Fillingham, M. Siahbazi, J. Greenblatt, K. Baetz, and D. Figeys.** 2010. Defining the budding yeast chromatin-associated interactome. *Mol Syst Biol* **6**:448.
44. **Lambert, J. P., L. Mitchell, A. Rudner, K. Baetz, and D. Figeys.** 2009. A novel proteomics approach for the discovery of chromatin-associated protein networks. *Mol Cell Proteomics* **8**:870-882.
45. **Lauffart, B., S. J. Howell, J. E. Tasch, J. K. Cowell, and I. H. Still.** 2002. Interaction of the transforming acidic coiled-coil 1 (TACC1) protein with ch-TOG and GAS41/NuB1 suggests multiple TACC1-containing protein complexes in human cells. *Biochem J* **363**:195-200.

46. **Le Masson, I., D. Y. Yu, K. Jensen, A. Chevalier, R. Courbeyrette, Y. Boulard, M. M. Smith, and C. Mann.** 2003. Yaf9, a novel NuA4 histone acetyltransferase subunit, is required for the cellular response to spindle stress in yeast. *Mol Cell Biol* **23**:6086-6102.
47. **Lee, C., and J. Goldberg.** 2010. Structure of coatamer cage proteins and the relationship among COPI, COPII, and clathrin vesicle coats. *Cell* **142**:123-132.
48. **Lim, H. H., T. Zhang, and U. Surana.** 2009. Regulation of centrosome separation in yeast and vertebrates: common threads. *Trends Cell Biol* **19**:325-333.
49. **Lin, Y. Y., J. Y. Lu, J. Zhang, W. Walter, W. Dang, J. Wan, S. C. Tao, J. Qian, Y. Zhao, J. D. Boeke, S. L. Berger, and H. Zhu.** 2009. Protein acetylation microarray reveals that NuA4 controls key metabolic target regulating gluconeogenesis. *Cell* **136**:1073-1084.
50. **Lin, Y. Y., Y. Qi, J. Y. Lu, X. Pan, D. S. Yuan, Y. Zhao, J. S. Bader, and J. D. Boeke.** 2008. A comprehensive synthetic genetic interaction network governing yeast histone acetylation and deacetylation. *Genes Dev* **22**:2062-2074.
51. **Lindstrom, K. C., J. C. Vary, Jr., M. R. Parthun, J. Delrow, and T. Tsukiyama.** 2006. Isw1 functions in parallel with the NuA4 and Swr1 complexes in stress-induced gene repression. *Mol Cell Biol* **26**:6117-6129.
52. **Liu, B., L. Larsson, A. Caballero, X. Hao, D. Oling, J. Grantham, and T. Nystrom.** 2010. The polarisome is required for segregation and retrograde transport of protein aggregates. *Cell* **140**:257-267.
53. **Longtine, M. S., A. McKenzie, 3rd, D. J. Demarini, N. G. Shah, A. Wach, A. Brachat, P. Philippsen, and J. R. Pringle.** 1998. Additional modules for versatile and economical PCR-based gene deletion and modification in *Saccharomyces cerevisiae*. *Yeast* **14**:953-961.
54. **Lotterberger, F., A. Panza, G. Lucchini, and M. P. Longhese.** 2007. Functional and physical interactions between yeast 14-3-3 proteins, acetyltransferases, and deacetylases in response to DNA replication perturbations. *Mol Cell Biol* **27**:3266-3281.
55. **Measday, V., K. Baetz, J. Guzzo, K. Yuen, T. Kwok, B. Sheikh, H. Ding, R. Ueta, T. Hoac, B. Cheng, I. Pot, A. Tong, Y. Yamaguchi-Iwai, C. Boone, P. Hieter, and B. Andrews.** 2005. Systematic yeast synthetic lethal and synthetic dosage lethal screens identify genes required for chromosome segregation. *Proc Natl Acad Sci U S A* **102**:13956-13961.
56. **Mehta, M., H. Braberg, S. Wang, A. Lozsa, M. Shales, A. Solache, N. J. Krogan, and M. C. Keogh.** 2010. Individual lysine acetylations on the N-terminus of *S. Cerevisiae* H2A.Z are highly but not differentially regulated. *J Biol Chem*.
57. **Micialkiewicz, A., and A. Chelstowska.** 2008. The essential function of Swc4p - a protein shared by two chromatin-modifying complexes of the yeast *Saccharomyces cerevisiae* - resides within its N-terminal part. *Acta Biochim Pol* **55**:603-612.

58. **Millar, C. B., F. Xu, K. Zhang, and M. Grunstein.** 2006. Acetylation of H2AZ Lys 14 is associated with genome-wide gene activity in yeast. *Genes Dev* **20**:711-722.
59. **Mitchell, L., J. P. Lambert, M. Gerdes, A. S. Al-Madhoun, I. S. Skerjanc, D. Figeys, and K. Baetz.** 2008. Functional dissection of the NuA4 histone acetyltransferase reveals its role as a genetic hub and that Eaf1 is essential for complex integrity. *Mol Cell Biol* **28**:2244-2256.
60. **Ogiwara, H., A. Ui, S. Kawashima, K. Kugou, F. Onoda, H. Iwahashi, M. Harata, K. Ohta, T. Enomoto, and M. Seki.** 2007. Actin-related protein Arp4 functions in kinetochore assembly. *Nucleic Acids Res* **35**:3109-3117.
61. **Pan, X., P. Ye, D. S. Yuan, X. Wang, J. S. Bader, and J. D. Boeke.** 2006. A DNA integrity network in the yeast *Saccharomyces cerevisiae*. *Cell* **124**:1069-1081.
62. **Piperno, G., and M. T. Fuller.** 1985. Monoclonal antibodies specific for an acetylated form of alpha-tubulin recognize the antigen in cilia and flagella from a variety of organisms. *J Cell Biol* **101**:2085-2094.
63. **Piperno, G., M. LeDizet, and X. J. Chang.** 1987. Microtubules containing acetylated alpha-tubulin in mammalian cells in culture. *J Cell Biol* **104**:289-302.
64. **Reid, J. L., V. R. Iyer, P. O. Brown, and K. Struhl.** 2000. Coordinate regulation of yeast ribosomal protein genes is associated with targeted recruitment of Esa1 histone acetylase. *Mol Cell* **6**:1297-1307.
65. **Robinson, M. D., J. Grigull, N. Mohammad, and T. R. Hughes.** 2002. FunSpec: a web-based cluster interpreter for yeast. *BMC Bioinformatics* **3**:35.
66. **Roth, S. Y., J. M. Denu, and C. D. Allis.** 2001. Histone acetyltransferases. *Annu Rev Biochem* **70**:81-120.
67. **Sigala, B., M. Edwards, T. Puri, and I. R. Tsaneva.** 2005. Relocalization of human chromatin remodeling cofactor TIP48 in mitosis. *Exp Cell Res* **310**:357-369.
68. **Sikorski, R. S., and P. Hieter.** 1989. A system of shuttle vectors and yeast host strains designed for efficient manipulation of DNA in *Saccharomyces cerevisiae*. *Genetics* **122**:19-27.
69. **Smith, E. R., A. Eisen, W. Gu, M. Sattah, A. Pannuti, J. Zhou, R. G. Cook, J. C. Lucchesi, and C. D. Allis.** 1998. ESA1 is a histone acetyltransferase that is essential for growth in yeast. *Proc Natl Acad Sci U S A* **95**:3561-3565.
70. **Spange, S., T. Wagner, T. Heinzl, and O. H. Kramer.** 2009. Acetylation of non-histone proteins modulates cellular signalling at multiple levels. *Int J Biochem Cell Biol* **41**:185-198.
71. **Still, I. H., A. K. Vettaikorumakankauv, A. DiMatteo, and P. Liang.** 2004. Structure-function evolution of the transforming acidic coiled coil genes revealed by analysis of phylogenetically diverse organisms. *BMC Evol Biol* **4**:16.

72. **Swisher, K. D., and R. Parker.** 2010. Localization to, and effects of Pbp1, Pbp4, Lsm12, Dhh1, and Pab1 on stress granules in *Saccharomyces cerevisiae*. *PLoS One* **5**:e10006.
73. **Tong, A. H., G. Lesage, G. D. Bader, H. Ding, H. Xu, X. Xin, J. Young, G. F. Berriz, R. L. Brost, M. Chang, Y. Chen, X. Cheng, G. Chua, H. Friesen, D. S. Goldberg, J. Haynes, C. Humphries, G. He, S. Hussein, L. Ke, N. Krogan, Z. Li, J. N. Levinson, H. Lu, P. Menard, C. Munyana, A. B. Parsons, O. Ryan, R. Tonikian, T. Roberts, A. M. Sdicu, J. Shapiro, B. Sheikh, B. Suter, S. L. Wong, L. V. Zhang, H. Zhu, C. G. Burd, S. Munro, C. Sander, J. Rine, J. Greenblatt, M. Peter, A. Bretscher, G. Bell, F. P. Roth, G. W. Brown, B. Andrews, H. Bussey, and C. Boone.** 2004. Global mapping of the yeast genetic interaction network. *Science* **303**:808-813.
74. **Vizeacoumar, F. J., N. van Dyk, S. V. F, V. Cheung, J. Li, Y. Sydorskyy, N. Case, Z. Li, A. Datti, C. Nislow, B. Raught, Z. Zhang, B. Frey, K. Bloom, C. Boone, and B. J. Andrews.** 2010. Integrating high-throughput genetic interaction mapping and high-content screening to explore yeast spindle morphogenesis. *J Cell Biol* **188**:69-81.
75. **Wang, A. Y., J. M. Schulze, E. Skordalakes, J. W. Gin, J. M. Berger, J. Rine, and M. S. Kobor.** 2009. Asf1-like structure of the conserved Yaf9 YEATS domain and role in H2A.Z deposition and acetylation. *Proc Natl Acad Sci U S A* **106**:21573-21578.
76. **Wang, J., and J. Chen.** 2010. SIRT1 regulates autoacetylation and histone acetyltransferase activity of TIP60. *J Biol Chem* **285**:11458-11464.
77. **Wang, Q., Y. Zhang, C. Yang, H. Xiong, Y. Lin, J. Yao, H. Li, L. Xie, W. Zhao, Y. Yao, Z. B. Ning, R. Zeng, Y. Xiong, K. L. Guan, S. Zhao, and G. P. Zhao.** 2010. Acetylation of metabolic enzymes coordinates carbon source utilization and metabolic flux. *Science* **327**:1004-1007.
78. **Wilm, M., A. Shevchenko, T. Houthaeve, S. Breit, L. Schweigerer, T. Fotsis, and M. Mann.** 1996. Femtomole sequencing of proteins from polyacrylamide gels by nano-electrospray mass spectrometry. *Nature* **379**:466-469.
79. **Zhang, J., R. Sprung, J. Pei, X. Tan, S. Kim, H. Zhu, C. F. Liu, N. V. Grishin, and Y. Zhao.** 2009. Lysine acetylation is a highly abundant and evolutionarily conserved modification in *Escherichia coli*. *Mol Cell Proteomics* **8**:215-225.
80. **Zhao, S., W. Xu, W. Jiang, W. Yu, Y. Lin, T. Zhang, J. Yao, L. Zhou, Y. Zeng, H. Li, Y. Li, J. Shi, W. An, S. M. Hancock, F. He, L. Qin, J. Chin, P. Yang, X. Chen, Q. Lei, Y. Xiong, and K. L. Guan.** 2010. Regulation of cellular metabolism by protein lysine acetylation. *Science* **327**:1000-1004.
81. **Zhou, H., W. Hou, J. P. Lambert, R. Tian, and D. Figeys.** 2010. Analysis of low-abundance proteins using the proteomic reactor with pH fractionation. *Talanta* **80**:1526-1531.

CHAPTER 5: GENERAL DISCUSSION

In this thesis I have presented three global screens performed to probe the function of the *S. cerevisiae* KAT NuA4 *in vivo*. Stand-alone, each screen provides unique insights into NuA4 function. Moreover, the unbiased nature of these systematic analyses has fostered significant leaps in our understanding of NuA4 biology, providing clear evidence that NuA4 function impacts a diverse array of cellular processes outside of its traditional chromatin-mediated roles. As an integrated body of work, the NuA4 SL, SDL, and protein-associated networks present a complementary analysis platform to derive specific testable hypotheses with respect to NuA4 function *in vivo*. Below, I will discuss specific examples of how the datasets may be integrated and contextualize this body of work within the field of lysine acetylation.

5.1 Integration of datasets to predict NuA4 function

5.1.1 SL and SDL genetic interactions

NuA4 is a challenging protein complex to functionally dissect using genetic approaches. First, of the thirteen NuA4 subunits, only Eaf1 functions exclusively within NuA4 (12), as each of Eaf3, Eaf6, Yaf9, Swc4, Act1, Arp4, and Tra1 participate in one or more additional chromatin modifying protein complexes (6); Eaf3, Eaf5, and Eaf7 have recently been proposed to function as a discrete trimer independently from NuA4 (Auger et al., 2008); and Esa1, Yng2, Epl1, and Eaf6

form the related PicNuA4 KAT complex (2). Therefore, genetic interactions associated with the NuA4 genes encoding all but Eaf1 may not derive specifically from disruption of NuA4 complex function. Secondly, essential genes encode six of NuA4's subunits, including the catalytic subunit Esa1. Genetic analyses of the essential components must necessarily rely on the use of mutant alleles, in which all functions of the encoded protein may not be fully compromised. To circumvent these issues, we chose to genetically dissect NuA4 function through its non-essential subunits, relying on the identification of trends in the SL genetic interaction network to identify links between NuA4 and vesicle-mediated transport, the stress response, and the high degree of inter-connectivity of specific nodes in the SDL network to discover a direct role for NuA4 in septin dynamics, mediated at least in part by NuA4-dependent acetylation of the septin protein Shs1.

In principle it is now possible to utilize NuA4 SDL and SL interactions in a complementary fashion, as SL interactions can connect NuA4 to particular cellular functions and SDL interactions have the potential to identify direct pathways (1). This is an especially important concept in light of the growing list of NuA4 SL genetic interactions appearing in the literature. For instance, since the publication of our NuA4 SL genetic interaction network (12), two additional SL-SGA surveys, designed to assess SL genetic interactions of KATs and KDACs (9), and more broadly the vast majority of genes within the yeast genome (5), have contributed enormously to the identification of NuA4 SL genetic interactions. As a result of these large-scale efforts, in combination with the NuA4 SL dataset presented in Chapter 2, more than 500 SL (or SS) genetic interactions have now been identified

for the five non-essential subunits. Moreover, alleles of most essential NuA4 genes have been subjected to SL-SGA analysis (5, 7, 9), importantly including two alleles encoding catalytically inactive versions of Esa1 (*esa1-L254P* (4) and *esa1-531* (9)) as well as a hypomorphic allele (*esa1-Hm1* (9)). For *ESA1* alone, 452 genetic interactions have been identified altogether, linking the function of this lysine acetyltransferase to virtually every cellular process in yeast and thus solidifying the role of Esa1 as a genetic hub (Figure 5.1A). As such, NuA4 SL interactions in isolation are practically impossible to interpret, which makes the comparison with our SDL profile even more valuable. For instance, cross-referencing the cellular processes enriched within the *ESA1* SL network with classes of genes identified in the NuA4 SDL network provides a crude method to distinguish processes that may directly impacted by Esa1, from processes that may be disrupted as a secondary consequence, for example through non-specific transcriptional misregulation (Figure 5.2B, red text). A comparison of the number of NuA4 SDL interactions uncovered in the work presented in Chapter 3 (89) to previously published NuA4 genome-wide SL interactions (>500) (Supplemental Table 3.2), indeed suggests that while NuA4 function impacts a diverse array of cellular processes, it may directly function in only a handful of pathways.

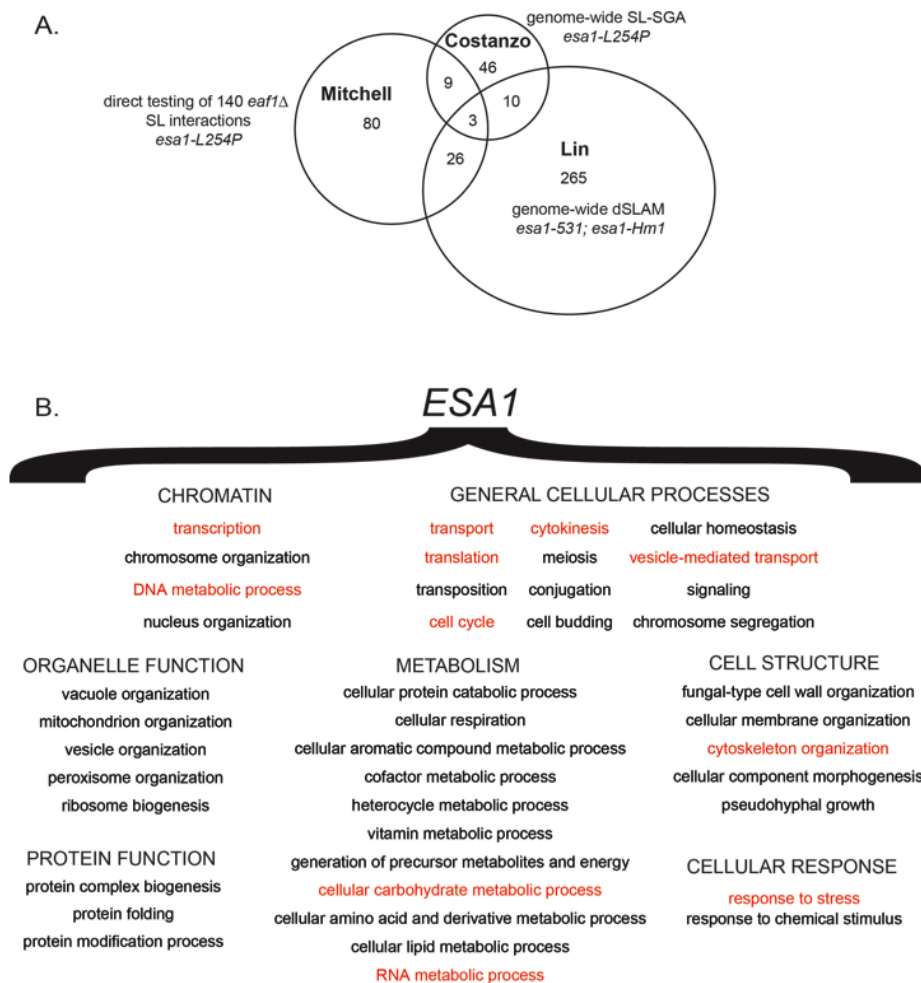


Figure 5.1: *ESA1* synthetic lethal genetic interactions link its function to a diverse array of cellular processes.

(A) Overlap of SL interactions from three different publications assessing *ESA1* function. The number of genes shared between datasets is presented in a Venn diagram. Mitchell *et al.* (12) directly tested 140 SL interactions identified for *EAF1* and used the *esa1-L254P* allele. Costanzo *et al.* (5) performed an SL-SGA screen using the same allele. Lin *et al.* (9) performed diploid-based synthetic lethal analysis by microarray (dSLAM) using two alleles of *ESA1*: (i) *esa1-531* which contains the L254P mutation as well as an additional substitution L346F; and (ii) a hypomorphic allele, *esa1-Hm1*. **(B)** Cellular processes linked to *ESA1* through SL analysis. Enrichments in cellular processes for within the set of 452 unique *ESA1* SL genetic interactions (as published at www.theBiogrid.org, version 3.1.70) were identified using GO Slim Mapper tool (<http://www.yeastgenome.org/cgi-bin/GO/goSlimMapper.pl>), by choosing “Yeast GO-slim Process”. Processes enriched within the dataset are organized by category (capital letters). Processes highlighted in red were also identified in the NuA4 SDL network.

5.1.2 Integrating SDL profiles of individual subunits to predict acetylation targets

Unlike SL-SGA analyses, very few SDL-SGA screens have been published to date (11, 14, 17). While these efforts have successfully identified enzyme-substrate relationships, a number of other interpretations can be made to explain the genetic basis underlying an SDL interaction. For instance, the hyper-activation of one pathway may overwhelm a compensatory pathway leading to the SDL phenotype. While a primary goal of the NuA4 SDL screen was to identify putative acetylation targets, it is likely that many, if not most, of the genes in the SDL network do not encode NuA4 substrates, but rather the interactions derive from alternative genetic origins. This is made even more likely due to the fact that a catalytically inactive *ESA1* allele was not used as a query strain. To narrow the list of NuA4 SDL genetic interactions to those derived from loss of the recruited action of NuA4 KAT activity, I propose an integrated approach making use of the knowledge we have gained with respect to the specific roles of non-essential NuA4 subunits in the complex. Specifically, *EAF1* interactions can be unambiguously assigned to NuA4, as *Eaf1* functions solely in the NuA4 complex (12). In principle, however, an *EAF1* SDL interaction could result from loss of NuA4 recruitment due to complex integrity disruption, and not necessarily depend on the ablated KAT activity observed in *eaf1* Δ cells. *YNG2* SDL interactions, while potentially dependent on the loss of NuA4 KAT activity observed in the absence of *Yng2*, could derive from *Yng2*'s role in either NuA4 or PicNuA4. Finally, *EAF5* and *EAF7*

encode NuA4 subunits that likely function to recruit NuA4, and therefore their SDL interactions may depend on their roles in the NuA4 recruitment domain. Together, this logic predicts that any SDL interaction shared by *EAF1*, *YNG2* and *EAF5/7* might depend specifically on the recruitment of NuA4-dependent acetyltransferase activity (Figure 5.2A). Applying these criteria narrows the list of 89 NuA4 SDL interactions to 10 (Figure 5.2B), including the septin genes *CDC11* and *SHS1*, characterized as part of the SDL work in Chapter 3. The remaining eight genes include *ALK2*, a kinase that functions in DNA damage repair; *ACT1*, which encodes the structural molecule actin, also a member of the NuA4 complex itself; *AKL1*, a kinase that participates in actin cytoskeleton organization; *ROX3*, an RNA polymerase II holoenzyme component; *RPN8*, a regulatory subunit of the proteasome; *SNC1* and *SMY2*, encoding proteins with roles in vesicle-mediated transport; and *WWM1*, an uncharacterized gene. Supporting this, an anti-acetyl lysine western blot detected that Ak11 is acetylated *in vivo* and analysis of Ak11-GFP localization in *eaf1Δ* mutants suggests its localization to the neck of small budded cells depends on NuA4 is altered (data not shown). Together, based on the interconnectivity of their SDL interactions with the specific NuA4 gene deletion mutants discussed above, the proteins encoded by these eight genes represent strong candidates as either direct NuA4 acetylation targets or as proteins involved in pathways directly regulated by NuA4 acetyltransferase activity.

A.

Interpretation of SDL Interaction			
	NuA4 specific	Acetylation-dependent	NuA4 recruitment
<i>EAF1</i>	YES	YES	YES
<i>YNG2</i>	NO (NuA4 OR PicNuA4)	YES	NO
<i>EAF5 or EAF7</i>	NO (NuA4 OR Eaf3/5/7)	NO	YES

B.

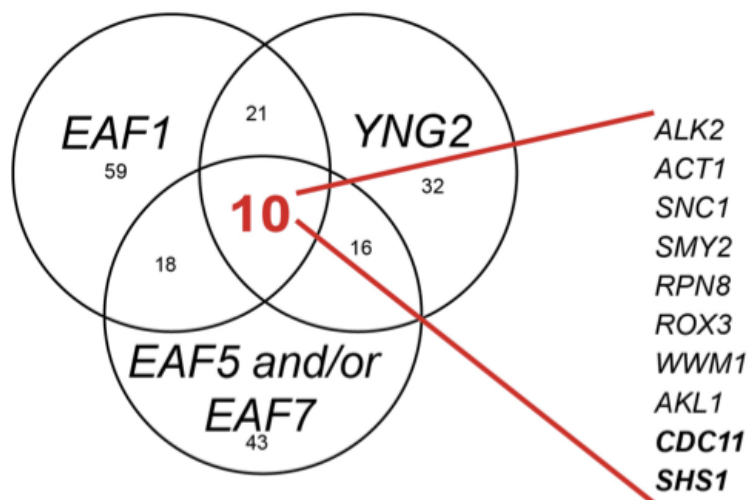


Figure 5.2: Integrating individual NuA4 mutant SDL profiles to predict substrates.

(A) A proposed method to interpret SDL interactions in order to isolate those specific to the recruited KAT activity of NuA4. (B) Venn diagram showing the overlap of *EAF1*, *YNG2*, and *EAF5/EAF7* SDL interactions, all predicted to be acetylation targets of NuA4. Based on the logic presented in (A), the list of putative candidate genes is represented in the sets of SL genetic interaction profiles (listed genes).

5.1.3 Integrating genetic interaction networks with NuA4 physical interactions and putative acetylation targets

Protein-protein interactions pinpoint direct connections within the cell and can therefore add tremendous insight to the functional relationships that may be inferred from SL or SDL genetic interactions. Moreover, additional layering of putative acetylation targets discovered through biochemical approaches such as our novel mChIP-KAT-MS technology or the NuA4 *in vitro* protein microarray (8) should be valuable to specifically identify acetylation targets within these networks. Making use of complementary datasets has proven effective to identify substrates of the Pho85 kinase in yeast, comparing genetic data generated from a *pho85Δ* systematic SDL screen to biochemical data derived from *in vitro* Pho85 kinase assays using proteome chips (13). We can now apply these same types of integrated analyses to the NuA4 complex. For instance, overlap discovered between the NuA4 SDL network and the physical interaction network include proteins encoded by *MSN4*, encoding the stress responsive transcription factor, and *ACT1*, encoding the actin structural molecule, which also serves a component of the NuA4 complex. Interestingly, in addition to the functional connections between NuA4 and Msn4 described in Chapter 2, which suggest NuA4 may acetylate Msn4, we have discovered NuA4-dependent 'heavy' acetylation sites on Msn4 using the mChIP-KAT-MS technique (data not shown); the next step is to determine whether these sites exist *in vivo* and/or whether mutation has any effect. Acetylation on actin, despite being discovered in mammalian systems (3), has not

been described in yeast, on either cytoskeletal actin or in our analysis of acetylation on NuA4 subunits (Chapter 4). However, regardless of acetylation status of the encoded protein, the overexpression of *ACT1* would be expected to have dire consequences *in vivo*, given the impact NuA4 may have on the actin cytoskeleton, as discussed in Chapter 3, as well as the additional disruption to the already crippled NuA4 complex.

The network of NuA4 SDL hits may also be compared to the candidate substrates identified on the NuA4 *in vitro* protein acetylation microarray (8) as another method to predict the most likely NuA4 substrates. This comparison reveals two genes: *GSY2*, which encodes the major glycogen synthase enzyme in yeast (15), and *WHI5*, a repressor of G1 transcription (16). Gsy2 is an interesting example, as the function of the protein is thought to be controlled largely at the transcriptional level, at least in part by the Msn2/4 stress responsive transcription factors (15). Specifically, low glucose conditions trigger induction of *GSY2* expression and the subsequent accumulation of glycogen (15). That NuA4 represses Msn2/4-dependent genes under normal conditions, as shown in Chapter 2 and by others (10), suggests the SDL interaction caused by overexpression of *GSY2* in NuA4 mutant cells may be potentiated through an aberrant transcriptional program. However, the complementary SDL interaction/*in vitro* target data suggests direct acetylation of Gsy2 as an intriguing alternative hypothesis.

5.2 Systems biology approaches to study lysine acetylation

Through the analysis of NuA4, I have demonstrated that global genetic and proteomic screens provide highly relevant functional information to discover novel

proteins and pathways regulated by NuA4 KAT activity. Moreover, as outlined above, I believe that integration of these orthogonal datasets can now be used to derive specific testable hypotheses worthy of investigation in order to further discern the functions of NuA4 at the molecular level. Moving forward in the study of lysine acetylation in the budding yeast, establishing and integrating SDL and mChIP-KAT-MS networks for all yeast KATs presents a promising approach to elucidate enzyme-substrate relationships and begin to unravel the network of lysine acetylation in this organism. Further, analysis of data generated in this 'KAT-ologue', will benefit from pre-existing SL-SGA profiles for all KATs (5, 9).

In summary, a number of systems biology approaches provide excellent tools to study lysine acetylation *in vivo*. Specifically, powerful genetic screens have been developed in the budding yeast model system that can be implemented to assess the function of KAT enzymes. Similar global approaches, for instance RNA interference (RNAi) screens, have been adapted to explore gene function globally in mammalian cells and other model systems such as *C. elegans* that will be useful to study KAT function in higher eukaryotes. Moreover, methodology development, such as the coupling of proteomic and biochemical screening enabled through the mChIP-KAT-MS approach described in Chapter 4, and additional mass spectrometry based approaches, such as SILAC, represent important tools to link KATs to their cognate substrates *in vivo*. Despite these outstanding high throughput approaches, the validation of KAT-substrate relationships *in vivo* and the demonstration of biological consequences associated with particular acetylation events remain to be the rate-limiting step in the elucidation of lysine

acetylation networks. In short, the rigorous experimentation that is required to accomplish these goals is simply not amenable to high throughput analysis. Specific areas that need to be addressed include: (i) the development of more robust pan-anti-acetyl lysine antibodies; and (ii) technological and/or methodological developments in mass spectrometry devoted to producing even sequence coverage. Other areas that will speed the validation of specific acetylation events include (i) the declining cost of complete gene synthesis that enable more efficient testing of unacetylatable mutants to identify the biological outcome of acetylation; (ii) the generation of site specific antibodies; (iii) proteome-wide identification of acetyl lysine residues in a wide variety of eukaryotes and prokaryotes to allow cross-species comparison of acetylation; and (iv) the development of consensus sequence recognition motifs to predict acetylation sites *de novo* or assign probability scores to acetyl lysine datasets. In summary, moving towards a more complete understanding of the consequences of all lysine acetylation events is a daunting challenge but the integration of different types of genetic, proteomic, and biochemical data represents the most promising strategy.

5.3 References

1. **Boone, C., H. Bussey, and B. J. Andrews.** 2007. Exploring genetic interactions and networks with yeast. *Nat Rev Genet* **8**:437-449.
2. **Boudreault, A. A., D. Cronier, W. Selleck, N. Lacoste, R. T. Utley, S. Allard, J. Savard, W. S. Lane, S. Tan, and J. Cote.** 2003. Yeast enhancer of polycomb defines global Esa1-dependent acetylation of chromatin. *Genes Dev* **17**:1415-1428.
3. **Choudhary, C., C. Kumar, F. Gnad, M. L. Nielsen, M. Rehman, T. C. Walther, J. V. Olsen, and M. Mann.** 2009. Lysine acetylation targets protein complexes and co-regulates major cellular functions. *Science* **325**:834-840.
4. **Clarke, A. S., J. E. Lowell, S. J. Jacobson, and L. Pillus.** 1999. Esa1p is an essential histone acetyltransferase required for cell cycle progression. *Mol Cell Biol* **19**:2515-2526.
5. **Costanzo, M., A. Baryshnikova, J. Bellay, Y. Kim, E. D. Spear, C. S. Sevier, H. Ding, J. L. Koh, K. Toufighi, S. Mostafavi, J. Prinz, R. P. St Onge, B. VanderSluis, T. Makhnevych, F. J. Vizeacoumar, S. Alizadeh, S. Bahr, R. L. Brost, Y. Chen, M. Cokol, R. Deshpande, Z. Li, Z. Y. Lin, W. Liang, M. Marback, J. Paw, B. J. San Luis, E. Shuteriqi, A. H. Tong, N. van Dyk, I. M. Wallace, J. A. Whitney, M. T. Weirauch, G. Zhong, H. Zhu, W. A. Houry, M. Brudno, S. Ragibzadeh, B. Papp, C. Pal, F. P. Roth, G. Giaever, C. Nislow, O. G. Troyanskaya, H. Bussey, G. D. Bader, A. C. Gingras, Q. D. Morris, P. M. Kim, C. A. Kaiser, C. L. Myers, B. J. Andrews, and C. Boone.** 2010. The genetic landscape of a cell. *Science* **327**:425-431.
6. **Doyon, Y., and J. Cote.** 2004. The highly conserved and multifunctional NuA4 HAT complex. *Curr Opin Genet Dev* **14**:147-154.
7. **Hoke, S. M., J. Guzzo, B. Andrews, and C. J. Brandl.** 2008. Systematic genetic array analysis links the *Saccharomyces cerevisiae* SAGA/SLIK and NuA4 component Tra1 to multiple cellular processes. *BMC Genet* **9**:46.
8. **Lin, Y. Y., J. Y. Lu, J. Zhang, W. Walter, W. Dang, J. Wan, S. C. Tao, J. Qian, Y. Zhao, J. D. Boeke, S. L. Berger, and H. Zhu.** 2009. Protein acetylation microarray reveals that NuA4 controls key metabolic target regulating gluconeogenesis. *Cell* **136**:1073-1084.
9. **Lin, Y. Y., Y. Qi, J. Y. Lu, X. Pan, D. S. Yuan, Y. Zhao, J. S. Bader, and J. D. Boeke.** 2008. A comprehensive synthetic genetic interaction network governing yeast histone acetylation and deacetylation. *Genes Dev* **22**:2062-2074.

10. **Lindstrom, K. C., J. C. Vary, Jr., M. R. Parthun, J. Delrow, and T. Tsukiyama.** 2006. Isw1 functions in parallel with the NuA4 and Swr1 complexes in stress-induced gene repression. *Mol Cell Biol* **26**:6117-6129.
11. **Liu, C., D. van Dyk, Y. Li, B. Andrews, and H. Rao.** 2009. A genome-wide synthetic dosage lethality screen reveals multiple pathways that require the functioning of ubiquitin-binding proteins Rad23 and Dsk2. *BMC Biol* **7**:75.
12. **Mitchell, L., J. P. Lambert, M. Gerdes, A. S. Al-Madhoun, I. S. Skerjanc, D. Figeys, and K. Baetz.** 2008. Functional dissection of the NuA4 histone acetyltransferase reveals its role as a genetic hub and that Eaf1 is essential for complex integrity. *Mol Cell Biol* **28**:2244-2256.
13. **Sopko, R., and B. J. Andrews.** 2008. Linking the kinome and phosphorome--a comprehensive review of approaches to find kinase targets. *Mol Biosyst* **4**:920-933.
14. **Sopko, R., D. Huang, N. Preston, G. Chua, B. Papp, K. Kafadar, M. Snyder, S. G. Oliver, M. Cyert, T. R. Hughes, C. Boone, and B. Andrews.** 2006. Mapping pathways and phenotypes by systematic gene overexpression. *Mol Cell* **21**:319-330.
15. **Wilson, W. A., M. P. Boyer, K. D. Davis, M. Burke, and P. J. Roach.** 2010. The subcellular localization of yeast glycogen synthase is dependent upon glycogen content. *Can J Microbiol* **56**:408-420.
16. **Wittenberg, C., and S. I. Reed.** 2005. Cell cycle-dependent transcription in yeast: promoters, transcription factors, and transcriptomes. *Oncogene* **24**:2746-2755.
17. **Zou, J., H. Friesen, J. Larson, D. Huang, M. Cox, K. Tatchell, and B. Andrews.** 2009. Regulation of cell polarity through phosphorylation of Bni4 by Pho85 G1 cyclin-dependent kinases in *Saccharomyces cerevisiae*. *Mol Biol Cell* **20**:3239-3250.